TU Delft

Delft University of Technology

Physiology of aerobic yeast cultures under industrially relevant conditions

Hakkaart, Xavier

DOI
10.4233/uuid:9ba7c6c5-1807-410a-a0b8-c40cd9399dcf

Publication date
2019

Document Version
Final published version

Citation (APA)
Hakkaart, X. (2019). *Physiology of aerobic yeast cultures under industrially relevant conditions*. [Dissertation (TU Delft), Delft University of Technology]. https://doi.org/10.4233/uuid:9ba7c6c5-1807-410a-a0b8-c40cd9399dcf

Important note
To cite this publication, please use the final published version (if applicable).
Please check the document version above.

Copyright
Other than for strictly personal use, it is not permitted to download, forward or distribute the text or part of it, without the consent of the author(s) and/or copyright holder(s), unless the work is under an open content license such as Creative Commons.

Takedown policy
Please contact us and provide details if you believe this document breaches copyrights.
We will remove access to the work immediately and investigate your claim.

This work is downloaded from Delft University of Technology.
For technical reasons the number of authors shown on this cover page is limited to a maximum of 10.

Physiology of aerobic yeast cultures under industrially relevant conditions

X.D.V. Hakkaart

Physiology of aerobic yeast cultures under industrially relevant conditions

Proefschrift

ter verkrijging van de graad van doctor
aan de Technische Universiteit Delft,
op gezag van de Rector Magnificus prof. dr. ir. T.H.J.J. van der Hagen,
voorzitter van het College voor Promoties,
in het openbaar te verdedigen op donderdag 31 oktober 2019 om 12.30

door

Xavier Dominique Vincent HAKKAART

Ingenieur in Life Science and Technology
Technische Universiteit Delft, Nederland

geboren te Hilversum, Nederland.

Dit proefschrift is goedgekeurd door de promotoren

Prof. dr. P.A.S. Daran-Lapujade
Prof. dr. J.T. Pronk

Samenstelling promotiecommissie:

Rector Magnificus	voorzitter
Prof. dr. P.A.S. Daran-Lapujade	Technische Universiteit Delft, *promotor*
Prof. dr. J.T. Pronk	Technische Universiteit Delft, *promotor*
Onafhankelijke leden:	
Prof. dr. U. Hanefeld	Technische Universiteit Delft
Dr. ir. M.L.A. Jansen	Koninklijke DSM
Prof. dr. B. Teusink	VU Amsterdam
Prof. dr. P. Branduardi	University of Milano-Bicocca, Italy
Prof. dr.-Ing. R. Takors	University Stuttgart, Germany
Overige leden:	
Prof. dr. F. Hollman	Technische Universiteit Delft, *reservelid*

The research presented in this thesis was performed at the Industrial Microbiology Section, Department of Biotechnology, Faculty of Applied Sciences, Delft University of Technology, The Netherlands. The project was financed by the BE-Basic R&D Program, which was granted a FES subsidy from the Dutch Ministry of Economic Affairs

Keywords: Yeast, Physiology, Industrial conditions, Retentostat, Teaching

Printed by: Proefschriften.net

Front & Back: Tom van Bavel

Copyright © 2019 by X.D.V.. Hakkaart

ISBN 978-94-6384-064-4

An electronic version of this dissertation is available at
http://repository.tudelft.nl/.

Contents

Samenvatting		1
Summary		5
1	General introduction	9
2	*S. cerevisiae* aerobic retentostat cultures	31
3	*S. cerevisiae* under industrially relevant conditions	61
4	Improved low-pH tolerance of *S. cerevisiae*	81
5	Teaching microbial physiology	113
Outlook		125
Acknowledgements		127
References		133
Curriculum Vitæ		152
List of Publications		153

Samenvatting

Micro-organismen worden in de industriële biotechnologie ingezet voor het maken van een breed scala aan producten, waaronder voedingssupplementen, transportbrandstoffen, medicijnen en plastics, uit suikers van natuurlijke oorsprong. Ten opzichte van de petrochemische synthese van deze producten biedt industriële biotechnologie een duurzaamheidsvoordeel door een lagere CO_2-uitstoot en draagt hiermee bij aan de bio-gebaseerde economie.

Gisten zijn belangrijke industriële 'werkpaarden' voor de productie van vele van de hierboven genoemde producten. Bakkersgist – *Saccharomyces cerevisiae* – wordt gebruikt voor de grootschalige productie van bijvoorbeeld bioethanol, farneseen, humaan insuline en barnsteenzuur. Om deze producten kostenefficiënt te produceren, is een hoge opbrengst van het beoogde product op het substraat (bijvoorbeeld glucose) een essentiële voorwaarde. Het ontkoppelen van productvorming en groei is een aanpak om een zo hoog mogelijke productopbrengst te behalen. Dit is een uitdagende aanpak, aangezien microbiële stofwisselingsroutes juist evolutionair geoptimaliseerd zijn om substraat te gebruiken voor groei en voor het onderhoud van de cellulaire integriteit en levensvatbaarheid.

Voor dissimilatoire producten, waarvan de productie resulteert in de netto productie van ATP, is de ontkoppeling van groei en productvorming eerder onderzocht voor ethanolproductie van *S. cerevisiae* onder anaërobe condities. Voor vorming van niet-dissimilatoire producten zoals farneseen, humaan insuline, andere eiwitten en barnsteenzuur uit glucose is een netto consumptie van ATP benodigd. Deze productieprocessen zijn daardoor in de cel in competitie met de behoefte aan ATP voor groei en voor cellulair onderhoud. Het optimaliseren van de opbrengst van niet-dissimilatoire producten op glucose vraagt daardoor een sterke mate van energetische koppeling in de dissimilatie, waarbij netto ATP geproduceerd wordt. Wanneer *S. cerevisiae* glucose verademt tot CO_2 en water, levert dit achtmaal meer ATP dan wanneer glucose wordt vergist tot ethanol en CO_2. Om deze reden wordt de productie van niet-dissimilatoire producten bij voorkeur uitgevoerd onder omstandigheden die verademing van glucose mogelijk maken.

Het systematisch karakteriseren van de fysiologie van gisten onder nauwkeurig gecontroleerde kweekomstandigheden kan worden uitgevoerd in bioreactoren. In steady-state chemostaatculturen in bioreactoren wordt de specifieke groeisnelheid bepaald door de verdunningssnelheid, die ingesteld wordt door de onderzoeker. Hierdoor maakt chemostaatcultivatie het mogelijk om verschillende microbiële

stammen en/of kweekomstandigheden groeisnelheidsonafhankelijk te vergelijken. Praktische beperkingen bij het inregelen van de mediumtoevoersnelheid maken chemostaatculturen in bioreactoren op laboratoriumschaal ongeschikt voor fysiologische studies bij een verdunningssnelheid lager dan ongeveer 0,015 per uur. De retentostaat, een chemostaat waarbij een filter in de uitgaande vloeistofstroom van de bioreactor voor 100 % biomassaretentie zorgt, is een geschikt alternatief voor het bestuderen van microbiële cultures bij deze zeer lage groeisnelheden.

In **Hoofdstuk 2** is de fysiologie van niet-groeiende, volledig aërobe en volledig respiratoire (ademhalende) *S. cerevisiae* retentostaatcultures gekarakteriseerd. Deze studie concentreerde zich op industrieel relevante eigenschappen van de cultuur zoals levensvatbaarheid, robuustheid en de capaciteit van de glycolytische stofwisselingsroute. Voor het ontwerp van de experimenten werd gebruik gemaakt van een voorspellend model, zodat een geleidelijke transitie van de cultuur van groei naar nulgroei van de cultuur kon worden gerealiseerd. De retentostaatcultures werden gedurende een periode van twintig dagen gevolgd. In deze periode daalde de specifieke groeisnelheid van 0,025 per uur tot, uiteindelijk, een specifieke groeisnelheid lager dan 0,001 per uur. Aan het eind van deze experimenten werd nagenoeg al het geconsumeerde substraat voor de onderhoudsbehoeften van de cultures gebruikt, terwijl de levensvatbaarheid van de cultures hoger dan 80 % bleef. Door gebruik te maken van een regressieanalyse op de toename van biomassa, werd de specifieke ATP-onderhoudsbehoefte bij extreem lage groeisnelheden berekend. Deze werd ongeveer 35 % lager geschat dan voor eerdere cultures bij een vergelijkbare niet-groeiende status onder anaërobe condities. Hoewel de specifieke substraatconsumptiesnelheid van deze cultures zeer laag was, bleef de glycolytische capaciteit juist hoog.

In **Hoofdstuk 2** bleken de expressieniveaus van genen met een rol in de biosynthese van onder andere sterolen, vetten, aminozuren en ribosomen af te nemen tussen een specifieke groeisnelheid van 0.1 per uur en het bereiken van de niet-groeiende status. Daarentegen namen de expressieniveaus van genen die gerelateerd waren aan de reactie op stress juist toe. Deze resultaten kwamen grotendeels overeen met de observaties van de expressieniveaus in een vergelijkbare studie aan anaërobe retentostaatcultures. De toename van de resistentie tegen een warmte-schok bij zeer langzame groeisnelheden was reeds bekend, maar het niveau van deze resistentie in aërobe retentostaatcultures was ongeëvenaard, zelfs in vergelijking met de warmteschoktolerantie van cellen in de stationaire fase van aërobe batchculturen.

In **hoofdstuk 2** werden de zeer-langzaam-groeiende culturen gekarakteriseerd onder standaard laboratoriumcondities. Deze condities zijn echter niet volledig representatief voor de omstandigheden die micro-organismen ontmoeten in een grootschalig industrieel proces. In **Hoofdstuk 3** werd dezelfde giststam als in **Hoofdstuk 2** bestudeerd onder zeer-langzaam-groeiende condities die relevant zijn

voor het productieproces van barnsteenzuur en andere dicarboxylzuren. Bij deze industrieel relevante condities hoorde een lage extracellulaire pH van de cultuur (pH 3) en een hoog CO_2-niveau (50 %). In retentostaatcultures resulteerden deze condities in een tweemaal hogere energiebehoefte voor onderhoudsdoeleinden dan was waargenomen onder de standaard laboratoriumcondities. In de eerste tien dagen van de retentostaatcultures onder deze industrieel relevante condities daalde de levensvatbaarheid bovendien naar 50 %, wat overeenkwam met een achtmaal hogere specifieke afstervingssnelheid dan onder standaard laboratoriumcondities werd gevonden. Zowel de verhoogde energiebehoefte voor onderhoudsdoeleinden als de toegenomen specifieke afstervingssnelheid zouden een negatieve invloed kunnen hebben op een grootschalig industrieel proces. Om de effecten van de lage pH en hoge CO_2 condities te ontleden, werden de effecten van deze condities apart en in combinatie geanalyseerd in chemostaatculturen bij dezelfde verdunningssnelheid. Deze experimenten toonden aan dat de lage pH de oorzaak was van de negatieve fysiologische effecten. Met behulp van ammonium-gelimiteerde retentostaatcultures, waarbij eveneens een verhoogde afstervingssnelheid en groei-onafhankelijke ATP-consumptiesnelheid werden waargenomen onder de industrieel relevante condities, werd geconcludeerd dat de glucose-limitatie in de eerdere experimenten niet van grote invloed was op de lage levensvatbaarheid en hoge onderhoudsbehoeften van de cultuur. Hoewel de fysiologische reacties op een lage pH en een lage pH gecombineerd met een hoog CO_2 niveau, grote overeenkomsten vertoonden, werden grote verschillen waargenomen in genoom-wijde genexpressieprofielen. Een mogelijke uitleg hiervoor is te vinden in de manier waarop *S. cerevisiae* de lage pH en hoge CO_2 niveaus signaleert en intracellulair doorstuurt: beide signalen kruisen door delen van de celwand-integriteits-route, de hoge-osmolariteit-glycerolroute en de calcineurin signaleringsroute.

De zeer negatieve effecten van een lage extracellulaire pH op de levensvatbaarheid van *S. cerevisiae* die werden beschreven in **Hoofdstuk 3**, lieten ruimte voor de verbetering van de lage-pH-tolerantie van *S. cerevisiae*. Op basis van het grote aantal processen zowel binnenin als buiten gistcellen waarbij protonen een rol spelen, is het niet verrassend dat er slechts een klein aantal genetische interventies bekend is dat leidt tot een verbetering van de lage-pH-tolerantie van *S. cerevisiae*. In **Hoofdstuk 4** werd een laboratoriumevolutie-experiment opgezet om *S. cerevisiae*-stammen te selecteren die tolerant waren geworden tegen een zeer lage extracellulaire pH. Terwijl de niet-geëvolueerde stam niet in staat was te groeien bij een pH van 2.5 en lager, konden de stammen die geïsoleerd waren aan het eind van het evolutie-experiment groeien bij een pH van 2.1 of zelfs bij 2.05. Deze lage-pH-tolerante stammen hadden mutaties opgelopen in genen gerelateerd aan calciumhomeostase, onderhoud van de celwand, de samenstelling van het celmembraan en eiwitreparatie en -hergebruik. Op basis van de introductie van deze mutaties in een niet-geëvolueerde stamachtergrond en op basis van terugkruisingsexperimenten werd duidelijk dat specifieke mutaties in de genen *PMR1*, *MUK1* en *MNN4* een belangrijke rol speelden in het lage-pH-tolerante

fenotype. Hoewel de volledige genetische complexiteit die ten grondslag ligt aan deze lage-pH-tolerantie niet volledig werd opgehelderd, leverden de resultaten in **Hoofdstuk 4** wel verder inzicht in mogelijkheden om lage-pH-tolerantie direct in te bouwen bij *S. cerevisiae*.

Het begrip van microbiële groei en stofwisseling is een centraal leerdoel in academische vakken over microbiële fysiologie en biotechnologie. Dit begrip is essentieel om microbiële ecologie, medisce microbiologie en industriële microbiologie, waaronder ook de resultaten in **Hoofdstuk 2**, **3** en **4** vallen, volledig te doorgronden. In **Hoofdstuk 5** wordt een computer-seminar gepresenteerd dat tot doel heeft om academisch onderwijs in de microbiële fysiologie te ondersteunen. Chemostaatcultivatie is een zeer bekende onderzoeksmethode om microbiële fysiologie te bestuderen, die de onderzoeker in staat stelt om een kwantitatieve analyse van groei en stofwisseling van micro-organismen uit te voeren onder nauwkeurig gedefinieerde kweekcondities. Een chemostaatcultuur waarin de specifieke groeisnelheid wordt gelimiteerd door het energie-substraat kan wiskundig worden beschreven door vier vergelijkingen: een massabalans voor substraat, een massabalans voor biomassa, de Pirt-vergelijking die de verdeling van substraat over groei en onderhoudsdoeleinden beschrijft en een Monod-type vergelijking die de relatie tussen de opnamesnelheid van substraat en de substraatconcentratie beschrijft. Deze concepten zijn al decennialang onderdeel van het biotechnologiecurriculum bij de TU Delft. Het abstractieniveau van de relevante vergelijkingen en een gebrek aan interactieve visualisatie bleken een beperkende factor voor het praktische begrip van kwantitatieve microbiologie van studenten bij het BSc-vak Microbiële Fysiologie.

De basis van het in **Hoofdstuk 5** beschreven educatieve seminar wordt gevormd door 'Chemostatus', een speciaal MATLAB-gebaseerd programma, gecombineerd met een set vraaggestuurde simulaties. Door het variëren van een of meerdere parameters in de bovengenoemde vergelijkingen, geven de simulaties aan studenten de mogelijkheid direct te visualiseren hoe de steady-state condities beïnvloed worden. Deze simulaties leveren daarmee een platform voor discussie met elkaar en met docenten. Introductie van dit seminar bleek te zorgen voor een verbeterd inzicht in de onderliggende mechanismen, aangezien de introductie van het seminar gepaard ging met een toename van de gemiddelde score van studenten bij tentamenvragen gerelateerd aan microbiële fysiologie. Gezien alle documenten voor dit seminar, evenals de software, beschikbaar zijn gesteld, kan het seminar direct worden toegepast in andere academische vakken over microbiële fysiologie en kan het Chemostatus-programma ook buiten de context van academisch onderwijs worden gebruikt door mensen die hun kennis van microbiële fysiologie willen testen en verbeteren.

Summary

In industrial biotechnology, micro-organisms are used for making a wide range of products, including neutraceuticals, transport fuels, pharmaceuticals and plastics. The raw materials for these microbial processes are often sugars derived from natural resources. Industrial biotechnology offers an advantage with respect to the petrochemical synthesis of these products with respect to its sustainability in CO_2 emissions.

Yeasts are important industrial workhorses in industrial biotechnology, as they are used for making many of the abovementioned products. Baker's yeast – *Saccharomyces cerevisiae* – is used for the large-scale production of, for example, bioethanol, farnesene, human insulin and succinic acid. To achieve cost-efficient production processes, the high-yield conversion of substrate (e.g. glucose) to the product of interest is essential. A possible approach to achieve this goal is to uncouple microbial product formation from growth. This approach is challenging since, during evolution, microbial metabolism has been optimized for the use of substrate for growth and maintenance of cellular integrity and viability.

For dissimilatory products, whose synthesis by micro-organisms results in the net production of ATP, such as ethanol for *S. cerevisiae*, uncoupling of growth and product formation has previously been investigated under anaerobic conditions. For non-dissimilatory products such as succinic acid, farnesene and proteins, a net input of ATP is required and their production is in direct competition with the use of ATP and energy substrate for growth and maintenance. High-yield production of non-dissimilatory products therefore requires a high energy efficiency in dissimilation. During fully respiratory growth of *S. cerevisiae*, the ATP yield from glucose dissimilation is eight-fold higher than during fermentative growth. Aerobic, respiratory dissimilation of glucose is therefore highly favorable for non-dissimilatory product formation.

Systematic characterization of yeasts can be performed under strictly controlled conditions in bioreactors. When bioreactors are operated as steady-state chemostat cultures, the specific growth rate is determined by the dilution rate, which is set by the experimenter. Chemostat cultivation therefore permits comparisons between strains and/or conditions independent of the specific growth rate. Due to technical limitations in the rate of medium supply, chemostat cultivation in bench-top laboratory bioreactors is practically not feasible at extremely low dilution rates ($< 0.015\ h^{-1}$). The retentostat, a modification of the chemostat in which 100

% biomass retention in the reactor is achieved by placing a filter in the outflow line, offers a suitable alternative for the investigation of such extremely low growth rates.

In **Chapter 2**, the physiology of virtually non-growing, fully aerobic, fully respiring *S. cerevisiae* retentostat cultures was characterized. This study focused on industrially relevant traits, such as culture viability, robustness and glycolytic capacity. For the design of the experiments, a predictive model was used to gradually reach a non-growing state of the culture. Over the course of 20 days, the culture was characterised during its transition from a specific growth rate of 0.025 h^{-1} to a specific growth rate below 0.001 h^{-1}. During this transition, culture viability remained above 80 %, while at the end of the culture nearly all substrate was used for cellular maintenance. The maintenance-energy requirements for ATP, calculated based on regression analysis of the biomass accumulation, were estimated to be 35 % lower than in corresponding anaerobic cultures. Although the substrate consumption rate was low during the transition of these cultures to near-zero growth rates, the glycolytic capacity remained high even after prolonged periods of extreme substrate limitation.

In **Chapter 2**, the transcript levels of *S. cerevisiae* genes involved in biosynthesis of sterols, lipids, amino acids and ribosomes were found to be down-regulated during a decrease in specific growth rate from 0.10 h^{-1} to near-zero growth rates. Conversely, genes involved in stress-responses were up-regulated during this transition. These observations largely corresponded to those found in a previous study on anaerobic retentostat cultures. A increased heat-shock tolerance at very low specific growth rates had been reported previously, but the level of tolerance observed in the aerobic retentostat cultures was unprecedented, even relative to that of cells in the stationary phase of an aerobic batch culture.

The beneficial traits of slow-growing cultures shown in **Chapter 2** were observed under standard laboratory conditions, which are not fully representative of the conditions in large-scale industrial processes. In **Chapter 3**, the same yeast strain as was used in **Chapter 2** was studied at near-zero growth rates under conditions relevant for the industrial production of succinic acid. These industrially relevant conditions, which encompassed a combination of a low culture pH (pH 3) and high levels of CO_2 (50 %), resulted in a two-fold increase of the maintenance-energy requirements relative to those observed under standard laboratory conditions in **Chapter 2**. Moreover, the culture viability dropped below 50 % during the first 10 days of retentostat cultivation, corresponding to an eight-fold higher specific death rate than under standard conditions. The higher maintenance-energy requirements as well as the higher specific cell death rate can negatively affect process performance at industrial scale. By dissecting the impact of low pH and high CO_2 in chemostat cultures grown at the same dilution rate, the low pH was identified as the cause of the detrimental physiological responses. Ammonium-limited retentostat

cultures yielded similar observations on specific death rates and growth-independent ATP consumption, indicating that glucose limitation was not a key factor for the reduced viability and increased maintenance-energy requirement. Although the physiological responses to low pH and low pH combined with high CO_2 showed strong similarities, genome-wide transcriptional responses to these conditions were vastly different. This might be explained by crosstalk between signalling pathways for low extracellular pH and high CO_2, which partially overlaps via the cell wall integrity, high-osmolarity glycerol and calcineurin signalling pathways.

The strong negative effects of a low extracellular pH on the viability of slow-growing *S. cerevisiae* cultures that were observed in **Chapter 3**, call for an improvement of the low-pH tolerance of *S. cerevisiae* for industrial applications. Since the proton concentrations inside and outside the cell affect many processes, it is not surprising that only a small number of genetic interventions is known to lead to improved low-pH tolerance. In **Chapter 4**, an adaptive laboratory evolution experiment was designed to select for *S. cerevisiae* strains tolerant to extremely low extracellular pH. Whereas the non-evolved reference strain could not grow at culture pH values of 2.5 and below, the evolved strains showed growth at a pH of 2.1 and even at pH 2.05. These low-pH tolerant strains were shown to have accrued mutations related to calcium homeostasis, cell wall maintenance, membrane composition and protein turnover. Specific mutations in the genes *PMR1*, *MUK1* and *MNN4* were shown to contribute to a low-pH tolerant phenotype by backcrossing experiments and by their expression in a non-evolved genetic background . Although the genetic complexity that underlies the low-pH tolerance of the evolved strains was not fully resolved, the results presented in **Chapter 4** provided important new targets for engineering low-pH tolerance in *S. cerevisiae*.

Understanding microbial growth and metabolism is a core learning goal in academic courses on microbial physiology and biotechnology and are essential to fully grasp microbial ecology, medical biotechnology and microbial biotechnology, including the results presented in the other **Chapter 2**, **3** and **4** of this thesis. **Chapter 5** presents a computer-assisted workshop for use in academic courses on microbial physiology. Chemostat cultivation is an important research tool to study microbial physiology and allows researchers to perform quantitative analyses of growth and metabolism under tightly controlled conditions. An energy-substrate-limited chemostat culture can be described mathematically by four equations: the mass balance for substrate, the mass balance for biomass, the Pirt equation describing the distribution of energy substrate over growth and maintenance purposes and a Monod-type equation describing the concentration-dependent specific consumption rate of the growth-limiting substrate.

While these concepts have been part of biotechnology curricula at the TU Delft for the past decades, the abstract nature of the mathematical equations and the lack of interactive visualization proved a limiting factor for the operative

understanding of chemostat cultivation by students. To overcome these educational challenges a workshop was based on a specially designed, MATLAB-based program ('Chemostatus') and a set of question-guided simulations. Varying one or multiple core parameters of the above mentioned equations in these simulations enables students to observe how steady-state conditions are affected and to discuss these observations with their peers and teachers to gain deeper, intuitive insight in the underlying mechanisms. The introduction of this workshop coincided with an increase in the average grade in exam questions related to quantitative microbial physiology. As all required documents for this computer workshop, as well as the Chemostatus software, are freely available, it can be directly implemented in other academic microbial physiology courses or can be used by others interested in microbial physiology and chemostat cultivation to test and improve their knowledge.

CHAPTER 1

General introduction

Biotechnology and a sustainable economy

The awareness of the detrimental effects of an anthropogenic disbalance in the carbon cycle due to the emission of CO_2 from fossil feedstocks has increased in recent years [328, 175]. Fossil resources have accumulated over millions of years deep in the earth as oil and coal. In recent centuries, their use for the production of fuels and chemicals has resulted in emissions of significant amounts of CO_2, at a much faster rate than that of the formation of fossil resources. Besides emission of CO_2 by the use of fossil resources as fuels for air, sea and road transportation, the manufacturing of many other day-to-day products (e.g. plastics) contributes to the production of CO_2. In 2017, the transport and manufacturing sectors accounted for over 42 % of the total global CO_2 emissions, while electricity and heat accounted for another 46 % [221]. Compared to emissions in 1990, the global CO_2 emissions in 2017 were 63 % higher and the accelerated emission of CO_2 has resulted in a rise in the atmospheric level of CO_2 [221]. This increased level correlates with a rise of the global temperature [297], which comes with far-stretching consequences for e.g. agriculture [358], a rising sea level [214] and human migration [4]. Meanwhile, in the 2015 Paris Agreement, nearly all countries in the world agreed on the reduction of CO_2 emissions to limit the effects of global warming [6]. To accommodate the increasing world population and the rise in average living standard [151, 103], while mitigating climate change, there is an urgent need for technological innovation aimed at reducing CO_2 emissions.

Industrial biotechnology largely relies on the microbial conversion of organic substrates (e.g. glucose or sugar rich agricultural waste streams) to products of interest. These include commodity chemicals, transportation fuels, flavors, fragrances, proteins and pharmaceuticals [94, 21, 336, 225, 180, 167, 350] whose extraction from natural resources is inefficient, or whose production in petrochemical processes lead to a net emission of CO_2. The microbial conversion of plant biomass to products does not by itself contribute to the anthropogenic disbalance in CO_2 emissions and products from such conversion processes can be used as transportation fuels, plastics and structural materials [140, 141]. At the same time other aspects of the industrial process, for example the transportation of raw materials, the required electricity to run the process or the product use and disposal, can result in the emission of CO_2, which is systematically assessed by Life Cycle Assessment [244, 135]. Advances in all technologies required for the production of bio-based materials require a collaborative effort of biotechnologists with colleagues working in other disciplines to address the most pressing societal threat of the century: climate change.

From substrate to product: Substrate used for growth, product formation and maintenance

In an ideal industrial biotechnological process, a microbe is a catalyst for the conversion of substrate to product. Microbial cells are however evolutionary hardwired to consume substrate for the purpose of survival and proliferation. A wide range of substrates is first converted into a small set of precursor molecules, from which all (macro)molecules essential for the formation of biomass can be produced (i.e. proteins, nucleic acids, lipids and carbohydrates). These macromolecules all contain carbon as structural element and are constructed in a plethora of intracellular chemical reactions. This structure of metabolism gives rise to the analogy of a bowtie [161, 226] (Figure 1.1A). In the first part of the bowtie, dissimilation, the complexity of substrates is reduced towards the above mentioned precursor molecules, which leads to a reduction of the Gibbs free energy. The released Gibbs energy is conserved in the form of the cellular energy moieties, ATP (Adenosine Tri-Phosphate). In the mirroring part of the bowtie, the precursor molecules are used for the construction of all macromolecules that make up microbial cells, in a set of reactions that are together referred to as assimilation. The Gibbs free energy increases in the formation of macromolecules from the precursor molecules in assimilation, which therefore requires a net input of ATP. The energy input required for the formation of biomass to a large extent depends on the macromolecular composition of biomass [298, 333, 176]. In addition, ATP is required for the quality control of the constructed macromolecules (e.g. proofreading of DNA, RNA or protein synthesis) [298]. In heterotrophic organisms growing on glucose, the overall formation of biomass requires glucose both as building block and as an energy source to supply the required ATP. To this latter end, glucose is consumed and converted into a dissimilatory product whose production results in the net conservation of energy in the form of ATP. To keep the conditions inside a cell optimal for the performance of catabolic and anabolic reactions, gradients of molecules across these membranes need to be maintained (m_{ATP}, Figure 1.1B). Other cellular processes that do not lead to formation of new biomass are the repair or replacement of macromolecules. These cellular processes require the input of cellular energy in the form of the 'energy currencies' ATP and/or transmembrane electrochemical gradients and, in many micro-organisms, are independent of whether a cell is proliferating [250]. For the applications of industrial biotechnology, microbial biomass itself is the product of only few industrial processes (e.g. the production of baker's yeast for baking applications and the production of fungal mycelium as a meat surrogate). Besides biomass itself, two classes of products can be described: products that are formed in catabolic reactions (dissimilatory products) and products that are produced by anabolic reactions (non-dissimilatory products). Synthesis of non-dissimilatory products from a substrate such as glucose requires a net input of cellular energy (ATP) and/or a net input of electrons via cellular redox carriers such as NADH and NADPH (Figure 1.1).

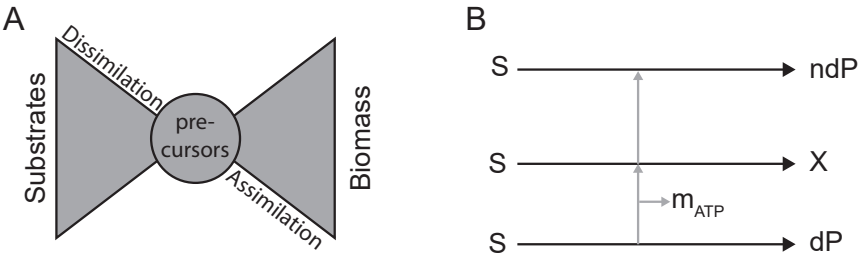

Figure 1.1: The structure of microbial metabolism in heterotrophs. A: Substrates are converted to central precursors in dissimilation and subsequently built up to the macromolecules that together make up biomass (proteins, lipids, nucleic acids, carbohydrates). B: Substrate (S), for instance glucose, is consumed for energetic and structural purposes in microbial metabolism. It is used as an energy source by its conversion into the dissimilatory product (dP), resulting in ATP (gray arrow) that can be used to assemble the macromolecules used for biomass (X) formation or for non-dissimilatory product formation (ndP). For both biomass formation as well as non-dissimilatory product formation substrate is also consumed as a building-block, indicated by black arrows.

To quantitatively evaluate the distribution of an energy substrate over growth and maintenance requirements in the absence of non-dissimilatory product formation, a mathematical description of substrate distribution was first proposed by S. John Pirt [250] in the Pirt equation (Equation 1.1). When, in a heterotrophic micro-organism, the limiting component in the medium is the (carbon- and) energy-source, and there is no production of non-dissimilatory products, the biomass-specific rate of substrate consumption (q_S, $mol_{substrate}\ g_{biomass}^{-1}\ h^{-1}$) is divided over growth (μ/Y_{XS}^{max}) and maintenance (m_S). In this equation μ denotes the specific growth rate (h^{-1}), and Y_{XS}^{max} the theoretical maximum yield of biomass on substrate ($g_{biomass}\ mol_{substrate}^{-1}$). This theoretical maximum yield of biomass on substrate is achieved in a virtual situation in which all of the substrate is used for biomass formation and substrate consumption for maintenance-energy requirements is therefore neglected. The maintenance-energy requirements (m_{ATP}; $mol_{substrate}g_{biomass}^{-1}\ h^{-1}$) are fulfilled by the dissimilation of the energy substrate and are dependent on the amount of ATP in this conversion (Y_{ATPS}, Equation 1.2). This linear relation between biomass specific substrate uptake rate (q_S) and the biomass specific growth rate (μ) allows to identify m_S when growth is zero and the slope of this relation is equal to $1/Y_{XS}^{max}$ (Figure 1.2A).

In the early days of quantitative microbial physiology research, Jacques Monod empirically described the relationship between specific growth rate and the substrate concentration (Equation 1.3) [217]. In this empirical relationship, the specific growth rate (μ) is dependent on the maximum specific growth rate (μ^{max}), the micro-organism's substrate-saturation constant for substrate (K_S) and the extracellular substrate concentration (C_S). The relationship known as the Monod equation (Equation 1.3) neglected maintenance-energy requirements. While this is

no problem when growth is limited by a substrate other than the energy substrate (and, therefore, m_S = 0), maintenance-energy requirements can constitute a large fraction of the overall consumption of an energy substrate during slow, energy-limited growth. To reconcile the Pirt equation and the Monod equation, the classical Monod-equation (Equation 1.3) requires an adaptation to an analogous equation describing the dependence of the biomass-specific substrate consumption rate (q_S) on the external substrate concentration (C_S; Equation 1.4). At the substrate-saturation constant (K_S), the specific substrate-uptake rate (q_S) is half of the maximum specific substrate-uptake rate (q_S^{max}) and at higher substrate concentrations the specific substrate-uptake rate approaches q_S^{max} (Figure 1.2B).

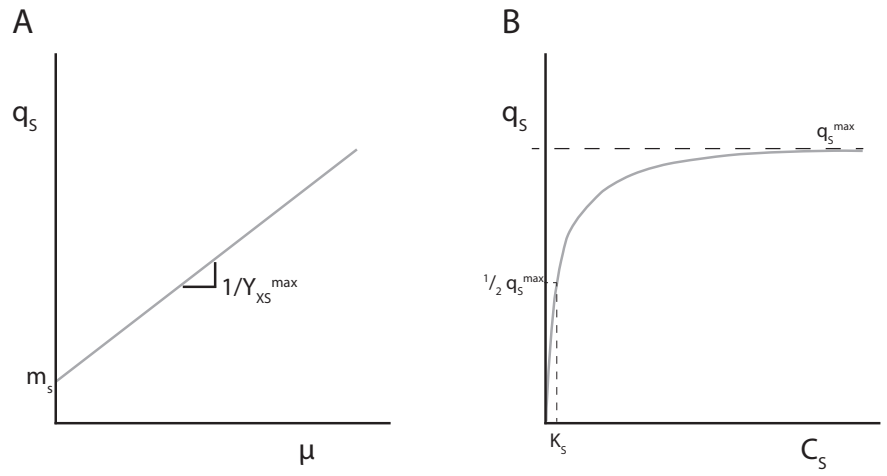

Figure 1.2: Key relations in quantitative microbial physiology A: The relation between the specific growth rate (μ) and the specific substrate uptake rate (q_S) based on the Pirt-equation (Equation 1.1). B: The relation between the extracellular substrate concentration (C_S) and the specific substrate uptake rate (q_S), based on Monod-type kinetics (Equation 1.4)

$$q_S = \frac{\mu}{Y_{XS}^{max}} + m_S \tag{1.1}$$

$$m_S = m_{ATP} Y_{ATP/S} \tag{1.2}$$

$$\mu = \mu^{max} \frac{C_S}{K_S + C_S} \tag{1.3}$$

$$q_S = q_S^{max} \frac{C_S}{K_S + C_S} \tag{1.4}$$

For the biosynthesis of non-dissimilatory products, the Pirt equation requires an extension for the distribution of substrate over growth, cellular maintenance processes and product formation (Equation 1.5). In analogy to biomass formation, formation of a non-dissimilatory product requires the consumption of substrate to provide the building block(s) for synthesis of the product, and simultaneous consumption of substrate to provide the free energy required for the synthesis of the product. The biomass specific rate of product formation is denoted by q_P, while the Y_{PS}^{max} is the maximum theoretical product yield in the absence of maintenance and growth.

$$q_S = \frac{\mu}{Y_{XS}^{max}} + \frac{q_P}{Y_{PS}^{max}} + m_S \tag{1.5}$$

The production rate q_P cannot yet be theoretically predicted, and hence empirical relations between growth and product formation – $q_P(\mu)$-relations – have to be experimentally derived for each combination of product, micro-organism and physicochemical process conditions. For some products a linear positive correlation of product formation and growth was observed, such as in the case of resveratrol-production by *S. cerevisiae* [339] (Figure 1.3A). Although for these products the biomass specific production rate (q_P) is highest at the maximum growth rate, the concomitant formation of biomass results in a suboptimal yield of product on substrate. Other $q_P(\mu)$-relations have also been observed, that for instance leading to a distinct q_P-optimum at a low specific growth rate or even a negative correlation between specific growth rate and product formation, as observed for the production of melanin in *Aspergillus nidulans* [272] and the production of penicillin with *Penicillium chrysogenum* [253]. Even for two different proteins, amylase and the human insulin precursor, that were heterologously produced in the same *S. cerevisiae* strain background and that share key intracellular processes required for production, the $q_P(\mu)$-relation was found to be quite different when produced in the same *S. cerevisiae* strain background [192]. For each of these types of $q_P(\mu)$-relations, the maximum theoretical product yield is achieved in the absence of growth and the absence of substrate consumption for cellular maintenance processes (Figure 1.3).

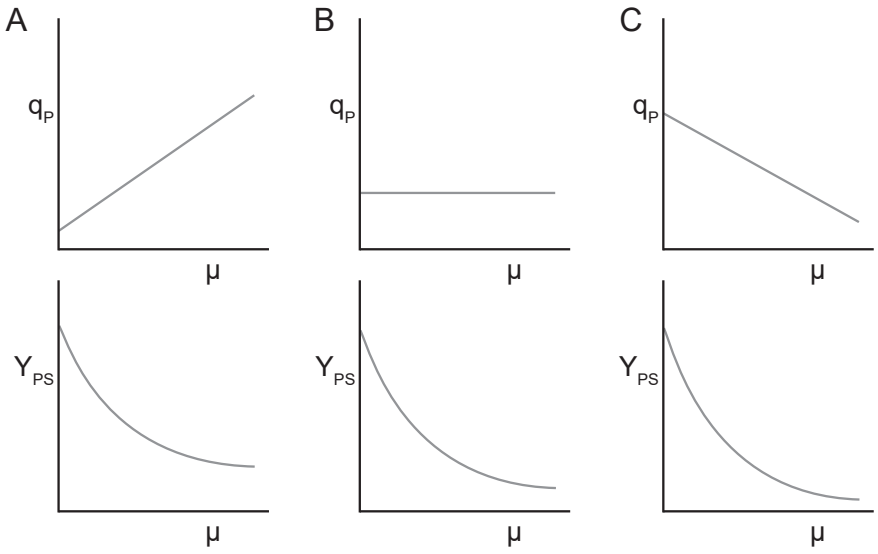

Figure 1.3: Various relations between the specific product formation rate for non-dissimilatory products (q_P) and the growth rate (μ) (top row). A: a positive correlation between q_P and μ, for example resveratrol-production by an engineered *Saccharomyces cerevisiae* background [339], B: Constant production of Penicillin by *Penicillium chrysogenum* [253] at any of the tested growth rates. C: hypothetical negative relation between q_P and μ. Other (non-linear) relations are possible, see for example human serum albumin production by *Pichia pastoris* [259]. The corresponding yield of product on substrate for the q_P(μ)-relations in the top row (bottom row) is highest growth is minimized.

Titer, Rate and Yield determine the efficiency of an industrial biotechnological process

The economic performance of processes in industrial biotechnology is of great importance, and is determined by the capital investments, the costs to run the process and the earnings of selling the product. For bulk products, financial margins are generally small and the economic feasibility is at stake at each stage of the industrial process. Three process parameters are determinants for the economic feasibility of an industrial process: titer, rate and yield (TRY) [123]. At a high titer, the product purification in downstream processing is facilitated. At a high rate of product formation, the capital expenses, i.e. the costs for the construction of the factory, can be reduced as unit operations can be scaled down. The costs for substrate are a significant contributor to the costs of the biotechnological production of bulk chemicals[148]. In such processes, a high yield of product on substrate, requiring efficient conversion and low by-product formation, is a prerequisite for process economics. Each step in the process upstream or downstream of the fermentation can lead to losses of the substrate or product,

which decreases the overall yield of the whole process, highlighting the necessity of efficient microbial production. Besides titer, rate and yield, also the purity of the product, the robustness of the microbe and process towards external perturbations are determining factors for the success of the large scale manufacturing of bulk products [123, 156].

Workhorses in industrial biotechnology

The industrial biotechnology sector has historically relied on a relatively small number of microbial species – the so-called industrial workhorses. These were chosen for practical reasons such as ease of cultivation, ease of characterization, genetic accessibility or their natural ability to produce a product of interest. Bacteria (e.g. *Escherichia coli*, *Bacillus subtilis*, *Corynebacterium glutamicum*), yeasts (e.g. *Saccharomyces cerevisiae*, *Pichia pastoris*, *Ogataea parapolymorpha*, *Yarrowia lipolytica*) and filamentous fungi (e.g. *Penicillium chrysogenum*, *Aspergillus niger*, *Trichoderma reesei*) have all been used in large-scale industrial processes (e.g. [178, 89, 164, 270, 111, 51]). In these industrial-scale processes, the size of the bioreactors can range from 1 000 to 2 000 000 liters [60]. Academic and industrial research was for a long time largely based on the native production of a compound by a micro-organism isolated from nature, which was subsequently further improved through cycles of random mutagenesis and screening for improved production, a process that is nowadays referred to as 'classical strain improvement'. For example, the antibiotic penicillin is produced by *P. chrysogenum* at low levels. Over the last decades, improvements in production by multiple orders of magnitude [315, 317] have been achieved by classical strain improvement. Intensive classical strain improvement of *A. niger* for citric acid production [288] and of *C. glutamicum* for production of the amino acids glutamate and lysine [178] have likewise led to optimized industrial processes.

Applications of the industrial workhorse *S. cerevisiae*

The unicellular budding yeast *S. cerevisiae* has an especially long track record of applications by mankind in wine, beer and bread making [189, 181], for which it has the Generally Regarded As Safe (GRAS) status from the United States Food and Drug Administration. The applications of *S. cerevisiae* have been extended to bioethanol production as a biofuel, at a market size of 100 billion liters in 2016 [216]. The intensification of the production of beer, bread and bioethanol has been based on extensive experimental studies of this yeast and has selected for strains that are robust to the conditions in these large industrial processes [14, 227, 120, 79, 323].

In 1996, the sequencing of the genome of *S. cerevisiae* gave access to all 6000 genes encoded on its 16 chromosomes [122] and was a major inspiration for the development of genome-wide analysis tools. Genetic engineering of this yeast is particularly easy due to its efficient use of homologous recombination of DNA [262, 170], that allows the efficient and targeted integration of heterologous DNA. The development of tools for genetic engineering for this yeast have rapidly progressed in recent years by the application of the bacterial defense mechanism CRISPR/Cas9 [82, 204], which allows fast, simultaneous and efficient alteration, deletion or introduction of multiple DNA sequences in *S. cerevisiae*.

The introduction of heterologous DNA sequences allows researchers to alter the properties of *S. cerevisiae* for the improvement of industrial processes. Relevant modifications include the expansion of substrate range, improvement of robustness towards stress conditions and introducing the capability of non-native product formation and improving product yield and productivity. Strain engineering is based on the Design-Build-Test-Learn (DBTL) cycle (Figure 1.4), in which the advances in CRISPR/Cas9-mediated genetic engineering have strongly accelerated the build phase. For example, it is nowadays possible to simultaneously modify six or even eight loci, including introduction of heterologous genes, deletion native genes and alterations of other genes in a single transformation step [204, 357, 5], a process that, before the advent of CRISPR/Cas9 techniques, would have required at least six consecutive transformations. Technical advances in DNA synthesis and DNA sequencing have reduced their costs and have significantly advanced the use of *S. cerevisiae* as industrial workhorse and contributed to further acceleration of the Build and Test phases (Figure 1.4). The advances in analytic tools and strain characterization allow for the automation of strain design [205, 289] and the integration of data interpretation gives rise to a change from classical manual laboratory work to 'biofoundries', in which robot-mediated automation of laboratory work increases the throughput of work in strain construction and testing and eliminates human error. The resulting vast increase in data generation and the requirements for its interpretation are in part solved by using machine learning and artificial intelligence to go through subsequent cycles of the DBTL-cycle [237, 76]. To show the capabilities and pitfalls of such biofoundries, a recent study performed a 'pressure test' to produce ten non-native products within 90 days in a variety of microbial hosts, one of these being *S. cerevisiae*, and cell free systems [42]. Although this challenging goal was not fully met, the successful proof of production of six out of the ten products is a powerful illustration the potential of this fast developing field.

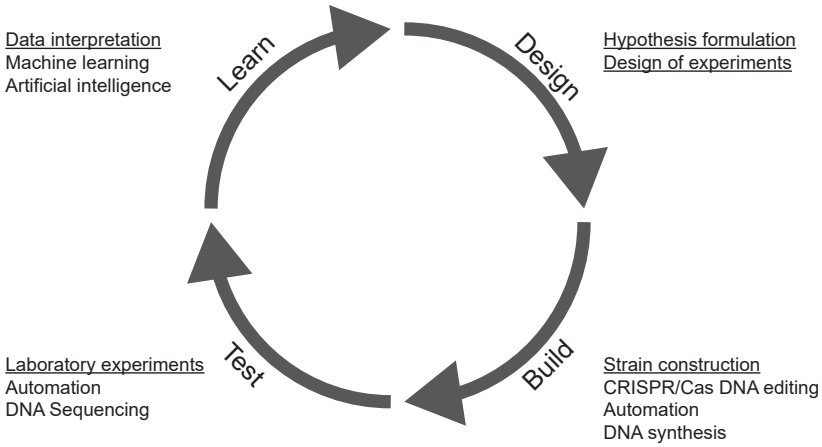

Figure 1.4: The Design-Build-Test-Learn cycle for industrial biotechnology. The iterative process of improvements starts with the formulation of an hypothesis and the design of the experiments to test this hypothesis. Underlined are the core tasks in each phase for metabolic engineering. Recent revolutionizing developments are indicated for each phase and are reviewed by [237].

Expanding the substrate and product ranges of *S. cerevisiae* for industrial applications

The use of agricultural residues (e.g. the stalks and leaves of corn or sugar cane bagasse) is beneficial compared to using only glucose as substrate, as these residues are not used for human consumption. These residues primarily consist of cellulose, hemicellulose and lignin. Although the lignin consists of hardly accessible aromatic compounds, the cellulose and hemicellulose can be treated to release glucose and a mix of mainly xylose and arabinose respectively [323]. Considerable efforts have been made to enable *S. cerevisiae* to convert xylose, arabinose and galacturonic acid, substrates that cannot be used by wild-type strains (e.g. [148, 26, 172, 347]). Efficient conversion of xylose and arabinose was enabled by the introduction of non-native (heterologous) genes [172, 347] and by the overexpression and deletion of native genes [148, 335]. As another example, the consumption of glycerol, a by-product in the classical bio-ethanol production or a compound that can be extracted from materials rich in oils and fats, is energetically favorable compared to the consumption of glucose for certain products. The improvement of glycerol consumption by *S. cerevisiae* has been achieved by expression of non-native genes and gene deletion [162, 352]. Lastly, engineering of the metabolism of natively consumed substrates such as galactose [179] or sucrose [207] aims for the use of abundantly available substrates other than glucose and enabling improved product yields [18, 206]. In many studies on the expansion of substrate range and acceleration of native substrate-consumption evolutionary engineering was successfully applied [348, 335, 142], both for direct strain improvement and the subsequent identification of causal mutations.

The expansion of the product range of *S. cerevisiae* far exceeds the expansion of the substrate spectrum in number of compounds addressed [158]. Heterologous products made by *S. cerevisiae* range from pharmaceuticals (e.g. human insulin [160, 343], taxol [77], artimisinic acid [265], opioids [114]), flavor compounds, neutraceuticals and other food additives (e.g. vanillin [131], resveratrol [339, 19], naringenin [166]), building blocks for polymer synthesis (e.g. lactic acid, succinic acid [20, 308, 238, 150], 1,3-propanediol [224] and ethylene [152]) and fuels (e.g. farnesene as a fuel precursor [274] and butanol [295]) and are reviewed by many others (e.g. [187, 169, 236, 109, 21, 227]). Some of these products (e.g. succinic acid, resveratrol, farnesene and human insulin) are produced on a large industrial scale. For many other products, academic literature shows proof of production by *S. cerevisiae*, but the optimization of Titer, Rate and Yield remains an outstanding challenge.

Optimized substrate dissimilation for product formation

The baker's yeast *S. cerevisiae* is well known for two dissimilatory products that lie at the basis of its classical applications in bread, beer and wine production: ethanol and CO_2. Under anaerobic conditions, fermentation of a mole of glucose via the Embden-Meyerhoff glycolysis results in 2 moles of pyruvate, yielding 2 moles of ATP per mol of consumed glucose (Figure 1.5). The 2 moles of NADH produced in this pathway are re-oxidized via the conversion of pyruvate to ethanol and CO_2.

Under fully aerobic conditions, two modes of catabolism are possible. At a low rate of glucose consumption, the catabolism of *S. cerevisiae* is fully respiratory, with CO_2 and water as the sole dissimilatory end products and yielding 16 ATP per glucose (more below). In the Crabtree-positive yeast *S. cerevisiae*, catabolism at high glucose consumption rates is performed by a mix of the two above mentioned mechanisms, a phenomenon known as the 'Crabtree effect' [70, 257]. The production of *S. cerevisiae* biomass for the baking industry, a process requiring large ATP-investments, is most optimally performed under fully respiratory conditions, for which the eight-fold higher yield of ATP on substrate in dissimilation compared to fermentative conditions (16 vs 2 ATP per glucose respectively, Figure 1.5), results in a high biomass yield on substrate [246]. Most of the non-native products mentioned above are non-dissimilatory products, and hence require the net input of ATP and redox-equivalents. Similarly, a higher maximum yield of non-dissimilatory product formation can be achieved under aerobic fully respiratory conditions instead of anaerobic conditions.

Optimal energy conservation under aerobic conditions requires the full respiration of substrate. At a P/O ratio of 1.0 (see legend to Figure 1.5), respiratory glucose dissimilation by *S. cerevisiae* yields 16 ATP per glucose: 4 ATP from substrate-level

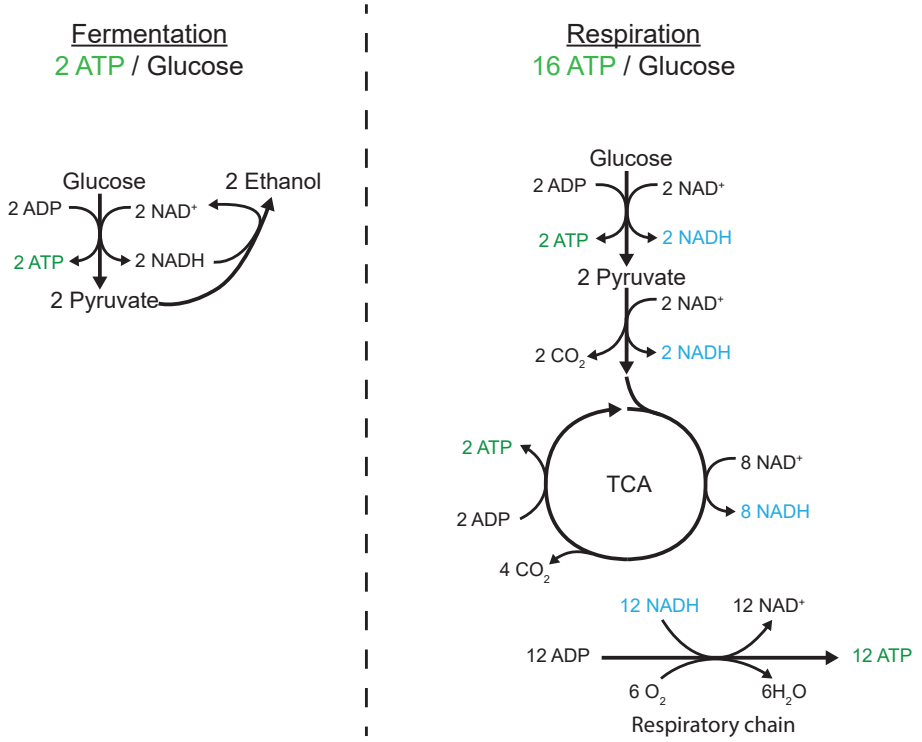

Figure 1.5: Intracellular dissimilation of glucose by *S. cerevisiae* can occur by two modes to generate ATP. Fermentation of glucose to ethanol occurs under anaerobic conditions, in which case glucose is converted via the Embden-Meyerhof glycolysis into two pyruvate. This results in the generation of 2 ATP per glucose via substrate level phosphorylation and 2 NADH. NADH is the electron carrier in dissimilation. In the absence of an external electron acceptor, pyruvate is converted into ethanol and CO_2, thereby regenerating the 2 NADH. Under full respiration glucose is converted via the Embden-Meyerhoff glycolysis into two pyruvate, forming 2 ATP per glucose and 2 NADH. The two pyruvate are further converted to Acetyl-CoA and submitted to the tricarboxylic acid (TCA) cycle. In total this results in the formation of 2 more GTP via substrate level phosphorylation (for the purpose of visualisation depicted as ATP), 6 CO_2 and 10 more NADH. The electrons transferred to 2 $FADH_2$ are depicted as 2 NADH for the purpose of visualisation. The 12 NADH, holding all electrons initially available in glucose, are reoxidized in the respiratory chain, where the electrons are accepted by 6 oxygen molecules, to form 6 H_2O. The efficiency of the respiratory chain is determined by the P/O ratio, the number of ATP generated per atom of oxygen, which is estimated in *S. cerevisiae* to be 1.0 for NADH as well as for $FADH_2$ [333].

phosphorylation and 12 ATP that are generated by oxidative phosphorylation in the mitochondria. The 24 available electrons from glucose are transferred to 10 NADH and 2 $FADH_2$ in the reactions in the Embden-Meyerhof glycolysis and the tricarboxylic acid (TCA) cycle (Figure 1.4). The respiratory chain is located in the inner mitochondrial membrane and, in canonical electron transport chains, consists of a set of five proteins that form complexes (in *S. cerevisiae* named alternative NADH-dehydrogenase and Complex II-V). In the first four steps going from the NADH-dehyrogenase or Complex II to Complex IV, the electrons from NADH and $FADH_2$ are transferred to oxygen (O_2). This electron transfer is coupled to the

translocation of protons over the intermitochondrial membrane. The fifth complex of the respiratory chain harvests this potential energy of the resulting chemi-osmotic proton gradient by coupling the influx of protons to the formation of ATP from ADP and inorganic phosphate (Pi) (Figure 1.5).

In *S. cerevisiae* the respiratory chain for oxidation of intramitochondrial NADH starts with the NADH dehydrogenase Ndi1, which is located on the inside of the inner mitochondrial membrane. In contrast to the Complex I-type NADH dehydrogenase complexes found in many other eukaryotes, Ndi1 does not translocate protons upon accepting the electrons from NADH, but transfers instead electrons to Complex III via ubiquinone. Similarly, cytosolic NADH can be reoxidized by Nde1 and Nde2, which perform the same reaction as Ndi1, but are located at the outer side of the inner mitochondrial membrane. At Complex II succinate is converted to fumarate, a reaction involved in the tricarboxylic acid cycle, and which transfers electrons to Complex III via $FADH_2$ and ubiquinone. In Complex III the electrons are then transferred to cytochrome c and 2 protons are transported. Lastly the electrons are transferred from cytochrome c to the final electron acceptor O_2 at Complex IV, resulting in the additional translocation of 4 protons (Figure 1.6). The influx of protons at Complex V, the mitochondrial F1-F0 ATPase complex, is stoichiometrically coupled to the formation of ATP.

The efficiency of ATP-generation is determined by the concerted action of the respiratory chain complexes and is described by the P/O-ratio: the ratio between ATP-generation and electrons transferred to oxygen. The proton gradient that is generated by the first four complexes of a respiratory chain cannot be fully used for ATP-generation, as the proton gradient is used for transport of proteins and small molecules into the mitochondria [171], due to proton leakage and proton slip of the ATP-synthase (Complex V) [128, 222] or due to the incomplete electron transfer in the respiratory chain that results in the formation of reactive oxygen species [312].

In all known aerobically growing yeasts species, Complex II – V are conserved, while there is variation in the configuration of the protein complexes involved in accepting electrons from NADH. In contrast to *S. cerevisiae*, other yeast species, e.g. *Yarrowia lipolytica*, *Komagataella phaffi* (*Pichia pastoris*), *Ogataea parapolymorpha* (*Hansenula parapolymorpha*), harbor a large multi-subunit protein complex (Complex I) that couples the transfer of electrons from NADH to Complex III to the translocation of 4 protons (Figure 1.6). As activity of a Complex I protein complex results in a larger number of protons being translocated across the mitochondrial membrane than is possible in *S. cerevisiae*, its presence in non-*Saccharomyces* yeasts could increase the number of ATP molecules generated at Complex V.

In the absence of non-dissimilatory product formation, the ATP is consumed for the purpose of growth and maintenance-energy requirements. Therefore, when more protons are transported in the respiratory chain, resulting in an increase in the ATP yield on substrate (Y_{ATPS}), this should coincide with an increase in the theoretical maximum biomass yield of biomass (Y_{XS}^{max}) or non-dissimilatory product (Y_{PS}^{max}), as the consumption of substrate as an energy source for biomass or non-dissimilatory product formation is reduced. Under the assumption that the maintenance-energy requirements (m_{ATP}) and biomass composition are not significantly affected by a change in the composition of the respiratory chain, the biomass yield of yeast strains using a proton-translocating NADH-reductase could be higher than for yeasts using a NADH-dehydrogenase as the entry point of the respiratory chain that does not translocate protons.

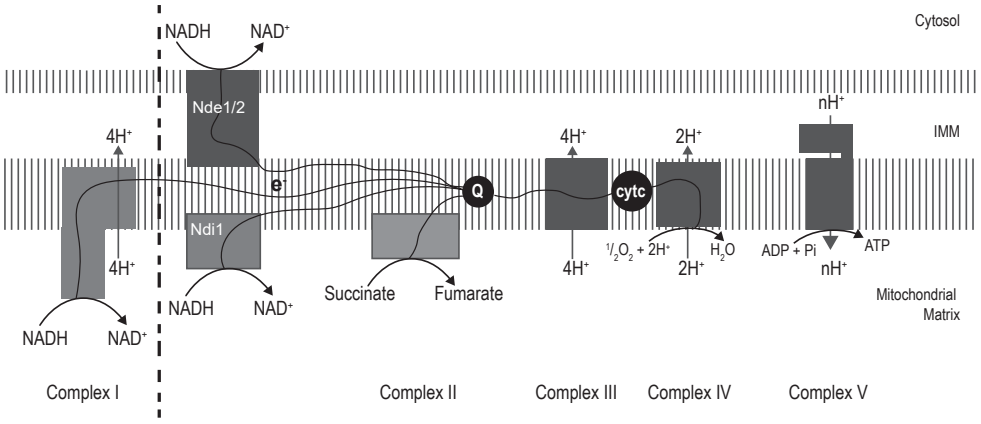

Figure 1.6: The respiratory chain in yeasts. In *S. cerevisiae* the site of NADH dehydrogenase activity is performed by the non-proton-translocating Ndi1 for NADH from the mitochondrial matrix and Nde1 and Nde2 for cytosolic NADH. Other yeast species such as *P. pastoris* or *O. parapolymorpha* have a proton-translocating Complex I (NADH dehydrogenase) with a stoichiometry of 4 protons (H^+) per NADH. The exact orientation of the alternative NADH dehydrogenases (Ndi1, Nde1 and Nde2 in *S. cerevisiae*) towards the mitochondrial matrix or the cytosol is unknown. The electrons are transferred to ubiquinone (Q) in the inner mitochondrial membrane. Complex II (succinate dehydrogenase) is part of the tricarboxylic acid cycle. The electrons transferred from succinate reach ubiquinone via $FADH_2$. Ubiquinone transfers the electrons to Complex III (cytochrome bc1 complex), which couples the transfer of electrons to cytochrome c (cyt c) in the inner mitochondrial membrane to the transport of 4 protons. The electrons from cytochrome c are transferred to oxygen in complex IV (cytochrome c oxidase), resulting in the export of 2 protons. The proton gradient across the inner mitochondrial membrane generated by the concerted action of Complex I-IV is used by Complex V (ATP synthase) for the formation of ATP from ADP and Pi (inorganic phosphate).

Quantitative physiology of *S. cerevisiae* for industrial applications

In large-scale microbial manufacturing processes, the large size of bioreactors results in imperfect mixing and inhomogeneity of the process. These variations in substrate or oxygen availability, temperature and pH give rise to heterogeneity in the cell population [106, 37, 136] and can each have negative effects on the process performance [177, 134]. As robustness of industrial workhorses to such perturbations is of great importance for the overall process performance, the understanding of the physiological responses under these conditions is intensively studied at a laboratory scale [60].

Experimental approaches for the study of quantitative physiology

Experimental tools for the characterization of unicellular micro-organisms such as *S. cerevisiae* vary in size and in the control of physicochemical conditions (e.g. temperature, pH or substrate feeding regimes). Classically batch cultures, in which all nutrients are available in excess and the micro-organism can grow at its maximum growth rate, were used for the characterization of microbes. The experimental set-ups in which such characterizations can be performed include, but are not limited to, microtiter plates, shake flasks and bioreactors. Downscaling of the culture size to shake flasks or microtiter plates facilitates experimentation, especially when many experiments are performed in parallel. The advantage of the use of bioreactors for strain characterization is the larger number of parameters that can be controlled. For example, in bioreactors the pH of a culture can be strictly controlled by online-analysis and feedback-control by the automated addition of base or acid solutions and the transfer of oxygen is strongly enhanced by sparging of air through the medium and due to stirring of the culture. Contrarily, gas transfer in shake-flask cultures and microtiter plates is notoriously poor and other than the addition of buffers for pH control, adequate control is not possible.

To study the substrate consumption and distribution over growth, product formation and maintenance-energy requirements, the specific growth rate (μ) is a key experimental variable. The linear relation between the growth rate and the consumption rate of the energy substrate (the Pirt equation, Equation 1.1) dictates that a decrease in substrate supply should result in a decrease in the growth rate. This reduction of substrate supply can be achieved in bioreactors by selectively feeding fresh medium with a limiting nutrient (e.g. the carbon- and energy source). Prolonged control of the growth rate in a bioreactor can be achieved by continuously limiting the substrate supply by the inflowing medium and the withdrawal of spent medium in a 'chemostat' [229]. In the almost seventy years since the introduction of this experimental tool it has been used for a wide variety of purposes. First, the chemostat was used as a method for studying microbial selection and competition [230], based on the natural occurrence of mutations in growing populations. Prolonged cultivation under nutrient-limiting conditions allowed for the enrichment

of beneficial spontaneous mutations in cell populations, which would outcompete the original population [84]. When the advantages and limitations of prolonged chemostat cultures were known, it was also used for limited time periods for the characterization of microbial physiology and systems biology [35, 66, 144].

The behavior of a chemostat culture can be expressed mathematically by mass balances for biomass and substrate. The substrate is supplied to the bioreactor by the (liquid) inflow and is then either consumed in the bioreactor by the biomass or removed from the bioreactor by means of the outflow (Equation 1.6). The biomass is produced in the bioreactor by the biomass through the conversion of substrate and removed with the broth by means of the outflow of the bioreactor (Equation 1.7).The two mass balances are connected through the Monod- and Pirt-equations (Equations 1.1 & 1.4).

$$\frac{dC_S}{dt} = F_{in}C_{S,in} - F_{out}C_{S,out} - q_S C_X V_L \tag{1.6}$$

$$\frac{dC_X}{dt} = -F_{out}C_{X,out} + \mu C_X V_L \tag{1.7}$$

Due to the continuous feeding of substrate, nutrient-limiting growth of biomass and the continuous removal of biomass and residual substrate, the conversion rates in a chemostat eventually become constant. This situation in which also in- and outflows, the volume of the culture and all other physicochemical parameters are constant, is called a steady state. In ideally mixed steady-state cultures, the accumulation of substrate and biomass (dC_S/dt and dC_X/dt respectively) both equal zero, and the specific growth rate of the micro-organism during this state is equal to the dilution rate – defined as the outflow of the reactor divided by the volume of the reactor ($D = F_{out}/V_L$). Characterization of *S. cerevisiae* cultures that are in steady state at the same dilution rate then allows for the analysis of responses to only one parameter, e.g. the studied strain, or variations in (limiting) nutrients [303, 68, 30], products or physicochemical conditions [1, 339, 152, 173, 345, 264, 8]. The biomass yield and – when applicable – the product yield of a strain grown in chemostat cultures at steady state is a direct read-out of the substrate and energy-distribution of the strain over growth, product formation and maintenance-energy requirements [339, 173, 72, 2] when the specific growth rate is imposed by the chosen dilution rate. The specific growth rate can be varied in chemostat cultures by growing a set of steady-state cultures at a range of different dilution rates, which allows for accurate estimation of the maintenance-energy requirements and the maximum biomass yield ($Y_{X/S}^{max}$) [306].

The specific growth rate, nutrient availability and other physicochemical conditions in chemostat cultures play an important role in the regulation of cell homeostasis. For growth *S. cerevisiae* goes through the cell cycle (Figure 1.7A). The sensing of

the extracellular environment in *S. cerevisiae* involves signaling pathways, in which several proteins orchestrate the coupling of sensing to transcriptional responses. The residual glucose concentration, which is usually low in glucose-limited chemostat cultures, is sensed via a signaling pathway of PKA, TORC1 and Sch9, all inactivating Rim15 in the presence of high glucose concentrations [59, 275]. While these signaling pathways are to date not fully elucidated, it has been shown that the protein kinase Rim15 activates the transcription factors Msn2/4 and Gis1, both targeting stress-inducible genes and genes required for the adaptation and survival to the glucose starvation [290] (Figure 1.7B). Similarly, the concentration of the preferred nitrogen source ammonium is sensed via TORC1 and Sch9 [59], again integrating the nutrient signals via Rim15. The strong limitation of nutrients in chemostat cultures indeed elicits the expression of the robustness genes under the control of Rim15, and their expression inversely correlates with the growth rate [260] while it positively correlates with the the physiological stress tolerance of these yeast cultures [355, 194, 119]. Besides the sensing of nutrient availability, environmental stress conditions such as heat, oxidative agents or high osmotic pressure and the sensing of the integrity of the cell wall [14, 117, 116, 50] overlap with the responses to nutrient depletion and limitation [115, 260] (Figure 1.7B). These complex, intertwined signaling networks triggered by environmental cues are tightly coordinated to optimize the survival of the organism. Several of the stress-responsive sensing pathways are shown to block progression of the cell cycle [101] (Figure 1.7A). in the absence of nutrients (e.g. glucose), *S. cerevisiae* can leave the active cell cycle and reside in a vegitative 'G0' state [344, 110] (Figure 1.7A). In cases where cell survival cannot be ensured, the eukaryotic organism *S. cerevisiae* is able to commit to a programmed cell death program [199, 40], a highly regulated process that is aimed at degradation of damaged cells from the population. In extreme stress conditions, or for stresses that *S. cerevisiae* is not able to sense, cell death can be established by a seemingly non-regulated loss of membrane integrity [349, 93].

Retentostat cultures: analysis of near-zero growth rates

Although uncoupling of growth and product formation is industrially desirable unless biomass is the intended product, and slow growth elicits stress tolerance in *S. cerevisiae* [194, 24], there are practical limitations to the lowest dilution rates at with a chemostat can be operated. When the feed rate of a chemostat is too low, the otherwise continuous supply of substrate is changed into a feed-famine regime, with short pulses of substrate availability alternating with the absence of substrate in the system, which elicits different physiological effects than continuous feeding [27, 299]. To circumvent this limitation of chemostat cultures and explore the scientific terra incognita of growth rates below 0.015 h^{-1}, the retentostat was designed as a dedicated continuous cultivation device. The retentostat is a modification of the chemostat in which the outflow port is equipped with full biomass retention device (e.g. a filter). This experimental set-up was first proposed

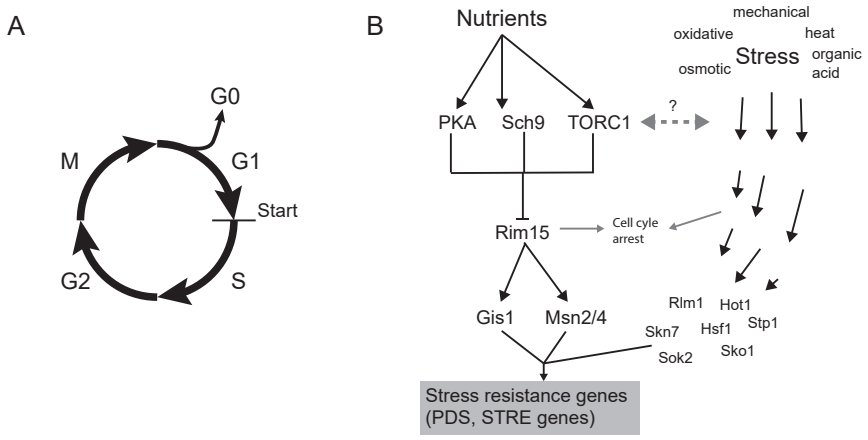

Figure 1.7: Regulation of growth and stress responses. A: The cell cycle in *S. cerevisiae*. Cells in the active cell cycle go through G1 and after passing Start are committed to complete the Synthesis (S), G2 and Mitosis (M) phases. Cells can leave the active cell cycle in the absence of nutrients and be in a vegetative state, the 'G0' state [344, 110]. B: Signaling pathways that regulate nutrient or stress responses. In the presence of nutrients, PKA and TORC1 are activated, while TORC1 activates Sch9. PKA, TORC1 and Sch9 all inhibit Rim15 [59, 275]. in the absence of nutrients, the inhibition of Rim15 by PKA, TORC1 and Sch9 is lost, upon which the stress inducible genes and stationary phase genes are activated via the transcription factors Msn2/4 and Gis1 respectively. The stress responses to osmotic, oxidative, mechanical, heat and organic acid stresses are sensed via multi-protein signaling pathways (e.g. the Cell Wall Integrity (CWI), High-Osmolarity Glycerol (HOG)), each resulting in the activation of a subset of transcription factors (e.g. Rlm1, Hot1, Stp1, skn7, Hsf1, Sok2 or Sko1) regulating the stress response [301, 14, 118, 117, 219]. There is (extensive) cross-talk between these stress-signaling pathways (e.g. [267]). Further cross-talk between the nutrient sensing pathways and stress signaling pathways (e.g. [80]) is aimed at the concerted regulation of homeostasis and regulation of the cell cycle. Figure adapted from [25].

by Chesbro *et al.* [54] and, just like in a chemostat, is based on a constant inflow of fresh medium to supply a growth-limiting energy substrate to the culture. The outflow of this culture is filtered and all biomass is retained in the bioreactor, and therefore the biomass balance does not include a factor describing the outflow (Equation 1.8). This cell retention results in a progressive increase of the biomass concentration (C_X) in the bioreactor (Figure 1.8A). As, consequently, the supplied substrate has to be distributed over an ever larger amount of biomass, the specific substrate uptake rate (q_S) decreases until it reaches the rate at which it is just enough to fulfill the maintenance-energy requirements (Figure 1.8B, m_S). In this situation, the specific growth rate (μ) approximates zero (Figure 1.8C). This gradual decline of the specific growth rate to near-zero values makes the retentostat an ideal experimental set-up to determine the maintenance-energy requirements of a micro-organism. The production of protease by *Bacillus licheniformis* has been investigated in retentostat cultures for prolonged periods of time [327]. This study identified a linear correlation between specific product formation and specific growth rates, but its formation was stopped after prolonged cultivation and the supplied

substrate was used for biosynthetic and maintenance purposes. Modeling of these results led to the conclusion that the determining factor for product formation in the absence of growth is the magnitude of the substrate consumption for maintenance purposes.

$$\frac{dC_X}{dt} = \mu C_X V_L \tag{1.8}$$

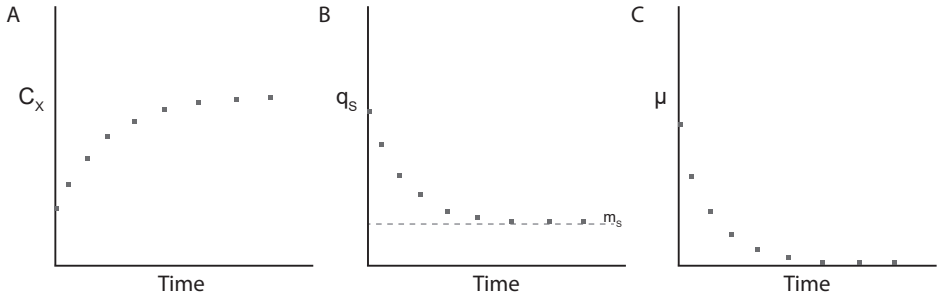

Figure 1.8: The expectation of culture parameters in a retentostat at a constant maintenance-energy requirement (m_S). Due to the filter in the outflow port ensuring 100 % biomass retention, biomass will accumulate from the start of the experiment (A). As the limiting substrate is distributed over more biomass, the specific substrate uptake rate will decrease over time (B) and consequently the growth rate decreases (C). After prolonged cultivation the substrate supplied per cell is only sufficient to meet the maintenance-energy requirements (m_S), but not for growth.

The first analysis of *S. cerevisiae* in a recycling bioreactor was not aimed at reaching extremely low growth rates, but was inspired by an interest in increasing the biomass concentration in a culture with a fixed substrate inflow at a range of specific growth rates [252]. The first retentostat cultures of *S. cerevisiae* with full biomass retention, enabling extremely low specific growth rates, were performed under anaerobic conditions [28] allowing for the precise quantification of maintenance-energy requirements. Over the course of 22 days of retentostat cultivation, the specific growth rate of these cultures decreased to below 0.001 h^{-1}, while the viability did not decrease below approximately 80 %. Under anaerobic conditions, ethanol is the sole dissimilatory product, and as growth was virtually absent, the ethanol yields at near zero-growth rates closely corresponded to the theoretical maximum [28]. The stoichiometric coupling of ATP-generation and ethanol formation allowed for the accurate quantification of the maintenance-energy requirements. Under these conditions, the maintenance-energy requirements estimated from chemostat cultures grown at a range of growth rates of 0.025 h^{-1} to 0.2 h^{-1} (1 $mmol_{ATP}.g_X^{-1}.h^{-1}$) and the value derived from retentostat cultures [28], closely corresponded. In contrast to the growth-rate independent maintenance-energy

requirements of *S. cerevisiae*, the first prokaryotes characterized in retentostats, *Escherichia coli* and *Bacillus polymyxa*, showed decreased maintenance-energy requirements at extremely low growth rates [54, 13, 327]. This 'stringent response', which represents a cellular programme for 'economizing' energy metabolism, is triggered by the alarmone ppGpp, whose accumulation at low growth rates sets off a down-regulation of genes involved in energy-intensive processes such as protein turnover [13, 45]. A stringent response was, however, not found in all prokaryotes studied in retentostat cultures [54, 13, 326, 305, 154, 99, 100].

The anaerobic glucose-limited retentostat cultures of *S. cerevisiae* [28] showed traits that are normally attributed to a cultures under starvation conditions. The accumulation of storage carbohydrates, the elevated tolerance to heat shock and the increased expression of genes involved in halting and exiting the cell cycle, were observed in these retentostat cultures and even in glucose-limited cultures at growth rates above 0.025 h^{-1} [27, 29]. During nutrient starvation of *S. cerevisiae*, senescent cells, which have left the active cell cycle and reside in G_0, a state that is commonly observed in nutrient-depleted conditions, accumulate [344, 127], (Figure 1.8). Based on analysis of cellular morphology, actin structures and analysis of the expression level of several specific transcripts in single cells [24], this accumulation did not occur in retentostat cultures. These observations suggested that the cells in a retentostat culture are homogeneous in their cellular state, and are clearly different for cells subjected to glucose starvation.

A key difference between retentostat cultures and starving cultures was that culture viability was maintained for prolonged periods of time in retentostat cultures, while viability rapidly decreased upon subsequent starvation [27]. Moreover, the accumulation of storage-polymers in the retentostat cultures, was reverted upon starvation. The rate of storage-polymer consumption during starvation suggested a 2-3 orders of magnitude decrease in maintenance-energy requirements. The transcriptional changes at near-zero growth rates showed a reduction of the expression level of biosynthesis-related genes and an increase in the expression of autophagy-related genes [29], observations that matched with the protein levels at near-zero growth rates [22]. The comparison of the genome-wide transcriptional responses to strong carbon- and energy limitation at near-zero growth rates and starvation showed rapid and fast downregulation of the expression of ribosomal proteins, RNA-binding proteins, in other words the core machinery of biosynthesis was down-regulated [27]. The subtle equilibrium between metabolic activity, growth and viability was investigated in retentostat cultures of a strain with a deletion in the central player of nutrient-sensing pathways (*RIM15*). This strain was not able to adapt to the extreme carbon- and energy source limitation and was not able to achieve near-zero growth, since it was unable to properly arrest its cell cycle. Consequences of this inability included a lower robustness and viability and higher maintenance-energy requirements than that of the reference strain. In the anaerobic retentostat cultures, biomass formation was successfully stopped and

uncoupled from the formation of the dissimilatory product ethanol. To investigate the possibility of achieving near-maximal yields of a non-dissimilatory product in the absence of growth, a similar analysis in retentostat cultures under fully aerobic conditions would be beneficial, due to the higher yield of ATP on substrate (see above). In addition, the beneficial traits observed in the anaerobic retentostat cultures (i.e. maintained metabolic activity, viability, high robustness) remain to be verified under aerobic conditions, both for non-producing and producing strains.

Outline of this thesis

The research presented in this thesis was funded by the BE-Basic foundation, an international public-private partnership that develops industrial biobased solutions for a sustainable society. In this partnership, the project that led to this thesis contributed to the flagship 'Genomics for Industrial Fermentation'. Uncoupling of non-dissimilatory product formation from biomass formation, by achieving processes in which the biomass remains viable and metabolically active but does not grow, is a key challenge in industrial biotechnology. To produce non-dissimilatory products at a large scale, the net input of cellular energy in the form of ATP and redox-equivalents is in direct competition with the formation of biomass and the fulfillment of maintenance-energy requirements. The efficiency of dissimilation, being the energy harvested in the form of ATP, is a determining factor of the maximum product yields that can be obtained.

Previous studies performed at the Industrial Microbiology group at TU Delft investigated the responses of *S. cerevisiae* to near-zero growth rates under anaerobic conditions. However, a higher ATP yield on substrate makes aerobic conditions more attractive for the production of non-dissimilatory products. **Chapter 2** of this thesis describes the first physiological and transcriptional characterization of fully respiring *S. cerevisiae* cultures under near-zero growth conditions. Design and interpretation of the aerobic retentostat experiments was supported by mathematical models of feeding regimes and regression analysis based on the equations presented above. The industrial context of this work was reflected by a focus on energetics, robustness and metabolic capacity of *S. cerevisiae*.

While **Chapter 2** focused on the physiology of aerobic yeast cultures under close to optimal conditions normally used in laboratory experiments, these conditions are not always the same in large-scale industrial processes. In **Chapter 3**, industrially relevant conditions for the production of dicarboxylic acids were chosen for a case study. These conditions comprised slow growth, low pH and high CO_2 levels. By means of chemostat and retentostat cultivation, this study aimed at dissecting the physiological impacts of these potentially adverse process conditions. The strong adverse effects of low pH found in **Chapter 3** highlighted the importance of robustness of industrial microbial workhorses such as *S. cerevisiae* to the conditions

met in large-scale industrial processes. The aim of **Chapter 4** was to identify novel targets for the improvement of performance of *S. cerevisiae* at low pH. By adaptive laboratory evolution of a laboratory strain, genome sequence analysis and reverse engineering in a non-evolved background, this study aimed to identify novel target mutations that improve growth under low pH conditions.

In **Chapters 2**, **3** and **4**, physiological responses of aerobic yeast cultures were investigated under a variety of conditions. The interpretation of these results strongly relied on key concepts in quantitative microbial physiology. These concepts are core learning objectives in the BSc and MSc curricula in Life Science & Technology (LST), taught jointly by the University of Leiden and Delft University of Technology. **Chapter 5** describes the design and implementation of a workshop that focuses on these concepts by using the dedicated simulator software 'Chemostatus'. This workshop allows students and teachers to discuss and interpret microbial physiology in an interactive and step-by-step way to gain thorough understanding of these otherwise rather abstract concepts. The aim of publication of this chapter was to make this tool available for others interested in teaching or studying quantitative microbial physiology.

CHAPTER 2

Maintenance-energy requirements and robustness of *Saccharomyces cerevisiae* at aerobic near-zero specific growth rates

Tim Vos
Xavier D.V. Hakkaart
Erik A.F. de Hulster
Ton J.A. van Maris
Jack T. Pronk
Pascale A.S. Daran-Lapujade

This chapter has been published in Microbial Cell Factories (2016) [340]. https://doi.org/10.1186/s12934-016-0501-z

Abstract

Background

Saccharomyces cerevisiae is an established microbial platform for production of native and non-native compound. When product pathways compete with growth for precursors and energy, uncoupling of growth and product formation could increase product yields and decrease formation of biomass as a by-product. Studying non- growing, metabolically active yeast cultures is a first step towards developing ***S. cerevisiae*** as a robust, non-growing cell factory. Microbial physiology at near-zero growth rates can be studied in retentostats, which are continuous-cultivation systems with full biomass retention. Hitherto, retentostat studies on ***S. cerevisiae*** have focused on anaerobic conditions, which bear limited relevance for aerobic industrial processes. The present study uses aerobic, glucose-limited retentostats to explore the physiology of non-dividing, respiring ***S. cerevisiae*** cultures, with a focus on industrially relevant features.

Results

Retentostat feeding regimes for smooth transition from exponential growth in glucose-limited chemostat cultures to near-zero growth rates were obtained by model-aided experimental design. During 20 days of retentostats cultivation, the specific growth rate gradually decreased from 0.025 h^{-1} to below 0.001 h^{-1}, while culture viability remained above 80%. The maintenance requirement for ATP (m_{ATP}) was estimated at 0.63 ± 0.04 $mmol_{ATP} \cdot g_{biomass}^{-1} \cdot h^{-1}$, which is ca. 35% lower than previously estimated for anaerobic retentostats. Concomitant with decreasing growth rate in aerobic retentostats, transcriptional down- regulation of genes involved in biosynthesis and up-regulation of stress-responsive genes resembled transcriptional regulation patterns observed for anaerobic retentostats. The heat- shock tolerance in aerobic retentostats far exceeded previously reported levels in stationary-phase batch cultures. While in situ metabolic fluxes in retentostats were intentionally low due to extreme caloric restriction, off-line measurements revealed that cultures retained a high metabolic capacity.

Conclusions

This study provides the most accurate estimation yet of the maintenance-energy coefficient in aerobic cultures of ***S. cerevisiae***, which is a key parameter for modeling of industrial aerobic, glucose-limited fed- batch processes. The observed extreme heat-shock tolerance and high metabolic capacity at near-zero growth rates demonstrate the intrinsic potential of ***S. cerevisiae*** as a robust, non-dividing microbial cell factory for energy-intensive products.

Background

The yeast *Saccharomyces cerevisiae* is an established microbial host for the production of native yeast metabolites as well as non-native products [158]. Production of many of these compounds, including phenylpropanoids, isoprenoids, heterologous proteins and lipids [46, 339, 192] from glucose requires a net input of ATP. The maximum ATP yield from glucose is obtained when its dissimilation occurs exclusively via respiration. In *S. cerevisiae*, a completely respiratory sugar metabolism requires aerobic conditions and sugar-limited cultivation at low to intermediate specific growth rates [319]. In industry, these requirements are usually met by sugar-limited, aerobic fed-batch cultivation. Due to oxygen-transfer and cooling constraints, aerobic fed-batch processes typically involve low specific growth rates [320, 138]. However, biomass-specific production rates (q_P) of products whose biosynthesis from sugar requires a net input of ATP typically show a positive correlation with specific growth rate [339, 192, 165, 152]. Understanding and, ultimately, breaking this correlation between growth and product formation by improving specific rates of product formation at low specific growth rates, is an important target for optimizing productivity and product yields in aerobic, sugar-limited fed-batch cultures.

In addition to the relation between q_P and specific growth rate, microbial product formation at low specific growth rates is strongly influenced by the metabolic-energy requirement of microorganisms for maintaining cellular integrity and viability. In a first analysis, this maintenance-energy requirement is often assumed to be growth-rate independent [339, 304]. Distribution of carbon- and energy substrate over growth and cellular maintenance can then be described by the Pirt equation [250], which can be modified to include ATP-requiring product formation (see equation in Figure 2.1). The Pirt equation describes how the fraction of the energy substrate that needs to be dissimilated to fulfill maintenance energy requirements increases as the specific growth rate in, for example, an aerobic, sugar-limited fed-batch process decreases. In slow-growing aerobic industrial fed-batch processes this increasing impact of maintenance requirements has a major negative impact on product yields and productivities [339].

Analysis of the physiology of extremely slow growing yeast cultures can provide relevant, quantitative information on the maintenance-energy requirements of *S. cerevisiae* and for developing this yeast into a non-growing cell factory [28, 27, 29, 25, 22]. Retentostats are continuous cultivation devices with full biomass retention that have been designed to study microbial physiology at near-zero growth rates [326, 99]. Retentostat cultivation typically starts with a steady-state chemostat culture, operated at a low dilution rate. After reaching steady state, the chemostat culture is switched to retentostat mode by redirecting the effluent through a filter unit that ensures full biomass retention (Figure 2.1). The

constant, growth-limiting feed of glucose will then result in biomass accumulation (C_X), while the amount of substrate available per cell per unit of time decreases over time (Figure 2.1). This decreased substrate availability results in decreasing specific substrate consumption rates (q_S) which, after prolonged retentostat cultivation, asymptotically approach the cellular energy-substrate requirement for maintenance (m_S). Since, in this situation, no energy-substrate is available for growth, the specific growth rate (μ) asymptotically approaches zero (Figure 2.1).

Retentostat cultures have mostly been used in the early 1990's to investigate the response of prokaryotes to extreme energy limitation. At extremely low growth rates, many bacteria, including *Escherichia coli*, display an alarmone-mediated stringent response. This coordinated response enables cultures to more efficiently withstand nutrient scarcity by down regulation of energy-intensive cellular processes and, therefore, a reduction of the maintenance-energy requirement [327, 13, 12]. Retentostats have recently been used to study the physiology of *S. cerevisiae* at near-zero growth rates under anaerobic conditions [28, 27, 29, 25, 22]. Even at extremely low specific growth rates, the maintenance requirement of *S. cerevisiae* in these anaerobic chemostat cultures was shown to be growth-rate independent [28]. A decrease of the ATP-turnover of non-growing cultures was only observed when anaerobic, retentostat-grown *S. cerevisiae* cultures were switched to glucose starvation and energy metabolism became dependent on metabolism of storage

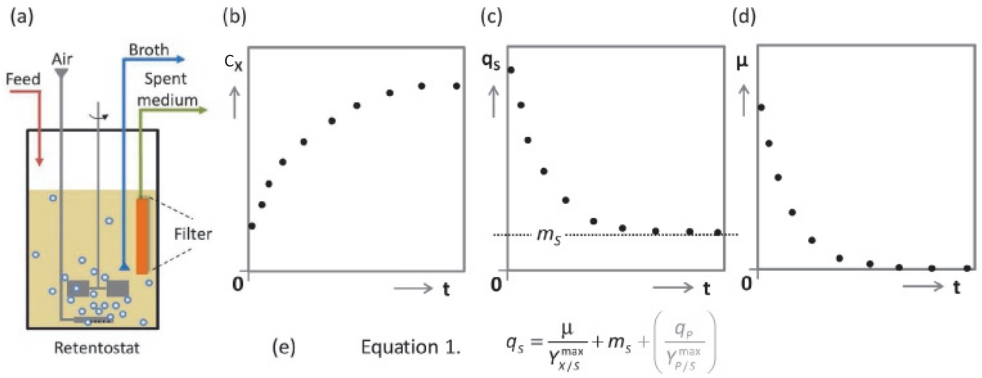

Figure 2.1: Schematic representation of retentostat set-up and simulated profiles of biomass accumulation (C_X), glucose consumption rate (q_S) and biomass specific growth rate (μ) during prolonged retentostat cultivations. The retentostat is a continuous bioreactor system in which the outflow can be switched from whole-broth removal to complete cell retention through a filter probe **(a)**. After switching from chemostat cultivation to retentostat mode, biomass accumulates in the bioreactor **(b)**, which gradually decreases the glucose availability per unit of biomass. This decrease ultimately results **(c)** in specific glucose consumption rates that can only meet energy demands for cellular maintenance (m_S), thereby causing near-zero specific growth rates **(d)**. The distribution of the carbon and energy source over growth, maintenance and product formation (not indicated in the plots) is mathematically captured by an extended Pirt equation **(e)**, in which $Y_{X/S}^{max}$ is the maximum theoretical biomass yield, q_P is the specific production rate of a product whose synthesis requires metabolic energy and $Y_{P/S}^{max}$ is the maximum theoretical yield of this product on substrate.

carbohydrates [27]. Transcriptome responses during anaerobic retentostats encompassed many genes whose transcription was previously shown to be growth-rate correlated in faster growing cultures, as well as an increased expression of genes involved in resistance to a variety of stresses [14]. Consistent with the latter observation, yeast cells grown at low specific growth rates acquire a strongly increased robustness towards heat shock and an increased chronological life span [27, 195].

Since previous retentostat studies on *S. cerevisiae* were exclusively performed under anaerobic conditions, it remains unclear how oxygen availability affects its physiology at extremely low specific growth rates. Oxygen is known to have multiple effects on cellular biology. Even in *S. cerevisiae*, which has a rather low efficiency of oxidative phosphorylation, fully respiratory dissimilation of glucose yields eightfold more ATP than alcoholic fermentation, which is the sole dissimilatory pathway under anaerobic conditions [333]. This higher ATP yield supports higher biomass yields and, if the maintenance-requirement for ATP (m_{ATP}) is the same in aerobic and anaerobic cultures, should lead to a lower m_S than observed in anaerobic cultures. Since biomass yield and maintenance-energy requirement affect the dynamics of retentostats, these differences should also be taken into account in the design of feed regimes that result in a smooth transition from exponential growth to near-zero growth rates. Despite the industrial relevance of maintenance-energy requirements, accurate experimental estimates of m_S and m_{ATP} for aerobic, sugar-limited cultures of *S. cerevisiae* on synthetic medium are not available. The assumption that m_{ATP} in aerobic cultures is the same as in anaerobic cultures [314], can result in over- or underestimation of the m_S of aerobic cultures. In anaerobic cultures, presence of the anaerobic growth factor oleic acid [331] and of ethanol and organic acids might increase m_{ATP}. Similarly, detoxification of reactive oxygen species (ROS) and repair of ROS-induced damage may lead to increased maintenance energy requirements in aerobic cultures [147]. ROS, which can contribute to cellular aging, could also accelerate cell death of aerobic, non-dividing and chronologically aging yeast cultures [49]. A further question that remains to be addressed is whether and to what extent extremely slow-growing *S. cerevisiae* cultures retain a high metabolic capacity, which is a prerequisite for efficient product formation. Previous studies showed that glucose-limited aerobic cultures of *S. cerevisiae* retain a high capacity of glycolysis (the highway for sugar assimilation) at specific growth rates down to 0.05 h^{-1} [322], but no data are available on the glycolytic capacity at near-zero growth rates.

The goal of the present study is to quantitatively analyse maintenance-energy requirement, robustness and glycolytic capacity of *S. cerevisiae* in aerobic cultures grown at near-zero growth rate. To this end, regimes for aerobic retentostat cultivation were designed and implemented that enabled a smooth transition from exponential growth to near-zero growth rates. In addition to quantitative physiological analyses, transcriptome analysis was performed to

investigate cellular responses to near-zero growth in aerobic cultures and to compare these with previously published transcriptome data obtained from anaerobic retentostats.

Results

Design of a regime for smooth transition to near-zero growth rates in aerobic retentostats

Growth rate dynamics and biomass accumulation in retentostat cultures mainly depend on two condition- dependent and strain-specific parameters: the theoretical maximal biomass yield ($Y_{X/S}^{max}$) and the maintenance coefficient (m_S). To predict the impact of these parameters on growth dynamics in aerobic retentostat cultures, a model based on the Pirt definition of resource allocation (see Figure 2.1) was used. $Y_{X/S}^{max}$ was estimated from published data on aerobic, glucose-limited chemostat cultures of the *S. cerevisiae* strain used in this study (0.5 g_X. g_S^{-1} [322]). Since no accurate estimates for the aerobic m_S are available, model-based simulations were performed with a range of m_S values that were based on the m_S calculated from anaerobic retentostat experiments (biomass-specific glucose consumption for maintenance: 0.5 mmol.g_X^{-1}.h^{-1}, [28]) and assuming a P/O ratio of 1.0 for aerobic, respiring cultures of *S. cerevisiae* [333, 104], which leads to an eight-fold higher ATP yield from respiratory sugar dissimilation than from alcoholic fermentation.

Initial model simulations were performed based on the assumption that no loss of viability occurs during retentostat cultivation and with the same feed regime that was previously used for anaerobic retentostats (constant dilution rate of 0.025 h^{-1} and a glucose concentration in the feed of 20 g.L^{-1} [28]). This resulted in a predicted accumulation of biomass to a concentration of ca. 45 g.L^{-1}, Figure 2.2, blue line), which was considered to present a substantial risk of clogging the filter unit. Moreover, in this simulation, near-zero growth rates (i.e. specific growth rates below 0.001 h^{-1}) were only reached after multiple weeks of operation (Figure 2.2, blue line), which was considered to be impracticable.

Near-zero growth rates can be reached faster by decreasing the glucose concentration in the medium for the retentostat culture ($C_{S,MR}$) compared to the glucose concentration in the medium for the chemostat culture ($C_{S,MC}$). However, care should be taken to avoid scenarios in which the glucose supply changes suddenly or transiently decreases below the culture's maintenance-energy demand, which might affect cellular viability. Introduction of an additional medium mixing vessel (Figure 2.2), whilst maintaining a constant flow of medium (F_V) and allowed for a controlled, smooth transition of the ingoing glucose concentration ($C_{S,in}$) into the retentostat culture, thereby a constant dilution rate. To incorporate the mixing vessel the model was expanded with Equation 2.2 and simulations were performed for experimental design of $C_{S,MR}$ and the volume of the mixing vessel (V_S in liters) (Figure 2.2).

$$\frac{dC_{S,in}}{dt} = \frac{F_V}{V_S}C_{S,MR} - \frac{F_V}{V_S}C_{S,in} \quad (2.2)$$

Figure 2.2 depicts the modeling output when $C_{S,MR}$ equals $C_{S,MC}$ (blue lines) and when $C_{S,MR}$ was decreased to 7.5 or 5 $g.L^{-1}$ (solid red and green lines, respectively) assuming an m_S of 0.011 $g.g_X^{-1}.h^{-1}$.

In the simulations, values of $C_{S,MR}$ of 5 $g.L^{-1}$ and lower resulted in 'negative growth', indicating that the model predicted glucose starvation and cell death. Since, in extremely slow growing cultures, glucose is predominantly used for maintenance, growth dynamics in retentostats are particularly sensitive to variations in m_S. Accordingly, a 20 % change in m_S resulted in a five-fold difference in the predicted specific growth rates after 20 days of retentostat cultivation (dashed lines in Figure 2.2). Based on these simulations, operational conditions were chosen such that the prediction complied to the following requirements: (i) near-zero growth rates ($\mu < 0.001$ h^{-1}) achieved within 2 weeks of retentostat cultivation, (ii) prevention of sudden changes in q_S and glucose starvation, (iii) the conditions led to a sizeable difference between initial and final biomass concentrations, (iv) previous criteria met for a range of m_S values, and (v) final biomass concentration kept below 30 g L^{-1} to prevent filter clogging (Figure 2.2, red line). The chosen operational conditions are described in Figure 2.2, and correspond to the red line.

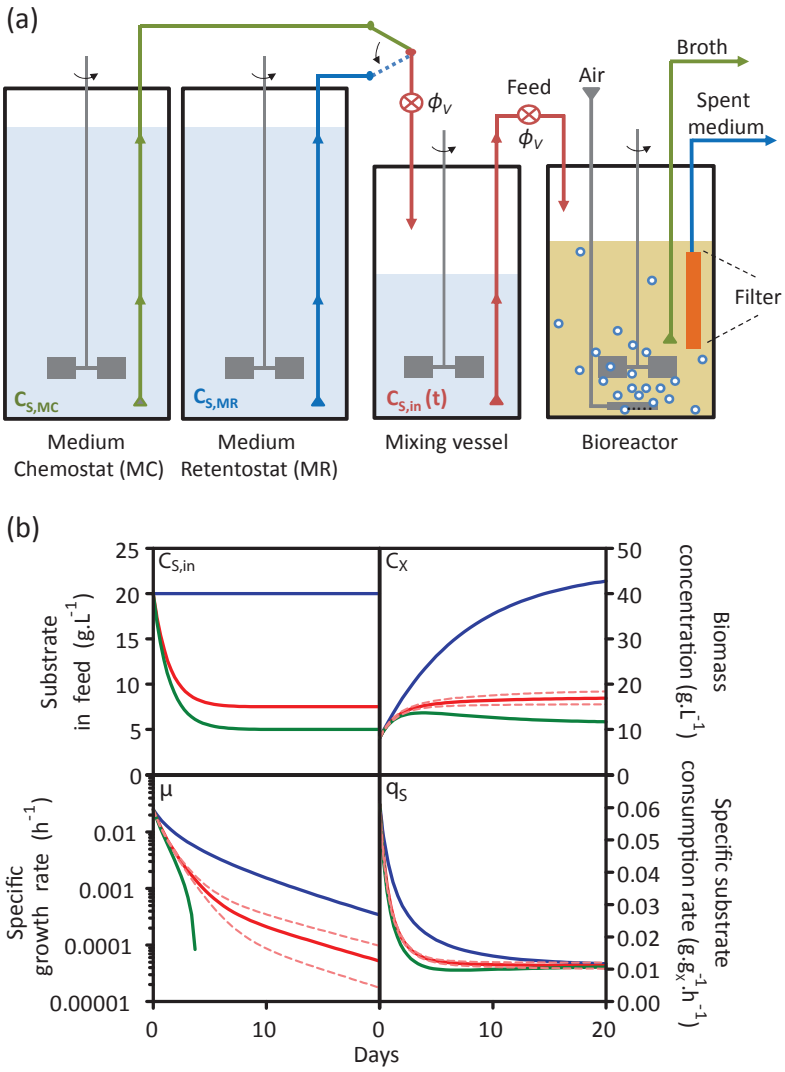

Figure 2.2: Setting up aerobic retentostat cultures. **a** Retentostat cultures (bioreactors) were started from a steady-state chemostat culture with an ingoing glucose concentration ($C_{S,MC}$) of 20 $g.L^{-1}$. At the start of the retentostats (t = 0 h), the feed to the mixing vessel was switched to the medium reservoir for the retentostat cultivation (as indicated by the *arrow*). The process was modelled for three different concentrations of glucose in the medium reservoir for the retentostat cultures ($C_{S,MR}$). **b** Profiles of biomass concentration (C_X), specific glucose consumption rate (q_S) and specific growth rate (μ) in time were predicted with a mathematical model, based on glucose concentration in the feed coming from the mixing vessel. Blue lines indicate a scenario in which $C_{S,MC}$ = $C_{S,MR}$ = 20 $g.L^{-1}$, green lines indicate $C_{S,MR}$ = 5 $g.L^{-1}$, and red lines indicate $C_{S,MR}$ = 7.5 $g.L^{-1}$. Dotted lines indicate simulations for which 10 % higher or lower maintenance values were considered in the model (see "Methods" section). The operational conditions applied in the experiments in this study correspond to the red lines

Maintenance-energy requirements in aerobic retentostat cultures

In four independent retentostat cultures, biomass accumulated reproducibly over a period of ca. 20 days. The final biomass concentrations were ca. threefold higher than those in the preceding chemostat culture (Figure 2.3a). However,the experimentally observed biomass accumulation was substantially higher than predicted from model simulations (Figure 2.3a). One factor that might contribute to this apparent discrepancy was the biomass viability which, in the model simulations, was assumed to remain at 100 % throughout the retentostats experiments. Indeed, flow-cytometric analysis of cellular integrity indicated that, over 20 days of retentostat cultivation, culture viability decreased to ca. 85 % (Figure 2.3b). Colony-forming unit counts confirmed that ca. 70 % of the cells in the population were able to sustain growth after 20 days in retentostat culture. This apparent loss of the cells' capacity to divide contrasted with the retention of cellular integrity and has been previously reported for anaerobic retentostat cultures [25]. It may result from various factors, such as the irreversible degradation of macromolecules necessary for duplication, but may also result from loss of reproductive capacity during CFU plating assays. To prevent the risk of underestimating culture viability, viable biomass concentrations were therefore calculated based on flow cytometry-based viability assays (Figure 2.3a). Based on these observations, a low but significant death rate of $4.7 \cdot 10^{-4}$ h^{-1} was calculated. However, correcting for viability only explained part of the difference between the observed and modelled biomass accumulation profiles.

As mentioned above, the exact value of m_S is expected to have a strong impact on biomass accumulation profiles in retentostat cultures. Assuming specific growth-rate independent maintenance, the aerobic m_S was estimated from the calculated specific growth rate and glucose consumption rates of *S. cerevisiae* in the aerobic retentostats, using biomass concentrations corrected for viability (Figure 2.4a). During 20 days of retentostat cultivation, specific growth rates in all four replicate experiments decreased from 0.025 h^{-1} in steady-state to values below $8 \cdot 10^{-4}$ h^{-1}, representing doubling times of over 36 days. The average specific glucose-consumption rate the cellular substrate requirement exclusively necessary converged to 0.039 ± 0.003 $mmol.g_X^{-1}.h^{-1}$, representing for maintenance energy purposes (Figure 2.4b). Considering an *in vivo* P/O ratio in *S. cerevisiae* of 1.0 [333], the aerobic ATP requirement of *S. cerevisiae* for maintenance (m_{ATP}) calculated from these experiments was 0.63 ± 0.04 $mmol_{ATP}.g_X^{-1}.h^{-1}$. This value is ca. 30 % lower than the m_{ATP} previously estimated from anaerobic retentostats cultures [28] (Figure 2.4b).

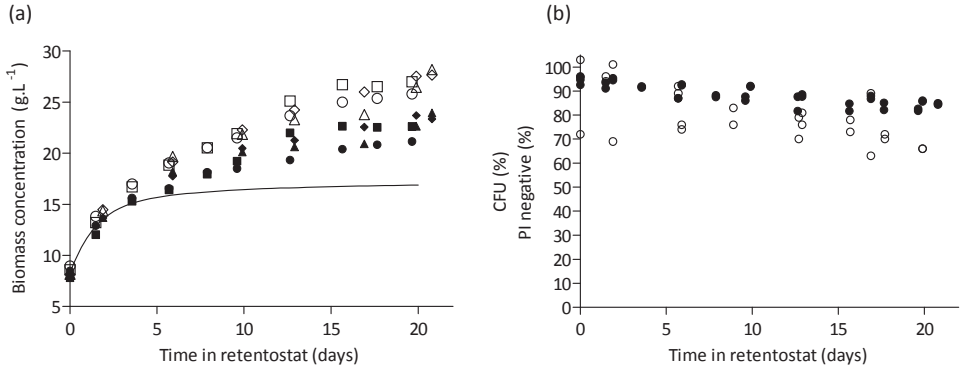

Figure 2.3: Biomass accumulation and culture viability during prolonged retentostat cultivation. **a** Predicted biomass accumulation profile (*line*), measured biomass dry weight concentrations (*open symbols*), and viable biomass concentration (*closed symbols*) from four replicate retentostat cultures. **b** Culture viability estimated by flow cytometric analysis of propidium iodide-stained cells (closed symbols), and viability estimated from colony forming unit counts (*open symbols*)

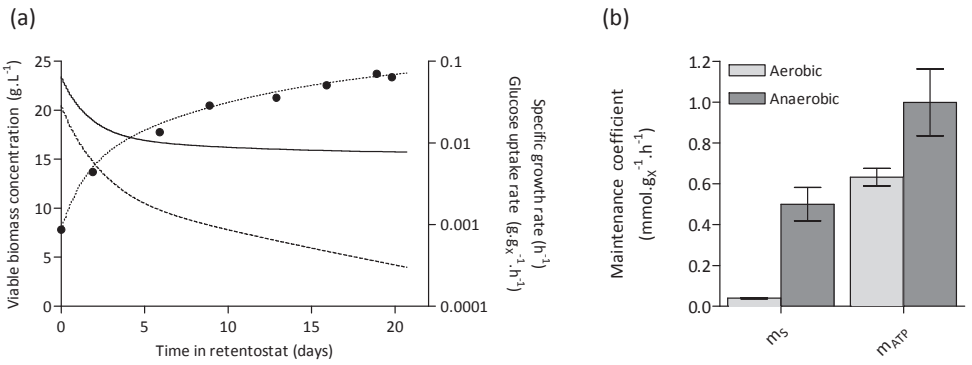

Figure 2.4: Growth kinetics and m_S in retentostat cultures. **a** Specific glucose-consumption rate (q_S, solid line) and specific growth rate (μ, dashed line) calculated by non-linear regression of the accumulation of viable- and total biomass over time (see "Methods" section). The closed symbols and dotted line represent the viable biomass and linear regression of the viable biomass, respectively. Data are shown for a single representative retentostat experiment. **b** Glucose and ATP requirements for maintenance (m_S and m_{ATP}, respectively) of aerobic and anaerobic retentostat cultures (anaerobic data obtained from [28]). The aerobic m_{ATP} was calculated based on a P/O ratio of respiring *S. cerevisiae* cultures of 1.0 [333]

Transcriptional reprogramming in aerobic retentostats: involvement of 'growth-rate responsive' genes

Over the course of the aerobic retentostat experiments, 1375 genes (ca. one-fifth of the genome) were differentially expressed. In comparison, aerobic batch cultures transitioning from exponential growth, through a post-diauxic phase, into stationary phase, resulted in 1690 differentially expressed genes (using the same analysis software and statistical criteria as in the present work, Additional file 1) [24]. One third (458 genes) of the 1375 genes identified in the present retentostat dataset overlapped with the aerobic batch data-set. The 1375 differentially expressed genes identified in the present study could be separated in two clusters with clear, specific-growth-rate dependent transcript profiles (Figure 2.5). Cluster 1 harboured 600 genes whose expression displayed a positive correlation with specific growth rate (Figure 2.5). As anticipated, this cluster showed an over-representation of genes involved in typical growth-related processes, including protein, ribosome, amino acid, nucleotide and lipid biosynthesis (Table 2.1). Consistent with this observation, cluster 1 also showed an overrepresentation of genes whose expression is controlled by transcription factors that are involved in this response: Fhl1, Rap1 and Sfp1, Gcn4 and Met32 (Table 1). Genes involved in sterol metabolism (including 15 of the 19 *ERG* genes involved in ergosterol synthesis) and pentose-phosphate pathway were also over-represented in cluster 1. Cluster 2 grouped the remaining 775 differentially expressed genes, whose transcript levels showed a negative correlation with specific growth rate (Figure 2.5). This cluster was most strongly enriched for genes involved in stress response, and more specifically targets of Skn7 and Cad1, as well as for genes involved in signal transduction and protein turnover (Table 2.2). Accordingly, cluster 2 was strongly enriched for targets of the stress-responsive transcription factor pair Msn2/Msn4 (55 out of 166 genes, p-value $4{\cdot}29\ 10^{-11}$) [117].

A positive correlation with specific growth rate of the expression levels of genes involved in anabolic processes and a negative correlation of those of stress-responsive genes, was previously shown in aerobic chemostat cultures grown at specific growth rates of 0.05 h^{-1} and above [44, 260, 32]. Clusters 1 and 2 showed a substantial overlap with these previously identified sets of growth-rate responsive genes (Additional file 2).

Table 2.1: Overrepresentation of functional categories among the differentially expressed genes in cluster 1 (See Figure 2.5). [a]: Number of genes present in both the cluster and the functional category. [b] Total number of genes in the functional category [c] A Bonferroni corrected p-value cut-off of 0.05 was used and -values indicate the probability of finding the same number of genes in a random set. [d] Functional categories originate from the Munich Information Centre for Protein Sequences (MIPS), Gene Ontology (GO) or transcription factor binding datasets (TF) described in the Methods section.

	Functional category	**k[a]**	**n[b]**	**p-value[c]**
MIPS[d]	PROTEIN SYNTHESIS	138	511	$4.98 \cdot 10^{-31}$
	Ribosomal proteins	95	277	$4.29 \cdot 10^{-29}$
	Ribosome biogenesis	106	343	$2.46 \cdot 10^{-28}$
	Amino acid metabolism	69	243	$3.31 \cdot 10^{-15}$
	METABOLISM	221	1530	$5.87 \cdot 10^{-11}$
	Metabolism of the aspartate family	26	64	$1.75 \cdot 10^{-8}$
	Metabolism of methionine	18	36	$3.52 \cdot 10^{-7}$
	Tetracyclic and pentacyclic triterpenes metabolism	16	36	$2.84 \cdot 10^{-5}$
	Purine nucleotide/nucleoside/nucleobase metabolism	22	66	$4.58 \cdot 10^{-5}$
	Nucleotide/nucleoside/nucleobase metabolism	48	230	$4.81 \cdot 10^{-5}$
	Isoprenoid metabolism	16	41	$2.55 \cdot 10^{-4}$
	Sulfur metabolism	7	8	$3.51 \cdot 10^{-4}$
	Sulfate assimilation	7	8	$3.51 \cdot 10^{-4}$
	Metabolism of the cysteine-aromatic group	23	80	$4.79 \cdot 10^{-4}$
	Aminoacyl-tRNA-synthetases	15	39	$7.46 \cdot 10^{-4}$
	ENERGY	58	360	$1.69 \cdot 10^{-2}$
	Pentose-phosphate pathway	10	24	$2.20 \cdot 10^{-2}$
GO[d]	Translation	117	345	$6.31 \cdot 10^{-36}$
	Cellular amino acid biosynthetic process	44	101	$1.10 \cdot 10^{-16}$
	Ribosome biogenesis	46	178	$1.13 \cdot 10^{-7}$
	Oxidation reduction	60	270	$1.24 \cdot 10^{-7}$
	Metabolic process	76	389	$2.49 \cdot 10^{-7}$
	Steroid biosynthetic process	15	24	$2.73 \cdot 10^{-7}$
	Sterol biosynthetic process	15	28	$5.46 \cdot 10^{-6}$
	Methionine biosynthetic process	16	32	$6.13 \cdot 10^{-6}$
	Maturation of SSU-rRNA	22	62	$2.28 \cdot 10^{-5}$
	Sulfate assimilation	9	11	$3.49 \cdot 10^{-5}$
	rRNA processing	43	195	$8.44 \cdot 10^{-5}$
	Methionine metabolic process	10	15	$1.36 \cdot 10^{-4}$
	Lipid biosynthetic process	18	52	$7.16 \cdot 10^{-4}$
	Ergosterol biosynthetic process	7	9	$2.66 \cdot 10^{-3}$
TF[d]	*FHL1*	75	208	$1.64 \cdot 10^{-24}$
	RAP1	51	145	$1.31 \cdot 10^{-15}$
	SFP1	20	50	$1.41 \cdot 10^{-6}$
	GCN4	37	182	$8.70 \cdot 10^{-4}$
	HAP1	27	120	$2.60 \cdot 10^{-3}$
	MET32	9	24	$4.06 \cdot 10^{-2}$

Table 2.2: Overrepresentation of functional categories among the differentially expressed genes in cluster 2 (see Figure 2.5). [a]: Number of genes present in both the cluster and the functional category. [b] Total number of genes in the functional category [c]: A Bonferroni corrected p-value cut-off of 0.05 was used and -values indicate the probability of finding the same number of genes in a random set. [d]: Functional categories originate from the Munich Information Centre for Protein Sequences (MIPS), Gene Ontology (GO) or transcription factor binding datasets (TF) described in the Methods section.[e]: MSN2/4 transcription factor dataset originates from [117] [

	Functional category	**k[a]**	**n[b]**	**p-value[c]**
MIPS[d]	UNCLASSIFIED PROTEINS	194	1140	$4.13 \cdot 10^{-5}$
	Oxidative stress response	21	56	$7.17 \cdot 10^{-4}$
	CELL RESCUE, DEFENSE AND VIRULENCE	101	558	$9.06 \cdot 10^{-3}$
	Degradation of polyamines	5	5	$1.98 \cdot 10^{-2}$
	ENERGY	70	360	$2.14 \cdot 10^{-2}$
	CELLULAR COMMUNICATION	50	239	$4.60 \cdot 10^{-2}$
	Cellular signalling	44	202	$4.71 \cdot 10^{-2}$
GO[d]	Signal transduction	24	74	$4.64 \cdot 10^{-3}$
	Protein amino acid phosphorylation	36	141	$1.11 \cdot 10^{-2}$
	Proteasomal ubiquitin- dependent protein catabolic process	9	16	$3.95 \cdot 10^{-2}$
	Oxidation reduction	56	270	$3.96 \cdot 10^{-2}$
	Negative regulation of gluconeogenesis	7	10	$4.55 \cdot 10^{-2}$
TF[d]	MSN2/MSN4 [e]	55	166	$4.29 \cdot 10^{-11}$
	SKN7	43	175	$6.59 \cdot 10^{-4}$
	YAP7	36	152	$9.78 \cdot 10^{-3}$
	CAD1	12	32	$4.40 \cdot 10^{-2}$

To investigate how cellular responses to near-zero growth rates differed between aerobic and anaerobic cultures, we compared transcriptome data from the present study with those obtained in a previous transcriptome analysis of anaerobic retentostats of the same *S. cerevisiae* strain [14]. Anaerobic retentostat cultivation yielded 2661 differentially expressed genes, based on the same range of specific growth rates and applying the same statistical criteria as in the present study. This number of genes is almost two-fold higher than observed in the aerobic retentostats (Additional file 3). Synthetic medium, pH and temperature in the anaerobic retentostats were the same as those used in the present study, except for the addition of the anaerobic growth factors Tween-80 (a source of oleic acid) and ergosterol in the previous study.

Differences in the responses of anaerobic and aerobic retentostats were investigated by identifying genes that showed a specific transcriptional response to near-zero growth rates in either aerobic or anaerobic retentostats (Figure 2.6). Among 182 genes whose expression increased at extremely low growth rates in anaerobic retentostat cultures, only functional categories related to aerobic respiration, were significantly enriched (Figure 2.6). 31 out of 74 genes involved in the cellular function aerobic respiration were specifically up-regulated in anaerobic retentostats, including 8 *COX* genes, which encode subunits of the mitochondrial inner-membrane cytochrome *c* oxidase. Genes involved in this functional category were not over-represented among the responsive genes identified in aerobic retentostat cultures, indicating that up-regulation of respiration-related genes is a specific adaptation to anaerobic slow growing and/or aging cultures. Among the 686 genes whose expression showed a reduced expression at near-zero growth rates under anaerobic conditions, functional categories related to protein synthesis were significantly enriched (Figure 2.6).

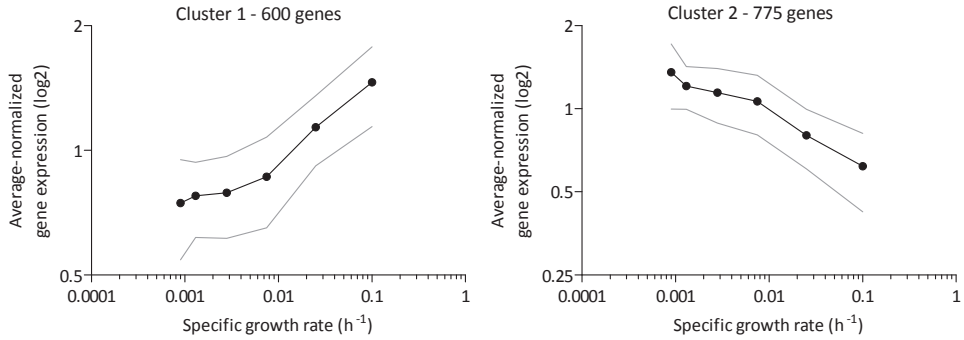

Figure 2.5: K-mean clustering of the 1375 genes with significant growth-rate dependent expression profiles. Retentostat data were combined with data from aerobic glucose-limited chemostats grown at μ= 0.10 h^{-1} (see "Methods" section). The p-value threshold for significant differential expression was set to 0.01. For each cluster, averaged-normalized expression values are depicted as a function of specific growth rate (see "Methods" section). Grey dotted lines show the standard deviation of averaged expression values

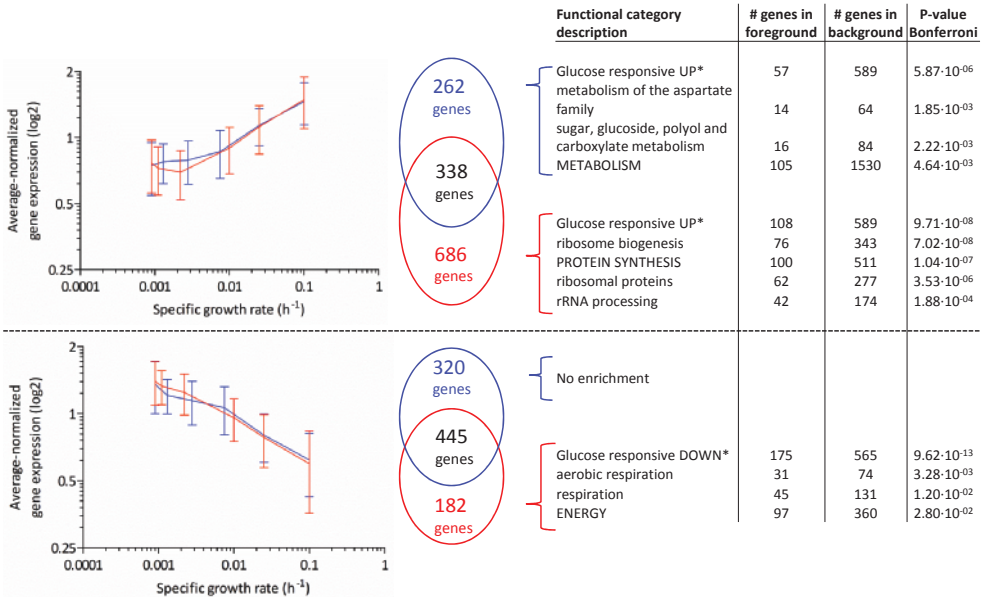

Functional category description	# genes in foreground	# genes in background	P-value Bonferroni
Glucose responsive UP*	57	589	$5.87 \cdot 10^{-06}$
metabolism of the aspartate family	14	64	$1.85 \cdot 10^{-03}$
sugar, glucoside, polyol and carboxylate metabolism	16	84	$2.22 \cdot 10^{-03}$
METABOLISM	105	1530	$4.64 \cdot 10^{-03}$
Glucose responsive UP*	108	589	$9.71 \cdot 10^{-08}$
ribosome biogenesis	76	343	$7.02 \cdot 10^{-08}$
PROTEIN SYNTHESIS	100	511	$1.04 \cdot 10^{-07}$
ribosomal proteins	62	277	$3.53 \cdot 10^{-06}$
rRNA processing	42	174	$1.88 \cdot 10^{-04}$
No enrichment			
Glucose responsive DOWN*	175	565	$9.62 \cdot 10^{-13}$
aerobic respiration	31	74	$3.28 \cdot 10^{-03}$
respiration	45	131	$1.20 \cdot 10^{-02}$
ENERGY	97	360	$2.80 \cdot 10^{-02}$

Figure 2.6: Comparison between aerobic and anaerobic growth-rate dependent gene expression at near-zero growth rates. Transcriptome datasets of aerobic (blue) and anaerobic (red) experiments covered a specific growth rate range between 0.1 h^{-1} and values below 0.001 h^{-1}, with an equal number of data points ([29] and Figure 2.5). The p-value threshold for significant differential expression was 0.01. Overlapping and exclusive gene groups within the clusters, presented as Venn diagrams, were mined for overrepresentation of genes involved in specific functional categories with a Bonferroni-corrected p-value threshold of 0.05 (see "Methods" section). Genes in the foreground represent number of genes present in both the cluster and the functional category, Genes in the background represent the total number of genes in the functional category. Asterisk Glucoseresponsive gene sets are derived from [168]

Extreme heat-shock tolerance of yeast cells grown in aerobic retentostats

Studies in aerobic chemostats, anaerobic retentostats and aerobic stationary-phase batch cultures showed that slow growth of *S. cerevisiae* increases its stress tolerance, most often measured as its ability to survive exposure to high temperatures [28, 195, 24]. The aerobic chemostat cultures, grown at a specific growth rate of 0.025 h^{-1}, which preceded the retentostat cultures were already remarkably heat-shock tolerant, with 50 % of the population surviving a 115 min exposure to a temperature of 53 °C (Figure 2.7a). After 10 days of retentostat cultivation, when the specific growth rate had decreased below 0.001 h^{-1}, this t_{50} had increased to 4 h. This t_{50} value is approximately fourfold higher than previously described for extremely heat-shock tolerant cultures, such as aerobic stationary-phase and anaerobic retentostat cultures (Figure 2.7a). To the best of our knowledge, this heat-shock tolerance is the highest measured to date in *S. cerevisiae*.

In previous studies, a high heat-shock tolerance of *S. cerevisiae* was found to

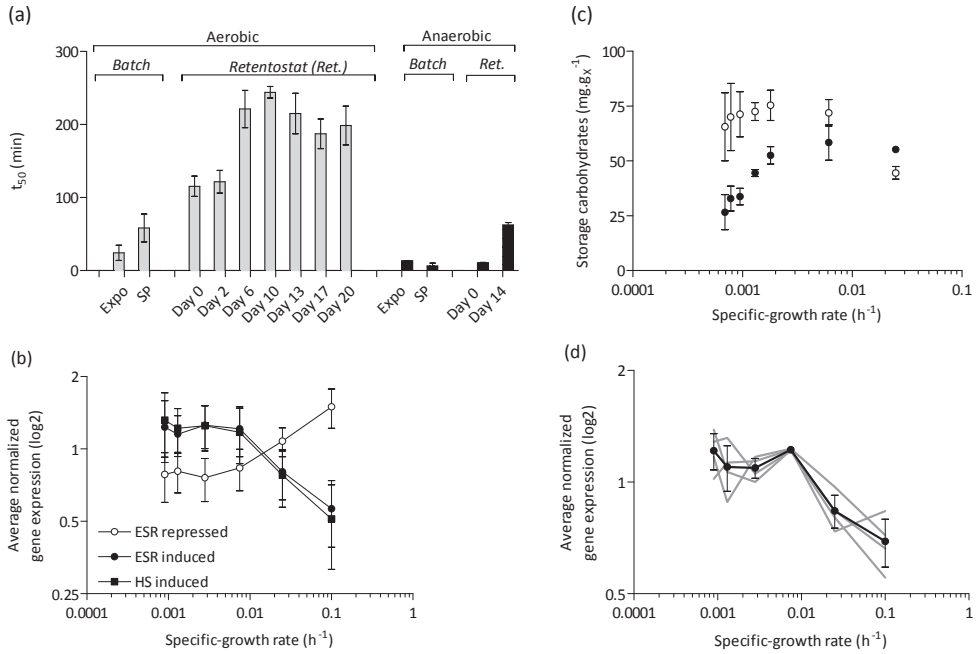

Figure 2.7: Heat-shock tolerance of aerobic and anaerobic retentostat and batch cultures. **a** Data on heat shock tolerance of anaerobic retentostat cultures and from batch cultures are taken from previous studies [13, 34]. Batch cultures were characterized during the exponential growth phase (expo) and after ca. 2 h in stationary phase (SP) [24]. t_{50} represents incubation time at 53 °C at which 50 % of the initial viable cell population was still alive. **b** Transcript levels of genes that exhibit a significant growth-rate dependent expression in retentostat, and are also known to respond to environmental stress and heat shock according to [117, 91]. **c** Cellular contents of trehalose (open symbols) and glycogen (closed symbols) during prolonged retentostat cultivation. **d** Average-normalized expression profiles of genes involved in trehalose metabolism (see "Methods" section)

correlate with increased transcript levels of many known stress-responsive genes [28, 24]. Consistent with these earlier observations, transcript levels of *Msn2/4* gene targets, as well as genes that were previously shown to be responsive to environmental stresses (ESR induced: 110 out of 281, p-value $1.17 \cdot 10^{-30}$; heat shock in an Msn2/4-independent manner (125 ESR repressed: 170 out of 563, p-value $3.31 \cdot 10^{-48}$) or to growth rate and, therefore, with heat-shock tolerance in out of 427, p-value $3.11 \cdot 10^{-21}$), correlated with specific the aerobic retentostat cultures (Figure 2.7b) [117, 91]. Heat-shock proteins function as chaperones that prevent aggregation of thermally damaged proteins, unfold them, or mark them for degradation [29]. Of 76 genes known to encode heat-shock proteins, seven showed increased mRNA levels at near-zero growth rates (*SSA3*, *HSP26*, *HSP42*, *XDJ1*, *CWC23*, *EUG1* and *HSP60*) [104]. Disaggregation and (re)folding activities of heat-shock proteins are ATP dependent and maintaining intracellular ATP levels has been shown to be crucial for heat-shock survival of stationary-phase batch cultures [24, 245]. High contents of the intracellular carbohydrate storage materials

trehalose and glycogen (>10 % of biomass dry-weight, Figure 2.7c) may have contributed to the extreme heat-shock tolerance of yeast cells grown in aerobic retentostat cultures by supplying the ATP that is required to combat heat stress (Figure 2.7c). In addition to intracellular trehalose concentrations, expression of the trehalose-metabolism related genes *TPS1*, *TPS2*, *ATH1* and *NTH1* increased substantially when retentostat cultures approached near-zero growth rates (Figure 2.7c, d) [245, 61]. The strong increase of intracellular trehalose concentrations in the aerobic retentostat cultures represents a marked difference with published data on anaerobic retentostats, in which intracellular trehalose levels were low and glycogen was the predominant storage carbohydrate [27].

Aerobic retentostat cultures retain a high glycolytic capacity at near-zero growth rates

Glycolysis, together with glucose transport, pyruvate decarboxylase and alcohol dehydrogenase, represents the pathway for alcoholic fermentation in *S. cerevisiae*. Respiratory cultures of this yeast maintain a high capacity for fermentative metabolism (fermentative capacity), which allows *S. cerevisiae* to rapidly increase its glycolytic flux in response to, for example, oxygen depletion and/or exposure to high sugar concentrations [316, 69, 321]. In aerobic glucose-limited chemostat cultures of the *S. cerevisiae* CEN.PK113-7D strain, fermentative capacity is essentially growth-rate independent at specific growth rates between 0.05 and 0.3 h^{-1}, [322]. The fermentative capacity of 7.5 $mmol_{ethanol}.g_X^{-1}.h^{-1}$ measured in the well with the fermentative capacity found previously at aerobic chemostats (D = 0.025 h^{-1}, Figure 2.8a), matched these higher specific growth rates [322]. After 18 days of aerobic retentostat cultivation, a significantly lower (p-value < 0.05) fermentative capacity of 4.5 mmol ethanol g_X^{-1} h^{-1} was measured (Figure 2.8a). The corresponding glucose-consumption rate was 45-fold higher than the specific rate of glucose consumption measured in the retentostat at this time point.

The decrease of the fermentative capacity in the aerobic retentostats coincided with a decrease of the transcript levels of a subset of glycolytic genes, some of which encoded major isoforms of glycolytic enzymes [292]. Expression levels of *HXK2* encoding hexokinase 2, first step in glycolysis, *FBA1* encoding the single fructose-bisphosphate aldolase, *PGK1* encoding the single phosphoglycerate kinase, *GPM1* encoding the major phosphoglycerate mutase, *ENO1* and *ENO2* paralogs encoding the two yeast enolases, *PYK1* also known as *CDC19*, encoding the major pyruvate kinase, last step in glycolysis, and *PDC1* encoding pyruvate decarboxylase 1 responsible for the first step in the fermentative pathway leading to ethanol, were stable during the initial phase of the retentostat cultures, but significantly and substantially decreased at growth rates below 0.002 h^{-1} (Figure 2.8b). Pair-wise comparison of transcriptome data for day 0 and day 16 of the retentostats (corresponding to specific growth rates of 0.025 and 0.0009 h^{-1}, respectively)

showed at least a twofold difference in expression levels of *HXK2*, *PGK1*, *GPM1*, *ENO2* and *PDC1*. Over-representation of binding sites for Rap1/Gcr1 in their promoter regions suggests that these transcription factors may be involved in their transcriptional regulation at near-zero growth rates. This hypothesis is further supported by the observation that 51 of the 145 gene targets of the transcription factor Rap1 were part of cluster 1 (Figure 2.4, Table 2.1). While we cannot exclude that decreased glucose transport was also involved in the reduction of fermentative capacity, no difference was observed in *HXT* gene expression at near-zero growth rates.

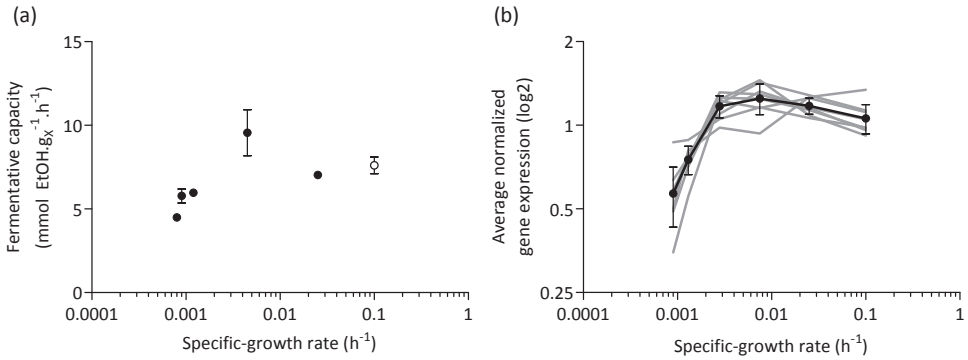

Figure 2.8: Fermentative capacity and expression levels of glycolytic genes in *S. cerevisiae* at near-zero growth rates. **a** Fermentative capacity, measured off-line as the specific rate of ethanol formation upon exposure of anaerobic cell suspensions to excess glucose. Fermentative capacity assays were performed on independent duplicate retentostat cultures, sampled at different time points. The open symbol corresponds to data from [322]. **b** Log2 average-normalized gene expression of *HXK2*, *FBA1*, *PGK1*, *GPM1*, *ENO1*, *ENO2*, *PYK1*, and *PDC1* during retentostat cultivation, plotted as a function of specific growth rate (see "Methods" section)

Discussion

Estimation of maintenance-energy requirements from aerobic retentostats

Initially developed by microbial ecologists to explore the 'twilight zone' between exponential growth and starvation [326, 327, 13, 12, 281, 280], the retentostat has recently seen a revival in studies on industrial microorganisms [99]. A key advantage of retentostat cultivation for application- inspired research is that it enables an accurate, quantitative estimation of microbial maintenance-energy requirements [99]. The conventional method for determining m_S does not measure, but estimates the specific rate of energy-substrate consumption in non-growing cultures, based on extrapolation of measurements on chemostat cultures that are actively growing (often at specific growth rates of 0.05 h^{-1} and above). Since, at these specific growth rates, substrate consumption for maintenance is relatively small as compared to the overall consumption rate of the energy substrate, m_S values calculated via this procedure are sensitive to small measurement errors [339, 99]. Moreover, chemostat-based estimation of m_S is based on the assumption that this parameter is growth-rate independent. Studies on several prokaryotes have shown that this assumption is not always valid and that, at extremely slow growth rates, several bacteria down-regulate ATP-turnover and thereby reduce substrate consumption for maintenance [13, 54].

Even at extremely low specific growth rates, the energetics of aerobic, glucose-limited retentostat cultures of *S. cerevisiae* could be adequately described with a growth-rate independent m_S. The same conclusion was drawn earlier for anaerobic, glucose-limited retentostat cultures of this yeast [28]. The value of m_S estimated from the aerobic retentostat cultures was 0.039 $mmol_{glucose}.g_X^{-1}.h^{-1}$. There are surprisingly few, invariably chemostat-based, estimates of the m_S of aerobically grown *S. cerevisiae*. Four decades ago, Rogers and Stewart [269] calculated an m_S of 0.07 $mmol_{glucose}.g_X^{-1}.h^{-1}$ based on aerobic chemostat cultures of a diploid *S. cerevisiae* strain, grown at pH 5.5 on a complex medium. This value is 75 % higher than the m_S found in the present study. Recently, based on aerobic chemostat cultures of the same haploid *S. cerevisiae* strain that is used in the present study, grown at pH 5.5, we estimated an m_S that was even 2.5-fold higher than calculated from the aerobic retentostats [192]. It should, however, be noted that the latter study used a growth medium that contained high concentrations of copper, which may have negatively affected cellular energetics.

Based on an assumed P/O ratio of 1.0 [333, 104, 285, 329], the maintenance requirement for ATP (m_{ATP}) estimated from the aerobic retentostat cultures was 0.63 $mmol_{ATP}.g_X^{-1}.h^{-1}$, a value 35 % lower than previously estimated based on anaerobic retentostat cultures of the same *S. cerevisiae* strain [28]. One possible explanation for this difference is that anaerobic growth indeed results in a higher m_S, for instance as a result of increasing proton leakage across membranes due to the presence of the fermentation products ethanol and acetic acid. Additionally, the anaerobic growth factor oleic acid, which is added to anaerobic chemostat media as the oleate ester Tween-80, has been shown to negatively affect growth energetics [331]. Alternatively, the assumed P/O ratio of 1.0 might be wrong. However, if this were the sole reason for the observed difference, the actual P/O ratio would have to be close to 1.7, which falls outside the range of estimates for this parameter from several quantitative physiological studies on *S. cerevisiae* [333, 104, 285, 329]. The lower m_{ATP} under aerobic conditions, makes it unlikely that the presence of oxygen or generation of ROS in respiration increases maintenance-energy requirements. Maintenance-energy requirements are well known to depend on growth conditions, for example on the presence of weak organic acids [248, 332, 1], and may additionally be strain dependent. The present study demonstrates that retentostat cultivation offers a robust way to estimate m_S. The large impact of this parameter on the performance of large-scale industrial fed-batch processes provides a strong impetus for using this, somewhat technically demanding, approach for determining and comparing maintenance-energy requirements of different production hosts under carefully controlled, industrially relevant experimental conditions.

Extreme heat-shock tolerance of aerobic retentostat cultures

In industrial processes, yeast cells face a variety of stresses, including high concentrations of CO_2 and other products, inhibitors in low-grade media, fluctuations in nutrient availability (e.g. during biomass recycling and 'repitching' in beer fermentation) and high as well as low temperatures [278, 120]. Here we show that aerobic retentostat cultures of *S. cerevisiae* grown at near-zero growth rates acquire an extreme resilience to heat shock. We recently reported that stationary-phase, glucose-grown aerobic batch cultures of *S. cerevisiae* are much more heat-shock tolerant than the corresponding anaerobic cultures [24]. This difference was tentatively attributed to the much faster transition from exponential growth to nutrient depletion in anaerobic batch cultures, which do not exhibit the second, slow growth phase on ethanol that is characteristic for aerobic glucose-grown batch cultures of *S. cerevisiae*. The hypothesis that this fast transition prevented a full induction of heat-shock tolerance was consistent with the earlier observation that anaerobic retentostat cultures, which undergo a slow transition to near-zero growth rates, exhibit a much higher heat-shock tolerance than anaerobic stationary-phase batch cultures [24]. The present study shows that, despite a very similar 'conditioning', the heat-shock tolerance of aerobic retentostat cultures is much more pronounced than in anaerobic retentostats (four to fivefold higher t_{50}, Figure 2.7a). Indeed, to our knowledge, the heat-shock tolerance of the aerobic retentostat

cultures is the highest reported to date for *S. cerevisiae*. These observations indicated that a smooth transition from exponential growth to (near-)zero growth in aerobic cultures provides an optimal conditioning for heat-shock tolerance in this yeast. Further research is required to assess whether this conclusion can be extended to include conditioning for other industrially relevant stresses, such as freezing/ drying, osmotic stress and oxidative stress.

Intracellular concentrations of trehalose and regulation of genes involved in its metabolism showed a remarkable correlation with the different levels of heat-shock tolerance in aerobic retentostats. Trehalose can act as an energy reserve, and has also been proposed to be directly involved in heat shock resistance [337, 155, 286]. However, recent evidence suggests that secondary, so called 'moon-lighting' functions of the trehalose-6-phosphate synthase Tps1, rather than trehalose itself, contribute to cell integrity during heat shock [245]. Additionally, different expression levels of other stress-induced proteins and different membrane composition, resulting from the inability of anaerobic cultures to synthesize unsaturated fatty acid and sterols, may contribute to the different heat-shock tolerance of aerobic and anaerobic *S. cerevisiae* cultures [331, 43, 346].

S. cerevisiae down-regulates glycolytic gene expression but maintains a high fermentative capacity at near-zero growth

Protein synthesis is the single most ATP-intensive process in living cells [298], and especially proteins with relatively high expression levels and short turnover times are expected to represent a significant metabolic burden to cells grown under severely calorie-restricted retentostat cultivation regimes. In actively growing *S. cerevisiae* cultures, glycolytic enzymes make up a significant fraction of the total cellular protein [71]. The half-life of most glycolytic proteins in *S. cerevisiae* grown in glucose-excess conditions range between 5 and 20 h, excluding Tdh1, Tdh2, Gpm2, and Eno1, for which half-lives of over 100 h have been determined [56]. These reported half-lives are much lower than the amount of time that the cells reside in retentostat; protein turnover of glycolytic proteins could therefore significantly contribute to the energy requirements of *S. cerevisiae* at near-zero growth. Under many conditions, this yeast exhibits a large overcapacity of the glycolytic pathway. Indeed, a substantial loss of fermentative capacity has previously been observed during prolonged cultivation of *S. cerevisiae* in aerobic, glucose-limited chemostat cultures (50 % after 100 generations) [149]. This loss was attributed to mutations that reduced the metabolic burden of synthesizing large amounts of glycolytic proteins. Although retentostat-grown cells retained a high glycolytic capacity, this decreased by ca. 40 % at extremely low specific growth rates. It is, however, unlikely that evolutionary adaptation caused this reduction in glycolytic capacity, since the average number of generations in the retentostat experiments was approximately three as a consequence of the biomass retention. Instead, the reduced mRNA levels of several

glycolytic genes suggest a transcriptional down-regulation of this key pathway at extremely low growth rates. Furthermore, glycolytic genes *PGK1* and *PYK1* that are considered to be constitutively expressed at high levels [242], displayed ca. twofold reduced transcript levels at near-zero growth (Figure 2.8), and shows that glycolytic promoters for the expression of (heterologous) proteins should be carefully selected.

Impact of oxygen availability on transcriptional reprogramming at near-zero growth rates

The specific growth rate profiles and experimental conditions employed in the aerobic retentostat cultures very strongly resembled those applied in a previous study on anaerobic retentostats of the same *S. cerevisiae* strain. Gene sets that showed a transcriptional response in these retentostat experiments showed a strong over-representation of growth-rate responsive genes identified by Fazio *et al.* [105]. These authors used chemostats, grown at specific growth rates of 0.03 h^{-1} and higher, to explore transcriptional responses under different aerobic and anaerobic nutrient-limitation. Of the set of 268 growth-rate-responsive genes identified in their study, 115 genes were also found to show growth-rate dependent expression at the very low specific growth rates studied in the aerobic and anaerobic retentostats (Additional file 3). Despite this clear overlap in transcriptional responses, the number of genes that showed a transcriptional response to the shift to near-zero growth rates was two-fold higher in the anaerobic retentostats than in the aerobic retentostats. As discussed above, ATP yields from respiratory and fermentative glucose dissimilation differ by a factor of approximately 8. As a consequence, at any specific growth rate, specific rates of glucose consumption (q_S) in anaerobic glucose-limited cultures are higher than in the corresponding aerobic cultures. For example, at a specific growth rate of 0.025 h^{-1}, the q_S in anaerobic glucose-limited chemostat cultures (2.3 $mmol.g_X^{-1}.h^{-1}$ (Additional file 4, [28]), was ca. eight-fold higher than in the corresponding aerobic chemostat cultures [0.3 $mmol.g_X^{-1}.h^{-1}$ (Additional file 4)]. Simple Monod-kinetics [217] predict that this difference should also be reflected in the concentration of the growth-limiting nutrient. Indeed, residual glucose concentrations in these anaerobic and aerobic cultures were 0.3 and 0.07 mM, respectively (Additional file 4 and [29]). The consequence of these differences is that aerobic and anaerobic retentostat cultures operate in a different range of residual glucose concentrations. Concomitantly, a set of previously identified glucose-responsive transcripts were specifically over-represented under anaerobiosis among genes which were transcriptionally up and down regulated with specific growth rate in retentostat cultures (Figure 2.6) [168]. This comparison identifies differences in glucose concentration as a major cause of the different transcriptome profiles of aerobic and anaerobic retentostat cultures.

Conclusion

Glucose-feeding regimes of retentostat cultures were optimized by model simulations to enable a first characterization of glucose-limited, aerobic cultures of *S. cerevisiae* during a smooth transition to extremely low specific growth rates. Quantitative analysis of these retentostats enabled the most accurate estimation to date of the growth-rate-independent maintenance-energy requirement of this yeast. Aerobic, glucose-limited retentostat cultures of *S. cerevisiae* showed a high viability, an extremely high heat-shock tolerance and retained an overcapacity of the fermentative pathway, thus illustrating the potential of this yeast to be developed for robust product formation in the absence of growth. This study shows that retentostat cultures, although technically demanding, offer unique possibilities for quantitative analysis of industrially relevant aspects of microbial physiology.

Methods

Yeast strain and shake-flask cultivation

The prototrophic strain *S. cerevisiae* CEN.PK113-7D (*MATa, MAL2-8c, SUC2*s [97, 228]) was used in this study. Stock cultures were grown in 500 mL shake flasks containing 100 mL YPD medium (10 $g.L^{-1}$ Bacto yeast extract, 20 $g.L^{-1}$ Bacto peptone and 20 $g.L^{-1}$ d-glucose). After addition of glycerol (20 % v/v) to early stationary-phase cultures, 1 mL aliquots were stored at −80 °C. Shake-flask precultures for chemostat experiments were grown in 500 mL shake flasks containing 100 mL of synthetic medium, set to pH 6.0 with 2 M KOH prior to autoclaving and supplemented with 20 $g.L^{-1}$ d-glucose [332]. These shake-flask cultures were inoculated with 1 mL of frozen stock culture and incubated in an orbital shaker at 200 rpm and at 30 °C.

Chemostat cultivation

Chemostat cultivation was performed in 2-liter bioreactors (Applikon, Delft, the Netherlands) equipped with a level sensor to maintain a constant working volume of 1.4 L. The culture temperature was controlled at 30 °C and the dilution rate was set at 0.025 h^{-1} by controlling the medium inflow rate. Cultures were grown on synthetic medium, prepared as described previously [332] but with the following modifications: the glucose concentration was increased to 20 $g.L^{-1}$ glucose ($C_{S,MC}$), the amount of trace-element and vitamin solutions were increased to 1.5 and 2 $mL.L^{-1}$ respectively [332], and 0.25 $g.L^{-1}$ Pluronic 6100 PE antifoaming agent (BASF, Ludwigshafen, Germany) was used. Fresh medium was supplied to the bioreactor from a 3-liter stirred mixing vessel (Applikon, Delft, The Netherlands) whose working volume (V_S) of 1.2 L was controlled by a level sensor and which was stirred continuously at 500 rpm. The mixing vessel was equipped with a sampling port. Medium was added to the mixinging reactor by automatic addition from a medium reservoir, with a flow rate (F_V) of 35 mL h^{-1} correspond to the dilution rate in the bioreactor. Cultures were sparged with air (0.5 vvm) and stirred at 800 rpm. Culture pH was kept constant at 5.0 by automatic addition of 10 % NH_4OH. Chemostat cultures were assumed to be in steady state when, after at least 6 volume changes, culture dry weight and the specific carbon dioxide production rates changed by less than 3 % over 2 consecutive volume changes. Steady-state carbon recoveries of chemostat cultures included in this study were above 98 %. Chemostat experiments performed at a dilution rate of 0.10 h^{-1} were performed as described above, with the following modifications: cultures were grown on synthetic medium [332] without modifications, with 7.5 $g.L^{-1}$ glucose, 1 $mL.L^{-1}$ trace elements solution, and 1 $mL.L^{-1}$ vitamin stock solution.

Retentostat cultivation

After reaching a steady-state in chemostat cultures, the retentostat phase was started by switching the reactor effluent to an outflow port equipped with an autoclavable Applisense filter assembly (Applikon), consisting of a hydrophobic polypropylene filter with a pore size of 0.22 µm and a stainless steel hollow filter support. Prior to autoclaving, the filter was wetted by overnight incubation in 96 % ethanol, and subsequently rinsed with a phosphate buffer saline solution (containing per 1 L demi-water: 8 g NaCl, 0.2 g KCl, 1.44 g Na_2HPO_4,

0.24 g KH_2PO_4, and HCl to adjust the final pH to 7.4). To control biomass accumulation, the medium reservoir connected to the mixing vessel (see above) was exchanged for a reservoir containing standard synthetic medium [332] supplemented with 7.5 $g.L^{-1}$ glucose ($C_{S,MR}$) and 0.25 $g.L^{-1}$ pluronic 6100 PE antifoam. Consequently, the concentration of growth-limiting substrate glucose entering the bioreactor [$C_{S,in}$ in ($g.L^{-1}$)] decreased over time [t in (h)] according to Equation 2.3.

$$C_{S,in} = (C_{S,MC} - C_{S,MR})e^{\frac{-F_V t}{V_S}} + C_{S,MR} \quad (2.3)$$

In this equation, $C_{S,MC}$ and $C_{S,MR}$ correspond to the glucose concentrations in the medium entering the mixing vessel during the chemostat and the retentostat phase respectively. During retentostat cultivaton, culture pH was controlled by automatic addition of 2 M KOH. Sampling frequency and sample volume were minimized to limit the impact of sampling on biomass accumulation inside the reactor. Culture purity was routinely checked by microscopy and by plating on synthetic medium agar containing 20 $g.L^{-1}$ glucose and 20 mM LiCl [65]. Full biomass retention was confirmed by plating filtered effluent on YPD containing 2 % (w/v) agar.

Predicting retentostat growth kinetics

Operational conditions to enable a smooth transition of the retentostat cultures to near-zero growth rates, were defined with a mathematical model that simulates growth kinetics of yeast during aerobic retentostat cultivation equation for biomass (Equation 2.4) was solved using MATLAB® (See Additional files 5, 6, 7). Essentially, the mass balance ode45 solver, by incorporating the substrate mass balance (Equation 2.5), with the Pirt relation [251] (Equation 2.1; Figure 2.1e).

$$\frac{dC_X}{dt} = \mu C_X \quad (2.4)$$

$$\frac{dC_S}{dt} = \frac{F_V}{V}(C + S, in - C_S) - q_S C_X \quad (2.5)$$

In these equations, C_X ($g.L^{-1}$) is the biomass concentration in the retentostat, μ (h^{-1}) is the specific growth rate, C_S ($g.L^{-1}$) is the residual substrate concentration, $C_{S,in}$ ($g.L^{-1}$) is the substrate concentration in the feed, F_V/V (h^{-1}) is the dilution rate, and q_S ($g.g_X^{-1}.h^{-1}$) is the biomass-specific glucose consumption rate. The specific substrate consumption rate can be described by the Pirt relation (Equation 2.1), in which $Y_{X/S}^{max}$ [$g.g^{-1}$] is the maximum biomass yield on glucose, and m_S ($g.g_X^{-1}.h^{-1}$) is the maintenance coefficient. Because retentostats were glucose limited and $C_{S,in} \gg CS_S$, the glucose concentration in the retentostat was assumed to be in a pseudo-steady state such that $dC_S/dt \approx 0$.

To run simulations, the model required inputs for variables V (bioreactor volume) (L), F_V (flow rate) ($L\ h^{-1}$), $C_{S,MC}$ ($g.L^{-1}$), $C_{S,MR}$ ($g.L^{-1}$), and V_S (L), and generated time-dependent profiles for biomass accumulation, glucose concentration in the feed, specific glucose consumption rates, and specific growth rates for a range of m_S values. The final operational conditions chosen for the retentostat experiments are indicated in Figure 2.2.

Regression analysis of biomass accumulation in retentostat

The maintenance-energy requirements and biomass-specific death rate of *S. cerevisiae* in aerobic retentostat were estimated from a least-squares regression analysis of data points for the biomass concentration (dry-weight) and the viable biomass concentration over time, using a MATLAB model (see Additional files 8, 9, 10, 11, 12). From these parameters, the specific growth rate and substrate consumption rates were derived. The curve shape was determined by the solution of the following ordinary differential equations with the smallest sum of square errors:

$$\frac{dC_{X_V}}{dt} = \mu C_{X_V} - k_d C_{X_V} \tag{2.6}$$

$$\frac{dC_{X_d}}{dt} = k_d C_{X_V} \tag{2.7}$$

$$\frac{dC_S}{dt} = \frac{F_V}{V}(C + S, in - C_S) - q_S C_{X_V} \tag{2.8}$$

In these equations, $C_{X,V}$ is the viable biomass concentration ($g.L^{-1}$), k_d is the death rate (h^{-1}). Equation 2.1 was used to define the specific substrate consumption rate (q_S). variables: V (L), F_V (L h^{-1}), $C_{S,MC}$ ($g.L^{-1}$), $C_{S,MR}$ ($g.L^{-1}$), The model required input for the biomass concentrations measured at different time points, and the following V_S (L) and $Y_{X/S}^{max}$. A value for m_S was approximated using parameter estimation. The time-dependent change of q_S and μ during the course of the retentostat followed from the regression analysis (see Additional files 8, 9, 10, 11, 12). To respect small differences in operational variables per experiment, regression analyses were performed separately on each independent retentostat experiment.

Determination of substrate, metabolites and biomass concentration

Prior to culture dry weight assays, retentostat samples were diluted in demineralized water. Culture dry weight was measured by filtering exactly 10 mL of an appropriate dilution of culture broth over pre-dried and pre-weighed membrane filters (pore size 0.45 µm, Gelman Science), which were then washed with demineralized water, dried in a microwave oven (20 min, 350 W) and reweighed. Supernatants were obtained by centrifugation of culture samples (3 min at 16,000 ×*g*) and analysed by high-performance liquid chromatography (HPLC) analysis on a Agilent 1100 HPLC (Agilent Technologies, Santa Clara, CA, USA), equipped with an Aminex HPX-87H ion-exchange column (BioRad, Veenendaal, The Netherlands), operated with 5 mM H_2SO_4 as the mobile phase at a flow rate of 0.6 $mL.min^{-1}$ and at 60 °C. Detection was by means of a dual-wavelength absorbance detector (Agilent G1314A) and a refractive-index detector (Agilent G1362A). Residual glucose concentrations in chemostat and retentostat cultures were analysed by HPLC after rapid quenching of culture samples with cold steel beads [209].

Gas analysis

The exhaust gas from chemostat cultures was cooled with a condenser (2 °C) and dried with a PermaPure Dryer (model MD 110-8P-4; Inacom Instruments, Veenendaal, the Netherlands) prior to online analysis of carbon dioxide and oxygen with a Rosemount NGA 2000 Analyser (Baar, Switzerland).

Viability

Samples from retentostat cultures were added to Isoton II diluent (Beckman Coulter, Woerden, Netherlands), pre-heated at 53 °C, to a final concentration of 10^7 cells.mL^{-1}, and incubated at 53 °C for at least 200 min. Loss of viability was monitored by sampling at 20 min intervals. Samples were immediately cooled on ice and subsequently stained with PI and analysed by flow cytometry as described above. Heat-shock resistance was represented by t_{50}, the incubation time at 53 °C that lead to a 50 % decrease in viability. To calculate t_{50}, survival curves were fitted with a sigmoidal dose–response curve in Graphpad® Prism, version 4.03.

Glycogen and trehalose assays

1 mL broth was sampled from the retentostat or chemostat and immediately added to 5 mL of cold methanol (−40 °C), mixed and centrifuged (4400×g, −19 °C, 5 min). The supernatant was decanted and pellets were resuspended in 5 mL cold methanol, pelleted again and stored at −80 °C. Pellets were then resuspended and diluted in 0.25 M Na_2CO_3, and further processed as previously described [241]. Trehalose was directly measured by HPLC. Glucose released from glycogen was measured by HPLC after overnight incubation of samples at 57 °C with α-amyloglucosidase (from *Aspergillus niger*, Sigma-Aldrich, Zwijndrecht, Netherlands).

Fermentative capacity assays

Samples containing exactly 100 mg dry weight of biomass from retentostat cultures were harvested by centrifugation at 5000 *×g* for 5 min, washed once, and resuspended in 10 mL fivefold concentrated synthetic centrifugation at 5000 *×g* for 5 min, washed once, and medium (pH 6, [332]). Subsequently, these cell suspensions were introduced into a 100 mL reaction vessel maintained at 30 °C, which was kept anaerobic with a constant flow (10 mL min^{-1}) of water-saturated CO_2. After addition of 40 mL demineralized water and 10 min of pre-incubation, 10 mL glucose solution (100 g L^{-1}) was added, and 1 mL samples were taken at 5 min intervals. After centrifugation, ethanol concentrations in supernatants were determined by HPLC. Fermentative capacity, calculated from the increase in ethanol concentration during the first 30 min of the experiments, was expressed as $mmol_{ethanol\ produced} \cdot g_{dry\ yeast\ biomass}{}^{-1} \cdot h^{-1}$. During the assay period, the increase in biomass concentration was negligible, and the increase in ethanol concentration was linear with time and proportional to the amount of biomass added.

Transcriptome analysis

Microarray analysis was performed with samples from independent triplicate steady-state chemostat cultures and duplicate retentostat cultures of *S. cerevisiae* strain CEN.PK113-7D sampled at 5 time points, comprising a total dataset of 13 microarrays. Sampling for transcriptome analysis was carried out by using liquid nitrogen for rapid quenching of mRNA turnover [247]. Prior to RNA extraction, samples were stored in a mixture of phenol/chloroform and TEA buffer at −80 °C. Total RNA extraction, isolation of mRNA, cDNA synthesis, cRNA synthesis, labeling and array hybridization was performed as described previously [213], with the following modifications. The quality of total RNA, cDNA, aRNA and fragmented aRNA was checked using an Agilent Bioanalyzer 2100 (Agilent Technologies,

Santa Clara, CA). Hybridization of labelled fragmented aRNA to the microarrays and staining, washing and scanning of the microarrays was performed according to Affymetrix instructions.

The 6383 yeast open reading frames were extracted from the 9335 transcript features on the YG-S98 microarrays. To allow comparison, all expression data were normalized to a target value of 240 using the average signal from all gene features. To eliminate variation in genes that are essentially not expressed, genes with expression values below 12 were set to 12 and the genes for which the average expression was below 20 for all 13 arrays were discarded. The coefficient of variation of the mean transcript data of replicate retentostats was approximately 10 %, similar to the reproducibility usually observed in replicate steady state chemostat cultures [68]. The expression of housekeeping genes *ACT1*, *HHT2*, *SHR3*, *PDA1*, *TPI* and *TFC1* [307] remained stable for both strains at all tested growth rates (average coefficient of variation 11 ± 4 % see Additional file 13).

To perform a differential expression analysis based on gene expression profiles across the different growth rates, EDGE version 1.1.291 [200] was used with growth rate as covariate. Genes with expression profiles with a p-value below 0.01 were considered to significantly correlate with growth rate, and were clustered with k-means clustering using consensus clustering (GenePattern 2.0, Broad Institute, [261]). For display of specific growth rate dependent expression profiles, expression values were normalized per gene by dividing single expression values by the average expression value at all different growth rates. Averages ± standard deviation of these average-normalized values are shown in Figures 2.5,2.6,2.7 and 2.8.

Gene expression clusters were analysed for over-representation of functional annotation categories from the Munich Information Centre for Protein Sequences (MIPS) database (http://mips.gsf.de/genre/proj/yeast), the Gene Ontology (GO) database (http://geneontology.org/) and transcription factor binding (TF) according to [132], based on the hypergeometric distribution analysis tool described by Knijnenburg *et al.* [163]. Additional functional categories that were searched for enrichment originate from [117, 91, 334, 119] and are listed in Additional file 14.

Acknowledgements

We would like to thank Corinna Rebnegger, Rinke van Tatenhove-Pel and Pilar de la Torre Cortes for assistance in the experiments.

Availability of data

The transcriptome data have been made available at the GEO data repository under accession number GSE77842.
The supplementary files are available online at the journal's website: https://doi.org/10.1186/s12934-016-0501-z

CHAPTER 3

Physiological responses of *Saccharomyces cerevisiae* grown under industrially-relevant conditions: slow growth, low pH and high CO_2 levels

Xavier D.V. Hakkaart
Yaya Liu
Mandy B. Hulst
Anissa el Massoudi
Eveline J. Peuscher
Jack T. Pronk
Walter M. van Gulik
Pascale Daran-Lapujade

This chapter has been submitted for publication in Biotechnology and Bioengineering.

Abstract

Engineered strains of ***Saccharomyces cerevisiae*** are used for industrial production of succinic acid. Optimal process conditions for dicarboxylic-acid yield and recovery include slow growth, low pH and high CO_2. To quantify and understand how these process parameters affect yeast physiology, this study investigates individual and combined impacts of low pH (3.0) and high CO_2 (50 %) on slow-growing chemostat and retentostat cultures of the reference strain ***S. cerevisiae*** CEN.PK113-7D. Combined exposure to low pH and high CO_2 led to increased maintenance-energy requirements and death rates in aerobic, glucose-limited cultures. Further experiments showed that these effects were predominantly caused by low pH. Growth under ammonium-limited, energy-excess conditions did not aggravate or ameliorate these adverse impacts. Despite the absence of a synergistic effect of low pH and high CO_2 on physiology, high CO_2 strongly affected genome-wide transcriptional responses to low pH. Interference of high CO_2 with low-pH signaling is consistent with low-pH and high-CO_2 signals being relayed via common (MAPK-)signaling pathways, notably the cell wall integrity (CWI), high osmolarity glycerol (HOG) and calcineurin pathways. This study highlights the need to further increase robustness of cell factories to low pH for carboxylic-acid production, even in organisms that are already applied at industrial scale.

Introduction

Dicarboxylic acids are attractive platform molecules for production of a wide range of chemicals [20]. High-yield microbial conversion of glucose to dicarboxylic acids can be achieved through the reductive branch of the TCA cycle and requires elevated concentrations of dissolved carbon dioxide (CO_2) to promote carboxylation of pyruvate or phosphoenolpyruvate to oxaloacetate [9, 354, 356]. Cost efficiency and sustainability of industrial dicarboxylic-acid production can be increased by using culture pH values well below pKa_1 of the product (pKa_1 values of succinic, malic and fumaric acid are 4.16, 3.51 and 3.03 respectively). Production of the free acid prevents the need for co-production of large quantities of gypsum [3, 53]. In contrast to most carboxylic-acid producing prokaryotes, the yeast *Saccharomyces cerevisiae* can withstand both high CO_2 [8, 92, 263] and low pH [78, 331]. However, although *S. cerevisiae* grows at high CO_2, reduced biomass yields have been reported for respiring *S. cerevisiae* cultures grown at CO_2 values of 50 % and 79 % [8, 92, 263]. Similarly, *S. cerevisiae* can grow at pH values as low as pH 2.5, but only at significantly reduced specific growth rates [38, 78, 79, 98, 234].

Heterotrophic microorganisms dissimilate their carbon and energy substrate to supply ATP for biomass formation and for cellular maintenance [250, 251]. In yeast strains engineered for dicarboxylic-acid production, product formation and export costs ATP and therefore directly competes with growth and maintenance processes for ATP supply [3, 150, 324]. Slow growth in fed-batch cultures (typically at specific growth rates below 0.05 h^{-1}) limits consumption of substrate for biomass formation, which benefits product yields. However, a trade-off of this strategy is that the fraction of the energy substrate allocated to cellular maintenance increases with decreasing specific growth rate, thereby leaving less substrate available for energy-dependent product formation [138, 212, 341]. Despite its industrial relevance, quantitative understanding of maintenance-related processes in *S. cerevisiae* and their sensitivity to industrially relevant process conditions is far from complete. Previous studies showed that, while growth-rate independent [28, 340], the maintenance-energy requirement (m_S; $mmol_{glucose}.g_{biomass}^{-1}.h^{-1}$) of *S. cerevisiae* can be affected by the cultivation conditions [173, 191, 340]. For example, growth at pH 2.5 substantially reduces the maximum specific growth rate in batch cultures [38, 78, 79, 234] and increases activity of the plasma-membrane proton pumps, suggesting that low pH also affects m_S [38, 98]. Moreover, even under mildly acidic conditions, the presence of weak, membrane-permeable organic acids strongly increases energy-requirements for intracellular pH homeostasis [1, 331].

Although elevated CO_2 and low pH are relevant industrial process conditions for dicarboxylic-acid production and have both been reported to adversely affect yeast physiology, their effects on maintenance-energy requirements and viability of slow growing *S. cerevisiae* cultures have not yet been quantitatively analyzed. To address this knowledge gap, a non-producing *S. cerevisiae* laboratory strain was grown at low and near-zero specific growth rates using a combination of glucose-limited chemostat and retentostat cultures, at a low pH (pH 3) and elevated CO_2 concentrations (50 % CO_2). Additionally, cultures were grown under ammonium-limited, energy-excess conditions at low pH. Quantitative analysis of rates, yields and culture viability was used to dissect physiological impacts of low pH and high CO_2. Furthermore, transcriptome analysis was employed to elucidate regulatory responses to these conditions.

Results

Low pH and high CO_2 levels cause increased death rate and maintenance-energy requirements in glucose-limited retentostat cultures of *S. cerevisiae*

The physiological responses of the *S. cerevisiae* laboratory strain CEN.PK113-7D under conditions relevant for industrial dicarboxylic acid production (aerobic, 50 % CO_2, pH 3.0) were investigated at near-zero growth rates in retentostat cultures. In these retentostat cultures, a filter in the effluent line enabled full biomass retention [99]. At a constant feed rate of glucose, biomass accumulates and the supplied substrate per cell gradually decreases and growth ceases until virtually all substrate is used to fulfill maintenance-energy requirements [28, 340]. Because the industrially relevant conditions applied in this study were expected to increase m_S relative to standard laboratory conditions (i.e., pH 5.0 and sparging with air, [173, 340], the asymptotic decrease of the glucose concentration in the feed, as previously applied for laboratory conditions [340], was not applied (Figure 3.1A, B). Instead, the substrate concentration in the feed was kept constant. This higher rate of substrate supply enabled the culture dry weight to accumulate to higher concentrations (Figure 3.1C, D). Culture viability, based on membrane integrity (PI staining) and reproductive capacity (CFU) was substantially lower under the industrially relevant conditions that under standard laboratory conditions (Figure 3.11 E, F). Furthermore, the lower viable biomass concentration at near-zero growth rates in the retentostat cultures grown under industrially relevant conditions indicated a higher m_S than under laboratory conditions.

Time-dependent regression analysis of substrate and product concentrations was previously shown to enable accurate estimates of specific growth rate, specific substrate-consumption rate, first-order death rate and mS in carbon and energy limited yeast retentostat cultures [340]. In contrast to growth under standard laboratory conditions, growth under industrially relevant conditions caused a strong decrease of the viable biomass concentration after the first 10 days of cultivation, which prevented use of regression analysis for data obtained beyond day 10 (Figure 3.1C, G).

Figure 3.1: *See next page.* Physiological characterization of *S. cerevisiae* CEN.PK113-7D in duplicate glucose-limited, aerobic retentostat cultures, grown at pH 3 and 50 % CO_2 (left column) and in quadruplicate cultures grown under reference conditions (pH 5, 0.04 % CO_2; right column)[340]. A & B: Glucose concentration in influent during retentostat cultivation. C & D: Biomass dry weight (open symbols) and viable biomass dry weight estimated by propidium iodide (PI) staining (closed symbols). The vertical line indicates the time until which data points were included in regression analysis for biomass accumulation (see main text for detailed explanation). E & F: Viability of retentostat cultures based on PI staining (closed symbols) and Colony Forming Units (CFU) (open symbols). G & H: Regression-based biomass-specific growth rate (μ, gray lines) and biomass-specific glucose uptake rate (black lines) during the first 10 d of retentostat cultivation. Viable biomass concentrations used for regression analysis were based on PI staining. The vertical line indicates the time until which data points were included in the regression analysis for biomass accumulation (see main text for detailed explanation).

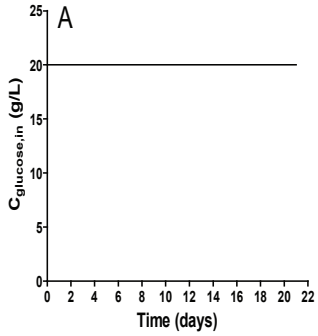
A
$C_{glucose,in}$ (g/L)
Time (days)

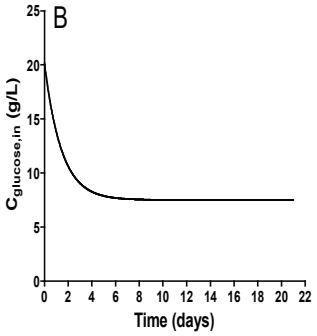
B
$C_{glucose,in}$ (g/L)
Time (days)

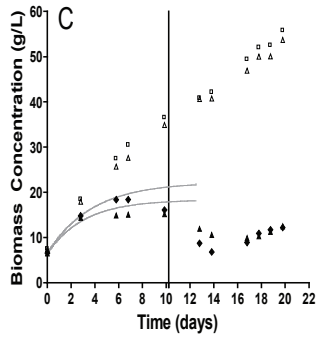
C
Biomass Concentration (g/L)
Time (days)

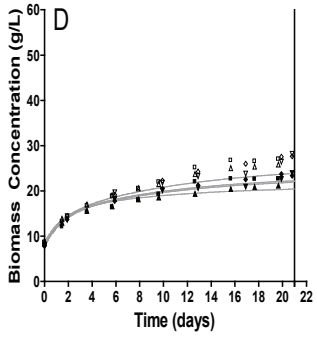
D
Biomass Concentration (g/L)
Time (days)

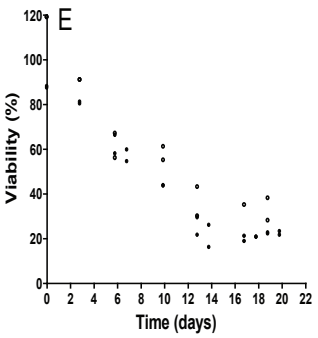
E
Viability (%)
Time (days)

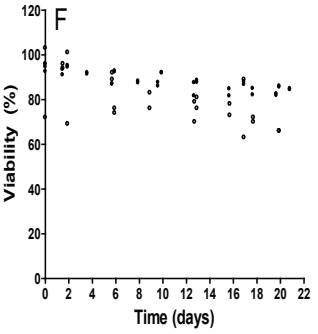
F
Viability (%)
Time (days)

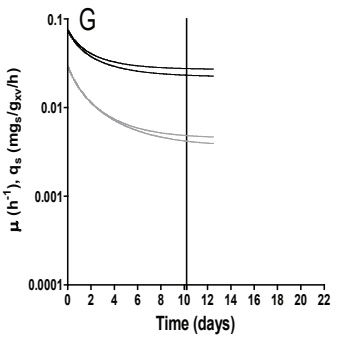
G
μ (h^{-1}), q_s ($mg_s/g_{xv}/h$)
Time (days)

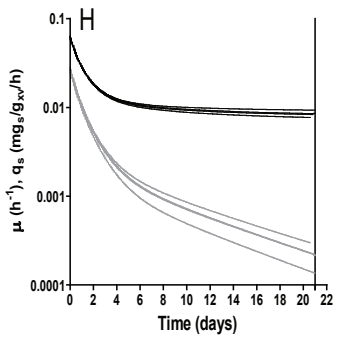
H
μ (h^{-1}), q_s ($mg_s/g_{xv}/h$)
Time (days)

Regression analysis showed that, although higher than the lowest growth rate reached under laboratory conditions (0.0008 h^{-1}, Figure 3.1H), the specific growth rate of retentostat cultures grown under the industrially relevant conditions was already extremely low at 10 days of cultivation (0.0045 ± 0.0003 h^{-1}, Figure 3.1G). This difference was partially due to an 8-fold higher death rate under industrially relevant conditions than under laboratory conditions (0.0039 ± 0.0005 h^{-1} vs 0.00047 h^{-1}; Figure 3.2). Moreover, the m_S calculated by regression analysis was more than 2-fold higher under industrially relevant conditions (0.0908 ± 0.0085 $mmol_S.g_{X,viable\ biomass}^{-1}.h^{-1}$ vs 0.039 ± 0.003 $mmol_S.g_{X,viable\ biomass}^{-1}.h^{-1}$, Figure 3.2). Throughout retentostat cultivation, residual glucose concentrations remained between 0.01 and 0.07 mM. These results demonstrate that the combination of an extremely low growth rate, low pH and high CO_2 has marked adverse effects on the physiology of *S. cerevisiae*.

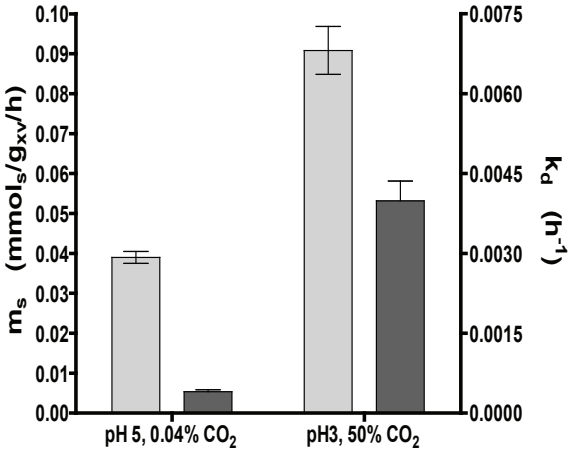

Figure 3.2: Maintenance-energy requirements and first-order death rate in pH 5, 0.04 % CO_2 reference conditions and in industrially relevant pH 3, 50 % CO_2 conditions in carbon-limited retentostat cultures of *S. cerevisiae* CEN.PK113-7D. These parameters were derived based on regression analysis of the biomass and viable biomass accumulation (see materials and methods and Appendix 1 for details). Light grey bars and dark grey bars present maintenance energy requirements and first-order death rates, respectively.

High maintenance-energy requirements and death rates result from low pH rather than high CO_2 levels

To further explore the extreme physiological response of *S. cerevisiae* in retentostat cultures grown under industrially relevant conditions, the effects of low pH and high CO_2 concentration at low growth rates were investigated separately and in combination. These experiments were performed in glucose-limited chemostat cultures grown at the same dilution rate (0.025 h^{-1}) as the retentostats, but without cell retention (Figure 3.1). In energy-limited chemostat cultures grown at a fixed dilution rate, differences in biomass yield ($Y_{X/S}$) can provide strong indications for differences in maintenance-energy requirements [173]. Under laboratory conditions (low CO_2, pH 5) at 0.025 h^{-1}, *S. cerevisiae* invests ca. 20 % of the consumed glucose in cellular maintenance [340], resulting in a biomass yield of 0.416 ± 0.005 $g_X.g_S^{-1}$. Despite small deviations in medium composition (higher concentrations of biotin and iron

sulfate in the present study), the biomass yield of 0.419 ± 0.009 $g_X.g_S^{-1}$ measured in the present study was entirely consistent with the yield observed by Vos *et al.* [340].

Irrespective of culture pH, increasing CO_2 levels to 50 % did not significantly affect biomass yields at a dilution rate of 0.025 h^{-1} relative to those observed under standard laboratory conditions (Table 3.1). Conversely, growth at pH 3 led to a significantly lower biomass yield than at pH 5, both at standard and at elevated CO_2 levels (7.4 % and 9.7 % decrease, respectively; 0.419 ± 0.009 g_x/g_s vs 0.388 ± 0.005 $g_X.g_S^{-1}$; $p < 0.001$ for pH 5 vs pH 3 when sparged with compressed air and 0.411 ± 0.006 $g_X.g_S^{-1}$ vs 0.371 ± 0.004 $g_X.g_S^{-1}$; $p < 0.02$ for pH 5 vs pH 3 at 50 % CO_2). These results showed that the higher m_S in retentostat cultures grown at high CO_2 and low pH resulted from the low pH rather from the high CO_2.

Measurements, by three different methods (CFU, PI and CFDA staining, Table 3.1 and Appendix 2), showed that, irrespective of CO_2, low pH led to a strongly reduced viability of glucose-limited chemostat cultures. Conversely, increasing the CO_2 levels did not significantly affect culture viability. Assuming that cells measured as non-viable did not contribute to biomass formation or glucose consumption, specific rates were corrected for viability based on PI staining, resulting in higher specific growth rates (μ) and biomass-specific substrate uptake rates (Table 3.1).

Table 3.1: Physiology of *S. cerevisiae* CEN.PK113-7D in aerobic glucose-limited chemostat cultures grown at a dilution rate of 0.025 h^{-1}. 'Replicates' indicates the number of biological replicates. Superscripts indicate the number of biological replicates for individual analyses when these deviate from the number presented under 'Replicates'. ND: not determined. Biomass specific rates (q-values) were calculated based on viable biomass (xv), estimated by PI staining. At both CO_2 values, cultures at pH 3 and at showed oscillations in dissolved oxygen, exhaust CO_2 and exhaust oxygen levels.

pH **CO_2 in inlet gas (%)**	**5** **0.04**	**5** **50**	**3** **0.04**	**3** **50**
Culture replicates	4	5	3	4
D (h^{-1})	0.026 ± 0.001	0.025 ± 0.001	0.025 ± 0.001	0.025 ± 0.000
Biomass yield ($g_X.g_S^{-1}$)	0.419 ± 0.009	0.409 ± 0.005	0.388 ± 0.005	0.372 ± 0.004
Viability PI (%)	97 ± 1	96 ± 4	71 ± 1	85 ± 3
Viability CFDA (%)	96 ± 2	98 ± 0	81 ± 2	92 ± 2
Viability CFU-FACS (%)	92 ± 1^2	85 ± 10^5	73 ± 2^2	74 ± 1^2
μ (h^{-1})	0.027 ± 0.001	0.026 ± 0.000	0.035 ± 0.001	0.03 ± 0.001
$q_{glucose}$ ($mmol.g_{XV}^{-1}.h^{-1}$)	0.358 ± 0.016	0.357 ± 0.008	0.508 ± 0.011	0.443 ± 0.023
q_{O2} ($mmol.g_{XV}^{-1}.h^{-1}$)	1.019 ± 0.087	ND	1.361 ± 0.102	ND
q_{CO2} ($mmol.g_{XV}^{-1}.h^{-1}$)	1.042 ± 0.094	ND	1.394 ± 0.138	ND
$C_{glucose}$ ($g.L^{-1}$)	0.011 ± 0.003	0.013 ± 0.001	0.005 ± 0.003	0.010 ± 0.006
Carbon recovery (%)	100.0 ± 4.1	ND	93.0 ± 4.5	ND
RQ (q_{CO2}/q_{O2})	1.023 ± 0.016	ND	1.024 ± 0.043	ND
Glycogen content ($mg.g_X^{-1}$)	35.3±3.3	32.6±2.2	46.4±3.2^2	30.4±1.9
Trehalose content ($mg.g_X^{-1}$)	19.4±3.7	18.3±1.94	12.64±1.1^2	9.7±1.7

Growth under ammonium-limited, energy-excess conditions does not reduce death rates at low pH and increases non-growth associated glucose consumption rates

Since glucose acts as energy substrate as well as carbon source, the high death rates and maintenance-energy requirements observed at pH 3 might reflect a cellular energy shortage. Therefore, physiological responses of *S. cerevisiae* were also investigated in near-zero growth rate retentostat cultures grown at pH 3 and pH 5 under ammonium-limited, glucose-excess conditions. These cultures were started from ammonium-limited chemostat cultures grown at a low dilution rate of 0.023 h^{-1}. The biomass concentration increased during the first 15 days of retentostat cultivation, after which it stabilized (Figure 3.3C). Culture viability in ammonium-limited chemostats grown at pH 3 (50 %; Figure 3.3E) was very low in comparison with viabilities observed in glucose- and ammonium-limited chemostat cultures grown at pH 5 (Figures 3.1F and 3.3F) and in glucose-limited cultures grown at pH 3 (Figure 3.1E). During ammonium-limited retentostat cultivation at pH 3, the total viable biomass concentration did not increase significantly (Figure 3.3C). Based on biomass and viability measurements towards the end of the retentostat experiments, the specific growth rate had decreased to 0.0006 ± 0.0001 h^{-1} (Table 3.2)) As the viable biomass concentration remained virtually constant during retentostat cultivation, this growth rate equaled the death rate. The combination of nitrogen-limited growth and its associated excess availability of glucose clearly did not prevent adverse effects of low pH at near-zero growth rates. However, the substantially lower death rate in ammonium-limited retentostats indicated that growth under energy-source excess enabled *S. cerevisiae* to better survive prolonged exposure to low-pH stress than energy-source-limited growth.

Throughout the ammonium-limited retentostat cultivation, residual glucose concentrations remained above 10 $g.L^{-1}$, confirming that cultures were not energy-limited. Ethanol concentrations remained below 15 $g.L^{-1}$ and, therefore, below reported toxic levels [113]. Residual ammonium concentrations were below detection limit (0.02 $mg.L^{-1}$) in all samples. In ammonium-limited chemostat cultures 93 % of the supplied nitrogen was recovered in biomass. In contrast, only 35-40 % of supplied nitrogen was used for biomass formation after prolonged ammonium-limited retentostat cultivation. The remaining 60-65 % of the supplied nitrogen was lost in the effluent as proteins and peptides (Table 3.2).

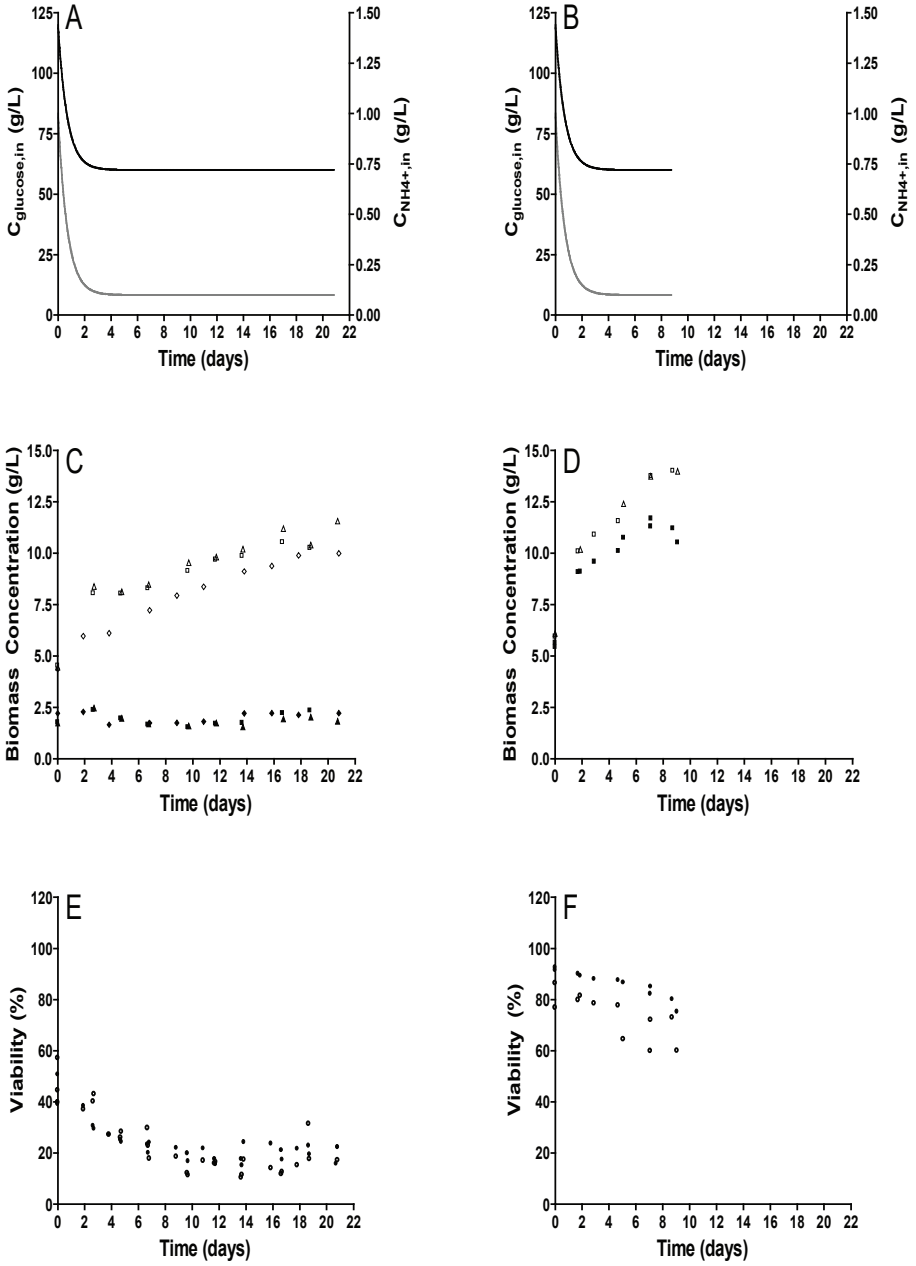

Figure 3.3: Physiological characterization of *S. cerevisiae* CEN.PK113-7D in triplicate nitrogen-limited retentostat cultures at pH 3 (left column) and in duplicate reference condition at pH 5 [191]. A & B: Medium glucose (black line) and nitrogen (gray line) concentration during retentostat cultivation. C & D: Biomass accumulation for cell dry weight (open symbols) and viable biomass (closed symbols) quantified by PI staining. E & F: Viability of retentostat cultures based on PI staining (closed symbols) and Colony Forming Units (CFU; open symbols)

Table 3.2: Physiology of *S. cerevisiae* CEN.PK113-7D in aerobic ammonium-limited chemostat and retentostat cultures. Data present the average and standard deviation of triplicate experiments from steady-state (chemostat) and near-zero growth (retentostat) cultures. q's indicate biomass specific values. Subscripts indicate the considered compound. X: biomass; byproducts: the sum of acetate, succinic acid, lactic acid and glycerol; N,in: nitrogen consumed; N,out: sum of nitrogen excreted in the form of protein and free amino acids; N,X: nitrogen conserved in biomass. BDL: below detection limit.

Culture Phase **pH**	**Chemostat** **3**	**Retentostat end** **3**
Culture replicates	3	3
D (h^{-1})	0.023 ± 0.004	0.023 ± 0.004
μ (h^{-1})	0.053 ± 0.001	0.0006 ± 0.0001
Yield ($g_X.g_{glucose}^{-1}$)	0.048 ± 0.002	0.0016 ± 0.0002
Viability PI (%)	43 ± 5	20 ± 3
Viability CFDA (%)	46 ± 3	12 ± 3
Viability CFU (%)	47 ± 7	17 ± 6
qglucose ($mmol.g_{Xv}^{-1}.h^{-1}$)	6.1 ± 0.4	2.2 ± 0.2
q_{O2} ($mmol.g_{Xv}^{-1}.h^{-1}$)	2.00 ± 0.3	0.83 ± 0.16
q_{CO2} ($mmol.g_{Xv}^{-1}.h^{-1}$)	12.5 ± 0.8	4.6 ± 0.2
$q_{ethanol}$ ($mmol.g_{Xv}^{-1}.h^{-1}$)	10.2 ± 0.6	4.1 ± 0.5
$q_{byproduct}$ ($mmol.g_{Xv}^{-1}.h^{-1}$)	0.36 ± 0.01	0.18 ± 0.06
$Y_{ethanol/glucose}$ ($mol.mol_s^{-1}$)	1.71 ± 0.03	1.83 ± 0.09
$C_{glucose}$ ($g.L^{-1}$)	33.77 ± 1.09	11.22 ± 0.15
Carbon recovery (%)	99 ± 1	100 ± 2
RQ value (q_{CO2}/q_{O2})	6.8 ± 1.2	5.9 ± 1.0
$q_{N,in}$ ($mmol_N.g_{Xv}^{-1}.h^{-1}$	0.079 ± 0.002	0.0034 ± 0.000
$q_{N,out}$ ($mmol_N.g_{Xv}^{-1}.h^{-1}$	0.007 ± 0.000	0.0022 ± 0.000
$q_{N,X}$ ($mmolN/g_{xv}/h$)	0.073 ± 0.001	0.0014 ± 0.000
C_N ($g.L^{-1}$)	BDL	BDL
Nitrogen-recovery (%)	101.0 ± 1.0	106 ± 9
Glycogen content ($mg.g_x^{-1}$)	22 ± 2.0	66 ± 1.8
Trehalose content ($mg.g_x^{-1}$)	35 ± 0.3	20 ± 1.0
Biomass composition	C1H1.87O0.63N0.089P0.012S0.0016	C1H1.85O0.59N0.061P0.012S0.0012

The non-constant death rate of the nitrogen-limited retentostat cultures prevented use of the regression model to estimate maintenance-energy requirements. Instead, metabolic flux analysis (MFA) was used to derive and compare rates of ATP turnover in the absence of growth at the end of the glucose- and ammonium-limited retentostat experiments (vertical line in Figure 3.1C,D and final points in Figure 3.3C, D; input parameters used for the MFA are specified in Appendix 3. Because the biomass protein content was much lower in the ammonium-limited cultures [191], a condition-dependent biomass composition (Table 3.2) was a key input to the MFA-model. For the glucose-limited cultures, a previously reported biomass composition for glucose-limited chemostat cultures of the same strain was used (D = 0.022 h^{-1}, [176]). Additionally, the *in vivo* P/O-ratio was assumed to be 1.0 [333]. The ATP hydrolysis rate derived from the MFA model for glucose-limited cultures at pH 5 closely matched the m_{ATP} derived from the regression model (Figure 3.2, Figure 3.4). Under glucose limitation, a decrease in pH from 5 to 3 resulted in a 3.7 fold increase of the calculated ATP-hydrolysis rate at near-zero growth rates (0.58 and 2.13 $mmol_{ATP}.g_{X,viable}^{-1}.h^{-1}$, respectively). The differences between the ATP-hydrolysis rate at pH 3 derived from MFA (Figure 3.4) and the m_{ATP} from the regression model at pH 3 under glucose-limitation (Figure 3.2,

estimated with a P/O-ratio of 1.0) can be explained by the different method of parameter estimation and the residual growth due to the high death rates under this condition. At pH 3, this non-growth associated rates of ATP turnover was 2.9 fold higher in ammonium-limited retentostats (6.14 $mmol_{ATP}.g_{X,viable}^{-1}.h^{-1}$) than in the corresponding glucose-limited cultures (Figure 3.4).

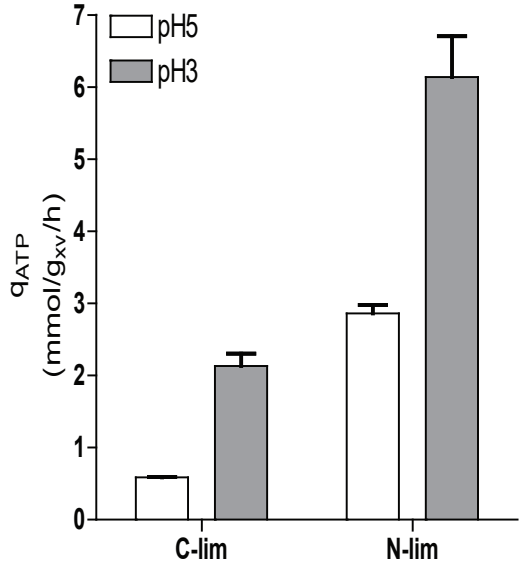

Figure 3.4: Maintenance energy requirements (glucose-limited cultures; C-lim) and non-growth associated energy requirements (ammonium-limited cultures; N-lim) of *S. cerevisiae* CEN.PK113-7D during growth at pH 5 and at pH 3 in retentostat cultures based on metabolic flux analysis. White bars: pH 5, grey bars: pH 3 (and 50 % CO_2 for glucose-limited cultures). Data for glucose-limited cultures grown at pH 5 are from Vos *et al.* 2016 [340], data for ammonium-limited cultivation at pH 5 are from Liu *et al.* 2019 [191].

Growth at low pH and/or high CO_2 cause extensive transcriptional rearrangements

Transcriptional responses of glucose-limited chemostat cultures to high CO_2, low pH or both was explored to gain further insight in the mechanisms underlying the reduced biomass yield, the increased maintenance energy requirements and increased cell death under industrially relevant conditions. Pair-wise differential gene-expression analysis against the reference at pH 5 and 0.04 % CO_2 (absolute fold-change (FC) >2 and false-discovery rate (FDR) < 0.005, see Materials and Methods) revealed large differences in yeast transcriptional responses to the different conditions for 50 % CO_2 alone (42 genes, blue), pH 3 alone (259 genes, yellow) and 50 % CO_2 and pH 3 combined (145 genes, green) (Figure 3.5A, Greek

letters correspond with subsets in Figure 3.5B).

To investigate common and specific responses to high CO_2 and low pH conditions, the corresponding sets of differentially expressed genes were analyzed (Figure 3.5B, sections in Venn diagram denoted with α-η). A set of 42 genes that were differentially expressed in response to high CO_2 only (Figure 3.5B, αβζ) did not reveal a clear enrichment for specific functional categories. The largest response was observed at pH 3, with 267 differentially expressed genes (Figure 3.5B, δεζ). This gene set showed an overrepresentation of genes involved in plasma-membrane and cell-wall organization (Figure 3.5C, δεζ, yellow). The same functional categories were overrepresented among 154 genes that were differentially expressed (Figure 3.5B, βγδ) when high CO_2 and low pH were combined (Figure 3.5C, βγδ, green).

A set of 13 genes that, irrespective of culture pH, were differentially expressed in response to high CO_2 (Figure 3.5B,β) consisted of genes involved in gluconeogenesis (*ICL1*, *PKC1* and *FBP1*, all upregulated at high CO_2), while *NCE103*, encoding carbonic anhydrase, was down-regulated. Among 48 genes that were differentially expressed in response to low pH, both at high and low CO_2 (Figure 3.5B,δ), genes involved in ammonium transport and plasma-membrane processes were overrepresented (Figure 3.5C, δ). This set comprised 18 genes that were commonly up-regulated, 18 that were commonly down-regulated and 12 genes that displayed opposite responses to low pH at low and high CO_2 (see Appendix 4). Of the latter 12 genes, five (*PIR4*/*YJL158C*, *TIP1*/*YBR067C*, *SVS1*/*YPL163C*, *SRL1*/*YOR247W*, *TIR2*/*YOR010C*) encode cell-wall proteins, with *PIR4*, *TIP1*, *SRL1* and *TIR2* described as mannoproteins. An unexpectedly large transcriptional response, involving no fewer than 598 genes (Figure 3.5A), was observed in response to high CO_2 at low pH. Of this large set of genes, many encoded proteins involved in processes related to cell wall, cell membrane and ergosterol biosynthesis (Appendix 4).

The scale of transcriptional response to glucose-limited retentostat cultivation at near-zero growth rates was similar for laboratory and industrial conditions, with 569 and 531 differentially expressed genes, respectively (Figure 3.5D). Notable differences between laboratory and industrial conditions included the regulation of *PDR12*, which encodes a plasma-membrane transporter in weak organic acid tolerance [249, 313], that responded in opposite directions under the two conditions, and the enrichment of genes encoding extracellular proteins and/or involved in cell wall processes among the genes whose expression was positively correlated with increasing growth rate under laboratory conditions but not industrial conditions (Appendix 5).

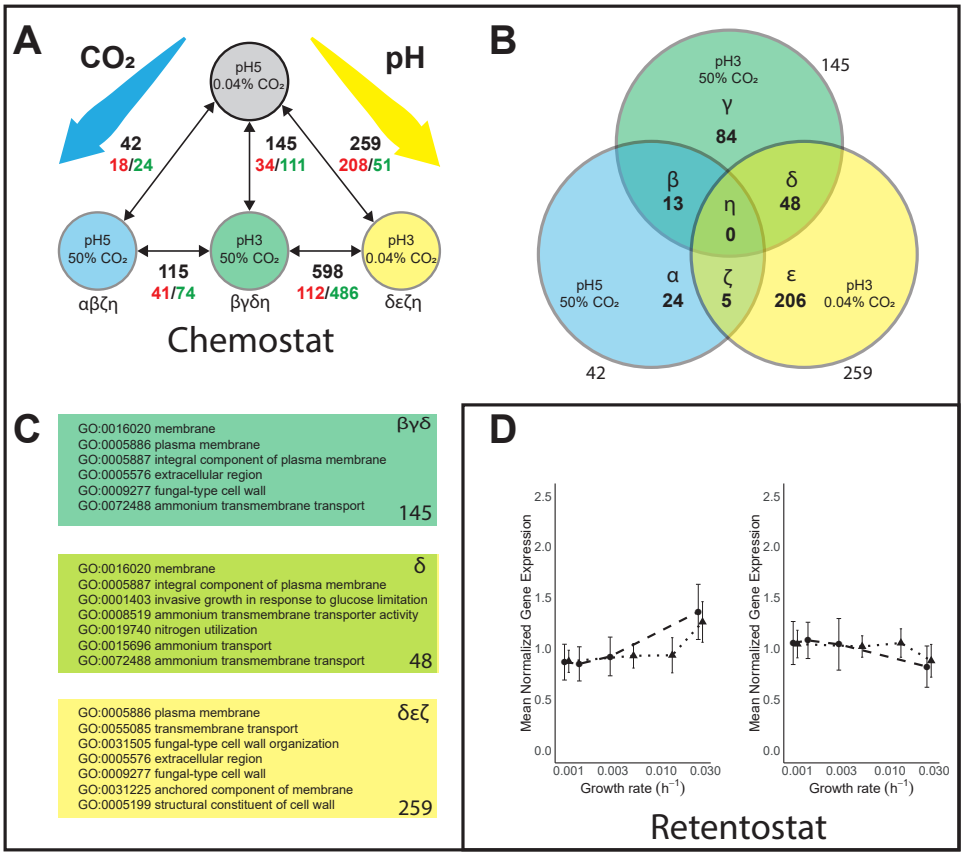

Figure 3.5: Differential Gene expression and Gene Set analysis in response to high CO_2, low pH, the combination of high CO_2 and low pH (A,B,C) and to near-zero growth rates (D,E,F,). (A) Pairwise comparisons between steady-state chemostat conditions to high CO_2 (blue), low pH (yellow), its combination (green) versus a 'laboratory conditions" reference (grey), as well as against the combination of the conditions (low pH, high CO_2). Black numbers indicate total number of differentially expressed genes (|FC| >2, FDR < 0.005, see Materials and methods), red numbers indicate up-regulated genes, green numbers indicate down-regulated genes. (B) Venn diagram of total differentially expressed (DE) genes based on pairwise comparison against the "laboratory conditions" reference, corresponding to the black numbers in panel A. Sections in the Venn diagram are indicated with Greek letters (α-η) (C) Enriched Gene Ontology sets based on Hyper-geometric distribution analysis (Bonferroni corrected $p < 0.05$ for: pH 3, 50 % CO_2 (145 genes, dark green top panel, corresponding to βγδ in panel B); the overlap between pH 3 and pH 3, 50 % CO_2 conditions (48 genes, light green middle panel; δ in panel B); low pH conditions (259 genes, yellow bottom panel, δεζ in panel B). See Appendix S4 for full tables. (D) Mean-normalized gene expression for genes with a positive (left) and negative (right) correlation with specific growth rate, based on Vos *et al.* [340] for "laboratory conditions" (black dots, dashed line) and "industrial conditions" (black triangles, dotted line). Error bars represent standard deviation of the mean-normalized expression of the gene set. Bonferroni corrected p-values for the "laboratory conditions (pH 5, 0.04 % CO_2)" up: $1.46 \cdot 10^{-89}$, down: $1.9 \cdot 10^{-4}$. "industrial conditions" (pH 3 50 % CO_2), up: $2.96 \cdot 10^{-26}$, down: $9.8 \cdot 10^{-16}$.

Discussion

This study was designed to quantify and dissect adverse physiological effects on *S. cerevisiae* of process conditions that are relevant for dicarboxylic acid production (low pH, high CO_2 and slow growth). Elevated CO_2 (50 %) did not, by itself, affect the biomass yield or viability of *S. cerevisiae* as compared to those under reference conditions (Table 3.1), and, accordingly, triggered only a weak transcriptional response (Figure 3.5). This result appears to contradict results from two independent previous studies on the same strain, performed at CO_2 levels of 50 and 79 %, under fully respiratory conditions [8, 92, 263]. This apparent discrepancy may be related to the lower specific growth rates applied in the present study (0.025 h^{-1} and below, while the cited earlier studies used 0.10 h^{-1}). Indeed, robustness of *S. cerevisiae* to various other stresses is inversely correlated with growth rate [23, 27, 32, 195].

In contrast to the apparent insensitivity of slow-growing cultures to high CO_2, a low culture pH caused increased maintenance-energy requirements in glucose-limited cultures, both at high and at low CO_2 (Figure 3.2, Figure 3.4). Moreover, both in glucose- and in ammonium-limited cultures, growth at low pH led to a reduced culture viability. A low extracellular pH results in a large proton gradient across the cell membrane and might increase proton influx via passive diffusion. To maintain intracellular pH homeostasis, *S. cerevisiae* can expel protons via the plasma-membrane ATPase Pma1 [38, 98], a process that is an intrinsic part of maintenance-energy metabolism (Figure 3.4). In glucose-limited chemostat cultures, no changes in the expression of genes encoding for proteins involved in proton homeostasis, including *PMA1* and genes encoding subunits of the vacuolar V-ATPase, were observed. However, in glucose-limited retentostat cultures, *PMA1* and *PMA2* expression did show a positive correlation with specific growth rate (Figure 3.6A,B).

Figure 3.6: *See next page.* Transcriptional responses of gene sets related to proton homeostasis and diffusion (A,B,C,D), genes responsive to signaling pathways involved in low pH stress (E, H,I,J) and cell wall synthesis (F) from Lesage and Bussey, 2006 [182] and cell wall stress (G) from Boorsma *et al.*, 2004 [31]. The number of genes in each gene set is indicated in the panels. Left figures indicate per gene mean-normalized expression from chemostats. Right figures indicate the per gene mean-normalized expression versus growth rate for retentostat cultures under "laboratory" condition (black dots, dashed line) and "industrial" conditions (black triangles, dotted line). Mean-normalization was performed on the separate experiments and prohibits intercomparing the expression levels. Error bars in each plot indicate the standard deviation of the per gene mean-normalized expression of all genes in the subset.

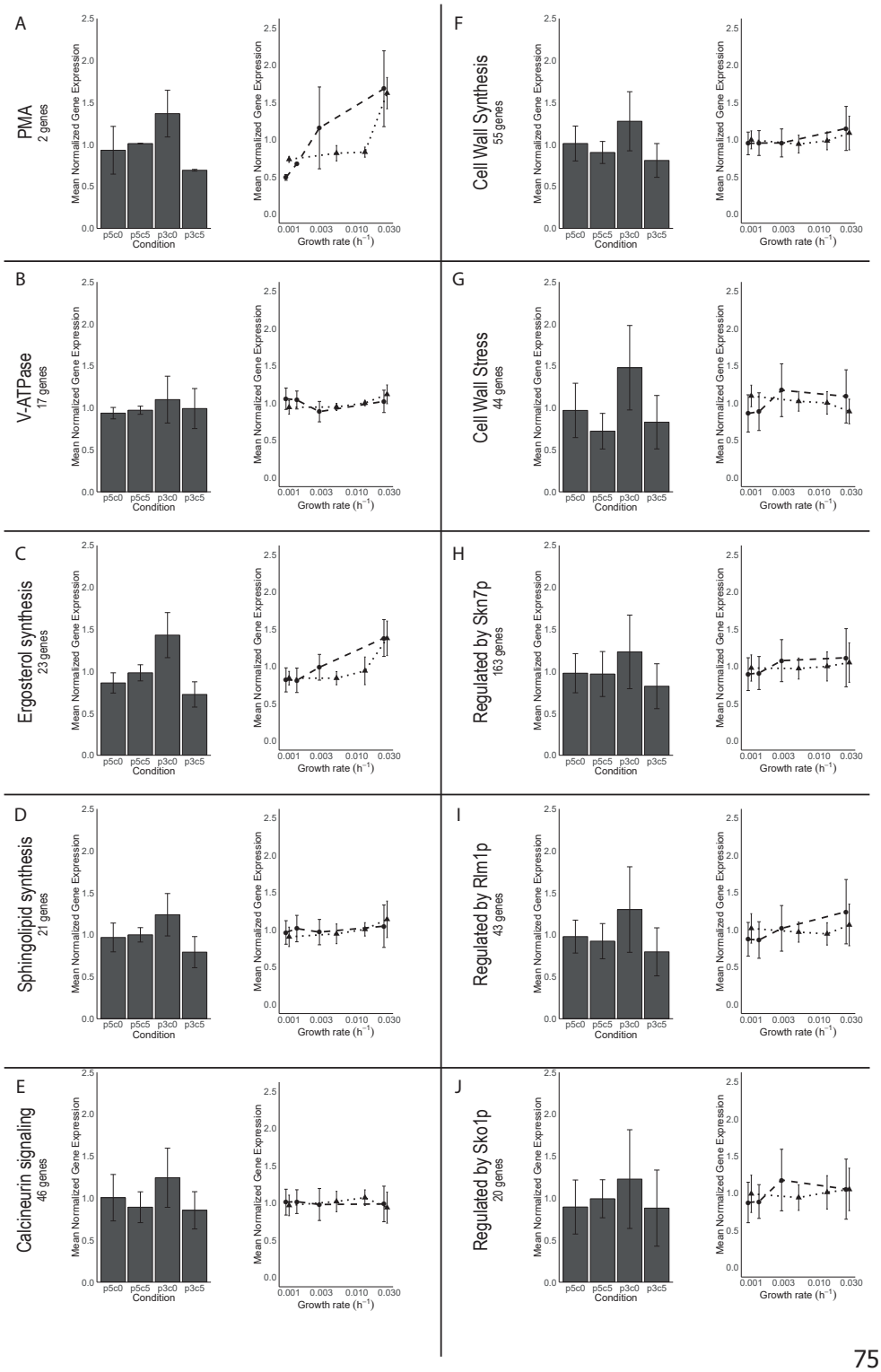
A
PMA
2 genes
B
V-ATPase
17 genes
C
Ergosterol synthesis
23 genes
D
Sphingolipid synthesis
21 genes
E
Calcineurin signaling
46 genes
F
Cell Wall Synthesis
55 genes
G
Cell Wall Stress
44 genes
H
Regulated by Skn7p
163 genes
I
Regulated by Rlm1p
43 genes
J
Regulated by Sko1p
20 genes
Mean Normalized Gene Expression
Condition
p5c0 p5c5 p3c0 p3c5
Growth rate (h⁻¹)
0.001 0.003 0.010 0.030

During ammonium-limited growth, additional mechanisms might explain the increase in non-growth associated energy requirements (Figure 3.4). Futile cycling of ammonia and ammonium across the plasma membrane could require addition proton pumping via Pma1 [62, 191] and might be aggravated at low pH. Additionally, presence of ethanol in the ammonium-limited cultures (up to 15 $g.L^{-1}$) might stimulate proton leakage across the plasma membrane and thus trigger an increase in ATP-mediated proton export [188, 198]. Together, the results of this study indicate that high death rates of slow-growing cultures at low pH cannot be directly attributed to energy-limited growth or increased maintenance energy-requirements.

Yeast transcriptional responses to near-zero growth rates in glucose-limited retentostat cultures were highly similar under laboratory and industrially relevant conditions, indicating that the different death rates and maintenance-energy requirements under these conditions (Figure 3.1 and 3.2) did not trigger extensive transcriptional reprogramming. In chemostat cultures, pronounced transcriptional responses to low pH involved many genes involved in cell wall synthesis and stress. Proteins located outside the plasma membrane, including cell wall proteins, are directly exposed to the extracellular medium. As the isoelectric point (pI) of a protein determines its folding and functionality, activity of these proteins may be particularly sensitive to low extracellular pH [282]. Failure to replace inactive extracellular proteins, either through accumulation of inactive protein or through a limited capacity for their replacement, may therefore be a key contributor to cell death, increased maintenance energy requirements or both at low pH.

While neither synergistic nor antagonistic physiological effects of low pH and high CO_2 were observed, transcriptional responses to the combination of these environmental conditions strongly differed from the transcriptional responses to either low pH or high CO_2 (Figure 3.5). In particular, high CO_2 levels appeared to dampen the transcriptional response to low pH. Low pH stress triggers transcriptional regulation of genes under control of the cell wall integrity (CWI), high-osmolarity glycerol (HOG) and calcineurin signaling pathways [73] and cytosolic pH acts as a sensor for PKA-signaling [86, 235]. Additionally, sensing of CO_2 is relayed through sphingolipid-mediated sensing, via the kinases Pkh1 and Pkh2, to the central nutrient sensor Sch9 [254]. Extensive crosstalk between these signaling pathways enables cellular homeostasis [48, 80, 107, 112, 267]. Accordingly, genes under control of the transcription factors regulated by these signaling pathways (Skn7p, Rlm1p, Sko1p, Figure 3.6E, H, I, J) were upregulated at pH 3, as were gene sets involved in cell wall synthesis [182] and cell wall stress [31]. However, these gene sets did not respond during growth at pH 3 at 50 % CO_2 (Figure 3.6F, G). While the present data do not enable elucidation of the precise nature of the cross-talks between pH and CO_2 signaling, in *S. cerevisiae*, two interactions between the abovementioned signaling pathways could provide further leads of investigation. First, cell wall integrity is sensed by the GPI-anchored nano-spring Wsc1 [90], ultimately activating CWI and PKA pathways [115]. The kinases Pkh1 and Pkh2 that relay the CO_2 signal

to Sch9 are also essential for Pkc1 activation of the CWI pathway [145, 183, 254] and phosphorylate the kinases Ypk1 and Ypk2 that in turn phosphorylate the CWI MAP Kinase Mpk1/Stl2 [268, 277]. Second, at high extracellular CO_2 conditions bicarbonate accumulates intracellularly, improves buffering of the cytosol, and attenuates the cytosolic pH [34, 92]. Both the cytosolic pH and bicarbonate are direct signals for PKA signaling [34, 86, 309]. Phosphoproteomic analysis of the proteins in the CWI, HOG and PKA signaling pathways could prove an efficient strategy to elucidate the observed interplay of high CO_2 and low pH signaling [208] , which could be supported by analysis of the in vivo cytosolic pH at high CO_2 and low pH conditions by the pH-dependent GFP-derivative pHluorin [235].

The present study indicates that sensitivity to high CO_2 is unlikely to be a major concern for the development of robust yeast cell factories for production of dicarboxylic acids. Instead, minimizing maintenance-energy requirement and death rate at low pH was identified as a major objective for strain improvement. Even in the absence of product formation, low pH was shown to augment the trade-off, at low specific growth rates, between a reduced allocation of substrate to biomass formation and increased relative contribution of maintenance-energy requirements. The strongly increased m_S at low pH is clearly disadvantageous for industrial scale production of dicarboxylic acids and, moreover, is likely to be further enhanced in the presence of high product concentrations. For example, high concentrations of organic acids have been shown to cause increased maintenance-energy requirements at low pH [1, 2]. From an economic perspective, the physiological impacts of low pH on *S. cerevisiae* constitute a trade-off between fermentation costs and costs for downstream processing. The complexity of the observed physiological and transcriptional responses indicates that improving robustness under industrial conditions is unlikely to be achieved by individual genetic modifications. Instead, exploration of yeast biodiversity [239], evolutionary engineering [203] and/or genome-shuffling approaches [201, 296] may offer interesting possibilities.

Materials and Methods

Strain and strain maintenance

S. cerevisiae CEN.PK113-7D [97, 228] was used in this study. The strain was stored at -80 ºC in 1 mL aliquots in YPD (10 g/L Bacto yeast extract, 20 g/L Bacto peptone, 20 g/L glucose) supplemented with 30 % (v/v) glycerol.

Aerobic, glucose-limited bioreactor cultures

Glucose-limited chemostat and retentostat cultures were grown in 2-L bioreactors (Applikon, Delft, The Netherlands) at a working volume of 1.4 L, essentially as described by [340]. Chemically defined medium containing 20 g/L glucose was used for chemostat and retentostat cultures. The inflowing gas (0.5 vvm) was either compressed air (0.04 % CO_2) or an in-line mix of 50 % compressed air and 50 % pure CO_2 (>99.7 % purity, Linde Gas Benelux, Schiedam, The Netherlands). The two gas flows were precisely controlled with mass flow controllers (Brooks, Hatfield, PA, USA) and mixed in a ratio of 1:1. A detailed description of pre-culture preparation, bioreactor operation and medium composition is given in Appendix 1.1.

Chemostat cultures were assumed to be in steady state when, after at least 5 volume changes under the same process conditions, culture dry weight (see below) changed by less than 4 % over two consecutive volume changes. Glucose-limited cultures grown at pH 3 showed oscillations of CO_2 and O_2 concentrations in the off-gas with a frequency of 5-8 hours, but were sampled regardless of the oscillations. These oscillations subsided upon approaching severe calorie restriction in the retentostat phase after 3 days.

Aerobic, ammonium-limited bioreactor cultures

Ammonium-limited retentostats grown at pH 3 were preceded by a chemostat phase under the same nutrient limitation, essentially as described before [191]. Details on bioreactor operation and media composition of these nitrogen-limited cultures are given in Appendix 1.2. Ammonium-limited chemostat cultures were assumed to be in steady state when, after four volume changes, biomass dry weight, CO_2 production rate and residual glucose and ethanol concentrations in the effluent differed by less than 5 % over three consecutive volume changes.

Off-gas analysis, biomass and extracellular metabolite determinations

Concentrations of O_2 and CO_2 in the exhaust gas of bioreactors were quantified with a paramagnetic/infrared off-gas analyzer (NGA 2000, Baar, Switzerland). For glucose-limited cultures, biomass concentrations were determined by filtering duplicate, exact volumes of culture broth, diluted to an approximate concentration of 2.5 g biomass/L, over pre-dried Supor 47 membrane filters with a 0.45 µm pore size (Pall Laboratory, Port Washington, NY, USA) as described by [257] . Biomass concentrations in ammonium-limited cultures were analyzed by essentially the same procedure with the exception that filters were dried in an oven instead of in a microwave. Procedures for analysis of extracellular metabolites are

described in detail in Appendix 1.3.

Viability

Viability measurements in retentostats were based on colony-forming-unit (CFU) counts, which indicate reproductive capacity of single cells [340]. For glucose-limited chemostats, CFU counts were obtained by sorting 96 single events detected by a FACS Aria™ II SORP Cell Sorter (BD Biosciences, Franklin Lakes, NJ) on a YPD plate (in quintuplicate, see Appendix 1.4 for details). To measure viability based on membrane integrity, cells were stained with the fluorescent dye propidium iodide (PI) [340]. Staining of single-cell esterase activity with 5-CFDA-AM was used to evaluate metabolic activity [24]. Flow cytometry was done on a BD-Accuri C6 with a 488 nm excitation laser (Becton Dickinson, Franklin Lakes, NJ). For each sample, over 10,000 events in fluorescence channel 3 (670 LP) were analyzed for PI and in fluorescence channel 1 (530/30 nm) for 5-CFDA-AM. The forward-scatter height (FSC-H) threshold was set to 80,000.

Regression analysis of biomass accumulation in glucose-limited retentostats

Quantification of maintenance-energy requirements and death rate in glucose-limited retentostats was done by model-based regression analysis of biomass accumulation over time [340]. The fitted model parameters were a constant first-order death rate and a growth-rate independent maintenance-energy coefficient. The maximum theoretical yield of biomass on substrate ($Y_{X/S}^{max}$) was set to a fixed value of 0.5 g_X/g_S. This analysis generated quantitative estimates of specific growth rate and glucose consumption rates during the first, dynamic phase of retentostat cultivation (see Results).

Carbon and nitrogen balances and rate calculations

Carbon and nitrogen recoveries were calculated based on measurements of substrate and product concentrations in the gas and liquid phases and gas and liquid in- and outflow rates. Ethanol evaporation from bioreactors was quantified [63] and taken into account in the calculation of specific ethanol-production rates. Specific growth rates in nitrogen-limited retentostat cultures were calculated as described by [28].

Transcriptome analysis

Detailed descriptions of sampling procedures [213, 247], total RNA extraction [279] , mRNA enrichment and RNA sequencing (Novogene, Hong Kong, China & Baseclear, Leiden, The Netherlands), alignment (STAR, [85]) and mapping (ht-seq count [10]) of reads against the S288C genome [96], TMM-normalization (EdgeR R-package, [266]), gene set enrichment (piano R-package, [330]) and trend analysis with the regression-based growth rate (see above) as variable (maSigPro R-package [58, 231]) are provided in Appendix 1.5.

Biomass composition, glycogen and trehalose determination

Biomass elemental composition and biomass protein content were quantified as described previously [174, 176]. After sampling for analysis of the intracellular storage carbohydrates glycogen and trehalose [340], pellets were stored at -80 ºC. Samples were processed [241] and analyzed as described in Appendix 1.6.

Metabolic flux analysis

Metabolic flux analysis was performed as described previously [67], with two modifications to the stoichiometric model: biomass composition was re-defined based on measured biomass elemental composition and reduction of acetaldehyde to ethanol was incorporated as ethanol was a main product of ammonium-limited aerobic cultures.

Availability of data

The supplementary files are available online at `https://www.tudelft.nl/tnw/over-faculteit/afdelingen/biotechnology/research-groups/industrial-microbiology/pascale-daran-lapujade-group/`

CHAPTER 4

Adaptive laboratory evolution and reverse engineering of low-pH tolerance in *Saccharomyces cerevisiae*

Xavier Hakkaart
Jordi Geelhoed
Philip A. de Groot
Marijke A.H. Luttik
Elsemiek Kranendonk
Dominic Dijksman
Jean-Marc G. Daran
Jack T. Pronk
Pascale Daran-Lapujade

This chapter has been submitted for publication in Applied and Environmental Microbiology

Abstract

Low-pH tolerance of ***Saccharomyces cerevisiae*** is a relevant trait for industrial production of carboxylic acids. However, few genetic modifications that enhance this trait have hitherto been identified. The limited success of targeted engineering approaches is largely explained by the tight maintenance of intracellular pH by complex regulatory networks. In this study, an adaptive laboratory evolution strategy was applied to decrease the minimum permissive pH of the laboratory strain ***S. cerevisiae*** CEN.PK113-7D from 2.6 to pH 2.1. independently evolved, low-pH tolerant strains showed mutations in genes involved in calcium signaling, cell-wall maintenance, membrane composition and protein turnover.

Combined reverse engineering and backcrossing enabled the identification of single and combined mutations that enabled growth at extremely low pH. Specific mutations in ***PMR1***, encoding the Golgi Ca^{2+}/Mn^{2+}-ATPase, already increased low-pH tolerance of ***S. cerevisiae***. Mutations in ***MUK1*** and ***MNN4*** were ineffective when introduced individually, but did synergistically improve low-pH tolerance when introduced together in an unevolved background. The results of this study show the genetic complexity underlying low-pH tolerance and provide further insights for the understanding and engineering of this trait.

Importance

Tolerance to low pH is an important microbial feature for industrial carboxylic acids production. However, the complex, pleiotropic effects of low extracellular pH prohibits the ***a priori*** identification of genetic targets and makes the improvement of microbial tolerance to low pH via genetic engineering a daunting task. In this study, a strategy based on Adaptive Laboratory Evolution (ALE) successfully enabled the identification of such genetic targets in the industrial and model yeast ***Saccharomyces cerevisiae***. Growth at incrementally decreasing pH over 450 generations substantially increased the low pH range of ***S. cerevisiae*** laboratory strains. Specific mutations in calcium signaling (***PMR1***), cell wall maintenance (***MNN4***) and protein degradation (***MUK1***) found in the evolved strains substantially improved pH tolerance when transplanted into non-evolved strains. These findings not only hold the potential to improve ***S. cerevisiae***-based carboxylic acid production processes, but also bring new insights in the mechanisms involved in low-pH tolerance.

Introduction

Microbially produced carboxylic acids are platform molecules for chemical synthesis of bioplastics and a wide range of other products [276, 52, 354]. When, during industrial microbial production of carboxylic acids, a near-neutral pH is maintained by base titration, subsequent recovery of the free acid results in excessive formation of by-products such as gypsum [150, 3]. The economic feasibility and sustainability of microbial carboxylic-acid production can therefore be improved by performing fermentation processes below the pKa_1 of the product. Obviously, such an approach requires low-pH tolerant industrial microorganisms [150, 109]. Strains of the model organism and industrial yeast *Saccharomyces cerevisiae* typically grow optimally at pH values of 5.0-5.5 [331] and some strains have been reported to grow at pH values down to 2.5 [331, 79, 38]. However, the combination of high organic acid concentrations and low pH negatively affects yeast physiology and, thereby, process performance (e.g. [196, 2, 215, 239]).

The intracellular concentration of protons affects most cellular processes. *S. cerevisiae* has therefore evolved complex mechanisms to tightly maintain pH homeostasis [233, 102]. While gene-expression and knock-out studies generated valuable information, the low-pH responses in *S. cerevisiae* are still incompletely understood. Responses to low extracellular pH involve signaling pathways that are not specific to low-pH tolerance. Notably, two MAPK pathways, the cell-wall integrity (CWI) and hyper-osmotic glycerol (HOG) signaling pathways [74, 73, 75, 47, 159], as well as calcineurin-mediated signaling [74], are activated during exposure to low extracellular pH values. At the physiological level, exposure to suboptimal pH values leads to activation of membrane transporters for protons, such as the plasma-membrane ATPase Pma1 and the multi-component vacuolar ATPase [331, 38, 39]. In addition, exposure to low pH triggers changes in cell wall composition [7, 220] and organization of the actin cytoskeleton [220]. These responses to low pH ultimately increase ATP costs for cellular maintenance and thereby decrease biomass yield on sugar [2, 78, 129]. Moreover, exposure to low pH decreases culture viability [129, 75].

Adaptive laboratory evolution (ALE) is a strategy for understanding and improving complex microbial phenotypes [203, 87]. ALE studies have been extensively used to investigate and improve tolerance of *S. cerevisiae* to a wide range of toxic compounds (e.g. [124, 125, 294, 324]). However, to date only two studies [75, 108] focused on low-pH tolerance in this yeast. De Melo *et al.* [75] performed ALE on an industrial strain isolated from a Brazilian bioethanol factory (JP1), which had already been selected for low-pH tolerance by repeated exposure to an in-line acid-wash step during industrial biomass recycling [79, 17]. After laboratory evolution, they obtained an evolved yeast strain (JP1M) capable of growth at pH 2. To our knowledge, this value represents the lowest reported permissive pH for growth of *S. cerevisiae*. The evolved strain exhibited a deficiency in neutral trehalase activity, a marker of cAMP-PKA signaling, along with an improved culture viability at low pH [75]. However, the proposed role of neutral trehalase deficiency in low-pH tolerance was not experimentally verified. Fletcher *et al.* [108] evolved the laboratory strain *S. cerevisiae* CEN.PK113-7D for faster growth at a suboptimal but permissive pH of 2.8. Using whole-genome sequencing and reverse engineering, they identified causal mutations for low-pH tolerance. In particular, low-pH tolerance was improved by reverse engineering of mutations in genes involved in ergosterol biosynthesis (*ERG5*) and iron homeostasis (*FRE1*) into an unevolved strain. The results of this study further supported the notion that mechanisms involved in tolerance to weak organic acids (weak-acid stress) and strong

inorganic acids (low-pH stress) only partially overlap [159].

The goal of the present study is to identify novel genetic targets in *S. cerevisiae* CEN.PK113-7D for improving low-pH tolerance by using ALE and reverse engineering of mutations acquired by evolved, low-pH tolerant strains. To complement an earlier study aimed at optimizing growth at a permissive pH [108], ALE experiments were specifically designed to decrease the minimum permissive pH for growth. Candidate causal mutations for low-pH tolerance were identified by whole-genome sequencing of independently evolved strains. Two parallel strategies were implemented to assess the physiological relevance of individual mutations as well as potential combinatorial effects. A direct reverse-engineering approach involved introduction of single and multiple acquired mutations into a non-evolved, low-pH sensitive strain. In parallel, backcrossing was used to enrich mutations with a beneficial impact on low-pH tolerance.

Results

Decreasing the minimal permissive pH of *S. cerevisiae* by ALE

To identify an adequate starting pH of ALE experiments, the pH range of the popular prototrophic laboratory strain *S. cerevisiae* CEN.PK113-7D was determined in shake flask cultures. In agreement with previous reports [331, 79, 78, 190], this strain was found to have a pH optimum for specific growth rate of around 5. A 20 % lower specific growth rate was observed at pH 3 and the strain did not grow on synthetic medium with glucose at pH values of 2.5 and below (Figure 4.1A).

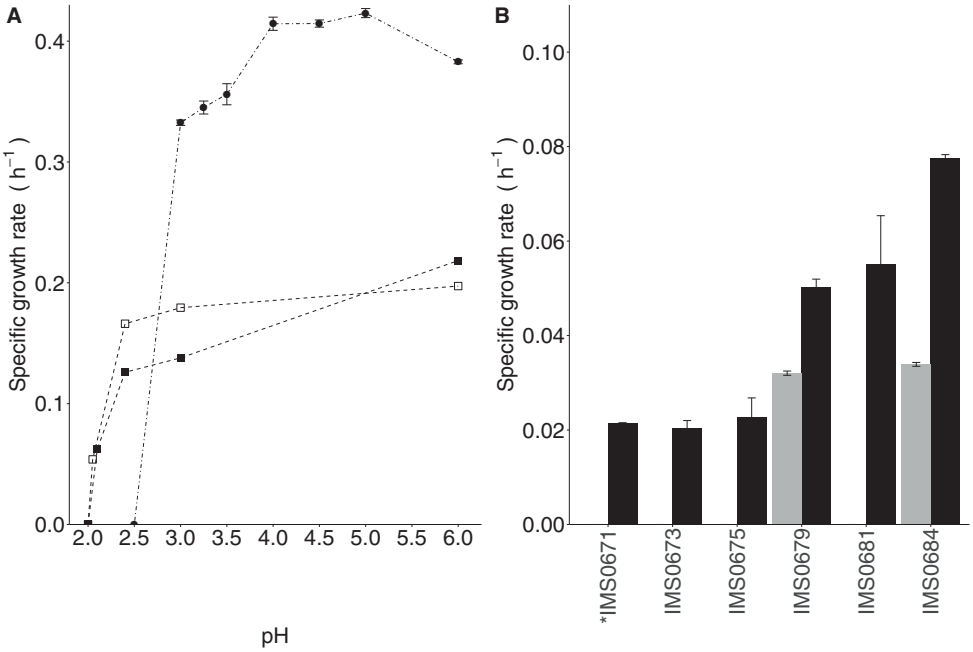

Figure 4.1: Adaptive Laboratory Evolution extends the low pH range of *S. cerevisiae* **A)** pH dependency of the specific growth rate of *S. cerevisiae* CEN.PK113-7D (dots) and of samples taken at the end of ALE experiments I and II (closed and open squares, respectively), in SMUD medium. **B)** Specific growth rates of single colony isolates from ALE experiments I (IMS0671, IMS0673, IMS0675) and II (IMS0679, IMS061, IMS0684) at pH 2.1 (dark grey bars) and at pH 2.05 (light grey bars) in independent duplicate shake-flask cultures (*IMS0671 was measured in a single culture). Error bars represent average deviation from the mean of duplicate cultures.

Two independent serial-transfer experiments were started at pH 2.8 and exposed to a progressively decreasing pH (Figure 4.1A, Supplementary data figure S1). ALE experiments I and II were transferred 88 and 101 times, corresponding to approximately 428 and 475 generations, respectively. Cultures were generally transferred to fresh medium after at least two generations. At the lowest pH values at which growth occurred, the final OD_{660} measurements of the cultures did not exceed 2 (Supplementary data figure S1). Specific growth rates of the resulting evolved populations were measured at pH 6.0, 3.0, 2.7, 2.4 and 2.1/2.05 (Figure 4.1B). The two populations grew, with a specific growth rate of

approximately 0.05 h^{-1}, at pH 2.1 for ALE experiment I and at pH 2.05 for ALE experiment II (Figure 1B). Eight single colonies were isolated from each ALE experiment and tested for growth at pH 3 and 2.1 (Supplementary data figure S2). The single-colony isolates from the ALE experiments grew slower than the non-evolved strain CEN.PK113-7D at pH 3 and all but one grew at pH 2.1. Three representative strains from ALE experiment I (IMS0671, IMS0673, IMS0675), and from ALE experiment II (IMS0679, IMS0681 and IMS0684) were retained for further analysis at pH 2.1 and pH 2.05. The strains from experiment II clearly outperformed the strains from experiment I at pH values of 2.1 and below (Figure 4.1B). Two strains (IMS0679 and IMS0684) grew at pH 2.05, just like the population from ALE experiment II from which they had been isolated (Figures 4.1A and B).

Identification of potential causal mutations by whole genome sequencing of low-pH tolerant strains

Sequencing of the genome of the six evolved, low-pH tolerant strains revealed multiple single-nucleotide mutations and copy-number variations relative to the genome of the parental strain CEN.PK113-7D. Strains isolated from ALE experiment I (IMS0671, IMS0673, IMS0675) showed a duplication of a region on chromosome XIII carrying 12 genes, while an adjacent region on the same chromosome arm, carrying 33 genes including *GAS1*, was triplicated (Figure 4.2, Table 4.1, Supplementary data table S5). In strains from ALE experiment II (IMS0679, IMS0681 and IMS0684), the copy number of only *GAS1* was six-fold higher than in the reference strain. Low-pH tolerant strains evolved by Fletcher *et al.* (2016) [108] also contained a partial duplication of the right arm of chromosome XIII carrying *GAS1*. These observations strongly implicated *GAS1* in low-pH tolerance of the evolved strains. Additionally, strains IMS0679 and IMS0681 carried a duplication and IMS0684 a triplication of a part of chromosome IX and chromosome XII, together covering 91 genes and the chromosome IX centromere (Table 4.1, Supplementary data table S3 and S4).

Figure 4.2: *See next page.* Two ALE experiments were performed with *S. cerevisiae* at incrementally decreasing pH conditions. Three strains were isolated from each ALE experiment. Mutations identified in strains isolated from ALE experiment I **A)** and ALE experiment II **B)** from whole genome sequencing analysis. The relative coverage depth of the respective strains (blue) is compared with the relative coverage depth of the non-evolved reference strain *S. cerevisiae* CEN.PK113-7D (red) along the 16 chromosomes (I-XVI). Mutations resulting in amino-acid changes are indicated at the relative location in the chromosomes. Protein names in green indicate genes in which mutations were found in both ALE experiments. **C)** Venn diagram of genes with mutations in ALE experiment I (blue) and ALE experiment II (yellow), **D)** For genes mutated in both ALE experiments the nucleotide position of the mutation is indicated, along with the resulting amino acid change and causal change in the codon (capital letters). The mutations indicated above and below the schematic ORF indicate mutations found in ALE experiments I and II, respectively. When an insertion or single-nucleotide change caused a premature stop-codon, the location of the new stop codon is indicated with a red asterisk and the codon mutation is indicated in red. Blue bars represent sequences that encode known functional parts of proteins: for *MUK1* the Vps9-domain is indicated [41] and for *UBR1* (left to right) the UBHC domain, the RING-H2 domain [353] and the C-terminal auto-inhibition site [351, 88].

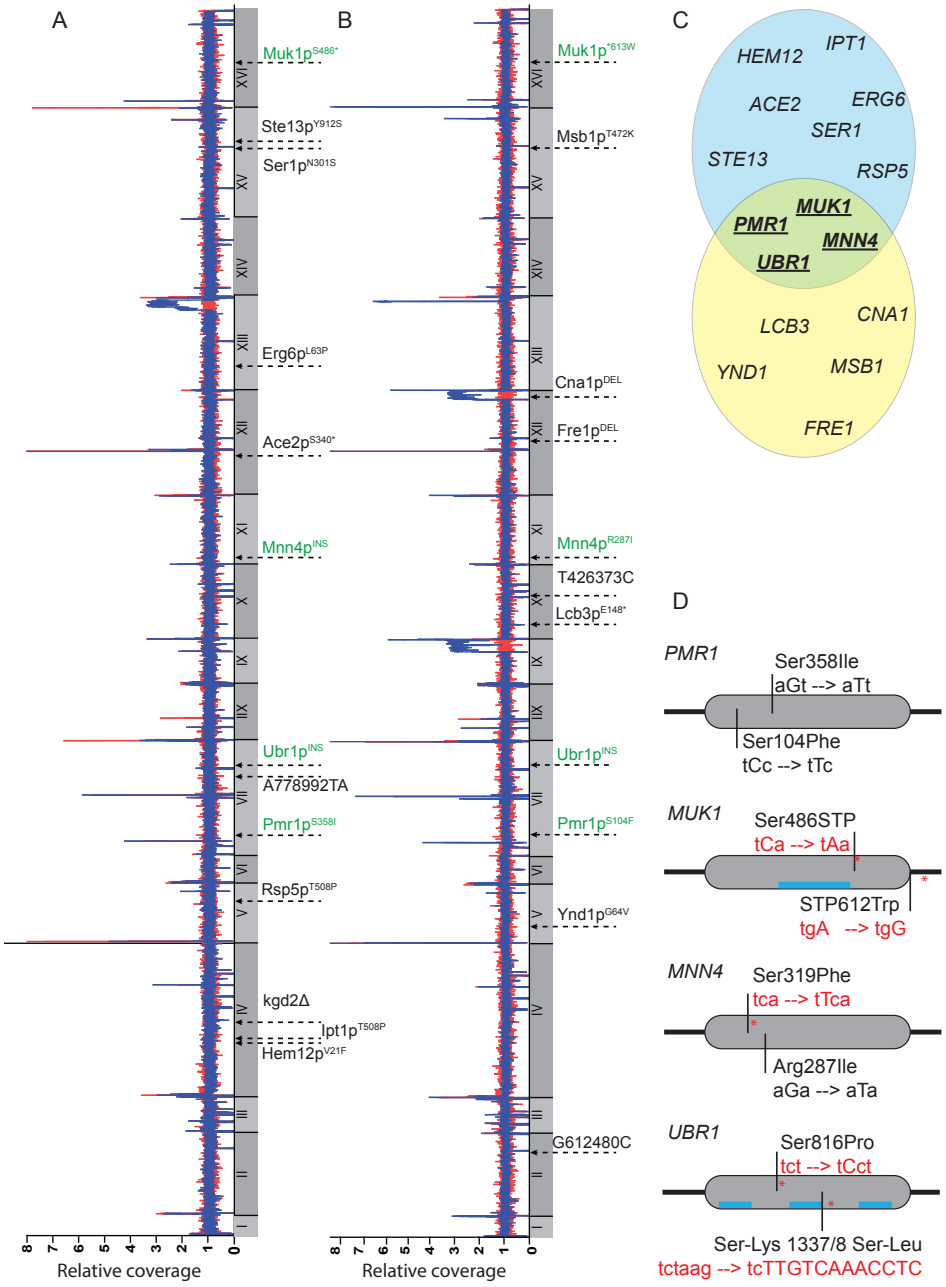
A
Muk1p S486*
Ste13p Y912S
Ser1p N301S
Erg6p L63P
Ace2p S340*
Mnn4p INS
Ubr1p INS
A778992TA
Pmr1p S358I
Rsp5p T508P
kgd2Δ
Ipt1p T508P
Hem12p V21F
Relative coverage
B
Muk1p *613W
Msb1p T472K
Cna1p DEL
Fre1p DEL
Mnn4p R287I
T426373C
Lcb3p E148*
Ubr1p INS
Pmr1p S104F
Ynd1p G64V
G612480C
Relative coverage
C
HEM12
IPT1
ACE2
ERG6
SER1
STE13
RSP5
MUK1
PMR1
MNN4
UBR1
LCB3
CNA1
YND1
MSB1
FRE1
D
PMR1
Ser358Ile
aGt --> aTt
Ser104Phe
tCc --> tTc
MUK1
Ser486STP
tCa --> tAa
STP612Trp
tgA --> tgG
MNN4
Ser319Phe
tca --> tTca
Arg287Ile
aGa --> aTa
UBR1
Ser816Pro
tct --> tCct
Ser-Lys 1337/8 Ser-Leu
tctaag --> tcTTGTCAAACCTC

For analysis of single-nucleotide variations, only genes affected in all three strains from an ALE experiment were taken into account (Figure 4.2,Table 4.1). This restriction yielded a set of 16 genes, of which four were mutated in all six strains (*MNN4*, *MUK1*, *PMR1*, *UBR1*), while 13 genes were mutated in a single ALE experiment (*ACE2*, *ERG6*, *HEM12*, *IPT1*, *RSP5*, *SER1* and *STE13* in experiment I and *LCB3*, *YND1*, *MSB1*, *FRE1* sand *CNA1* in experiment II (Figure 4.2, Table 4.1)). These 16 genes encoded proteins involved in six cellular functions: heme biosynthesis (*HEM12*), sphingolipid metabolism (*IPT1*, *LCB3*, *SER1*), multivesicular body and vacuolar degradation pathways (*RSP5*, *UBR1*, *STE13*, *MUK1*), ergosterol biosynthesis (*ERG6*), cell wall maintenance (*MNN4*, *MSB1*, *ACE2*, *YND1*), and cation homeostasis and sensing (*FRE1*, *PMR1*, *CNA1*). Strains from ALE experiment II showed a partial loss of mitochondrial DNA (affecting *OLI1*, *ATP6* and *COX1*, Supplementary data table S5), while strains from ALE experiment I showed a loss of *KGD2*, which is required for a functional Krebs cycle (Table 4.1). Consistent with these mutations, cultures from ALE experiment I and II did not grow on solid plates with ethanol and glycerol as carbon source.

Table 4.1: Mutations in evolved strains obtained by serial transfer at progressively decreasing culture pH. Open reading frames with non-synonymous mutations, indicated as amino-acid changes in the encoded proteins, and copy-number variations (CNV) found in three sequenced, evolved strains from ALE experiment I (strains IMS0671, IMS0673 and IMS0675) and ALE experiment II (strains IMS0679, IMS0681 and IMS0684). Protein descriptions and cellular functions are obtained from yeastgenome.org. Mutations that were unique to any of the six strain strains are listed in Supplementary data table S7

Systematic name	Gene name	ALE experiment I	ALE experiment II	Protein description	Cellular function
YDR047W	*HEM12*	Val-21-Phe		uroporphyrinogen decarboxylase	Heme biosynthesis
YDR072C	*IPT1*	Thr-508-Pro		Inositolphospho-transferase	Sphingolipid metabolism
YER005W	*YND1*		Gly-65-Val	Apyrase with wide substrate specificity	Protein glycosylation
YER125W	*RSP5*	Ser-444-Phe		NEDD4 family E3 ubiquitin ligase	Protein degradation
YGL167C	***PMR1***	**Ser-358-Ile**	**Ser-104-Phe**	High affinity Ca^{2+}/Mn^{2+} P-type ATPase;	Calcium transport
YGR184C	***UBR1***	**insertion: Ser-816-Pro early stopcodon**	**disruption**	E3 Ubiquitin ligase in N-end rule degradation	Protein degradataion
YJL134W	*LCB3*		Glu-148-STP	Long-chain base-1-phosphate phosphatase,	Sphingolipid metabolism
YKL201C	***MNN4***	**Disruption**	**Arg-287-Ile**	Positive regulator of mannosylphosphate transferase Mnn6p;	Cell wall maintenance
YLR131C	*ACE2*	Ser-340-STP		Transcription factor required for septum destruction after cytokinesis	Cell wall maintenance
YLR214W	*FRE1*		disruption/insertion	Ferric reductase and cupric reductase	Cation homeostasis
YLR433C	*CNA1*		Leu413, Asp414->His413	Catalytic subunit of calcineurin	Cation sensing
YML008C	*ERG6*	Leu-63-Pro		Delta(24)-sterol C-methyltransferase; ergosterol synthesis	Ergosterol synthesis
YOR184W	*SER1*	Asn-301-Ser		3-phosphoserine aminotransferase	Sphingolipid metabolism

Table 4.1: (Table continued)

YOR188W	*MSB1*		Thr-472-Lys	Positive regulator of 1,3-beta-glucan ssynthesis and the Pkc1p-MAPK pathway	Cell wall maintenance
YOR219C	*STE13*	Tyr-912-Ser		Dipeptidyl aminopeptidase;	Protein degradation
YPL070W	***MUK1***	**Ser-486-STP**	**STP-613-Trp**	Guanine nucleotide exchange factor	Protein degradation

Chromosome	**ALE experiment I**	**ALE experiment II**	**Comment**
CHR IV	0x (733220-733880)		internal deletion of *KGD2* (*YDR148C*)
CHR IX		2x (318000 - Right telomere)	Genes encoded in this region are listed in Table S3.
CHR XII		2x (934000 - right telomere)	Genes encoded in this region are listed in TableS4.
CHR XIII	2x (786000-814000)		Genes encoded in this region are listed in Table S5.
CHR XIII	3x (814000- Right telomere)		Genes encoded in this region are listed in Table S5.
CHR XIII	6x (858600-865900)		Genes encoded in this region are listed in Table S5.
mtDNA		0x (31000 - 82400)	Genes encoded in this region are listed in Table S6

Reverse engineering of low-pH tolerance

The occurrence of mutations in *PMR1*, *MUK1*, *MNN4* and *UBR1* and increased copy number of *GAS1* (Figure 4.2, Table 4.1, Supplementary data table S5) in the two independent ALE experiments strongly suggested a role of these five genes in low-pH tolerance. The GPI-anchored Gas1 cell-wall 1,3-beta-glucanosyltransferase contributes to cell-wall organization and integrity by crosslinking β-glucans [255]. Plasmid-based, multi-copy overexpression of *GAS1* was previously shown to improve low-pH tolerance [211]. Genomic integration of a single additional copy of *GAS1* under the control of its native promoter and terminator in the *SGA1* locus of an unevolved strain did, however, not improve its specific growth rate at pH 2.7 (Figure 4.3).

UBR1 encodes an E3-ubiquitin ligase [16]. Mutations in the evolved strains removed an auto-inhibitory site and affected the RING-domain in Ubr1 (Figure 4.2D), thereby probably abolishing its ubiquitination activity. Deletion of *UBR1* in an non-evolved strain did, however, not result in an increased growth rate at pH 2.7 (Figure 4.3) nor at pH 2.8 (Supplementary data figure S3). *MUK1* gene encodes a guanine-nucleotide exchange factor involved in vesicle-mediated transport [243]. Although the two mutations in *MUK1* caused a premature stop codon (Figure 4.2D), conservation of

the Vps9 domain (Figure 4.2D) suggested that Muk1 activity might still be present in the evolved strains. None of these *MUK1* mutations led to improved growth at pH 2.7 or pH 2.8 upon their introduction in a non-evolved strain (Figure 4.3, Supplementary data figure S3). *MNN4* encodes a positive regulator of mannosyl phosphorylation by Mnn6p [232]. Since the impact of the mutations found in *MNN4* on protein activity could not be predicted, the *mnn4-1* and *mnn4-2* mutations were introduced into a non-evolved reference strain. Their introduction resulted in a 25 % lower growth rate at pH 2.7 (Figure 4.3), Student t-test p-value < 0.006). In contrast, introducing the mutations in *PMR1* found in strains IMS0675 and IMS0684 into an unevolved strain did significantly increase its specific growth rate at pH 2.7 and 2.8, by ca. 28 % and 32 % respectively (Figure 4.3 and S3). These results indicated a role of the Pmr1 P-type ATPase, which transports Ca^{2+} and Mn^{2+} from the cytosol to the Golgi-lumen [11], in low-pH tolerance.

To explore potential synergistic effects, the sets of four mutations occurring in strains IMS0675 and IMS0684 were reconstructed in an unevolved reference strain, leading to strains IMX1961 (*pmr1-1 muk1-1 mnn4-1 ubr1Δ*) and IMX1962 (*pmr1-2 muk1-2 mnn4-2 ubr1Δ*). While the low-pH tolerance of strain IMX1961 was improved relative to that of the non-evolved strain at pH 2.7, this was not the case for IMX1962 (Figure 4.3). The pH tolerance of both strains was lower than that of strains carrying only a pmr1 mutation, suggesting antagonistic effects of the combined mutation at a permissive pH.

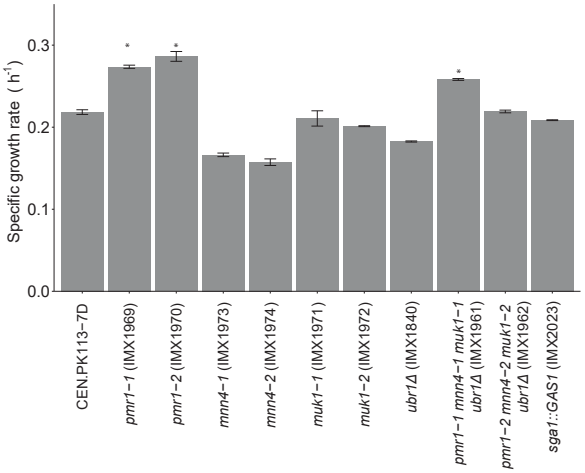

Figure 4.3: Specific growth rate in shake-flask cultures on SMUD medium at pH 2.7 of *S. cerevisiae* CEN.PK113-7D (unevolved parent strain) and congenic strains carrying specific, reverse engineered mutations identified in evolved, low-pH tolerant strains. Data are represented as average ± average deviation from the mean of independent duplicate growth experiments for each strains. Significantly different growth rates as compared to the reference CEN.PK113-7D are indicated with an asterisk (two-sided Student's T-test, p <0.01).

During the ALE experiments, culture pH was incrementally decreased to decrease the minimum permissive pH for growth of the evolving population. The mutations might therefore, conceivably, have contributed to a lower permissive pH rather than to an increased specific growth rate at a suboptimal but still permissive pH. To evaluate whether the mutations in *GAS1*, *UBR1*, *MUK1*, *MNN4* or *PMR1* extended the low pH range to below pH 2.5 when introduced separately or together, a microtiter plate assay was used (Figure 4.4). Introduction of an extra copy of *GAS1* led to a decreased minimum permissive pH, but not to an increased specific growth rate at pH 2.7 (Figure 4.4C). As observed for growth at pH 2.7, single mutations in *UBR1*, *MUK1* and *MNN4* did not improve growth at non-permissive pH when introduced in non-evolved strains, while introduction of the mutated alleles *pmr1-1* and *pmr1-2* did (Figure 4.4D-J). While strains IMX1961 and IMX1962, carrying mutations in all four genes, did not perform as well as strains with a single *PMR1* mutation at pH 2.7, they displayed the same phenotype as *pmr1-1* or *pmr1-2* 'only' strains at pH 2.5 and below (Figure 4.4K,L, vs E,F). To evaluate whether mutations in strains *MUK1*, *MNN4* and *UBR1* had a beneficial effect on growth at pH of 2.5 and below in the absence of mutations in *PMR1*, strains carrying mutations in these genes, but not in *PMR1* were constructed. Combination of the mutations of ALE experiment II (*muk1-2*, *mnn4-2* and deletion of *UBR1*) enabled growth at pH 2.4 (Figure 4.4 N). In contrast, no such effect was observed when the mutations found in these genes in ALE experiment I were combined (Figure 4.4 M). Meanwhile, none of these reverse engineered strains matched the low-pH tolerance of the evolved strains (Figure 4.4A,B), suggesting that other mutations than the five presently selected and tested contributed to this acquired phenotype.

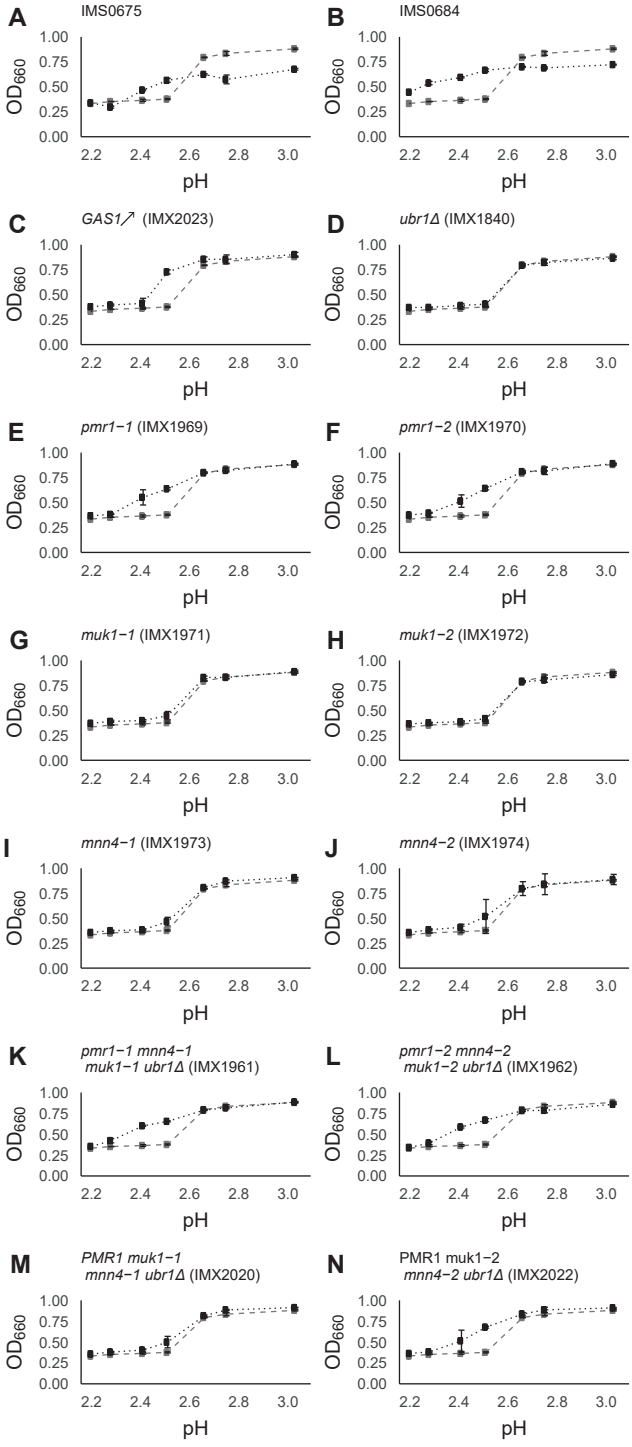
A
IMS0675
B
IMS0684
C
GAS1↗ (IMX2023)
D
ubr1Δ (IMX1840)
E
pmr1−1 (IMX1969)
F
pmr1−2 (IMX1970)
G
muk1−1 (IMX1971)
H
muk1−2 (IMX1972)
I
mnn4−1 (IMX1973)
J
mnn4−2 (IMX1974)
K
pmr1−1 mnn4−1
muk1−1 ubr1Δ (IMX1961)
L
pmr1−2 mnn4−2
muk1−2 ubr1Δ (IMX1962)
M
PMR1 muk1−1
mnn4−1 ubr1Δ (IMX2020)
N
PMR1 muk1−2
mnn4−2 ubr1Δ (IMX2022)
OD660
1.00
0.75
0.50
0.25
0.00
2.2
2.4
2.6
2.8
3.0
pH

Figure 4.4: *See previous page.* Characterization of the effect of specific mutations identified in ALE experiments I and II on growth of *S. cerevisiae* at pH values that are non-permissive for the parental strain CEN.PK113-7D. All strains were grown in four independent microtiter plates at the indicated pH and final OD_{660} was measured after 3 (pH 2.4 and above) or 5 days (pH 2.3 and below) of incubation. An OD over 0.4 was considered as growth. For all panels, black dots and dashed lines indicates the pH tolerance profile of the unevolved strain CEN.PK113-7D. Relevant genotypes and strain names are indicated in each of the panels. For the genotype of IMS0675 and IMS0684 see Error bars show the standard deviation of the OD measurements of the four replicates.

Backcrossing to enrich for mutations contributing to low-pH tolerance

In the evolved, low-pH tolerant strains, many genes affected by mutations did not occur in all strains isolated from an ALE-experiment (Figure 4.2, Table 4.1). To minimize the time and resources invested in reverse engineering and still test all (combinations of) these mutations, a backcrossing approach was used to enrich causal mutations. Evolved strains IMS0675 and IMS0684 were backcrossed with an unevolved parent (IMK439), and the resulting F1 and F2 progenies were screened for pH tolerance (Figure 4.5) For each ALE experiment, three F1 strains and two F2 strains, selected (Figure 4.5A) based on similarity of their low-pH tolerance phenotype with that of their evolved parents (Figure 4.5B), were sequenced. Four strains obtained by backcrossing of strain IMS0675 (ALE experiment I) outperformed their parent (IMS0937, IMS0846, IMS0847 and IMS0947) in terms of final optical density and pH range, while the pH range and final optical density of IMS0944 strongly resembled its evolved parent. Strain IMS0950 showed a higher minimum permissive pH of 2.3 than its evolved parent IMS0675. Four strains obtained by backcrossing (IMS0942, IMS0848, IMS0849, IMS0953) showed the same pH range as their evolved parent IMS0684 (ALE experiment II), but consistently reached higher final optical densities.

The most strongly conserved mutations in F1 and F2 strains were expected to be important for pH tolerance. In ALE experiment I, a single mutation, *mnn4-1*, was conserved in all five F1 and F2 strains. In ALE experiment II, *ynd1-2*, *pmr1-2*, *cna1-2*, *muk1-2* and the CNV of chromosomes IX and XII, were also conserved in all five descendants (Table 4.2). Since the evolved strains were crossed with a uracil-auxotrophic strain, sequences on chromosome V of the evolved parent, which carried a functional *URA3* allele, were selected for in the F1 and F2 progeny. Enrichment of the Chromosome V-borne *ynd1-2* (ALE experiment II) might therefore result from co-segregation of *ynd1-2* with *URA3*, and not necessarily reflect a contribution to low-pH tolerance (Tables 4.1 and 4.2). The mutation in *cna1-2* in evolved strain IMS0684 was located on the duplicated arm of chromosome XII and had 100 % coverage, indicating that both copies of *cna1-2* were mutated. In the F2 strains IMS0950 and IMS0953, coverage for this mutation was ambiguous (only 50 %; Table 4.2), indicating that a single copy of the mutated allele *cna1-2* had been retained.

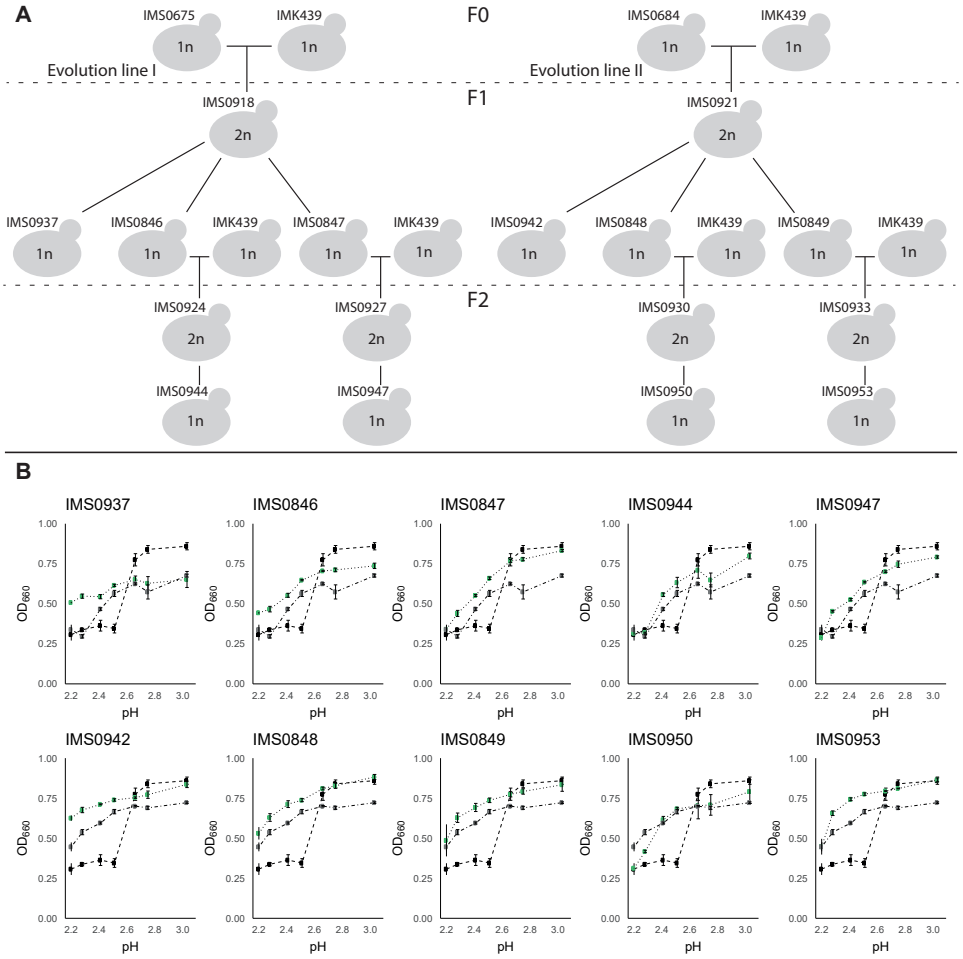

Figure 4.5: **A)** Backcrossing strategy. **B)** pH range for all selected haploid F1 and F2 strains (determined in microtiter plate, see Materials and Methods). All strains were measured at least in duplicate and error bars represent the average deviation from the mean. Top row: strains from ALE experiment I, bottom row: strains from ALE experiment II. Green dots represent the F1 or F2 strain, black dots represent the unevolved parent strain CEN.PK113-7D, gray dots represent the corresponding evolved strain (IMS0675 or IMS0684).

Other genes were conserved in most descendants: *rsp5-1*, *pmr1-1*, *erg6-1*, *muk1-1* and the CNV for chromosome XII (Table 4.2) for ALE experiment I and fre1-2 and CNV for XIII for ALE experiment (Table 4.2). As for *ynd1-2*, the Chromosome V-borne *rsp5-1* allele may have been co-enriched with *URA3* in the F1 and F2 progeny. Mutations in ergosterol synthesis (*erg5*) and disruption of *fre1* (ferric reductase) were previously implicated in improved growth of evolved *S. cerevisiae* at a permissive low pH [108]. However, neither the *fre1-2* mutation nor the *erg6-1* found in the present study were conserved in all F1 and F2 strains and therefore

did not appear to play a major role in the low-pH tolerance of the evolved strains.

Of the four mutated genes that were reverse engineered, those in *PMR1*, *MUK1* and *MNN4* were highly conserved after backcrossing, while *ubr1-1* and *ubr1-2* were lost in the majority of F1 and F2 strains. Since *UBR1* and *PMR1* are both located on chromosome VII, loss of the mutated *UBR1* genes must have resulted from an intrachromosomal cross-over. A single F2 strain from ALE experiment I that lacked *pmr1-1* (IMS0944), retained only three mutations of the 14 mutations found in its evolved parent (*MNN4*, *ERG6* and duplication of a region of chromosome XIII, Table 4.2).

Table 4.2: Retention or loss of mutations after backcrossing of evolved, low-pH tolerant strains. Conservation (X) or loss (0) of mutations identified in the evolved, low-pH-tolerant *S. cerevisiae* strains IMS0675 and IMS0684 in low-pH tolerant F1 and F2 progeny obtained after backcrossing with an non-evolved, low-pH intolerant reference strain. The matching grey color indicates from which F1 strain the F2 progeny originates (e.g., IMS0944 is a descendant of IMS0846). Mutations in *IOC2* were only found in IMS0684, but not in IMS0679 or IMS0681 and were therefore excluded from Table 4.2 and Figure 4.2.

ALE experiment I						
			F1		**F2**	
Gene name	**Locus**	**IMS0937**	**IMS0846**	**IMS0847**	**IMS0944**	**IMS0947**
MNN4	YKL201C	X	X	X	X	X
*RSP5**	YER125W	X	X	X	O	X
PMR1	YGL167C	X	X	X	O	X
ERG6	YML008C	X	X	O	X	O
MUK1	YPL070W	X	O	X	O	X
CHR XIII (2x,3x)		X (2x)	X (2x)	O	X (2x)	O
KGD2	YDR148C	O	X	X	O	X
HEM12	YDR047W	X	X	O	O	O
IPT1	YDR072C	X	X	O	O	O
UBR1	YGR184C	X	X	O	O	O
SER1	YOR184W	O	O	X	O	X
STE13	YOR219C	O	O	X	O	X
ACE2	YLR131C	X	O	O	O	O
ALE experiment II						
			F1		**F2**	
Gene name	**Locus**	**IMS0942**	**IMS0848**	**IMS0849**	**IMS0950**	**IMS0953**
*YND1**	YER005W	X	X	X	X	X
PMR1	YGL167C	X	X	X	X	X
CNA1	YLR433C	X	X	X	AMB (50%)	AMB (50%)
MUK1	YPL070W	X	X	X	X	X
CHR IX 3x		X (2x)	X (2x)	X (2x)	X (2x)	X (2x)
CHR XII 3x		X (2x)	X (2x)	X (2x)	X (2x)	X (2x)
GAS1 6x		X (5x)	X (3x)	X (3x)	O	X (3x)
FRE1	YLR214W	X	X	O	X	O
MNN4	YKL201C	X	O	X	O	O
MSB1	YOR188W	X	O	O	O	O
UBR1	YGR184C	O	X	O	O	O
LCB3	YJL134W	O	O	O	O	O
IOC2	YLR095C	O	O	O	O	O
MITO		O	O	O	O	O

Physiological characterization at pH 2.5 in shake flask cultures

To further investigate the effects of the observed mutations, the best performing strains from the reverse engineering approach (IMX1969, IMX1970, IMX1961 and IMX1962) and from backcrossing (IMS0937, IMS0944, IMS0947, IMS0942 and IMS0953) were characterized in shake-flask cultures at pH 2.5 on synthetic medium with glucose (SMUD) and compared with the evolved strains IMS0675 and IMS0684 and with the non-evolved strain CEN.PK113-7D. While CEN.PK113-7D was unable to grow at pH 2.5, the evolved strains grew at 0.26 h^{-1} (IMS0675) and 0.16 h^{-1} (IMS0684) (Figure 4.6A) and the cultures were fully viable (Figure 4.6B). Strains carrying only the *pmr1-1* or *pmr1-2* alleles (IMX1969 and IMX1970) were unable to sustain growth after a pre-culture at pH 2.5. In contrast, strains IMX1961 and IMX1962, which each carried four mutations in *PMR1*, *MUK1*, *MNN4* and *UBR1*, grew at 0.18 h^{-1} and at 0.14 h^{-1}, respectively (Figure 6A), but during exponential growth only about 75 % of the cultures was viable (Figure 6B). This decreased viability of the direct engineered strains compared to the evolved strains suggests that additional mutations in the evolved strains contribute to an improved viability under low pH conditions.

Backcrossed strains from ALE experiment I (IMS0937, IMS0944 and IMS0947) all grew at pH 2.5. The F1 strain IMS0937 and F2 strain IMS0947 (Figure 5) outperformed strain IMX1961, which carried reverse engineered mutations in *PMR1*, *MUK1*, *MNN4* and *UBR1*. As mutations in all of these four genes were retained in strain IMS0937, its higher specific growth rate at pH 2.5 should be attributed to other mutations retained it its genome (*rsp5-1*, *erg6-1*, *hem12-1*, *ipt1-1*, *ace2-1* and/or a duplication of the right arm of chromosome XIII). Although IMS0937 and IMS0947 had nearly identical specific growth rates at pH 2.5 (0.21 h^{-1} and 0.23 h^{-1}, respectively), the only common mutations between these two strains were *pmr1-1*, *muk1-1*, *mnn4-1* and *rsp5-1*. The culture of IMS0937 was fully viable, while the viability of the culture IMS0947 was higher than 90 % (Figure 4.6B). Strain IMS0944, in which only *mnn4-1*, *erg6-1* and the duplication of the right arm of chromosome XIII were retained, grew at pH 2.5. However, its specific growth rate was less than half than that of its evolved parent strain (Figure 4.6), and the culture viability was only 70 %. For ALE experiment II, F1 strain IMS0942 and F2 strain IMS0953 both outperformed their evolved parent strain IMS0684, with specific growth rates at pH 2.5 of 0.27 h^{-1} and 0.29 h^{-1} (Figure 4.6A) and culture viabilities of more than 80 %. The conserved mutations between IMS0942 and IMS0953 were *ynd1-2*, *pmr1-2*, *cna1-2*, *muk1-2*, an extra copy of the part of chromosome IX and XII and an increased copy number of *GAS1* (Table 4.2).

Physiological characterization in anaerobic bioreactor cultures at pH 2.5

Cultures in bioreactors were performed to quantitatively evaluate the performance of the engineered and evolved strains. Three strains derived from evolution line I were selected for this characterization, the evolved strain IMS0675, its F2 descendant IMS0947, and the reverse engineered strain IMX1961 (*pmr1-1 muk1-1*

mnn4-1 ubr1Δ). These strains differed in their respiratory competency as the reverse engineered strain IMX1961 was most likely capable to respire, while IMS0675 and its descendant IMS0947, both lacking a full *KGD2* allele, were most likely respiratory deficient. To exclude a potential impact of respiratory proficiency in the low-pH tolerance of these strains, the cultures were performed under anaerobiosis. The performance of the low-pH tolerant strains was compared with the non-evolved strain CEN.PK113-7D grown at pH 2.5 (Figure 4.7). As observed under aerobic environment, the unevolved strain CEN.PK113-7D did not grow at pH 2.5 (Figure 4.7A,E), even after 62 hours, while the evolved parental strain IMS0675 grew

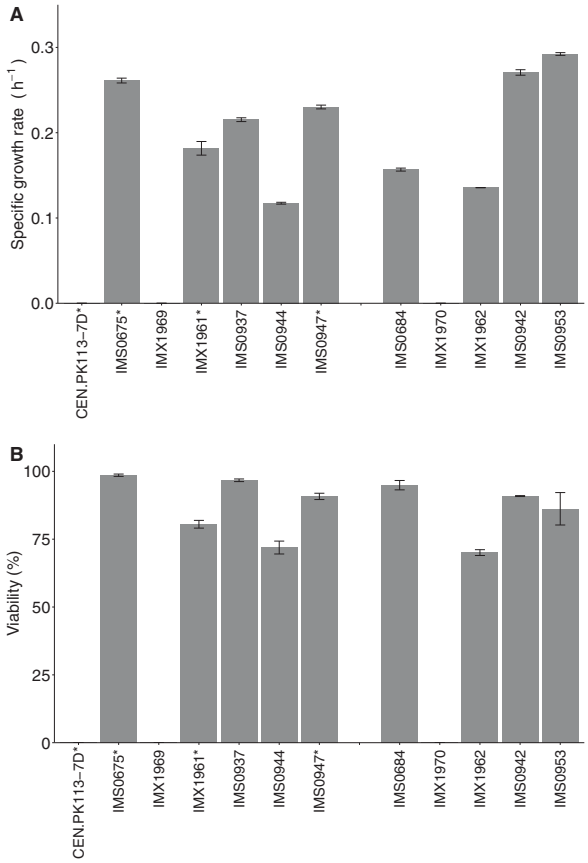

Figure 4.6: Maximum specific growth rate (A) and viability based on propidium iodide staining (B) of evolved strains IMS0675 and IMS0684, reverse engineered strains and backcrossed strains of ALE experiment I and II in shake flask cultures at pH 2.5. Strains were grown in duplicate shake flask cultures in SMUD at pH 2.5 with glucose as sole carbon and energy source. Data are represented as average ± average deviation from the mean of independent duplicate growth experiments for each strains. Strains were pre-cultured in SMUD at pH 2.5 prior to analysis of the growth rate. CEN.PK113-7D did not grow in the pre-culture at pH 2.5 and was hence inoculated from a culture grown at the permissive pH of 3.0. An asterisk indicates strains that were selected for characterization in anaerobic bioreactor cultures.

at a specific growth rate of 0.18 h^{-1} (Figure 4.7B,E). A decrease in growth rate is expected for *S. cerevisiae* from aerobic to anaerobic conditions (0.39 vs 0.31 h^{-1}, respectively for CEN.PK113-7D at pH 5 [24], which could partially explain the decreased growth rates observed in the anaerobic bioreactor cultures compared to the aerobic shake flask cultures at pH 2.5. Remarkably, while IMS0947 grew faster than IMX1961 in aerobic shake flask cultures at pH 2.5 (Figure 4.6A), under anaerobic conditions the reverse engineered strain IMX1961 grew at a specific growth rate of 0.12 h^{-1}, outperforming the F2 descendant IMS0947 which grew at a specific growth rate of 0.10 h^{-1} (Figure 4.7E). A positive correlation was observed between specific growth rate and biomass yield as strains IMS0675, IMX1961 and IMS0947 displayed a biomass yield to 0.058 ± 0.003 $g.g^{-1}$, 0.054 ± 0.001 g g^{-1} and 0.046± 0.000 $g.g^{-1}$ respectively. These values are substantially lower than the biomass yield under anaerobiosis of 0.094 ± 0.004 $g.g^{-1}$ at pH 5 [240, 292] and 0.076 ± 0.002 $g.g^{-1}$ at pH 2.7 [78] measured for the unevolved strain. The overall yield of biomass on ATP decreased from 13.27 $g.mol^{-1}$ for the unevolved strain at pH 5 [292] and 9.17 $g.mol^{-1}$ at pH 2.7 [78] to 8.15 $g.mol^{-1}$ for the evolved parent strain IMS0675 at pH 2.5 (Figure 4.7J). The evolved parent strain IMS0675 outperformed both IMX1961 and IMS0947 in specific growth rate and specific substrate consumption rate (Figure 4.7E,F). Moreover, the biomass yield and Y_{ATP} (Figure 4.7H,J) of IMS0947 were lower than of IMS0675, altogether suggesting that in neither IMX1961 nor IMS0947, the genotype required for the low-pH tolerance of the parent was fully reconstituted. In these experiments, the differences in viability between the IMS0675, IMX1961 and IMS0947 in the anaerobic cultures at pH 2.5 were smaller than in the aerobic shake flask cultures at pH 2.5 (Figure 4.6B, Figure 4.7G). The viability of the unevolved strain had dropped below 15 % after 40 hours of incubation.

Finally, to test the respiratory competence of these strains the sparging gas was switched from pure nitrogen to compressed air at the end of the cultures. Glucose consumption leads to ethanol accumulation and only respiration proficient strains can utilize ethanol as carbon source. While IMX1961, was able to grow aerobically on ethanol, the evolved strain IMS0675 and the backcrossed strain IMS0947, both lacking a full *KGD2* allele, were confirmed to be respiratory deficient. Considering the performance of the three tested strains under aerobic and anaerobic environment, respiratory competence is unlikely to have a substantial impact on the low-pH tolerance of the evolved and engineered strain.

Figure 4.7: *See next page.* Biomass and metabolite profiles of CEN.PK113-7D (A), IMS0675 (B), IMX1961 (C) and IMS0947 (D) in anaerobic bioreactor cultures in SMD medium at pH 2.5. Closed circles: OD_{660}. Open circles: glucose concentration. Closed squares: Glycerol. Open squares: Ethanol. Closed triangles: Biomass (Dry weight). Panels A-D display single representative cultures from a set of two independent duplicate cultures for each strain.The resulting specific growth rate based on the increase in OD_{660} (E), specific substrate consumption rate ($q_{glucose}$) (F), viability (G), Biomass yield (Y_{XS}) (H), Ethanol ($Y_{ethanol}$) and glycerol ($Y_{glycerol}$) yield (I) and ATP yield (Y_{ATP}) (J) could only be determined for the growing cultures (ie. All except CEN.PK11-7D). Data shown in panels E-J are represented as average ± average deviation from the mean of independent duplicate growth experiments for each strains. The raw data of panels E-J is provided in Supplementary data table S8 and has not been corrected for viability.

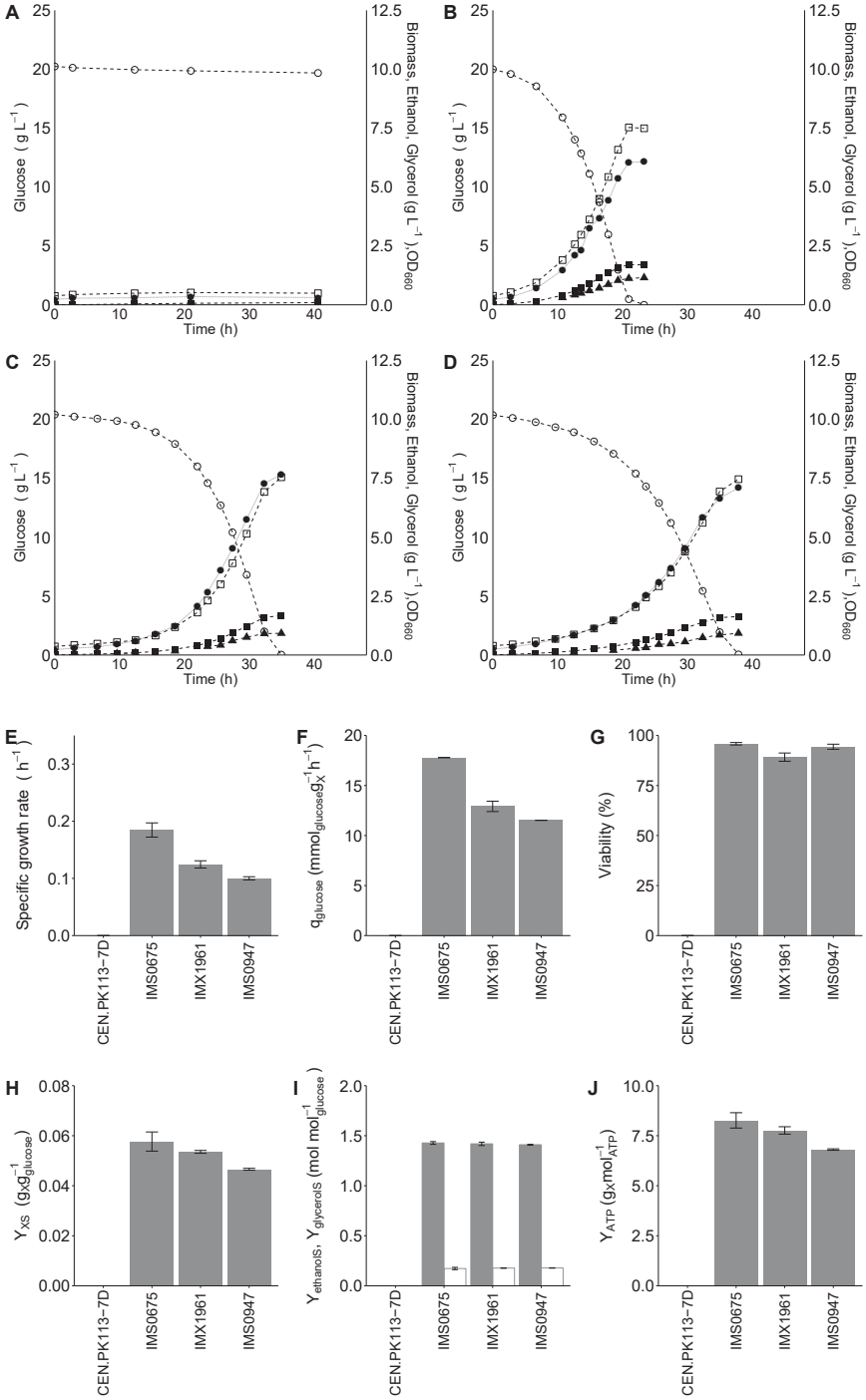
A
B
C
D
Glucose (g L−1)
Biomass, Ethanol, Glycerol (g L−1), OD660
Time (h)
E
Specific growth rate (h−1)
F
qglucose (mmolglucose gX−1 h−1)
G
Viability (%)
H
YXS (gX gglucose−1)
I
YethanolS, YglycerolS (mol molglucose−1)
J
YATP (gX molATP−1)
CEN.PK113−7D
IMS0675
IMX1961
IMS0947

Discussion

Adaptive laboratory evolution, involving serial transfer of batch cultures grown at progressively lower pH values, decreased the minimum permissive pH of *S. cerevisiae* CEN.PK113-7D from above 2.5 to 2.1. This change represents an over 2.5-fold increase of the permissive extracellular concentration of free protons. One evolved strain showed a specific growth rate at pH 2.5, a non-permissible pH for its parental strain *S. cerevisiae* CEN.PK113-7D, of 0.26 h^{-1}. This specific growth rate corresponds to approximately 60 % of the specific growth rate of the non-evolved strain at its optimum pH for growth (Figure 4.1A). These results illustrate the potential of laboratory evolution to improve complex, multi-gene traits.

The biomass yield in anaerobic batch cultures of the evolved low-pH tolerant strain IMS0675 at pH 2.5 (0.058 g biomass (g glucose)$^{-1}$, Figure 4.7, Supplementary data table S8) was substantially lower than biomass yields reported for its parental strain CEN.PK113-7D at permissive pH values but under otherwise similar conditions (0.094 $g.g^{-1}$ at pH 5 [240, 292]) and 0.08 $g.g^{-1}$ at pH 2.8 [78]). This low biomass yield is unlikely to be solely attributable to changes in biomass composition [333]. Instead, it suggests that, despite acquisition of mutations that improved low-pH tolerance, growth of evolved low-pH tolerant strains at low pH still requires a high rate of glucose dissimilation to support cellular maintenance. An increased maintenance-energy requirement has recently also been shown for growth of the parental strain CEN.PK113-7D at suboptimal but permissive pH values [173, 129]. Another remarkable feature of the evolved strains was the ability to retain a high viability at pH 2.5, while the unevolved strain was reported to exhibit a reduced viability at low pH conditions [129]. It can be speculated that the mechanisms underlying this superior robustness might come at a cost in term of ATP.

Indeed, next to an increased rate of proton leakage across the plasma membrane, which would necessitate increased ATP-dependent proton pumping, an increased rate of protein turnover could contribute increased maintenance energy requirements at extremely low pH. Even under optimal growth conditions, protein turnover is responsible for a large fraction of cellular maintenance-energy requirements in *S. cerevisiae* [36, 143]. At low extracellular pH, exposed cell wall and membrane proteins may be particularly susceptible to destabilization and/or denaturation, requiring their continuous turnover. In line with this notion, *GAS1*, which was amplified in two independent ALE experiments in this study and in a previous ALE study on low-pH tolerance [108], encodes a cell-wall polysaccharide-crosslinking enzyme [255, 256] that is directly exposed to the extracellular medium. Null mutants in *gas1* show reduced viability [256] and are sensitive to cell- wall stresses [258]. *GAS1* expression is induced at low pH [74] and overexpression of *GAS1* improves growth at suboptimal pH values (Figure 4.4A, [211, 210]). Expression of *GAS1* paralogs from acid-tolerant yeast species such as *Issatchenkia orientalis* similarly improves low-pH tolerance of *S. cerevisiae* [210]. Mutations in *MUK1*, *RSP5* and *UBR1* could also indicate a key role of increased

protein turnover, although *ubr1* mutations were not retained during backcrossing. A previous study showed that mutations in protein degradation pathways improved tolerance of *S. cerevisiae* to n-butanol [125], a chemical that is known to cause protein denaturation [359].

As individual *muk1-2* and *mnn4-2* mutations in non-evolved strains did not enhance low-pH tolerance, the present results suggest a synergy between the proteins encoded by the *muk1-2* and *mnn4-2* alleles (Figure 4.5, Table 4.2). Interestingly, Kao and Sherlock found $MNN4^{Lys924Glu}$ and $MUK1^{Ser441STP}$ mutations and Chiotti *et al.* found $MUK1^{Lys275STP}$ during prolonged cultivation in chemostat cultures that were not equipped with pH regulation [157, 55]. In the absence of pH control, utilization of ammonium, the nitrogen source in those cultures, causes strong acidification [137]. Mutations in *MNN4* and *MUK1* in these studies might therefore also reflect an adaptation to low pH. Both Muk1p and Mnn4p are involved in extracellular processes. Mnn4 regulates Mnn6, which is involved in mannosylphosphorylation of cell wall proteins [232, 311], while Muk1p, is in the multivesicular body (MVB) pathway for Golgi trafficking and endocytosis [243, 287]. The present study therefore supports a role for these proteins in low-pH tolerance.

The challenges involved in unravelling the signaling pathways involved in low-pH tolerance and the underlying cellular functions are illustrated by the *pmr1* mutations identified in the evolved low-pH tolerant strains. While a previous study specifically implicated mutations in *PMR1* in lactic-acid tolerance [108], our results indicate that the *pmr1-1* and *pmr1-2* mutations were sufficient to cause improved growth of *S. cerevisiae* at pH 2.7 and below in the absence of this monocarboxylate (Figure 4.4). Since deletion of *PMR1*, which encodes an ATP-dependent transporter that translocates Ca^{2+} from the yeast cytosol into the Golgi, negatively affects aerobic growth and causes extended lag phases (Supplementary data figure S4, [11, 335]), the *pmr1-1* and *pmr1-2* mutations clearly did not cause a complete loss of function. Both mutations changed polar serine residues to a hydrophobic amino acid in a transmembrane α-helix that is part of the ion-transport channel (S104) or in close proximity to it (S358) (Table 4.1, Supplementary data figure S6). Since serine residues play an important conformational role in (trans-membrane) α-helices [15], these mutations may well affect Ca^{2+} transport [202, 310]. Cytosolic Ca^{2+} is an important signaling molecule that, via the calcineurin pathway, affects regulation of cell wall synthesis, vesicle transport and lipid and sterol synthesis [64]. Calcium plays additional roles within the Golgi in protein glycosylation [81, 57] and cell wall modification [184], while alterations of the Ca^{2+} concentration can ultimately also affect protein folding and lipid synthesis in the ER [81, 283]. The hypothesis that the *pmr1-1* and *pmr1-2* mutations contributed to low-pH tolerance by influencing cytosolic Ca^{2+}-mediated signaling pathways is consistent with other mutations in the evolved strains that affected related processes: calcineurin signaling (*cna1-2*), cell wall maintenance and synthesis (*GAS1*, *mnn4-1*, *mnn4-2*, *ynd1-2*) and sphingolipid and sterol synthesis (*erg6-1*, *ipt1-1*, *lcb3-2*, *ser1-1*). Single mutations in *PMR1* could thus offer an evolutionary 'quick fix' by simultaneously

influencing multiple cellular processes that affect low-pH tolerance. Analyzing cytosolic Ca^{2+} concentrations in strains carrying *pmr1-1* and *pmr1-2* mutations with the Ca^{2+}-dependent photoprotein aequorin [57, 223] could help testing this hypothesis and analyzing the molecular mechanisms connecting low-pH tolerance and calcium signaling.

This study identifies specific mutations in calcium signaling, cell wall maintenance, membrane composition and protein turnover that lead to increased tolerance to low extracellular pH conditions. While ALE combined with reverse engineering has shown to be a powerful approach for the construction of strains with desired traits [125, 124, 338, 43], the genotype underlying low-pH tolerance could not be fully resolved. This study illustrates the need for high throughput strain construction as well as screening in ALE strategies for the identification of all mutations involved in phenotypes as complex as pH tolerance.

Materials and Methods

Strains and strain maintenance

S. cerevisiae strains used in this study are listed in Table 4.3. Stocks of *S. cerevisiae* CEN.PK113-7D, the reverse engineered and backcrossed strains (see below), were prepared by overnight growth in YPD (10 $g.L^{-1}$ Bacto yeast extract, 20 $g.L^{-1}$ Bacto peptone, 20 $g.L^{-1}$ glucose, demineralized water) in an Innova incubator shaker (New Brunswick Scientific, Edison, NJ) set to 200 rpm and 30 ºC. After adding glycerol to a final concentration of 30 %, 1.5 mL aliquots of these cultures were stored at -80 ºC. Frozen samples from evolution experiments were prepared in the same way.

Table 4.3: Yeast strains used in this study. Superscript symbols in the genotype of strains from backcrossing indicate extended copy number variation and are described in Table 4. The genes in chromosomal regions that showed copy number variations are described in Supplementary data *: Table S3, #: Table S1, : Table S2 and ^*:Table S3

Strain name	Genotype	Reference
CEN.PK113-7D	*MATa MAL2-8c SUC2*	[273, 228, 318]
Evolved strains		
IMS0671	Single colony isolate 1 from ALE experiment I	This study
IMS0672	Single colony isolate 2 from ALE experiment I	This study
IMS0673	Single colony isolate 3 from ALE experiment I	This study
IMS0674	Single colony isolate 4 from ALE experiment I	This study
IMS0675	Single colony isolate 5 from ALE experiment I	This study
IMS0676	Single colony isolate 6 from ALE experiment I	This study
IMS0677	Single colony isolate 7 from ALE experiment I	This study
IMS0678	Single colony isolate 8 from ALE experiment I	This study
IMS0679	Single colony isolate 1 from ALE experiment II	This study
IMS0680	Single colony isolate 2 from ALE experiment II	This study
IMS0681	Single colony isolate 3 from ALE experiment II	This study
IMS0682	Single colony isolate 4 from ALE experiment II	This study
IMS0683	Single colony isolate 5 from ALE experiment II	This study
IMS0684	Single colony isolate 6 from ALE experiment II	This study
IMS0685	Single colony isolate 7 from ALE experiment II	This study
IMS0686	Single colony isolate 8 from ALE experiment II	This study

Table 4.3: (continued)

Constructed strains		
IMX585	*MATa MAL2-8c SUC2 can1Δ::cas9-natNT2*	[204]
IMX1840	*MATa MAL2-8c SUC2 can1Δ::cas9-natNT2 ubr1Δ*	This study
IMX1927	*MATa MAL2-8c SUC2 can1Δ::cas9-natNT2 pmr1Δ::synPAM*	This study
IMX1928	*MATa MAL2-8c SUC2 can1Δ::cas9-natNT2 muk1Δ::synPAM*	This study
IMX1929	*MATa MAL2-8c SUC2 can1Δ::cas9-natNT2 mnn4Δ::synPAM*	This study
IMX1930	*MATa MAL2-8c SUC2 can1Δ::cas9-natNT2 pmr1Δ::synPAM muk1Δ::synPAM mnn4Δ::synPAM ubr1Δ*	This study
IMX1961	*MATa MAL2-8c SUC2 can1Δ::cas9-natNT2 pmr1Δ::pmr1-1 muk1Δ::muk1-1 mnn4Δ::mnn4-1 ubr1Δ*	This study
IMX1969	*MATa MAL2-8c SUC2 can1Δ::cas9-natNT2 pmr1Δ::pmr1-1*	This study
IMX1970	*MATa MAL2-8c SUC2 can1Δ::cas9-natNT2 pmr1Δ::pmr1-2*	This study
IMX1971	*MATa MAL2-8c SUC2 can1Δ::cas9-natNT2 muk1Δ::muk1-1*	This study
IMX1972	*MATa MAL2-8c SUC2 can1Δ::cas9-natNT2 muk1Δ::muk1-2*	This study
IMX1973	*MATa MAL2-8c SUC2 can1Δ::cas9-natNT2 mnn4Δ::mnn4-1*	This study
IMX1974	*MATa MAL2-8c SUC2 can1Δ::cas9-natNT2 mnn4Δ::mnn4-2*	This study
IMX2020	*MATa MAL2-8c SUC2 can1Δ::cas9-natNT2 pmr1Δ::PMR1 muk1Δ::muk1-1 mnn4Δ::mnn4-1 ubr1Δ*	This study
IMX2021	*MATa MAL2-8c SUC2 can1Δ::cas9-natNT2 pmr1Δ::PMR1 muk1Δ::muk1-2 mnn4Δ::mnn4-2 ubr1Δ*	This study
IMX2023	*MATa MAL2-8c SUC2 can1Δ::cas9-natNT2 sga1::GAS1*	This study
Backcrossing Diploid strains		
IMS0918	IMS0675 x IMK439 *MATa/α URA3/ura3Δ::Kan-MX*	This study
IMS0924	IMS0846 x IMK439 *MATa/α URA3/ura3Δ::Kan-MX*	This study
IMS0927	IMS0847 x IMK439 *MATa/α URA3/ura3Δ::Kan-MX*	This study
IMS0921	IMS0684 x IMK439 *MATa/α URA3/ura3Δ::Kan-MX*	This study
IMS0930	IMS0848 x IMK439 *MATa/α URA3/ura3Δ::Kan-MX*	This study
IMS0933	IMS0849 x IMK439 *MATa/α URA3/ura3Δ::Kan-MX*	This study

Table 4.3: (continued)

Backcrossing Haploid strains		
IMK439	CEN.PK113-1A *MATα ura3Δ::Kan-MX*	[125]
IMS0846	Low-pH tolerant isolate from IMS0918; *MATa URA3 hem12-1 ipt1-1 rsp5-1 pmr1-1 ubr1-1 mnn4-1 erg6-1 kgd2-1* CHRXIII*(2x)	This study
IMS0847	Low-pH tolerant isolate from IMS0918; *MATa URA3 rsp5-1 pmr1-1 mnn4-1 ser1-1 ste13-1 muk1-1 kgd2-1*	This study
IMS0937	Low-pH tolerant Isolate from IMS0918; *MATα URA3 hem12-1 ipt1-1 rsp5-1 pmr1-1 ubr1-1 mnn4-1 ace2-1 erg6-1 muk1-1* CHRXIII*(2x)	This study
IMS0944	Low-pH tolerant isolate from IMS0924; *MATα URA3 mnn4-1 erg6-1* CHRXIII*(2x)	This study
IMS0947	Low-pH tolerant isolate from IMS0927; *MATa rsp5-1 pmr1-1 mnn4-1 ser1-1 ste13-1 muk1-1 kgd2-1*	This study
IMS0848	Low-pH tolerant isolate from IMS0921; *MATa URA3 ynd1-2 pmr1-2 ubr1-2 fre1-2 cna1-2 muk1-2* CHRIX#(2x) CHRXII^(2x) *GAS1*\(3x)	This study
IMS0849	Low-pH tolerant isolate from IMS0921; *MATa URA3 ynd1-2 pmr1-2 mnn4-2 cna1-2 muk1-2* CHRIX#(2x) CHRXII^(2x) *GAS1*\(3x)	This study
IMS0942	Low-pH tolerant isolate from IMS0921; *MATa URA3 ynd1-2 pmr1-2 mnn4-2 fre1-2 cna1-2 msb1-2 muk1-2* CHRIX#(2x) CHRXII^(2x) *GAS1*\(5x)	This study
IMS0950	Low-pH tolerant isolate from IMS0930; *MATa URA3 ynd1-2 pmr1-2 fre1-2 cna1-2/ muk1-2* CHRIX#(2x) CHRXII^(2x)	This study
IMS0953	Low-pH tolerant isolate from IMS0933; *MATα URA3 ynd1-2 pmr1-2 cna1-2/ muk1-2* CHRIX#(2x) CHRXII^(2x) *GAS1*\(3x)	This study

Adaptive laboratory engineering (ALE)

To start the ALE experiments, frozen stock cultures of *S. cerevisiae* CEN.PK113-7D were inoculated into 500-mL shake flasks containing 100 mL chemically defined medium with urea as nitrogen source and glucose as sole carbon source (SMUD). This medium was essentially as described previously [332] but contained 38 mM urea and 38 mM K_2SO_4 instead of $(NH_4)_2SO_4$ and glucose (2 %) as sole carbon source. The pH was set to pH 2.8, 2.7, 2.6 or 2.5, with concentrated H_2SO_4 (97 %, Sigma-Aldrich, St. Louis, MO), before filter sterilization with 0.22 µm bottle top filters (Thermo Fisher Scientific, Waltham, MA). Shake-flask cultures were incubated at 30 ºC and at 200 rpm. Serial transfer was performed in 100-mL Erlenmeyer flasks containing 20 mL of the same medium. During serial transfer, the pH of the medium was decreased stepwise (pH 2.8, 2.7, 2.6, 2.5, 2.4, 2.35, 2.3, 2.28, 2.25). In subsequent serial transfers (pH 2.2, 2.15, 2.1, 2.05) potassium sulfate was omitted from the medium. At each transfer, a culture sample was diluted 50 – 100 fold in sterile medium with the same initial pH as the previous culture as well as in medium with the next lower initial pH in the series. The culture at the lower pH was only used to inoculate a subsequent serial transfer if it showed more than 2 doublings. When serial transfer was interrupted for technical or logistic reasons, experiments were re-started from the most recent frozen sample from a previous transfer. Culture purity was routinely checked by phase-contrast microscopy, by

testing for the CEN.PK113-7D characteristic lithium sensitivity [65] and by Sanger sequencing of the ITS-region of the whole population. To evaluate the respiratory capacity of the evolution cultures, an aliquot of the culture was plated on solid yeast extract peptone (see above) plates with ethanol (2 %) and glycerol (1 %) as carbon sources supplemented with 2 % (w/v) agar.
At the end of serial transfer experiments, the resulting culture was plated on YPD agar (YPD as described above with 2 % (w/v) agar). For each serial transfer experiment, eight colonies were picked and pre-grown in synthetic medium at pH 3.0. After microscopic inspection for culture purity, these cultures were sorted for single entities by a FACS Aria (BD Biosciences, Franklin Lakes, NJ) with a 70 µm nozzle, based on the FSC and SSC distribution as described before [33]. Five entities per culture were spotted separately onto a YPD plate. After incubation at 30 °C for two days, one of the five colonies was randomly chosen and inoculated into SMUD (pH 3.0). Prior to preparing frozen stocks (-80 °C) in 30 % glycerol, cells were cells were centrifuged (3000 *xg*, 5 min) and resuspended in synthetic medium [332] at pH 6.0 to prevent potential deterioration by exposure to low pH during freezing and thawing.

Molecular biology techniques

Diagnostic PCR was performed with DreamTaq polymerase (Thermo Scientific), according to the manufacturer's instructions. DNA fragments for Sanger sequencing or integration (see below) were amplified with Phusion Hot Start II High Fidelity Polymerase (Thermo Scientific). Desalted or PAGE-purified oligonucleotides (Sigma-Aldrich, St. Louis, MO) used as primers for PCR amplification are listed in Supplementary data table S1. Amplified DNA fragments were separated by electrophoresis on 1 % (w/v) agarose gels (Thermo Scientific) in TAE buffer or 2 % agarose gels in TBE buffer at 90 V for 30 min. PCR fragments were purified with a GenElute PCR Clean-Up kit (Sigma-Aldrich) or a Zymoclean Gel DNA Recovery kit (Zymo Research, Irvine, CA). Plasmids maintained in *Escherichia coli* DH5α (Z-competent transformation kit; Zymo Research, CA) were isolated using the Sigma Genelute Plasmid Kit (Sigma-Aldrich). Yeast genomic DNA was isolated with the SDS/lithium acetate protocol [193] with an additional washing step with 70 % ethanol, drying of the pellet for approximately 1 hour and resuspension in water or TE buffer.. .

Plasmid construction

Plasmids used in this study are listed in Table 4.4. Plasmids pUDR389, pUDR432, pUDR433, pUDR434, pUDR435 and pUDR436 were constructed by Gibson assembly (New England Biolabs, Beverly, MA) of two fragments, according to the manufacturer's recommendations. One of these fragments contained the 2µ origin of replication and two gRNA-recognition sites, while the other encode selection markers for maintenance in *S. cerevisiae* and *E. coli*, as described previously [204]. *E.coli* DH5-α was transformed by chemical transformation [146]. For construction of pUDR432 and pUDR433, the plasmid pROS12 was used as template for the backbone, while for pUDR434, pUDR435 and pUDR436 the plasmid pROS13 was used for this purpose, amplified with primer 6005 (Supplementary data table S1, [204]). To amplify the fragment with the 2µ-fragment and to introduce a *PMR1*, *MUK1*, *MNN4* and/or *UBR1* recognition site, primers 11289, 12824, 13353 or 13358 were used, respectively (Supplementary data table S1) with pROS12 as a template. The orientation of the gRNA-recognition sites in each plasmid was confirmed by PCR as described before [204], with primers 11138 and 5941 binding on the backbone and primers 13898, 13895, 13897

and 13896 binding in the recognition sites of *PMR1*, *MUK1*, *MNN4* and *UBR1*, respectively. For storage of yeast and *E. coli* strains, 30 % (v/v) glycerol was added to exponentially growing cultures and aliquots were stored at −80 °C.

Table 4.4: Plasmids used in this study. Plasmids used in this study for CRISR/Cas9 mediated strain engineering as described by Mans *et al.* 2015 [204]. The loci of the gRNA-recognition sites introduced in these plasmids are indicated. The synPAM locus is a synthetic sequence enabling the removal of a native locus and subsequent introduction of a mutated allele [271]. The plasmids used as template for amplification of the backbone and the corresponding yeast selection marker are indicated. For propagation in *E. coli* the backbone carried the AmpR selection marker. Primers used for amplification of the plasmid backbone and the 2µ-fragment [204] are listed in Supplementary data table S1.

Plasmid	Target	Target sequence (5' -> 3')	Template backbone / yeast selection marker [204]	Origin
pUDR114	synPAM (2x)	TGTAGAATTTCACCTAGACG	pROS12 / /*hphNT2*	[271]
pUDR119	*SGA1*	ATTGACCACTGGAATTCTTC	pMEL11 / amdSYM	[271]
pUDR389	*PMR1* (2x)	CATAAAAAGAGAGACCACTG	pROS13 / *kan-MX*	This study
pUDR432	*PMR1* + *MUK1*	ATCGATGAAAGTAATTTAAC + TTCTAGATTGGTTAATGCAA	pROS12 / *hphNT2*	This study
pUDR433	*MUK1* (2x)	TTCTAGATTGGTTAATGCAA	pROS12 / *hphNT2*	This study
pUDR434	*UBR1* (2x)	TAATCCCACAATATTCATAT	pROS13 / *kan-MX*	This study
pUDR435	*UBR1* + *MNN4*	TAATCCCACAATATTCATAT + ACGTAGAATTCAACCATAAC	pROS13 / *kan-MX*	This study
pUDR436	*MNN4* (2x)	ACGTAGAATTCAACCATAAC	pROS13 / *kan-MX*	This study

Strain construction

S. cerevisiae strains were transformed according to Gietz and Woods (2002) [121]. Mutants were selected on solid YP medium (demineralized water, 10 g·L^{-1} Bacto yeast extract, 20 g·L^{-1} Bacto peptone, 2 % (w/v) agar), supplemented with 200 mg·L^{-1} G418 and/or 200 mg·L^{-1} hygromycin B as required or on solid synthetic medium (2 % w/v agar) with acetamide (0.6 g·L^{-1}) as sole nitrogen source [293] and 6.6 g·L^{-1} potassium sulfate to compensate for the absence of ammonium sulfate and both contained 2 % glucose. In all cases, gene deletions and integrations were confirmed by colony PCR on randomly picked colonies, using the diagnostic primers listed in Supplementary data table S1 (Supplementary data).

For introduction of an extra copy of *GAS1* under the control of its native promoter and terminator, primers 14291 and 14292 were used to amplify the fragment from genomic DNA of CEN.PK113-7D and add 60-bp flanks homologous to sequences at the *SGA1*-locus. Transformation of the resulting fragment and pUDR119 to *S. cerevisiae* IMX585 (CEN.PK113-7D with a functional Cas9 [204]), followed by selection on SM-glucose with acetamide as sole nitrogen source, yielded strain IMX2023.

UBR1 was deleted by simultaneous transformation of a repair oligo (Supplementary data table S2) and plasmid pUDR434, yielding strain IMX1840. *PMR1*, *MUK1* and *MNN4* were deleted, along with introduction of synthetic PAM sites [271], by transformation of pUDR389 and a repair oligo made out of oligos 14195 and 14196 (*PMR1*), pUDR433 and a repair oligo made out of oligos 14191 and 14192 (*MUK1*), pUDR436 and a repair oligo made out of oligos 14193 and 14194 (*MNN4*). Combined deletion of *UBR1*, *PMR1*, *MUK1* and *MNN4* was performed by transforming the abovementioned repair oligos with plasmid pUDR432 and pUDR435, resulting in strain IMX1930, in which *ubr1* was deleted and *pmr1*, *muk1* and *mnn4*

were deleted with the introduction of a synthetic PAM site.

For introduction of the mutated alleles of *PMR1*, *MUK1* and *MNN4*, the loci were amplified from genomic DNA of IMS0675 or IMS0684 with primers 8641 and 11292 (*PMR1*), 12828 and 13757 (*MUK1*), 13356 and 13357 (*MNN4*). Transformation of these fragments, along with pUDR114 [271] that carries a gRNA targeting the synthetic PAM site, resulted in integration of the mutated alleles. Performing this transformation routine in IMX1927 resulted in strains IMX1969 (*pmr1-1*) and IMX1970 (*pmr1-2*), in IMX1928 resulted in strains IMX1971 (*muk1-1*) and IMX1972 (*muk1-2*), and in IMX1929 resulted in strains IMX1973 (*mnn4-1*) and IMX1974 (*mnn4-2*). Analogously, transformation of pUDR114 and these fragments into IMX1930 resulted in strains IMX1961 (*pmr1-1 muk1-1 mnn4-1 ubr1Δ*), IMX1962 (*pmr1-2 muk1-2 mnn4-2 ubr1Δ*). For the reconstitution of the native *PMR1* locus in IMX1930, genomic DNA of CEN.PK113-7D was used as a template with primers as described above, resulting in IMX2020 (*PMR1 muk1-1 mnn4-1 ubr1Δ*) and IMX2021 (*PMR1 muk1-2 mnn4-2 ubr1Δ*), respectively. All mutated alleles were confirmed by Sanger sequencing (Baseclear, Leiden, The Netherlands).

Backcrossing: mating, sporulation, spore isolation and germination

Evolved mutants (IMS0675 and IMS0684) were crossed with IMK439, a strain derived from CEN.PK113-1A by replacing its *URA3* gene with the Kan-MX marker gene [124]. CEN.PK113-1A is congenic with CEN.PK113-7D, but has the opposite mating type (MATα). For mating, parent strains were grown overnight in YPD in separate shake-flask cultures (30°C, 200 rpm). After another transfer to fresh YPD medium, amounts of mid-exponential-phase cells (OD_{660} of 8-10) corresponding to 1 mL of cell suspension with an OD_{660} of 3.4 were taken from both cultures and pooled. The resulting culture was centrifuged (2000 *xg*, 1 min), resuspended in 200 µL YPD and incubated at 12°C for at least 2 days, until 'shmoo formation' was observed by microscopic analysis (see below). Diploid strains were selected by plating on SMD agar plates with urea as nitrogen source that contained G418 and lacked uracil by making three restreaks and stocking the strains at -80°C as described above.

Sporulation of diploids and mass spore isolation was performed according to Gorter de Vries *et al.* (2019) with minor adaptations [126]. Diploid strains were grown over night in YPD in shake-flask cultures (30°C, 200 rpm). Sporulation in 2 % potassium acetate at pH 7.0 was done in the presence of 0.05 % glucose (20ºC, 200rpm). Presence of spores (asci) was microscopically checked (see below) after at least 48 h of incubation. Cells were then pelleted (1000 *xg*, 5 min), resuspended in softening buffer (10 mM dithiothreitol, 100 mM Tris-SO_4, pH set to 9.4 with H_2SO_4) and incubated at 30°C for 10 minutes. Cells were washed with demineralized water, resuspended in spheroplasting buffer (2.1 M sorbitol, 10 mM KH_2PO_4, pH set to 7.2 with 1M NaOH, 0.8 $g.L^{-1}$ zymolyase 20-T (AMS Biotechnology, Ltd. Abingdon, United Kingdom)) and incubated overnight at 30°C. Next, the culture was pelleted (1000 *xg*, 10 min), washed with demineralized water and resuspended in 0.5 % triton X-100 (Sigma-Aldrich, Zwijndrecht, The Netherlands). Spores were sonicated for 15 s at 50 Hz with an amplitude for 6 µm while kept on ice using a Soniprep 150 (MSE, London, United Kingdom). Isolation of spores was confirmed by microscopic inspection (see below). The suspension was diluted 1:1 with Isoton II diluent (Beckman Coulter, Woerden, The Netherlands) and sorted by fluorescence-activated cell sorting (FACS), using a BD FACSAria™ II SORP Cell Sorter (BD Biosciences, Franklin Lakes, NJ) equipped with a 70 µm nozzle and operated with filtered FACSFlow™ (BD Biosciences). Using a 488 nm laser, cell morphology was analyzed by plotting forward scatter (FSC) against side scatter (SSC). Prior to each

experiment, cytometer performance was checked by running a CS&T cycle with CS&T Beads (BD Biosciences). Drop delay for sorting was determined by running an Auto Drop Delay cycle with Accudrop Beads (BD Biosciences). Prior to sorting, 100,000 events were analyzed for each culture. On the basis of plots displaying forward scatter plotted against side scatter, a sorting region of interest ('gate') was selected for sorting. The gate was set in such a manner that smaller debris, spore clumps and cell clumps (if present) would be discarded. Single spores were sorted in 200 µL YPD in 96 well plates (Sigma Aldrich). The plates were incubated at 30°C for two days without shaking. The grown cultures originating from a single spore were, transferred to an empty 96 well plate and subsequently the determination of the low pH range of these cultures was performed as described below. The most tolerant strains were grown overnight in YPD in shake flask cultures and were stocked at -80ºC after adding glycerol to a final concentration of 30 %. The mating type of the selected strains was determined by PCR. Four F1- strains resulting from this procedure were (IMS0846-IMS0849) were mated with IMK439 and led to the strains IMS0944, IMS0947, IMS0950 and IMS0953 by following the procedures as described above.

Strain characterization

All strain characterizations in shake flask cultures were incubated at 30 ºC at 200 rpm in an Innova incubator shaker (Eppendorf Nederland B.V., Nijmegen, The Netherlands), unless stated otherwise. Growth rates were derived from the increase in optical density at 660 nm over at least 2,5 doublings. The spectrophotometer is indicated per characterization below.

pH range of CEN.PK113-7D

Growth experiments in shake flasks were started by inoculating CEN.PK113-7D from frozen stock cultures in synthetic medium, with urea as sole nitrogen source to prevent further acidification [197], glucose as the sole carbon source and set at the appropriate pH (2.5, 3.0, 3.25, 3.5, 4.0, 4.5, 5.0, 6.0) with either H_2SO_4 or KOH (SMUD). After this initial culture, cells were transferred to a pre-culture on the same medium and pH, at an initial OD_{660} of approximately 0.1. During exponential growth, cells were washed with demineralized water and transferred to a third shake flask at an initial OD_{660} of 0.2 in which the specific growth rate was calculated based on optical density measurements of at least five sample points over at least 2 doublings. The cultures were diluted with demineralized water to an OD_{660} between 0.1 and 0.3 and measured on a Libra S11 spectrophotometer (Biochrom, Cambridge, United Kingdom).

Screening of growth of single-colony isolates from ALE experiments at pH 3 and pH 2.1

Frozen stock cultures of single-colony isolates were inoculated in 20 mL SMUD at pH 3.0 in 100 mL Erlenmeyer flasks and incubated until they were in the exponential growth phase. Cells were then transferred to fresh medium at pH 3 (SMUD) and pH 2.10 (SMUD without K_2SO_4). The specific growth rate of these cultures was determined based on optical density measurements on a Libra S11 spectrophotometer (Biochrom). Three colonies from each of the two ALE experiments were chosen for further characterization.

Characterization of the minimum permissive pH of evolved strains

Evolved strains were characterized at the lowest pH at which growth was observed during the two ALE experiments, i.e. SMUD pH 2.05 and SMUD 2.1. Strains were inoculated

in synthetic medium at SMUD pH 3 (see above) until fully grown at 30 °C at 200 rpm in an Innova incubator shaker (Eppendorf Nederland B.V.). To obtain exponentially growing cultures, an aliquot was transferred to fresh medium at pH 3. Exponentially growing cultures were then transferred to fresh synthetic medium SMUD pH 2.1 and pH 2.05 (see above) at an initial OD_{660} of 0.1 - 0.3. Specific growth rates of these cultures were measured based on the increase in optical density on a Jenway 7200 Spectrophotometer (Jenway, Staffordshire, United Kingdom).

Shake flask characterization at pH 2.8, pH 2.7 and pH 2.5

Characterization of reverse engineered strains at pH 2.8 and pH 2.7 was performed in duplicate cultures in 500-mL shake flasks contained 100 mL medium. Cultures were inoculated from freezer stocks into SMUD pH 3.0 medium and grown until an OD_{660} of 10-20. Cells were the transferred to fresh SMUD medium at the same pH as used for the subsequent characterization (SMUD pH 2.8, pH 2.7 or pH 2.5) at an initial OD_{660} of 0.05 – 0.1. Mid-exponential phase cells were centrifuged (3000g , 5 min), washed with demineralized water and inoculated to fresh SMUD at the corresponding pH for growth characterization at an initial OD_{660} of 0.5 for characterization at pH 2.8 and 2.7 and an initial OD_{660} of 0.05 for pH 2.5 Maximum specific growth rates were calculated based on OD_{660} measurements on a Jenway 7200 Spectrophotometer (Jenway) as described above. Since the parental strain CEN.PK113-7D did not grow in SMUD pH 2.5, its pre-culture for characterization in SMUD pH 2.5 was grown in SMUD pH 3.0.

pH range analysis

For the analysis of the pH range of reverse engineered strains, backcrossed strains and their haploid progeny (see above), they were pre-grown overnight on YPD in at 30 °C in 15 mL Greiner Tubes. Of these precultures, 5 µL was added to 100 µL synthetic medium with a range of initial pH conditions in polystyrene microtiter plates (96 well flat bottom plate, Sigma-Aldrich). The pH of the medium was set such that it reached the intended value after addition of 5 % v/v of YPD. For each culture pH, duplicate plates were used. Upon inoculation, the 96 well plate was covered with a gas-permeable seal and statically incubated for 3-5 days at 30 °C. Prior to analysis, plates were shaken and the seal was removed. The final OD_{660} was measured on a GENIos Pro microplate spectrophotometer (Tecan, Männedorf, Switzerland).

Anaerobic bioreactor cultures

Shake-flask cultures on SMUD (pH 3) were inoculated with frozen stock cultures and grown until glucose depletion. Cells were then transferred to shake flasks containing fresh SMUD (pH 3) and grown until mid-exponential phase. These precultures were subsequently inoculated to anaerobic bioreactors at an initial OD_{660} of 0.2 - 0.3. Anaerobic bioreactor batch cultures were performed in synthetic medium with glucose as sole carbon source (20 $g.L^{-1}$), and ammonium sulfate as sole nitrogen source (5 $g.L^{-1}$) prepared as described before [331] and containing 0.2 $g.L^{-1}$ sterile antifoam C (Sigma-Aldrich), ergosterol (10 $mg.L^{-1}$) and Tween 80 (420 $mg.L^{-1}$) (SMD). The medium pH was set to 2.5 by addition of H_2SO_4. Culture pH was maintained at 2.5 by automatic addition of 2M KOH. Anaerobic batch cultures were grown in 2-L Applikon bioreactors (Applikon, Schiedam, The Netherlands) with a 1.2-L working volume, at 30 °C and at a stirrer speed of 800 rpm. Nitrogen gas (<10 ppm

oxygen) was sparged through the cultures at 0.6 L min^{-1} and bioreactors were equipped with Norprene tubing and Viton O-rings to minimize oxygen diffusion. All strains were tested in independent duplicate cultures. Biomass dry weight was determined as described previously by Postma *et al.* [257] and OD_{660} was measured on a Jenway 7200 spectrophotometer as described above. The exhaust gas was passed through a condenser kept at 2 °C and dried with a PermaPure Dryer (model MD 110-8P-4; Inacom Instruments, Veenendaal, the Netherlands). Carbon dioxide in the dried exhaust gas was measured with a Rosemount NGA 2000 Analyser (Baar, Switzerland). Supernatants were obtained by centrifugation of culture samples (3 min, 16,000 *xg*) and analyzed by high-performance liquid chromatography (HPLC) on an Agilent 1260 HPLC (Agilent Technologies, Santa Clara, CA), equipped with an Aminex HPX-87H ion-exchange column (BioRad, Veenendaal, The Netherlands), with 5 mM H2SO4 as the mobile phase and operated at 60 °C and at a flow rate of 0.6 $mL.min^{-1}$. Detection was by means of a dual-wavelength absorbance detector (Agilent G1314F) and a refractive-index detector (Agilent G1362A).

Microscopy and viability analysis

Phase-contrast microscopy with an Imager-Z1 microscope equipped with an AxioCam HR3 camera (Carl-Zeiss, Oberkochen, Germany), using an EC Plan-Neofluar 40x/0.75 Ph 2 M27 155 objective (Carl-Zeiss). For viability analyses based on membrane integrity, cells were incubated for 15 minutes in the dark with a final concentration of 0.02 mM propidium iodide (PI, Sigma Aldrich) and analyzed by fluorescence microscopy analysis. PI can enter cells that have lost membrane integrity, where it intercalates with nucleic acids. Propidium Iodide fluorescence was detected with filter set 14 (Ex. 510-560 nm, Bs FT 580 nm, Em. LP 590 nm; Carl Zeiss). Images were analyzed using ImageJ 1.46r (NIH, USA). At least 500 cells, detected by phase-contrast microscopy, were counted per sample and viability was expressed as the fraction of non-PI-stained cells in a sample.

Genome sequencing and analysis

For whole-genome sequencing, strains were grown on YPD at 30 °C and 200 rpm until glucose depletion. Genomic DNA was isolated with the Qiagen Genomic DNA buffer set kit (Qiagen, Venlo, The Netherlands) in combination with the Qiagen Genomic-tip 100/G. DNA concentrations were determined using a Qubit® Fluorometer 2.0 (Thermo Fisher Scientific). Sequencing was performed on a MiSeq (Illumina, San diego, CA) after TruSeq DNA PCR-free library preparation as described previously [300]. Reads were mapped onto the *S. cerevisiae* CEN.PK113-7D reference genome [273] using the Burrows-Wheeler alignment tool and further processing using SAMtools and Pilon for variant calling [185, 186, 342]. The datasets generated by genome sequencing for this study can be found in the NCBI database (`https://www.ncbi.nlm.nih.gov/`) under the bioproject PRJNA546594.

Acknowledgements

This work was performed within the BE-Basic R&D Program (http://www.be-basic.org/), which was granted a FES subsidy from the Dutch Ministry of Economic Affairs, Agriculture and Innovation (EL&I). Furthermore, we thank Mark Bisschops, Arthur Gorter de Vries, as well as partners in the BE-Basic project for valuable discussions. The authors thank Francine Boonekamp, Hannes Jürgens and Nicolò Baldi for practical assistance during the Adaptive

Laboratory Evolution experiment. Furthermore, the authors thank Pilar de la Torre Cortes for extensive expertise in whole genome sequencing of strains in this study and would like to thank Marcel van den Broek for help in the analysis of whole genome sequencing data. Lastly, the authors thank Susan Weening and Charlotte Koster for the advice and help in the backcrossing experiments.

Availability of data

The supplementary files are available online at `https://www.tudelft.nl/tnw/over-faculteit/afdelingen/biotechnology/research-groups/industrial-microbiology/pascale-daran-lapujade-group/`

CHAPTER 5

A simulator-assisted workshop for teaching chemostat cultivation in academic classes on microbial physiology

Xavier D.V. Hakkaart
Jack T. Pronk
Ton J.A. Van Maris

In my experience this facet of microbiology
- growth physiology -
has been severely diluted (practically and theoretically)
in many university degree programs
and now would be an opportune time
to redress ill-considered curriculum decisions.

Allan T. Bull, 2010

This chapter was published in the Journal of Microbiology and Biology Education **18-3**, (2017) [130].
https://dx.doi.org/10.1128%2Fjmbe.v18i3.1292

Abstract

Understanding microbial growth and metabolism is a key learning objective of microbiology and biotechnology courses, essential for understanding microbial ecology, microbial biotechnology and medical microbiology. Chemostat cultivation, a key research tool in microbial physiology that enables quantitative analysis of growth and metabolism under tightly defined conditions, provides a powerful platform to teach key features of microbial growth and metabolism.

Substrate-limited chemostat cultivation can be mathematically described by four equations. These encompass mass balances for biomass and substrate (Equations 5.1 and 5.2), an empirical relation that describes distribution of consumed substrate over growth and maintenance energy requirements (Pirt equation, Equation 5.3), and a Monod-type equation that describes the relation between substrate concentration and substrate-consumption rate (Equation 5.4). The authors felt that the abstract nature of these mathematical equations and a lack of visualization contributed to a suboptimal operative understanding of quantitative microbial physiology among students who followed their Microbial Physiology B.Sc. courses.

The studio-classroom workshop presented here was developed to improve student understanding of quantitative physiology by a set of question-guided simulations. Simulations are run on Chemostatus, a specially developed MATLAB-based program, which visualizes key parameters of simulated chemostat cultures as they proceed from dynamic growth conditions to steady state.

In practice, the workshop stimulated active discussion between students and with their teachers. Moreover, its introduction coincided with increased average exam scores for questions on quantitative microbial physiology. The workshop can be easily implemented in formal microbial physiology courses or used by individuals seeking to test and improve their understanding of quantitative microbial physiology and/or chemostat cultivation.

Introduction

Acquiring a quantitative insight into the interaction of micro-organisms with their growth environment and, specifically, the way in which nutrient availability affects microbial growth kinetics and biomass yields, is an essential learning objective in academic microbiology programmes. Understanding of this key aspect of microbial physiology is important across many domains of microbiology, including the design of experiments for isolation novel microorganisms from nature, the understanding and optimization of antibiotic therapies and the optimization of microbial product formation in industrial bioreactors. In view of the latter application, biotechnology and bioengineering curricula have historically emphasised the importance of mass balancing in microbial processes, as well as of the ensuing (biomass-specific) rates and microbial growth kinetics.

The chemostat is a continuous cultivation device that is especially suitable for quantitative physiological comparison of microorganisms under highly defined conditions [35, 217, 229, 139, 65, 218]. The power of the chemostat lies in the fact that, after inoculation and an initial dynamic phase (here referred to as non-steady state), the system approaches a state in which not only the physicochemical environment, but also all rates of production and consumption remain constant in time (hence called steady state). In ideally mixed, steady state chemostat cultures, the specific growth rate of the microorganisms equals the dilution rate of the system, which can be set by the experimenter.

Growth and substrate consumption of microorganisms in chemostat cultures can be described by a set of four equations [340]: The mass balances of biomass and growth-limiting substrate, an equation describing the distribution of the growth-limiting substrate over growth and maintenance processes and an equation describing the specific substrate consumption rate as a function of the substrate consumption (see the 'Prerequisite student knowledge'-section for an extensive description of the system). Operational knowledge of and insight into these equations is important for experimental design of chemostat experiments, to correctly interpret experimental data and, in general, to understand the impact of growth conditions on microbial growth and performance.

Quantitative microbial physiology in chemostat cultures is an integral part of the Microbial Physiology course that, for the past 10 years, two of us (J.T. P and A.J.A. v. M) taught together as part of a 2nd year B.Sc. curriculum in Life Science and Technology offered jointly by the Delft University of Technology and Leiden University (the Netherlands). Based on their experience in classroom teaching and evaluation of written exams, all three authors attributed the lower than desired operational knowledge on this topic to the somewhat abstract nature of the mathematical equations and, in particular, insufficient visualisation of the ways in which growth conditions affect growth of microorganisms in chemostat cultures.

Several models have been described in literature that describe chemostat cultivation processes. However, these models are generally aimed at users with advanced understanding of the subject and are therefore suboptimal for use in educational settings [284, 95]. To help students come to grip with the key quantitative aspects of non-steady state and steady state growth phases in chemostat cultures, we developed a simple, robust simulator that specifically visualises the time-dependent dynamics that ultimately result in steady state chemostat cultures. Around this simulator, we designed a question-guided workshop, in which students explore how individual experimental design parameters and/or key

characteristics of the microorganism itself influence the non-steady state and steady state behaviour of chemostat cultures. The workshop was held in a studio-classroom learning environment but can, in principle, be run on stand-alone computers.

Here, we describe the simulator, the accompanying lecture material, the questions used in the workshop and our experiences with the implementation of this workshop.

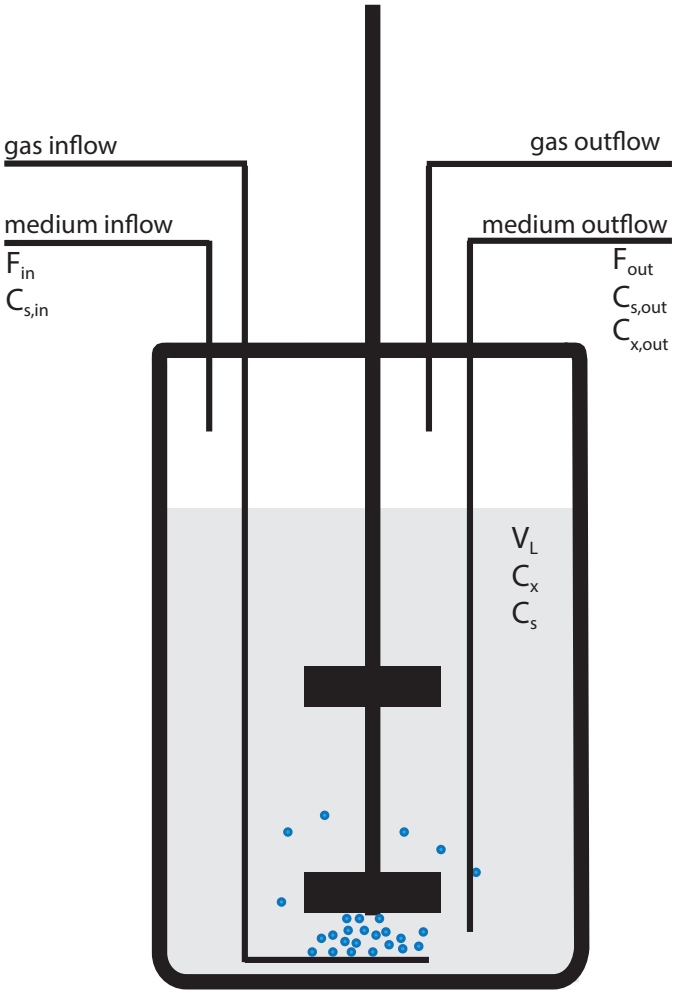

Figure 5.1: Schematic representation of a chemostat set-up. F_{in} and F_{out} are volumetric flows, V_L represents the liquid volume and C represents a concentration. Subscripts in and out denote transport respectively into or from the reactor. Subscript s denotes the carbon and energy-source (substrate) and subscript x denotes biomass.

Intended audience

The simulator-assisted workshop is intended for students who have proceeded in microbiology or (bio)chemical engineering majors with a focus on microbial physiology and/or microbial biotechnology. These students should have had general microbiology classes prior to the workshop and should have been introduced to the theory described below in 'Prerequisite student knowledge', preferably no longer than two weeks prior to the workshop. The workshop is most easily implemented into courses that already have a focus on microbial physiology.

Higher-level students and researchers aiming to improve their knowledge and understanding of quantitative physiology can also use the simulator without the accompanying workshop.

Prerequisite student knowledge

In a standard chemostat culture, fresh medium is continuously added to a cultivation vessel, (bio)reactor, while continuous removal of the spent medium containing biomass is controlled to maintain a constant volume. The fresh medium is typically designed in such a way that a single nutrient will limit growth, while all other medium components are in excess. This workshop focuses on chemostat cultures in which the energy substrate is the growth-limiting nutrient which, in organoheterotrophs, also acts as the carbon source. Growth in such chemostat cultures can be described according to two mass balances: a mass balance for the substrate (a non-volatile carbon and energy source) and a mass balance for biomass.

Description of chemostat cultures with these simple mass balance equations requires that three important criteria be met: (i) the culture needs to be ideally mixed, i.e., concentrations of biomass and substrate within the bioreactor should be identical to those in the outflow, (ii) the culture volume remains constant over time, and (iii) the inflow and outflow rates are equal. The characteristic parameter that can be fixed in a chemostat culture is the dilution rate (D, h^{-1}).

Substrate is added to the bioreactor as part of the fresh, sterile inlet medium. Once inside the reactor it can either be consumed by the microbe in the bioreactor or be removed with the spent medium (Figure 5.1). The microbe in the bioreactor will grow and at the same time be removed with the spent broth.

$$\frac{dM_S}{dt} = \frac{dC_S V_L}{dt} = V_L \frac{dC_S}{dt} = F_{in} C_{S,in} - F_{out} C_{S,out} - q_S C_X V_L \tag{5.1}$$

$$\frac{dM_X}{dt} = \frac{dC_X V_L}{dt} = V_L \frac{dC_S}{dt} = -F_{out} C_{X,out} - \mu C_X V_L \tag{5.2}$$

Distribution of energy substrate over growth and maintenance energy requirements, in the absence of ATP requiring product formation, can be described according to the Pirt equation (Equation 5.3), an empirical relation that assumes a growth rate-independent energy requirement for maintaining cellular viability and integrity [251, 250]. An important consequence of this assumption is that, as the growth rate decreases, a large fraction of the substrate needs to be dissimilated to meet maintenance requirements and is therefore not available for growth. The relationship between the specific consumption rate of the growth-limiting substrate (q_s, $g_s.g_x^{-1}.h^{-1}$) as a function of its concentration in the culture (C_s) can be described by Monod-type saturation kinetics (Equation 5.4) 4, [291, 83, 325]). This relation was used in the simulations rather than the traditional Monod equation for specific growth rate (μ). In situations where growth is limited by the energy substrate, the μ-based Monod equations are conceptually and mathematically incompatible with the concept of growth-rate-independent maintenance requirements. For a comprehensive review of practical aspects of chemostat cultivation, the reader is referred to [139, 65, 153].

To implement the theory described above in a mathematical simulation model, six parameters and three boundary limits were defined as inputs for the model to run: The dilution rate (D, h^{-1}), the maximum biomass-specific substrate uptake rate (q_s^{max}, $g_s.g_x^{-1}.h^{-1}$), the saturation constant for substrate consumption of the growth-limiting nutrient (K_s, $g.l^{-1}$), the maximum biomass yield ($Y_{x/s}^{max}$, $g_x.g_s^{-1}$), the biomass-specific maintenance-energy requirement (m_s, $g_s.g_x^{-1}.h^{-1}$), the substrate concentration in the fresh inflowing medium ($C_{s,in}$, $g.l^{-1}$), the initial biomass concentration ($C_{x,0}$, $g.l^{-1}$), the initial substrate concentration $C_{s,0}$, $g.l^{-1}$) and the total time for the model to run (Max time, days).

$$q_S = \frac{\mu}{Y_{X/S}^{max}} + m_S \tag{5.3}$$

$$q_S = q_S^{max} \frac{C_S}{K_S + C_S} \tag{5.4}$$

Learning objectives

Upon completion of the simulator-assisted workshops about the physiological concepts of energy-source limited chemostat cultivation, students will be able to :

1. Report the mass balances for substrate and biomass that describe a continuous cultivation
2. Report the assumptions that are required to describe steady state conditions
3. Explain and describe the non-steady state dynamics in biomass concentration and substrate concentration in chemostat cultivations that ultimately lead to steady state conditions
4. Describe the relation between the specific growth rate (μ) and the specific substrate uptake rate (q_s) through the Pirt-equation
5. Describe the relation between the specific substrate uptake rate (q_s) and extracellular substrate concentrations (C_s) through Monod-type kinetics
6. Identify the effect on the biomass yield $Y_{X/S}$ and the residual substrate concentrations (C_s) in steady state conditions of the following parameters:
    - Maintenance energy requirements (m_s)
    - Maximum biomass yield ($Y_{X/S}^{max}$)
    - Saturation constant for substrate (K_s)
    - Maximum substrate uptake rate (q_s^{max})
    - Dilution rate (D)
    - Substrate concentration in the inflowing medium ($C_{s,in}$)

    All these concepts are addressed in the workshop questions and can be tested with exam questions, for which examples are provided (Appendix 5).

Learning time

The entire workshop takes approximately four hours to complete. It starts with an introductory part, consisting of a set of introductory questions followed by a presentation by a teacher or course assistant. Subsequently, the students start working with the simulation programme and systematically tackle the guided questions. Finally, results are discussed plenary. It is crucial that students should be allowed sufficient time to 'wrestle' with the questions themselves.

- The workshop starts with the students answering the 'introductory questions' provided in Appendix 3 (25 minutes)
- An introductory presentation recapitulates the answers to the introductory questions and the operation of chemostat cultures. It also explains how the non-steady state dynamics can be analysed. The Power Point presentation in Appendix 2 can be used for this purpose (30 minutes)
- Students start the MATLAB program and familiarize themselves with the functions (20 minutes).
- Students answer the 'guiding questions' about non-steady state and steady state dynamics in chemostat cultures provided in Appendix 3. (120 minutes)
- The workshop ends with an interactive plenary discussion on the answers of the questions. (45 minutes)
- Students are encouraged to use the simulator to individually explore quantitative physiology outside of the workshop

Procedure

Materials

- Student computers that can either work with MATLAB (.m) files or that have the Chemostatus simulation programme installed as a stand-alone module (we have extensively tested this stand-alone version on Windows 7 64 bit). An installation manual is provided in Appendix 1. The MATLAB files as well as the stand-alone version can be requested by sending an email to chemostatus@gmail.com. Chemostatus cannot be installed as a stand-alone version on Mac or Linux computers.
- A studio classroom (i.e. a classroom with PCs or laptops on which Chemostatus simulator and Microsoft Excel can be run). The studio classroom should ideally enable students to work in pairs and have easy access for course assistants.
- Printed student questions, with introductory and guiding questions on separate sheets.
- A projector and screen.
- The Power Point presentation supplied in Appendix 2 or equivalent teaching material.
- A whiteboard or blackboard for the interactive discussion and explanation by teachers/course assistants at the end of the workshop.

Safety instructions

The workshop does not involve (biological) safety hazards (with the possible exception of student exposure to computer keyboards [302]).

Student instructions

Students are advised to work in pairs as this stimulates discussion of the observations. A key aspect to improve the learning experience in this workshop is address each question in a systematic order, answering three sub-questions: (i) which (qualitative) changes are to be expected based on the answers to the introductory questions, (ii) use the Chemostatus simulator and/or simulation data exported to Microsoft Excel to answer the question quantitatively, and (iii) combine knowledge of quantitative physiology and numerical answers to qualitatively understand the changes.

Chemostatus allows the user to change each of the input parameters at will and evaluate the output for six consecutive calculations. Time-dependent simulations provide insight into how steady state conditions are reached. Its outputs consists of plots of biomass concentration, substrate concentration, biomass-specific substrate consumption rate, specific growth rate and actual biomass yield on substrate from the start ('virtual inoculation') of the experiment until a predefined time point. The simulated data that are used to generate the plots can be exported to a Microsoft Excel file for further calculations.

Faculty instructions

It is important that the studio classroom does not only enable students to work on computers, but also enables them to follow instructions by teachers and/or course assistants (using beamer, blackboard and/or whiteboard. The required software (Chemostatus simulator, Microsoft Excel) should be installed and tested on the computers prior to the workshop. A manual for installation is available in Appendix 1. Note that, due to user administrator restrictions, installation of software may require involvement of professional support staff.

Prior to the workshop the pre-requisite knowledge should be explained during classroom lectures. The workshop starts by answering a set of (refresher) questions about steady state chemostat cultures (Appendix 3 ' Introductory questions') without using a computer. Preferably, the underlying concepts of chemostat cultivation should previously have been discussed in regular classroom teaching. The introductory set of questions aims to bring students to the entry level required for the rest of the workshop. Subsequently the answers are discussed. A PowerPoint presentation for teachers/course assistants has been supplied (Appendix 2) to be used during the workshop.

After discussing the relevant growth parameters, equations and assumptions as presented above, students are given 20 minutes to familiarize themselves with the Chemostatus simulator. After this, they are supplied with the set of guiding questions (Appendix 3 'guiding questions') that guide them through simulations of the physiological impacts of changes in different parameters. As stated above, we recommend that students work in pairs to facilitate discussions and peer learning. During this part of the workshop the teacher is available to address questions from students. Obviously, the goal here is not to answer the questions for students but to encourage them to find the answers themselves. Typically, this involves asking additional 'guiding' questions. Depending on the group size, the teacher might require support from course assistants. In our experience, a group of 50-60 students can be guided by three experienced teachers and/or teaching assistants.

After students have had sufficient time to answer the questions, the answers are discussed in a plenary session. The teacher can explain the answers to each of the questions, but can also point out other interesting observations during the non-steady state or steady state phases of the simulated cultures. Preferably, this involves running the Chemostatus on a computer connected to a large screen.

Suggestions for determining student learning

A stepwise approach to the questions, starting out with a formulation of the expected qualitative outcome of the simulations is, in our experience, a major success factor for this workshop. Teachers and course assistants can stimulate and verify this approach by engaging students in conversations themselves and by actively encouraging discussions about the questions among students.
At the end of the workshop the answers to the questions are discussed by the teachers in an interactive plenary session. The feedback from the students during this session provides the teacher with a clear view of student learning results. Written exam questions provide an effective way of testing the extent to which students master this subject. Quantitative physiology is a recurring topic in exams of our Microbial Physiology course. Examples of exam questions are provided (Appendix 5) with corresponding learning objectives.

Sample data

Answers to the student questions of the workshop are provided (Appendix 4).

Discussion

Field testing

- Prior to its use in the regular teaching program, the authors and two student volunteers tested the workshop for user friendliness and clarity.

- The workshop was used twice by as an integral part of their Microbial Physiology course at the Delft University of Technology (December 2015). The workshops, each attended by 60-70 students, were supervised by the three authors.

- The workshop was as an optional workshop in addition to a course on chemostat cultivation taught to eight PhD students by Professor J.G. Kuenen (emeritus professor at Delft University of Technology) and hosted by Professor K.N. Nealson of the Geobiology group in the Department of Earth Sciences, University of Southern California, Los Angeles. This course was held in April 2016.

Evidence of student learning

During the workshop students showed great involvement in the topic and came up with meaningful questions. Spontaneous, enthusiastic discussions occurred about the explanation of complex simulation results (e.g. 'overshoots' of biomass concentrations during non-steady state simulations due to a lower impact of maintenance energy requirements during fast growth). We consider this active involvement and feedback a good indicator that that the workshop enhanced student learning.

Two of the authors have taught quantitative microbial physiology for a full decade as part of their Microbial Physiology course, which they teach in a 'duo presentation' mode. Quantitative aspects of microbial growth is the subject of one of four questions in the final written exam. This question typically consists of 5 sub-questions for each of which scores of 0 - 10 are awarded. In 2014 and 2015 chemostat theory was only explained during lectures. The teachers were not satisfied with student scores for the quantitative physiology question and decided to implement the workshop described in this paper.

To analyze the effect of the workshop the average score per student for the sub-questions specifically dealing with steady-state chemostat cultures were evaluated for the two years before introduction and for the year of introduction of the workshop. The selected sub-questions and corresponding learning objectives are shown in Appendix 5. Upon introduction of the workshop in 2016, the average grade for these sub-questions was significantly higher than in the previous years for both the regular exam (Student's t-test; 2014 to 2016 $p < 0.001$; 2015 to 2016 $p < 0.001$) as well as the retake exam (Student's t-test; 2014 to 2016 p-value: < 0.05; 2015 to 2016 p-value: < 0.001). More importantly the fraction of students that now grasp these quantitative physiological concepts has increased by the introduction of the workshop, as shown by the higher 75% percentile compared to the previous two years (Figure 5.2, Panel A and B) and the increased percentage of students that passed the exam (Figure 5.2, Panel C and D).

At the Delft University of Technology, all courses are evaluated via student surveys and oral evaluation. The course of which this workshop was a new element was evaluated very positively and students specifically indicated the usefulness of the workshop on quantitative physiology.

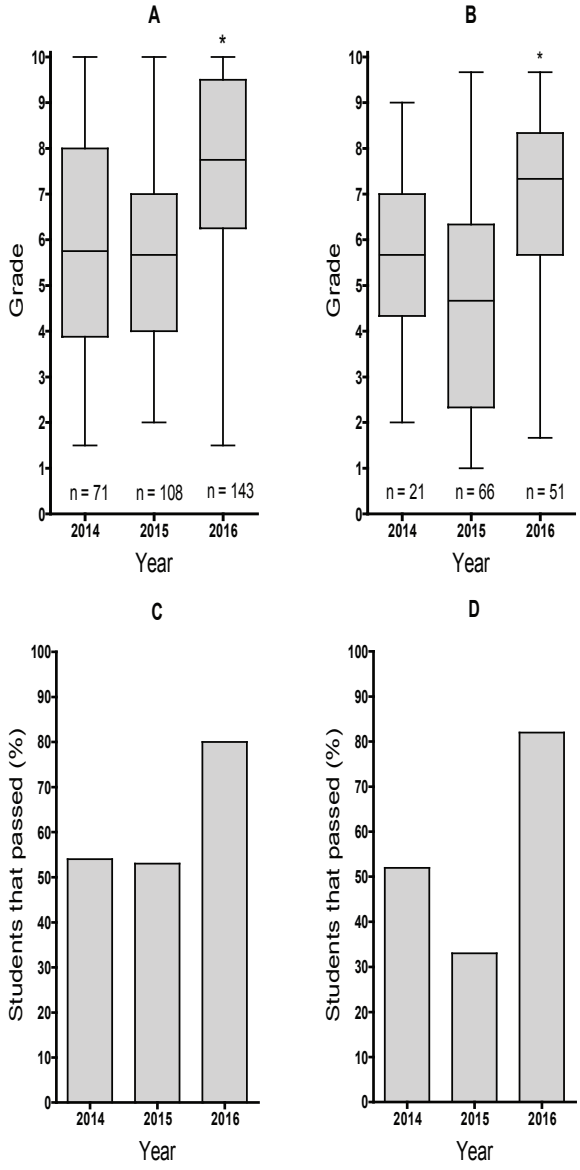

Figure 5.2: Student performance on exam questions concerning continuous cultivations before (2014 and 2015) and after the introduction of the simulator workshop (2016). A boxplot of the distribution of average grades of individual students on these questions for the regular exam (Panel A) and resit exams (Panel B) shows the minimum and maximum grades, the 25% and 75% quartiles (upper and lower limit of the box) and the median (black bar in the box). The asterisk indicates that the average grade was significantly higher than the two other years (p-value < 0.05 in a Student's t-test) Panel A: Student's t-test; 2014 to 2016 p < 0.001 ; 2015 to 2016 p-value < 0.001 Panel B: Student's t-test; 2014 to 2016 p-value: < 0.05; 2015 to 2016 p-value: < 0.001. The questions and the corresponding learning outcomes are provided in Appendix 5. In the Dutch educational system students pass with a grade of 5.5 or higher. The percentage of students passing the exam questions that specifically dealt with steady-state chemostat conditions is shown for the regular exams (Panel C) and resit exams (Panel D)

Possible modifications

This workshop is a complete activity that is ready for use as presented here. In its current format the workshop is held in one session, but can be split into two shorter sessions in which the first session focuses on the concepts and 'introductory questions' and the second session provides students with the opportunity to focus on the 'guiding questions'. To meet specific requirements of different student groups or courses, new sets of questions can be designed. Furthermore, the original MATLAB (.m) files can be requested by sending an email to chemostatus@gmail.com, providing the opportunity to implement new functions. The following modifications can contribute to additional learning:

- Without the accompanying questions and the structure of the workshop, advanced students can use the Chemostatus simulator outside the context of the workshop to deepen their understanding of key concepts of microbial physiology.
- The current version of the workshop is based on simulated data only. The accompanying questions could be extended with an exercise in which experimental chemostat data of a well-known microorganism (for the input parameters of the model are known or can be estimated based on simulations as part of the exercise) are compared to simulations.
- In microbial ecology, chemostat cultivation is a powerful tool to study competition for a limiting nutrient [133, 84, 229]. This concept could be implemented by introducing a second set of parameters, equations and mass balances. This would require the coding of the MATLAB program to be adapted. We would recommend not to add microbial competition as an additional subject in the current 4-h workshop, but, instead, make it the subject of a separate simulation workshop. Similarly, occurrence of mutants with altered growth kinetics might be simulated to gain a deeper understanding in (laboratory) evolution.
- Microbial product formation, which is of special interest in industrial biotechnology, could be implemented by introducing an additional mass balance for product and by providing the model with a relation between product formation and growth rate.

Acknowledgements

The authors would like to thank Prof. J.G. Kuenen for fruitful discussions on the contents and for field testing of the model at the University of Southern California (Los Angeles). We thank Leonor Guedes da Silva for valuable stimulating discussions on the MATLAB coding. The authors thank Maaike Voskamp and Joachim van Renselaar for testing the workshop for user-friendliness. In particular, we thank the 2016 class of our Microbial Physiology course at the Delft University of Technology for acting as highly constructive guinea pigs for this workshop.

Availability of data

The supplementary files are available online at the journal's website: https://dx.doi.org/10.1128%2Fjmbe.v18i3.1292

Outlook

The research described in **Chapter 2**, **3** and **4** systematically characterizes physiological responses of yeast strains to industrially relevant conditions. Interpretation of these results strongly relies on the fundamentals of microbial physiology – the consumption rate of substrate following Monod-type kinetics and substrate distribution over growth and maintenance processes described by the Pirt equation. **Chapter 5** describes a workshop and a simulation program that were specifically designed to make BSc-level students in Microbial Physiology familiar with these quantitative aspects of microbial growth. This tool was highly appreciated by BSc students participating in the Leiden-Delft curriculum in Life Science and Technology and, moreover, improved their understanding of quantitative aspects of microbial physiology, as reflected in their significantly improved performance in related exam questions. The contribution of this education tool to students' understanding of microbial physiology is not limited to the understanding of current and future students at TU Delft. Since its publication, the course material has been requested by colleagues from, amongst other countries, the United States of America, Sweden, Mexico, the United Kingdom and The Netherlands. With this workshop, our goal is to contribute to the understanding of quantitative microbial physiology for the next generation of biotechnology researchers worldwide.

The characterization and quantification of the maintenance-energy requirements under aerobic conditions of *S. cerevisiae* in **Chapter 2** and **3** provides valuable quantitative data for modeling of industrial-scale processes. The glycolytic capacity of *S. cerevisiae* under near-zero growth rates presented in **Chapter 2**, shows the potential of high rate production of non-dissimilatory products in the absence of growth. In **Chapter 3**, the same non-producing yeast strain was characterized under industrially relevant conditions for the microbial production of dicarboxylic acids with *S. cerevisiae*, pH 3 and 50 % CO_2, conditions that were chosen for the purpose of facilitate product recovery in downstream processing and to stimulate product formation, respectively. Growing *S. cerevisiae* under these conditions resulted in increased maintenance-energy requirements and strongly increased death rates, which could be attributed to the low pH.

The reduced performance of *S. cerevisiae* under low-pH conditions was further investigated in **Chapter 4**. The results expose an intrinsic trade-off between optimal conditions for product recovery and for microbial physiology during the microbial production process. The adaptive laboratory evolution approach in **Chapter 4** resulted in *S. cerevisiae* strains capable of growth at pH 2.1 and this study successfully identified genetic targets in *PMR1*, *MNN4* and *MUK1* to overcome the inability to grow at a pH below 2.5. These mutations are direct targets for further improvement of the industrial production of dicarboxylic acids as their implementation in industrial strains may directly improve their tolerance to low pH which could possibly improve product formation. Additionally, these results show the potential of using laboratory evolution for generating low-pH tolerant platform strains, that may subsequently be engineered for carboxylic acid production. The exact biological mechanism underlying the improved low-pH tolerance remains to be elucidated. Based on the prominent role of *PMR1* in low-pH tolerance in **Chapter 4** the characterization of intracellular calcium and the analysis of calcineurin-dependent responses such as adaptations of the cell wall and

cell membrane composition are a good starting point. This is supported by the improvement of low-pH tolerance by overexpression of (heterologous) *GAS1* observed in **Chapter 4** and in other recent studies, and the differential expression of genes involved in cell wall stress observed in **Chapter 3**. The best performing reverse engineered strains in **Chapter 4** – strains IMX1961 and IMX1962 - still exhibited high death rates compared to the strains evolved for low-pH tolerance. Further investigations of low-pH tolerance should focus on the mechanisms of cell death at low pH.

Protein turnover has been suggested to be a major contributor to maintenance-energy requirements of *S. cerevisiae* under optimal laboratory conditions, but it is unknown whether this is also the case under industrially relevant stresses such as low extracellular pH. Determination of the relative contribution of macromolecular turnover and the maintenance of gradients across biological membranes to the total maintenance energy requirements would provide another important step in the identification of approaches to reduce maintenance energy requirements.

Recent advances in genetic engineering of *S. cerevisiae* by CRISPR-techniques have greatly facilitated the construction of strains capable of making non-native non-dissimilatory products. Stepping from the extremely low product yields that are reported in many 'proof-of-concept' studies to reach high-yield product formation in industrial environments, continues to be a significant challenge. Designing genetic circuits based on condition-dependent expression is increasingly used to optimize product formation, taking into account trade-offs between growth rate, product yield and cellular robustness. The transcriptome datasets in **Chapter 2** and **3** can assist in promoter choice for designing genetic switches and in identification of metabolic pathways that require engineering to ensure product formation at near-zero growth rates.

Acknowledgements

The results in this thesis were not the results of a one-man-show, and therefore I am happy that I get to thank all of the people that helped in one way or another. It also brings me joy that this section is possibly the first thing you turn to upon opening this book (am I right?).

First and foremost my gratitude goes to my promotors, Jack Pronk and Pascale Daran-Lapujade for the support, freedom and constructive meetings. You've taught me many aspects of science and much more. As expected, the unexpected happened. Pascale, without your supervision I wouldn't have worked as hard, thought as critically about the results and wouldn't have been enriched with many good experiences, merci beaucoup. Our joint perseverance in characterization of product formation under near-zero growth honed my personality, especially since, in the end, it did not lead to a chapter in this thesis. That which does not kill us, makes us stronger . When coming back from holidays in France, I acted as your somewhat regular delivery service of Crème Anglaise, Sauce béchamel and Badoit sparkling water, avec plaisir. Jack, your enthusiasm about any aspect of science is a great inspiration. Thanks for the personal interest during all these years and for the trust in me as a teacher, the fun we had with 'fermentatiegymnastiek' with the first year students, and the fun discussions during the computer workshops for microbial physiology and far beyond. Your optimism and how you kept a bird's eye view of my project are very much appreciated.

You weren't an official supervisor, Mark, but your advice and help during my project were of great importance to get to the finish line. I admire your perseverance inside and outside academia, your innovative mind and how you set clear goals, I'm sure you'll go a long way.

Besides my direct supervisors for the duration of this PhD project, others have had a great influence on my personal growth and scientific developments. It feels like ages ago since I first stepped into the IMB group for a meeting about a Bachelor End Project (BEP) with Ton, but in reality that was only in 2010. Your inspirational pitch made me decide to join IMB! Stefan and Ton made my BEP a great endeavor, where I first got a taste of the freedom of working in science. For my Master thesis, Tim taught me all the ins and outs of the fermentation lab, and together with Pascale made me a partner in crime for the zero-growth work, resulting in Chapter 2 of this thesis. Thanks for your personal interest in me and for asking me as your paranymph! The adventures in the USA during my industrial internship at Mascoma prior to starting my PhD project at IMB were made into a success by the supervision of Allan, thanks! My co-workers Alyssa, Alex, Andrew, Brooks, Janet, Michelle and Rintze were of great support in the lab and fun outside of the lab. Lastly, the adventures in the USA gave me time to reflect on my future goals, make decisions on embarking on a PhD project, of which the fruitful results are now in your hands.

Several of the projects that led to this thesis have been based on collaborations. Hannes, I greatly enjoyed the shared supervision of Jildau and all our wild ideas on the project 'daddy', that at the last moment did not end up in this thesis. Yaya, our projects grew into

---

Friedrich Nietzsche

a collaboration by the nice complementation of the results presented in chapter 3. The Be-Basic FS10 meetings together with the academic project partners (Bas, Frank, Pascale, Phillipp, Walter and Yaya) and industrial partners (Alrik, Mickel and Viktor) were always pleasant and informative. Mickel, thanks for the bike-meetings on our way to Delft and some career advice here and there!

The core of IMB is kept running by the PIs, thanks for shaping the IMB-atmosphere Jack, Pascale, Robert, Jean-Marc and Ton. The core expertises of IMB are guarded and maintained by your devotion to the group and by the day to day care of the staff- and project-technicians. Thanks to the great care of Erik, assisted by Matthijs, Christiaan and Flip the fermentation labs are up and running continuously. It speaks for itself that without their help, this thesis would have had far fewer chapters, while not even all experiments made it to this final book. The same goes for Pilar and Melanie in the molecular biology lab, Marijke in Mickel's lab and Marcel for all the bioinformatics analyses. Marijke, good luck with your new company, I hope you'll be able to help many people! Also a big thanks for the help in the last stages of my PhD: for part of the results in chapter 4 and for proofreading this thesis! Flip, also a big thanks for the collaboration for part of the results in chapter 4, your helpfulness is one of your big assets!

During my PhD project alone, so many people have passed by the IMB group as colleagues and students. With such a dynamic group, everyone has contributed to this work in one way or the other. Some people I would like to thank in particular, but in a random order. To Arthur, Alex, Robert, Jasmine, Jonna, Maarten, Maria, Mario, Nick, Thomas and Thomas, thanks for making offices throughout the old and new building pleasant together! I'm passing by all the students with whom I've shared the office as well, but thanks to all of you too! IMB is much bigger than only one office, and all the other people contributing to the work atmosphere and the contents of this thesis in one way or another deserve my gratitude as much as the above mentioned office-mates do.

Robert, our office 'de Gazelle-Geit' will always be a fond memory, although I'd be surprised to ever find a hybrid of a gazelle and a goat in the wild. Do you remember who won the chair-race in the Applied Physics building? I think we both have a bit of a twisted mind, but in the most positive way you can imagine. Thanks for the fun, slightly absurd discussions, wild ideas and also for the guidance in the work that led to chapter 3. It was a great pleasure to be your paranymph together with Arthur, especially because there was plenty of material to fill your cabaret! Barbara, thanks for showing me how to combine fun and hard work and thanks for your career advice during my PhD. I solemnly swear never to kick trees again. Harmen, you showed me around the molecular biology lab at the beginning of my PhD project. Some parts of this thesis have greatly benefited from your initial help, thanks! Laura, you really have a heart of gold and your caring personality goes further than you probably imagine. At the start of our projects we shared bike rides back to The Hague, that were traded in for numerous cups of tea and coffee that helped me to reflect on work and life. I hope I could return the favor! Maarten, thanks for fun with discussions about hypothetical experiments, the quality control of word-jokes and for proofreading my introduction! Aurin, your wild enthusiasm for basically anything makes you for a great and greatly blunt discussion partner. Jasmine, sharing the office during the final stage of your PhD was a great joy, just like the "what vegetable am I eating" game that continued over WhatsApp. Your sense of humor and your contagious laugh created the right work atmosphere in our office. Arthur, thanks for many things! The scientific discussions, your goal-oriented mind and business attitude, the fun with climbing, skiing and other out-of-work activities. Your immense drive for anything

you do was a great push in the right direction for me too! I had great fun co-paranymphing with you for Robert's defence and in the preparation for his cabaret.

Work and play go hand in hand. Besides a trip to Gothenburg with Ioannis, Jasmine, Wesley, Nicolo and Hannes and – both work and play –, the skiing trips to Italy with Arthur, Nicolo and Susan, and to France with Anna, Arthur and Nicolo – being mostly play, a trip to France with Maarten and holidays with Sanne kept me going and provided the necessary distraction from PhD life.

Further distractions I found with bouldering-buddies. Although the frequency and the group size varied throughout the years at IMB, I'd like to thank Ewout, Maria, Susan, Arthur, Erik, Sofiia, Nicolo and Sanne for pushing me for that last boulder. Sofiia, your advice summarizes bouldering very eloquently: just go up.

During this project I have had the pleasure to be involved in the daily supervision of Eveline, Elsemiek, Maxime, Teun, Mandy, Dominic, Nicole, Jildau and Jordi. Eveline, your project provided the foundation for chapter 3 in this thesis and left many open questions, part of which were answered in subsequent work. Your diligent work attitude and friendly nature made it a pleasure to work with you. During your project, Elsemiek, we've made a very good start of the results in chapter 5. With my project being in the very early stages, we had many possibilities to explore and had to work with uncertainty. It has given me great pleasure to see you grow and find your passion in the years after. Maxime, your BEP during the move to the new building made the planning of your project challenging. Your hard work and drive contributed to new insights into the research line you worked on. Unfortunately the results from your project did not end up in this thesis, but that didn't hold you back in showing what you've got to offer! Teun, your dedication and strong attitude towards your project made it a pleasure to collaborate with you. Supervising you was also a battle of who was most stubborn. Did I win? I don't know. Even with the many set-backs in your project you did not change your mind about doing a PhD and moving to Sweden. Mandy, never ever tell me again that you're not creative! You set a goal and go for it, a quality of which you can be proud! Good luck with your PhD project in Leiden. Your work, Dominic, was the basis for a pivotal point in the work presented in chapter 5 of this thesis. Jordi, your project started in the final stages of my PhD project and left off where Dominic's project finished. You managed to make low pH tolerance something to directly engineer. I hope I have been able to contribute to your personal growth as well. I'm proud that you found a position at IMB that fits you so well. By far the majority of the work in chapter 3 of this book was performed by Jildau. Your hard work really paid off and it gave me so much pleasure to see you grow during the months that Hannes, you and I made up a great team! Wherever you move next, you'll be great! Your project, Nicole, in collaboration with Mieke and Marine, was possibly the most exciting and inventive project I contributed to, I had never expected to wrap a bioreactor in LED lights..! Sadly, the results never saw the (blue) light in the end. I know it is a cliché, but you should know that I have learned a lot from all of you, thanks!

Zonder het fantastische werk van Apilena, Astrid en Jannie bij de medium- en sterilisatiedienst, zouden de experimenten in het biotechnologie departement in Delft een stuk trager verlopen. Ik wil jullie bedanken voor jullie grote geduld en flexibiliteit om zelfs bij wispelturige autoclaven altijd een manier te vinden om iedereen tot hulp te zijn. Werken in het fermentatielab in het Kluyver of in TNW Zuid, betekent een regelmatig bezoekje aan de werkplaats. Pompen, rotoren, waterbaden of filterhouders die de goede zorgen van Marcel

of Arno nodig hadden, waren altijd in een mum van tijd weer klaar. Bedankt voor deze belangrijke ondersteuning van het onderzoekswerk. Met name de resultaten van hoofdstuk 3 zouden niet dezelfde vorm gehad hebben zonder de grote bijdrage van het gassenteam, en met name Erwin. Daarnaast zou de afdeling Biotechnologie een stuk minder veilig zijn zonder Johan, en zouden de GMO-regels een stuk minder strikt gevolgd worden zonder Marinka (en Pilar bij IMB). De lange traditie van borrels in 't Keldertje en in de botanische tuin bij Chateau de Jacques zou niet mogelijk zijn geweest zonder de enorme inzet van Sjaak, Tonnie, Joop, Robert, Nayyar en de rest van de BT-Feestcie. Jullie toewijding aan de BT-familie voor de talloze BT-feestjes, borrels, sportdagen, PhD-feestjes en vele andere activiteiten waren altijd een groot succes.

A special thanks goes to Louise van Swaaij. A PhD project is like climbing two mountains at the same time, one scientific and one of personal development. With your help I've gotten the tools to climb the highest one, thanks a lot.

Mathieu, who recently passed away so suddenly, I think back to your lectures, our meetings while I was on the board of Study association LIFE, but also to a study-trip to South Korea and your kind advise and interest in me during my PhD project. Your hard work for the Life Science & Technology curriculum in Delft and Leiden – a unique combination of two universities I herald wherever I go - made quality of education and the student's interest go hand in hand. You leave a great legacy, thank you!

My passion for teaching and my interest for life sciences were fed by your contagious enthusiasm, Hilde. And you even achieve to combine it with strict time-management! Our endless talks at the Klikspaanweg and thereafter a little less frequent in Delft, The Hague or Leiden, but always with the same fun, interest and nerd-factor were a great joy to me. Even when I had a flat tire with my racing bike in the middle of nowhere between Leiden and The Hague you and your Atos came to the rescue, thanks! Already at the time when we transferred the treasurer responsibilities at LIFE, we got along very well, Eveline. A listening ear, a laugh and a cup of tea were never far away when we met. You've often helped me to put things in perspective, even after you finished your PhD. I wish Diederik and you all the best in Woerden. Rarely have I met someone that is more ambitious, hard-working and nitty-gritty than you, Leonor. This definitely was an excellent match for the assignments during the MSc courses in Delft, discussions about science and non-science ever since. The MEC-meetings we organized in the old building were a great excuse to meet up for coffee every now and then. However close our offices were at TWN-Zuid, little did we meet up for lunch. Always busy bees, the two of us. Thanks for the support and fun! Our visits to De Doelen must have significantly decreased the average age during all the concerts that we attended, Eleonoor. Discussing our PhD projects over dinner, that were almost in-sync, was of course a necessity as well. Your caring nature, as well as your strong drive to pursue your self-set goals and interests – such as moving to Leuven – has impressed and inspired me very much! Your recent challenges outside of the TU Delft might be tough, but know that it is a matter of time before we can go to De Doelen again. Thanks for everything!

Sophie, thanks for all the dinners at Eazie and for dancing at Wesseling! Jonna, your keen eye for details and your strong drive and opinion make you a great asset to any team. The preparations in the last phase of my PhD project wouldn't have been as easy without your help as a paranymphs. I am happy to defend this thesis with both of you at my sides!

Bedankt voor de gezelligheid bij practica, colleges, feestjes en nog meer tijdens onze studie en bij de weekendjes weg en Sinterkerstennieuw, Danny, Els, Eleonoor, Esmee, Laura, Loes, Maaike, Maureen, Oscar en Tom. Lieve Bart, Doshima, Mette, Olga, Pieter, Rebekka, Tom en Thom. De Wielie als Kluit-head quarter is helaas niet meer, maar wanneer we samen zijn, samen eten, gaan we echt weer terug naar de basis van Kluit: een punt van reflectie en een punt van plezier. Vind ik leuk! Heren van DSF, de korte vakanties naar Normandië moeten we vooral in ere houden. Abram, Bart, Jan, Ken, Matthijs, Pieter, Thom, Tom en Vincent, bedankt voor alle ongepast harde humor, felle discussies en interesse in elkaar.

Een vriendschap vanuit groep 1 op de Hilversumse Schoolvereniging – inmiddels 25 jaar geleden – moet wel iets heel bijzonders zijn. Pieter, je brede kennis van geschiedenis, economie, politiek en interesse in nog veel meer helpen me vaak om mijn eigen ideeën aan te scherpen. Juist de discussies over alles in de wereld zijn een verademing buiten de wetenschap. Jouw en Nikki's trouwdag, waarbij ik jouw getuige was, staat voor altijd als een feestdag in mijn geheugen.

Lieve Hien, samen zijn we gegroeid onder de vleugels van pap en mam, wat ons 'positief kritisch' de wijde wereld in heeft gestuurd. Je houdt me als geen ander een spiegel voor, wat ik in alle jaren zeker nodig heb gehad. Ik ben blij dat we nog steeds samen kunnen optrekken. Het actieve en avontuurlijke leven dat je samen met Alwin hebt, is iets om trots op te zijn. Je gaat zo lekker je eigen weg.

Zonder jullie onvoorwaardelijke steun, pap en mam, was ik niet gekomen tot het schrijven van deze thesis, of tot nog heel veel minder. Altijd een luisterend oor, altijd het goede advies dat ik soms wel en soms nog niet kon horen. De reislust en fascinatie voor levende dingen zitten er bij Hien en mij goed in. Nature of nurture? Met n=2 en zonder negatieve controle zullen we het nooit zeker weten. Maar ook de menselijke maat, de intrinsieke motivatie en zorg voor een ander hebben jullie me meegegeven.

Lieve Sanne, voordat we er ERG in hadden riepen we samen OLE! Je laat me, je helpt me te zijn wie ik ben, te zijn wie we zijn. Ik vind je lief. Zonder jou had ik het einde van dit project niet gehaald. Ik kijk uit naar al onze komende avonturen.

References

[1] Abbott, D. A., Knijnenburg, T. A., De Poorter, L. M., Reinders, M. J., Pronk, J. T., and Van Maris, A. J. Generic and specific transcriptional responses to different weak organic acids in anaerobic chemostat cultures of *Saccharomyces cerevisiae*. *FEMS Yeast Research 7*, 6 (2007), 819–833.

[2] Abbott, D. A., Suir, E., Van Maris, A. J. A., and Pronk, J. T. Physiological and transcriptional responses to high concentrations of lactic acid in anaerobic chemostat cultures of *Saccharomyces cerevisiae*. *Applied and environmental microbiology 74*, 18 (2008), 5759–68.

[3] Abbott, D. A., Zelle, R. M., Pronk, J. T., and Van Maris, A. J. A. Metabolic engineering of *Saccharomyces cerevisiae* for production of carboxylic acids: Current status and challenges. *FEMS Yeast Research 9*, 8 (2009), 1123–1136.

[4] Adger, W. N., Arnell, N. W., Black, R., Dercon, S., Geddes, A., and Thomas, D. S. Focus on environmental risks and migration: Causes and consequences. *Environmental Research Letters 10*, 6 (2015).

[5] Adiego-Perez, B., Randazzo, P., Daran, J. M., Verwaal, R., Roubos, J. A., Daran-lapujade, P., and Oost, J. V. D. Multiplex genome editing of microorganisms using CRISPR-Cas. *FEMS Microbiology Letters 366* (2019), 1–19.

[6] Agreement, P. United nations framework convention on climate change. *Paris, France* (2015).

[7] Aguilar-Uscanga, B., and François, J. M. A study of the yeast cell wall composition and structure in response to growth conditions and mode of cultivation. *Letters in Applied Microbiology 37*, 3 (2003), 268–274.

[8] Aguilera, J., Petit, T., De Winde, J. H., and Pronk, J. T. Physiological and genome-wide transcriptional responses of *Saccharomyces cerevisiae* to high carbon dioxide concentrations. *FEMS Yeast Research 5*, 6-7 (2005), 579–593.

[9] Ahn, J. H., Jang, Y. S., and Lee, S. Y. Production of succinic acid by metabolically engineered microorganisms. *Current Opinion in Biotechnology 42* (2016), 54–66.

[10] Anders, S., Pyl, P. T., and Huber, W. Genome analysis HTSeq — a Python framework to work with high-throughput sequencing data. *Bioinformatics 31*, 2 (2015), 166–169.

[11] Antebi, A., and Fink, G. R. The yeast Ca^{2+}-ATPase homologue, *PMR1*, is required for normal Golgi function and localizes in a novel Golgi-like distribution. *Molecular biology of the cell 3*, 6 (1992), 633–654.

[12] Arbige, M., and Chesbro, W. relA and Related Loci are Growth Rate Determinants for *Escherichia coli* in a Recycling Fermenter. *Journal of General Microbiology 128* (1982), 693–703.

[13] Arbige, M., and Chesbro, W. R. Very slow growth of *Bacillus polymyxa*: Stringent response and maintenance energy. *Archives of Microbiology 132*, 4 (1982), 338–344.

[14] Attfield, P. V. Stress tolerance: The key to effective strains of industrial baker's yeast. *Nature Biotechnology 15*, 13 (dec 1997), 1351–1357.

[15] Ballesteros, J. A., Deupi, X., Olivella, M., Haaksma, E. E., and Pardo, L. Serine and threonine residues bend α-helices in the $\chi 1 = g^-$ conformation. *Biophysical Journal 79*, 5 (2000), 2754–2760.

[16] Bartel, B., Wünning, I., and Varshavsky, A. The recognition component of the N-end rule pathway. *The EMBO journal 9*, 10 (1990), 3179–89.

[17] Basso, L. C., Basso, T. O., and Rocha, S. N. Ethanol production in Brazil: The industrial process and its impact on yeast fermentation. In *Biofuel Production - Recent Developments and Prospects*, vol. 1. Intechopen, 2011, ch. 5, p. 596.

[18] Basso, T. O., de Kok, S., Dario, M., do Espirito-Santo, J. C. A., Müller, G., Schlölg, P. S., Silva, C. P., Tonso, A., Daran, J. M., Gombert, A. K., van Maris, A. J., Pronk, J. T., and Stambuk, B. U. Engineering topology and kinetics of sucrose metabolism in *Saccharomyces cerevisiae* for improved ethanol yield. *Metabolic Engineering 13*, 6 (2011), 694–703.

[19] Becker, J., Armstrong, G., Vandermerwe, M., Lambrechts, M., Vivier, M., and Pretorius, I. Metabolic engineering of for the synthesis of the wine-related antioxidant resveratrol. *FEMS Yeast Research 4*, 1 (oct 2003), 79–85.

[20] Becker, J., Lange, A., Fabarius, J., and Wittmann, C. Top value platform chemicals: Bio-based production of organic acids. *Current Opinion in Biotechnology 36*, Figure 1 (2015), 168–175.

[21] Becker, J., and Wittmann, C. Advanced biotechnology: Metabolically engineered cells for the bio-based production of chemicals and fuels, materials, and health-care products. *Angewandte Chemie - International Edition 54*, 11 (2015), 3328–3350.

[22] Binai, N. A., Bisschops, M. M. M., Breukelen, B. V., Mohammed, S., Loe, L., Pronk, J. T., Heck, A. J. R., Daran-lapujade, P., and Slijper, M. Proteome Adaptation of *Saccharomyces cerevisiae* to Severe Calorie Restriction in Retentostat Cultures. *Journal of Proteome Research 13* (2014).

[23] Bisschops, M. M., Luttik, M. A., Doerr, A., Verheijen, P. J., Bruggeman, F., Pronk, J. T., and Daran-Lapujade, P. Extreme calorie restriction in yeast retentostats induces uniform non-quiescent growth arrest. *Biochimica et Biophysica Acta - Molecular Cell Research 1864*, 1 (2017), 231–242.

[24] Bisschops, M. M., Vos, T., Martínez-Moreno, R., Cortés, P. d. l. T., Pronk, J. T., and Daran-Lapujade, P. Oxygen availability strongly affects chronological lifespan and thermotolerance in batch cultures of *Saccharomyces cerevisiae*. *Microbial Cell 2*, 11 (2015), 429–444.

[25] Bisschops, M. M., Zwartjens, P., Keuter, S. G., Pronk, J. T., and Daran-Lapujade, P. To divide or not to divide: a key role of Rim15 in calorie-restricted yeast cultures. *Biochimica et Biophysica Acta (BBA) - Molecular Cell Research* (jan 2014), 1–11.

[26] Biz, A., Sugai-Guérios, M. H., Kuivanen, J., Maaheimo, H., Krieger, N., Mitchell, D. A., and Richard, P. The introduction of the fungal d-galacturonate pathway enables the consumption of d-galacturonic acid by *Saccharomyces cerevisiae*. *Microbial Cell Factories 15*, 1 (2016), 1–11.

[27] Boender, L. G. M., Almering, M. J. H., Dijk, M., van Maris, A. J. a., de Winde, J. H., Pronk, J. T., and Daran-Lapujade, P. Extreme calorie restriction and energy source starvation in *Saccharomyces cerevisiae* represent distinct physiological states. *Biochimica et biophysica acta 1813*, 12 (dec 2011), 2133–44.

[28] Boender, L. G. M., de Hulster, E. A. F., van Maris, A. J. A., Daran-Lapujade, P. A. S., and Pronk, J. T. Quantitative physiology of *Saccharomyces cerevisiae* at near-zero specific growth rates. *Applied and environmental microbiology 75*, 17 (sep 2009), 5607–14.

[29] Boender, L. G. M., van Maris, A. J. A., de Hulster, E. A. F., Almering, M. J. H., van der Klei, I. J., Veenhuis, M., de Winde, J. H., Pronk, J. T., and Daran-Lapujade, P. Cellular responses of *Saccharomyces cerevisiae* at near-zero growth rates: transcriptome analysis of anaerobic retentostat cultures. *FEMS yeast research 11*, 8 (dec 2011), 603–20.

[30] Boer, V. M., de Winde, J. H., Pronk, J. T., and Piper, M. D. W. The genome-wide transcriptional responses of *Saccharomyces cerevisiae* grown on glucose in aerobic chemostat cultures limited for carbon, nitrogen, phosphorus, or sulfur. *The Journal of biological chemistry 278*, 5 (jan 2003), 3265–74.

[31] Boorsma, A., de Nobel, H., ter Riet, B., Bargmann, B., Brul, S., Hellingwerf, K. J., and Klis, F. M. Characterization of the transcriptional response to cell wall stress in *Saccharomyces cerevisiae*. *Yeast 21*, 5 (2004), 413–427.

[32] Brauer, M. J., Huttenhower, C., Airoldi, E. M., Rosenstein, R., Matese, J. C., Gresham, D., Boer, V. M., Troyanskaya, O. G., and Botstein, D. Coordination of growth rate, cell cycle, stress response, and metabolic activity in yeast. *Molecular biology of the cell 19*, 1 (jan 2008), 352–67.

[33] Brickwedde, A., Brouwers, N., Broek, M. V. D., Gallego Murillo, J. S., Fraiture, J. L., Pronk, J. T., and Daran, J.-M. G. Structural, physiological and regulatory analysis of maltose transporter genes in *Saccharomyces eubayanus* CBS 12357T. *frontiers in Microbiology 9*, August (2018), 1–18.

[34] Buck, J., and Levin, L. R. Physiological sensing of carbon dioxide/bicarbonate/pH via cyclic nucleotide signaling. *Sensors 11*, 2 (2011), 2112–2128.

[35] Bull, A. T. The renaissance of continuous culture in the post-genomics age. *Journal of industrial microbiology & biotechnology 37*, 10 (oct 2010), 993–1021.

[36] Canelas, A. B., Harrison, N., Fazio, A., Zhang, J., Pitkänen, J.-P., van den Brink, J., Bakker, B. M., Bogner, L., Bouwman, J., Castrillo, J. I., Cankorur, A., Chumnanpuen, P., Daran-Lapujade, P., Dikicioglu, D., van Eunen, K., Ewald, J. C., Heijnen, J. J., Kirdar, B., Mattila, I., Mensonides, F. I. C., Niebel, A., Penttilä, M., Pronk, J. T., Reuss, M., Salusjärvi, L., Sauer, U., Sherman, D., Siemann-Herzberg, M., Westerhoff, H., de Winde, J., Petranovic, D., Oliver, S. G., Workman, C. T., Zamboni, N., and Nielsen, J. Integrated multilaboratory systems biology reveals differences in protein metabolism between two reference yeast strains. *Nature Communications 1*, 9 (2010), 145.

[37] Carlquist, M., Fernandes, R. L., Helmark, S., Heins, A.-L., Lundin, L., Sørensen, S. J., Gernaey, K. V., and Lantz, A. E. Physiological heterogeneities in microbial populations and implications for physical stress tolerance. *Microbial cell factories 11*, 1 (jan 2012), 94.

[38] Carmelo, V., Bogaerts, P., and Sá-Correia, I. Activity of plasma membrane H^+-ATPase and expression of *PMA1* and *PMA2* genes in *Saccharomyces cerevisiae* cells grown at optimal and low pH. *Archives of Microbiology 166* (1996), 315–320.

[39] Carmelo, V., Santos, H., and Sá-Correia, I. Effect of extracellular acidification on the activity of plasma membrane ATPase and on the cytosolic and vacuolar pH of *Saccharomyces cerevisiae*. *Biochimica et Biophysica Acta - Biomembranes 1325*, 1 (1997), 63–70.

[40] Carmona-Gutierrez, D., Bauer, M. A., Zimmermann, A., Aguilera, A., Austriaco, N., Ayscough, K., Balzan, R., Bar-Nun, S., Barrientos, A., Belenky, P., Blondel, M., Braun, R. J., Breitenbach, M., Burhans, W. C., Buettner, S., Cavalieri, D., Chang, M., Cooper, K. F., Côrte-Real, M., Costa, V., Cullin, C., Dawes, I., Dengjel, J., Dickman, M. B., Eisenberg, T., Fahrenkrog, B., Fasel, N., Froehlich, K.-U., Gargouri, A., Giannattasio, S., Goffrini, P., Gourlay, C. W., Grant, C. M., Greenwood, M. T., Guaragnella, N., Heger, T., Heinisch, J., Herker, E., Herrmann, J. M., Hofer, S., Jiménez-Ruiz, A., Jungwirth, H., Kainz, K., Kontoyiannis, D. P., Ludovico, P., Manon, S., Martegani, E., Mazzoni, C., Megeney, L. A., Meisinger, C., Nielsen, J., Nystroem, T., Osiewacz, H. D., Outeiro, T. F., Park, H.-O., Pendl, T., Petranovic, D., Picot, S., Polčic, P., Powers, T., Ramsdale, M., Rinnerthaler, M., Rockenfeller, P., Ruckenstuhl, C., Schaffrath, R., Segovia, M., Severin, F. F., Sharon, A., Sigrist, S. J., Sommer-Ruck, C., Sousa, M. J., Thevelein, J. M., Thevissen, K., Titorenko, V., Toledano, M. B., Tuite, M., Voegtle, F.-N., Westermann, B., Winderickx, J., Wissing, S., Woelfl, S., Zhang, Z. J., Zhao, R. Y., Zhou, B., Galluzzi, L., Kroemer, G., and Madeo, F. Guidelines and recommendations on yeast cell death nomenclature. *Microbial Cell 5*, 1 (2018), 4–31.

[41] Carney, D. S., Davies, B. A., and Horazdovsky, B. F. Vps9 domain-containing proteins: Activators of Rab5 GTPases from yeast to neurons. *Trends in Cell Biology 16*, 1 (2006), 27–35.

[42] Casini, A., Chang, F. Y., Eluere, R., King, A. M., Young, E. M., Dudley, Q. M., Karim, A., Pratt, K., Bristol, C., Forget, A., Ghodasara, A., Warden-Rothman, R., Gan, R., Cristofaro, A., Borujeni, A. E., Ryu, M. H., Li, J., Kwon, Y. C., Wang, H., Tatsis, E., Rodriguez-Lopez, C., O'Connor, S., Medema, M. H., Fischbach, M. A., Jewett, M. C., Voigt, C., and Gordon, D. B. A Pressure Test to Make 10 Molecules in 90 Days: External Evaluation of Methods to Engineer Biology. *Journal of the American Chemical Society 140*, 12 (2018), 4302–4316.

[43] Caspeta, L., Chen, Y., Ghiaci, P., Feizi, A., Buskov, S., Hallstrom, B. M., Petranovic, D., and Nielsen, J. Altered sterol composition renders yeast thermotolerant. *Science 346*, 6205 (2014), 75–78.

[44] Castrillo, J. I., Zeef, L., Hoyle, D., Zhang, N., Hayes, A., Gardner, D., Cornell, M., Petty, J., Hakes, L., Wardleworth, L., Rash, B., Brown, M., Dunn, W., Broadhurst, D., O'Donoghue, K., Hester, S., T.P.J., D., Hart, S., Swainston, N., Li, P., Gaskell, S., Paton, N., Lilley, K., D.B., K., and Oliver, S. Growth control of the eukaryote cell: a systems biology study in yeast. *Journal of Biology 6*, 2 (2007), 4.

[45] Chatterji, D., and Kumar Ojha, A. Revisiting the stringent response, ppGpp and starvation signaling. *Current Opinion in Microbiology 4*, 2 (2001), 160–165.

[46] Chemler, J. A., Yan, Y., and Koffas, M. A. Microbial Cell Factories Biosynthesis of isoprenoids, polyunsaturated fatty acids and flavonoids in *Saccharomyces cerevisiae*. *Microbial Cell Factories 5*, 20 (2006), 1–9.

[47] Chen, A. K. L., Gelling, C., Rogers, P. L., Dawes, I. W., and Rosche, B. Response of *Saccharomyces cerevisiae* to stress-free acidification. *Journal of Microbiology 47*, 1 (2009), 1–8.

[48] Chen, D., Wilkinson, C. R. M., Watt, S., Penkett, C. J., Toone, W. M., Jones, N., and Bähler, J. High-Resolution Crystal Structure and *in Vivo* Function of a Kinesin-2 Homologue in *Giardia intestinalis*. *Molecular biology of the cell 19*, 1 (2007), 308–317.

[49] Chen, Q., Ding, Q., and Keller, J. N. The stationary phase model of aging in yeast for the study of oxidative stress and age-related neurodegeneration. *Biogerontology 6*, 1 (jan 2005), 1–13.

[50] Chen, R. E., and Thorner, J. Function and regulation in MAPK signaling pathways: Lessons learned from the yeast *Saccharomyces cerevisiae*. *Biochimica et Biophysica Acta - Molecular Cell Research 1773*, 8 (2007), 1311–1340.

[51] Chen, X., Zhou, L., Tian, K., Kumar, A., Singh, S., Prior, B. A., and Wang, Z. Metabolic engineering of *Escherichia coli*: A sustainable industrial platform for bio-based chemical production. *Biotechnology Advances 31*, 8 (2013), 1200–1223.

[52] Chen, Y., and Nielsen, J. Advances in metabolic pathway and strain engineering paving the way for sustainable production of chemical building blocks. *Current Opinion in Biotechnology 24*, 6 (2013), 965–972.

[53] Chen, Y., and Nielsen, J. Biobased organic acids production by metabolically engineered microorganisms. *Current Opinion in Biotechnology 37* (2016), 165–172.

[54] Chesbro, W., Evans, T., and Eifert, R. Very slow growth of *Escherichia coli*. *Journal of Bacteriology 139*, 2 (1979), 625–638.

[55] Chiotti, K. E., Kvitek, D. J., Schmidt, K. H., Koniges, G., Schwartz, K., Donckels, E. A., Rosenzweig, F., and Sherlock, G. The Valley-of-Death: Reciprocal sign epistasis constrains adaptive trajectories in a constant, nutrient limiting environment. *Genomics 104*, 6 (2014), 431–437.

[56] Christiano, R., Nagaraj, N., Fröhlich, F., and Walther, T. Global Proteome Turnover Analyses of the Yeasts *S. cerevisiae* and *S. pombe*. *Cell Reports* (nov 2014), 1959–1965.

[57] Colinet, A.-S., Sengottaiyan, P., Deschamps, A., Colsoul, M.-L., Thines, L., Demaegd, D., Duchene, M.-c., Foulquier, F., Hols, P., and Morsomme, P. Yeast Gdt1 is a Golgi-localized calcium transporter required for stress-induced calcium signaling and protein glycosylation. *Scientific Reports 6* (2016), 1–11.

[58] Conesa, A., Madrigal, P., Tarazona, S., Gomez-Cabrero, D., Cervera, A., McPherson, A., Szcześniak, M. W., Gaffney, D. J., Elo, L. L., Zhang, X., and Mortazavi, A. A survey of best practices for RNA-seq data analysis. *Genome Biology 17*, 1 (2016), 13.

[59] Conrad, M., Schothorst, J., Kankipati, H. N., Van Zeebroeck, G., Rubio-Texeira, M., and Thevelein, J. M. Nutrient sensing and signaling in the yeast *Saccharomyces cerevisiae*. *FEMS Microbiology Reviews 38*, 2 (2014), 254–299.

[60] Crater, J. S., and Lievense, J. C. Scale-up of industrial microbial processes. *FEMS Microbiology Letters 365*, 13 (2018), 1–5.

[61] Crowe, J. H. Thehalose as a "Chemical Chaperone": Fact and Fantasy. In *Molecular Aspects of the Stress Response: Chaperones, Membranes and Networks*, P. Csermely and L. Vigh, Eds. Landes Bioscience and Springer Science+Business Media, LLC All, 2007, ch. 13, p. 201.

[62] Cueto-Rojas, H. F., Milne, N., Helmond, W., Pieterse, M. M., Maris, A. J., Daran, J. M., and Wahl, S. A. Membrane potential independent transport of NH_3 in the absence of ammonium permeases in *Saccharomyces cerevisiae*. *BMC Systems Biology 11*, 1 (2017), 1–13.

[63] Cueto-Rojas, H. F., Seifar, R. M., Pierick, A. T., Heijnen, S. J., and Wahl, A. Accurate measurement of the *in vivo* ammonium concentration in *Saccharomyces cerevisiae*. *Metabolites 6*, 2 (2016).

[64] Cyert, M. S. Calcineurin signaling in *Saccharomyces cerevisiae*: How yeast go crazy in response to stress. *Biochemical and Biophysical Research Communications 311*, 4 (2003), 1143–1150.

[65] Daran-Lapujade, P., Daran, J. M., Luttik, M. A. H., Almering, M. J. H., Pronk, J. T., and Kötter, P. An atypical *PMR2* locus is responsible for hypersensitivity to sodium and lithium cations in the laboratory strain *Saccharomyces cerevisiae* CEN.PK113-7D. *FEMS Yeast Research 9*, 5 (2009), 789–792.

[66] Daran-Lapujade, P., Daran, J. M., van Maris, A. J. A., de Winde, J. H., and Pronk, J. T. *Chemostat-Based Micro-Array Analysis in Baker's Yeast*, vol. 54. Academic Press, 2008.

[67] Daran-Lapujade, P., Jansen, M. L. A., Daran, J.-M., van Gulik, W., de Winde, J. H., and Pronk, J. T. Role of Transcriptional Regulation in Controlling Fluxes in Central Carbon Metabolism of *Saccharomyces cerevisiae*. *Journal of Biological Chemistry 279*, 10 (2004), 9125–9138.

[68] Daran-Lapujade, P., Jansen, M. L. a., Daran, J.-M., van Gulik, W., de Winde, J. H., and Pronk, J. T. Role of transcriptional regulation in controlling fluxes in central carbon metabolism of *Saccharomyces cerevisiae*. A chemostat culture study. *The Journal of biological chemistry 279*, 10 (mar 2004), 9125–38.

[69] Daran-Lapujade, P., Rossell, S., van Gulik, W. M., Luttik, M. a. H., de Groot, M. J. L., Slijper, M., Heck, A. J. R., Daran, J.-M., de Winde, J. H., Westerhoff, H. V., Pronk, J. T., and Bakker, B. M. The fluxes through glycolytic enzymes in *Saccharomyces cerevisiae* are predominantly regulated at posttranscriptional levels. *Proceedings of the National Academy of Sciences of the United States of America 104*, 40 (oct 2007), 15753–8.

[70] de Deken, R. H. The Crabtree Effect: A Regulatory System in Yeast. *Journal of general microbiology 44*, 2 (1966), 149–156.

[71] de Groot, M. J. L., Daran-Lapujade, P., van Breukelen, B., Knijnenburg, T. A., de Hulster, E. A. E., Reinders, M. J. T., Pronk, J. T., Heck, A. J. R., and Slijper, M. Quantitative proteomics

and transcriptomics of anaerobic and aerobic yeast cultures reveals post-transcriptional regulation of key cellular processes. *Microbiology 153*, Pt 11 (nov 2007), 3864–78.

[72] De Kok, S., Yilmaz, D., Daran, J. M., Pronk, J. T., and Van Maris, A. J. A. *In vivo* analysis of *Saccharomyces cerevisiae* plasma membrane ATPase Pma1p isoforms with increased in vitro H^+/ATP stoichiometry. *Antonie van Leeuwenhoek, International Journal of General and Molecular Microbiology 102*, 2 (2012), 401–406.

[73] de Lucena, R. M., Elsztein, C., de Barros Pita, W., de Souza, R. B., de Sá Leitão Paiva Júnior, S., and de Morais Junior, M. A. Transcriptomic response of *Saccharomyces cerevisiae* for its adaptation to sulphuric acid-induced stress. *Antonie van Leeuwenhoek, International Journal of General and Molecular Microbiology 108*, 5 (2015), 1147–1160.

[74] de Lucena, R. M., Elsztein, C., Simões, D. A., and de Morais, M. A. Participation of CWI, HOG and Calcineurin pathways in the tolerance of *Saccharomyces cerevisiae* to low pH by inorganic acid. *Journal of applied microbiology 113*, 3 (2012), 629–40.

[75] De Melo, H. F., Bonini, B. M., Thevelein, J., Simões, D. A., and Morais, M. A. Physiological and molecular analysis of the stress response of *Saccharomyces cerevisiae* imposed by strong inorganic acid with implication to industrial fermentations. *Journal of Applied Microbiology 109*, 1 (2010), 116–127.

[76] de Ridder, D. Artificial intelligence in the lab: ask not what your computer can do for you. *Microbial Biotechnology 12*, 1 (2019), 38–40.

[77] DeJong, J. H. M., Liu, Y., Bollon, A. P., Long, R. M., Jennewein, S., Williams, D., and Croteau, R. B. Genetic engineering of taxol biosynthetic genes in *Saccharomyces cerevisiae*. *Biotechnology and Bioengineering 93*, 2 (2006), 212–224.

[78] Della-Bianca, B. E., de Hulster, E., Pronk, J. T., van Maris, A. J. A., and Gombert, A. K. Physiology of the fuel ethanol strain *Saccharomyces cerevisiae* PE-2 at low pH indicates a context-dependent performance relevant for industrial applications. *FEMS yeast research 14*, 8 (2014), 1196–205.

[79] Della-Bianca, B. E., and Gombert, A. K. Stress tolerance and growth physiology of yeast strains from the Brazilian fuel ethanol industry. *Antonie van Leeuwenhoek, International Journal of General and Molecular Microbiology 104*, 6 (2013), 1083–1095.

[80] Deprez, M.-A., Eskes, E., Wilms, T., Ludovico, P., and Winderickx, J. pH homeostasis links the nutrient sensing PKA/TORC1/Sch9 ménage-à-trois to stress tolerance and longevity. *Microbial Cell 5*, 3 (2018), 119–136.

[81] D'hooge, P., Coun, C., Van Eyck, V., Faes, L., Ghillebert, R., Mariën, L., Winderickx, J., and Callewaert, G. Ca^{2+} homeostasis in the budding yeast *Saccharomyces cerevisiae*: Impact of ER/Golgi Ca^{2+} storage. *Cell Calcium 58*, 2 (2015), 226–235.

[82] DiCarlo, J. E., Norville, J. E., Mali, P., Rios, X., Aach, J., and Church, G. M. Genome engineering in *Saccharomyces cerevisiae* using CRISPR-Cas systems. *Nucleic acids research 41*, 7 (apr 2013), 4336–43.

[83] Diderich, J. A., Schepper, M., van Hoek, P., Luttik, M. A. H., van Dijken, J. P., Pronk, J. T., Klaassen, P., Boelens, H. F. M., Teixeira de Mattos, M. J., van Dam, K., and Kruckeberg, A. L. Glucose Uptake Kinetics and Transcription of *HXT* Genes in Chemostat Cultures of *Saccharomyces cerevisiae*. *Journal of Biological Chemistry 274*, 22 (may 1999), 15350–15359.

[84] Dijkhuizen, D., and Hartl, D. Selection in Chemostats. *Microbiology Reviews 47*, 2 (1983), 150–168.

[85] Dobin, A., Davis, C. A., Schlesinger, F., Drenkow, J., Zaleski, C., Jha, S., Batut, P., Chaisson, M., and Gingeras, T. R. STAR: ultrafast universal RNA-seq aligner. *Bioinformatics 29*, 1 (2013), 15–21.

[86] Dolz-Edo, L., Guikema-van der Deen, M., Brul, S., and Smits, G. J. Caloric restriction controls stationary phase survival through PKA and cytosolic pH. *Aging Cell e12921*, January (2019).

[87] Dragosits, M., and Mattanovich, D. Adaptive laboratory evolution – principles and applications for biotechnology. *Microbial Cell Factories 12*, 1 (2013), 64.

[88] Du, F., Navarro-Garcia, F., Xia, Z., Tasaki, T., and Varshavsky, A. Pairs of dipeptides synergistically activate the binding of substrate by ubiquitin ligase through dissociation of its autoinhibitory domain. *Proceedings of the National Academy of Sciences 99*, 22 (2002), 14110–14115.

[89] Dufossé, L., Fouillaud, M., Caro, Y., Mapari, S. A., and Sutthiwong, N. Filamentous fungi are large-scale producers of pigments and colorants for the food industry. *Current Opinion in Biotechnology 26* (2014), 56–61.

[90] Dupres, V., Alsteens, D., Wilk, S., Hansen, B., Heinisch, J. J., and Dufrêne, Y. F. The yeast Wsc1 cell surface sensor behaves like a nanospring *in vivo*. *Nature chemical biology 5*, 11 (2009), 857–862.

[91] Eastmond, D. L., and Nelson, H. C. M. Genome-wide analysis reveals new roles for the activation domains of the *Saccharomyces cerevisiae* heat shock transcription factor (Hsf1) during the transient heat shock response. *Journal of Biological Chemistry 281*, 43 (2006), 32909–32921.

[92] Eigenstetter, G., and Takors, R. Dynamic modeling reveals a three-step response of *Saccharomyces cerevisiae* to high CO_2 levels accompanied by increasing ATP demands. *FEMS Yeast Research 17*, 1 (2017), 1–11.

[93] Eisenberg, T., Carmona-Gutierrez, D., Büttner, S., Tavernarakis, N., and Madeo, F. Necrosis in yeast. *Apoptosis 15*, 3 (2010), 257–268.

[94] Ekas, H., Deaner, M., and Alper, H. S. Recent advancements in fungal-derived fuel and chemical production and commercialization. *Current Opinion in Biotechnology 57* (2019), 1–9.

[95] Enfors, S. Simuplot 4. *Available on www.enfors.eu* (2015).

[96] Engel, S., Dietrich, F., Fisk, D., Binkley, G., Balakrishnan, R., Costanzo, M., Dwight, S., Hitz, B., Karra, K., Nash, R., Weng, S., Wong, E., Lloyd, P., Skrzypek, M.S.Miyasato, S., Simison, M., and Cherry, J. The Reference Genome Sequence of *Saccharomyces cerevisiae*: Then and Now. *G3 4*, 3 (2014), 389–398.

[97] Entian, K.-d., and Kötter, P. Yeast Genetic Strain and Plasmid Collections. *Methods in microbiology 36*, 06 (2007), 629–666.

[98] Eraso, P., and Gancedo, C. Activation of yeast plasma membrane ATPase by acid pH during growth. *FEBS Lett 224*, 188055588 (1987), 187–192.

[99] Ercan, O., Bisschops, M. M. M., Overkamp, W., Jørgensen, T. R., Ram, A. F., Smid, E. J., Pronk, J. T., Kuipers, O. P., Daran-Lapujade, P., and Kleerebezem, M. Physiological and Transcriptional Responses of Different Industrial Microbes at Near-Zero Specific Growth Rates. *Applied and Environmental Microbiology 81*, 17 (sep 2015), 5662–5670.

[100] Ercan, O., Smid, E. J., and Kleerebezem, M. Quantitative physiology of *Lactococcus lactis* at extreme low-growth rates. *Environmental microbiology 15*, 8 (aug 2013), 2319–32.

[101] Escoté, X., Zapater, M., Clotet, J., and Posas, F. Hog1 mediates cell-cycle arrest in G1 phase by the dual targeting of Sic1. *Nature Cell Biology 6*, 10 (2004), 997–1002.

[102] Eskes, E., Deprez, M. A., Wilms, T., and Winderickx, J. pH homeostasis in yeast; the phosphate perspective. *Current Genetics 64*, 1 (2018), 1–7.

[103] Estes, R. J., and Sirgy, M. J. Global Advances in Quality of Life and Well-Being: Past, Present, and Future. *Social Indicators Research 141*, 3 (2019), 1137–1164.

[104] Famili, I., Forster, J., Nielsen, J., and Palsson, B. O. *Saccharomyces cerevisiae* phenotypes can be predicted by using constraint-based analysis of a genome-scale reconstructed metabolic network. *Proceedings of the National Academy of Sciences of the United States of America 100*, 23 (nov 2003), 13134–9.

[105] Fazio, A., Jewett, M. C., Daran-Lapujade, P., Mustacchi, R., Usaite, R., Pronk, J. T., Workman, C. T., and Nielsen, J. Transcription factor control of growth rate dependent genes in *Saccharomyces cerevisiae*: a three factor design. *BMC genomics 9* (jan 2008), 341.

[106] Fernandes, R. L., Nierychlo, M., Lundin, L., Pedersen, a. E., Puentes Tellez, P. E., Dutta, a., Carlquist, M., Bolic, a., Schäpper, D., Brunetti, a. C., Helmark, S., a L Heins, Jensen, a. D., Nopens, I., Rottwitt, K., Szita, N., van Elsas, J. D., Nielsen, P. H., Martinussen, J., Sørensen, S. J., Lantz, a. E., and Gernaey, K. V. Experimental methods and modeling techniques for description of cell population heterogeneity. *Biotechnology advances 29*, 6 (2011), 575–99.

[107] Flamigni, E., and Dolci, G. The cell wall integrity checkpoint: coordination between cell wall synthesis and the cell cycle. *Yeast 27* (2010), 513–519.

[108] Fletcher, E., Feizi, A., Bisschops, M. M., Hallström, B. M., Khoomrung, S., Siewers, V., Nielsen, J., Hallström, B. M., Khoomrung, S., Siewers, V., and Nielsen, J. Evolutionary engineering reveals divergent paths when yeast is adapted to different acidic environments. *Metabolic Engineering 39*, October (2016), 0–1.

[109] Fletcher, E., Krivoruchko, A., and Nielsen, J. Industrial systems biology and its impact on synthetic biology of yeast cell factories. *Biotechnology and Bioengineering 113*, 6 (2015), 1164–1170.

[110] Forsburg, S. L., and Nurse, P. Cell cycle regulation in the yeasts *Saccharomyces cerevisiae* and *Schizosaccharomyces pombe*. *annual review of cell biology 7* (1991), 227–256.

[111] Frisvad, J. C., Møller, L. L. H., Larsen, T. O., Kumar, R., and Arnau, J. Safety of the fungal workhorses of industrial biotechnology: update on the mycotoxin and secondary metabolite potential of *Aspergillus niger*, *Aspergillus oryzae*, and *Trichoderma reesei*. *Applied Microbiology and Biotechnology 102*, 22 (2018), 9481–9515.

[112] Fuchs, B. B., and Mylonakis, E. Our paths might cross: The role of the fungal cell wall integrity pathway in stress response and cross talk with other stress response pathways. *Eukaryotic Cell 8*, 11 (2009), 1616–1625.

[113] Fujita, K., Matsuyama, A., Kobayashi, Y., and Iwahashi, H. The genome-wide screening of yeast deletion mutants to identify the genes required for tolerance to ethanol and other alcohols. *FEMS yeast research 6* (2006), 744–750.

[114] Galanie, S., Thodey, K., Trenchard, I. J., Filsinger Interrante, M., and Smolke, C. D. Complete biosynthesis of opioids in yeast. *Science 349*, August (2015), 1095–1100.

[115] García, R., Bravo, E., Diez-Muñiz, S., Nombela, C., Rodríguez-Peña, J. M., and Arroyo, J. A novel connection between the Cell Wall Integrity and the PKA pathways regulates cell wall stress response in yeast. *Scientific Reports 7*, 1 (2017), 1–15.

[116] García, R., Rodríguez-Peña, J. M., Bermejo, C., Nombela, C., and Arroyo, J. The high osmotic response and cell wall integrity pathways cooperate to regulate transcriptional responses to zymolyase-induced cell wall stress in *Saccharomyces cerevisiae*. *Journal of Biological Chemistry 284*, 16 (2009), 10901–10911.

[117] Gasch, A. P., Spellman, P. T., Kao, C. M., Carmel-Harel, O., Eisen, M. B., Storz, G., Botstein, D., and Brown, P. O. Genomic Expression Programs in the Response of Yeast Cells to Environmental Changes. *Molecular Biology of the Cell 11* (2000), 4241–4257.

[118] Gasch, A. P., and Werner-Washburne, M. The genomics of yeast responses to environmental stress and starvation. *Functional & integrative genomics 2*, 4-5 (sep 2002), 181–92.

[119] Gibney, P. A., Lu, C., Caudy, A. A., Hess, D., and Botstein, D. Yeast metabolic and signaling genes are required for heat-shock survival and have little overlap with the heat-induced genes. *Proceedings of the National Academy of Sciences 110*, 46 (2013), E4393–E4402.

[120] Gibson, B. R., Lawrence, S. J., Leclaire, J. P., Powell, C. D., and Smart, K. A. Yeast responses to stresses associated with industrial brewery handling. *FEMS Microbiology Reviews 31*, 5 (2007), 535–569.

[121] Gietz, R. D., and Woods, R. A. Transformation of yeast by lithium acetate/single-stranded carrier DNA/polyethylene glycol method. In *Methods in Enzymology*, vol. 350. 2002, pp. 87–96.

[122] Goffeau, A., Barrell, B. G., Bussey, H., Davis, R. W., Dujon, B., Feldmann, H., Galibert, F., Hoheisel, J. D., Jacq, C., Johnston, M., Louis, E. J., Mewes, H. W., Murakami, Y., Philippsen, P., Tettelin, H., and Oliver, S. G. Life with 6000 Genes. *Science 274*, November (1996), 562–567.

[123] Gong, Z., Nielsen, J., and Zhou, Y. J. Engineering Robustness of Microbial Cell Factories. *Biotechnology Journal 12*, 10 (2017), 1–9.

[124] González-Ramos, D., Gorter de Vries, A. R., Grijseels, S. S., van Berkum, M. C., Swinnen, S., van den Broek, M., Nevoigt, E., Daran, J.-M. G., Pronk, J. T., and van Maris, A. J. A. A new laboratory evolution approach to select for constitutive acetic acid tolerance in *Saccharomyces cerevisiae* and identification of causal mutations. *Biotechnology for Biofuels 9*, 1 (2016), 173.

[125] González-Ramos, D., van den Broek, M., van Maris, A. J., Pronk, J. T., and Daran, J.-M. G. Genome-scale analyses of butanol tolerance in *Saccharomyces cerevisiae* reveal an essential role of protein degradation. *Biotechnology for Biofuels 6*, 1 (2013), 48.

[126] Gorter de Vries, A. R., Koster, C. C., Weening, S. M., Luttik, M. A. H., Kuijpers, N. G. A., Geertman, J.-M. A., Pronk, J. T., and Daran, J.-M. G. Phenotype-independent isolation of interspecies Saccharomyces hybrids by dual-dye fluorescent staining and Fluorescence-Activated Cell Sorting. *Frontiers in Microbiology 10*, April (2019), 1–12.

[127] Gray, J. V., Petsko, G. A., Johnston, G. C., Ringe, D., Singer, R. A., and Werner-washburne, M. 'Sleeping Beauty': Quiescence in *Saccharomyces cerevisiae*. *Microbiology and molecular biology reviews 68*, 2 (2004), 187–206.

[128] Guerrero-Castillo, S., Araiza-Olivera, D., Cabrera-Orefice, A., Espinasa-Jaramillo, J., Gutiérrez-Aguilar, M., Luévano-Martínez, L. A., Zepeda-Bastida, A., and Uribe-Carvajal, S. Physiological uncoupling of mitochondrial oxidative phosphorylation. Studies in different yeast species. *Journal of Bioenergetics and Biomembranes 43*, 3 (2011), 323–331.

[129] Hakkaart, X. D., Liu, Y., Hulst, M. B., el Masoudi, A., Peuscher, E. J., Pronk, J. T., van Gulik, W. M., and Daran-Lapujade, P. A. S. Physiological responses of *Saccharomyces cerevisiae* to industrially relevant conditions: slow growth, low pH and high CO_2 levels. *Biotechnology and Bioengineering, Essentially as chapter 3 of this Thesis* (2019).

[130] Hakkaart, X. D. V., Pronk, J. T., and Maris, A. J. A. V. A Simulator-Assisted Workshop for Teaching Chemostat Cultivation in Academic Classes on Microbial Physiology. *Journal of Microbiology & biology education 18*, 3 (2017).

[131] Hansen, E., Lindberg Møller, B., Kock, G., Bunner, C., Kristensen, C., Jensen, O., Okkels, F., Olsen, C., Motawia, M., and Hansen, J. *De novo* biosynthesis of vanillin in fission yeast (*Schizosaccharomyces pombe*) and baker's yeast (*Saccharomyces cerevisiae*). *Applied and Environmental Microbiology 75*, 9 (2009), 2765–2774.

[132] Harbison, C., Gordon, D., Lee, T., Rinaldi, N., Macisaac, K., Danford, T., Hannett, N., Tagne, J., Reynolds, D., Yoo, J., and Others. Scoring and Clustering and Conservation Testing Assignment of Single Motif to Each Regulator. *Nature 431*, 7004 (2004), 1–5.

[133] Harder, W., Kuenen, J., and Matin, A. Microbial Selection in Continous Culture. *Journal of applied bacteriology 43* (1977), 1–24.

[134] Haringa, C., Deshmukh, A. T., Mudde, R. F., and Noorman, H. J. Euler-Lagrange analysis towards representative down-scaling of a 22 m^3 aerobic *S. cerevisiae* fermentation. *Chemical Engineering Science 170* (2017), 653–669.

[135] Hatti-Kaul, R., Törnvall, U., Gustafsson, L., and Börjesson, P. Industrial biotechnology for the production of bio-based chemicals - a cradle-to-grave perspective. *Trends in Biotechnology 25*, 3 (2007), 119–124.

[136] Heins, A. L., Lencastre Fernandes, R., Gernaey, K. V., and Lantz, A. E. Experimental and in silico investigation of population heterogeneity in continuous *Sachharomyces cerevisiae* scale-down fermentation in a two-compartment setup. *Journal of Chemical Technology and Biotechnology 90*, 2 (2015), 324–340.

[137] Hensing, M. C., Bangma, K. A., Raadonk, L. M., de Hulster, E., van Dijken, J. P., and Pronk, J. T. Effects of cultivation conditions on the production of heterologous α-galactosidase by *Kluyveromyces lactis*. *Applied Microbiology and Biotechnology 43*, 1 (1995), 58–64.

[138] Hensing, M. C., Rouwenhorst, R. J., Heijnen, J. J., van Dijken, J. P., and Pronk, J. T. Physiological and technological aspects of large-scale heterologous-protein production with yeasts. *Antonie van Leeuwenhoek 67*, 3 (1995), 261–279.

[139] Herbert, D., Elsworth, R., and Telling, R. C. The continuous culture of bacteria; a theoretical and experimental study. *Journal of general microbiology 14*, 3 (jul 1956), 601–22.

[140] Hermann, B. G., Blok, K., and Patel, M. K. Producing bio-based bulk chemicals using industrial biotechnology saves energy and combats climate change. *Environmental Science and Technology 41*, 22 (2007), 7915–7921.

[141] Hermann, B. G., and Patel, M. Today ' s and Tomorrow ' s Bio-Based Bulk Chemicals From White Biotechnology. *Applied Biochemistry And Biotechnology 136* (2007).

[142] Ho, P. W., Swinnen, S., Duitama, J., and Nevoigt, E. The sole introduction of two single-point mutations establishes glycerol utilization in *Saccharomyces cerevisiae* CEN.PK derivatives. *Biotechnology for Biofuels 10*, 1 (2017), 1–15.

[143] Hong, K. K., Hou, J., Shoaie, S., Nielsen, J., and Bordel, S. Dynamic 13C-labeling experiments prove important differences in protein turnover rate between two *Saccharomyces cerevisiae* strains. *FEMS Yeast Research 12*, 7 (2012), 741–747.

[144] Hoskisson, P. A., and Hobbs, G. Continuous culture - Making a comeback? *Microbiology 151*, 10 (2005), 3153–3159.

[145] Inagaki, M., Schmelzle, T., Yamaguchi, K., Irie, K., Hall, M. N., and Matsumoto, K. *PDK1* Homologs Activate the Pkc1–Mitogen-Activated Protein Kinase Pathway in Yeast. *Molecular and Cellular Biology 19*, 12 (1999), 8344–8352.

[146] Inoue, H., Nojima, H., and Okayama, H. High efficiency transformation of *Escherichia coli* with plasmids. *Gene 96* (1990), 23–28.

[147] Jamieson, D. J. Oxidative Stress Responses of the Yeast. *Yeast 1527* (1998), 1511–1527.

[148] Jansen, M. L., Bracher, J. M., Papapetridis, I., Verhoeven, M. D., de Bruijn, H., de Waal, P. P., van Maris, A. J., Klaassen, P., and Pronk, J. T. *Saccharomyces cerevisiae* strains for second-generation ethanol production: from academic exploration to industrial implementation. *FEMS yeast research 17*, 5 (2017), 1–20.

[149] Jansen, M. L. A., Diderich, J., Mashego, M., Hassane, A., de Winde, J. H., Daran-Lapujade, P. A. S., and Pronk, J. T. Prolonged selection in aerobic, glucose-limited chemostat cultures of *Saccharomyces cerevisiae* causes a partial loss of glycolytic capacity. *Microbiology 151*, 5 (may 2005), 1657–1669.

[150] Jansen, M. L. A., and van Gulik, W. M. Towards large scale fermentative production of succinic acid. *Current opinion in biotechnology 30* (2014), 190–7.

[151] Joel E Cohen. Human Population: The Next Half Century. *Science 302*, November (2003), 1172–1175.

[152] Johansson, N., Quehl, P., Norbeck, J., and Larsson, C. Identification of factors for improved ethylene production via the ethylene forming enzyme in chemostat cultures of *Saccharomyces cerevisiae*. *Microbial Cell Factories 12*, 1 (2013), 1–7.

[153] Jong-Gubbels, P. D., Bauer, J., Niederberger, P., Stückrath, I., Dijken, J. P. V., and Pronk, J. T. Physiological characterisation of a pyruvate-carboxylase-negative *Saccharomyces cerevisiae* mutant in batch and chemostat cultures. *Antonie van Leeuwenhoek 74* (1998), 253–263.

[154] Jørgensen, T. R., Nitsche, B. M., Lamers, G. E., Arentshorst, M., van den Hondel, C. a., and Ram, A. F. Transcriptomic insights into the physiology of *Aspergillus niger* approaching a specific growth rate of zero. *Applied and environmental microbiology 76*, 16 (aug 2010), 5344–55.

[155] Jules, M., Beltran, G., François, J., and Parrou, J. L. New insights into trehalose metabolism by *Saccharomyces cerevisiae*: *NTH2* encodes a functional cytosolic trehalase, and deletion of *TPS1* reveals Ath1p-dependent trehalose mobilization. *Applied and Environmental Microbiology 74*, 3 (2008), 605–614.

[156] Jullesson, D., David, F., Pfleger, B., and Nielsen, J. Impact of synthetic biology and metabolic engineering on industrial production of fine chemicals. *Biotechnology Advances 33*, 7 (2015), 1395–1402.

[157] Kao, K. C., and Sherlock, G. Molecular characterization of clonal interference uring adaptive evolution in asexual populations of *Saccharomyces cerevisiae*. *Nature Genetics 40*, 12 (2009), 1499–1504.

[158] Kavšček, M., Stražar, M., Curk, T., Natter, K., and Petrovič, U. Yeast as a cell factory: current state and perspectives. *Microbial Cell Factories 14*, 1 (2015), 94.

[159] Kawahata, M., Masaki, K., Fujii, T., and Iefuji, H. Yeast genes involved in response to lactic acid and acetic acid: acidic conditions caused by the organic acids in *Saccharomyces cerevisiae* cultures induce expression of intracellular metal metabolism genes regulated by Aft1p. *FEMS yeast research 6*, 6 (2006), 924–36.

[160] Kazemi Seresht, A., Cruz, A. L., de Hulster, E., Hebly, M., Palmqvist, E. A., van Gulik, W., Daran, J.-M., Pronk, J., and Olsson, L. Long-term adaptation of *Saccharomyces cerevisiae* to the burden of recombinant insulin production. *Biotechnology and bioengineering 110*, 10 (oct 2013), 2749–63.

[161] Kitano, H. Biological robustness. *Nature reviews. Genetics 5*, 11 (nov 2004), 826–37.

[162] Klein, M., Carrillo, M., Xiberras, J., ul Islam, Z., Swinnen, S., and Nevoigt, E. Towards the exploitation of glycerol's high reducing power in *Saccharomyces cerevisiae*-based bioprocesses. *Metabolic Engineering 38* (2016), 464–472.

[163] Knijnenburg, T. A., de Winde, J. H., Daran, J. M., Daran-Lapujade, P., Pronk, J. T., Reinders, M. J. T., and Wessels, L. F. A. Exploiting combinatorial cultivation conditions to infer transcriptional regulation. *BMC Genomics 8* (2007), 1–14.

[164] Knuf, C., and Nielsen, J. *Aspergilli*: Systems biology and industrial applications. *Biotechnology Journal 7*, 9 (2012), 1147–1155.

[165] Kocharin, K., and Nielsen, J. Specific growth rate and substrate dependent polyhydroxybutyrate production in *Saccharomyces cerevisiae*. *AMB Express 3*, 1 (2013), 1–6.

[166] Koopman, F., Beekwilder, J., Crimi, B., van Houwelingen, A., Hall, R. D., Bosch, D., van Maris, A. J., Pronk, J. T., and Daran, J.-M. *De novo* production of the flavonoid naringenin in engineered *Saccharomyces cerevisiae*. *Microbial Cell Factories 11*, 155 (2012).

[167] Koutinas, A. A., Vlysidis, A., Pleissner, D., Kopsahelis, N., Lopez Garcia, I., Kookos, I. K., Papanikolaou, S., Kwan, T. H., and Lin, C. S. K. Valorization of industrial waste and by-product streams via fermentation for the production of chemicals and biopolymers. *Chemical Society Reviews 43*, 8 (2014), 2587.

[168] Kresnowati, M. T., Van Winden, W. A., Almering, M. J., Ten Pierick, A., Ras, C., Knijnenburg, T. A., Daran-Lapujade, P., Pronk, J. T., Heijnen, J. J., and Daran, J. M. When transcriptome meets metabolome: Fast cellular responses of yeast to sudden relief of glucose limitation. *Molecular Systems Biology 2* (2006).

[169] Krivoruchko, A., and Nielsen, J. Production of natural products through metabolic engineering of *Saccharomyces cerevisiae*. *Current opinion in biotechnology 35C* (dec 2014), 7–15.

[170] Kuijpers, N. G. A., Chroumpi, S., Vos, T., Solis-Escalante, D., Bosman, L., Pronk, J. T., Daran, J.-M., and Daran-Lapujade, P. One-step assembly and targeted integration of multigene constructs assisted by the I-SceI meganuclease in *Saccharomyces cerevisiae*. *FEMS yeast research 13*, 8 (dec 2013), 769–81.

[171] Kulawiak, B., Höpker, J., Gebert, M., Guiard, B., Wiedemann, N., and Gebert, N. The mitochondrial protein import machinery has multiple connections to the respiratory chain. *Biochimica et Biophysica Acta - Bioenergetics 1827*, 5 (2013), 612–626.

[172] Kuyper, M., Harhangi, H. R., Stave, A. K., Winkler, A. A., Jetten, M. S., De Laat, W. T., Den Ridder, J. J., Op Den Camp, H. J., Van Dijken, J. P., and Pronk, J. T. High-level functional expression of a fungal xylose isomerase: The key to efficient ethanolic fermentation of xylose by *Saccharomyces cerevisiae*? *FEMS Yeast Research 4*, 1 (2003), 69–78.

[173] Lahtvee, P.-J., Kumar, R., Hallstrom, B. M., and Nielsen, J. Adaptation to different types of stress converge on mitochondrial metabolism. *Molecular Biology of the Cell 27*, 15 (2016), 2505–2514.

[174] Lameiras, F., Heijnen, J. J., and van Gulik, W. M. Development of tools for quantitative intracellular metabolomics of *Aspergillus niger* chemostat cultures. *Metabolomics 11*, 5 (2015), 1253–1264.

[175] Landeweerd, L., Surette, M., and van Driel, C. From petrochemistry to biotech: a European perspective on the bio-based economy. *Interface Focus 1*, 2 (feb 2011), 189–195.

[176] Lange, H. C., and Heijnen, J. J. Statistical reconciliation of the elemental and molecular biomass composition of *Saccharomyces cerevisiae*. *Biotechnology and bioengineering 75*, 3 (nov 2001), 334–44.

[177] Lara, A. R., Galindo, E., Ramírez, O. T., and Palomares, L. A. Living With Heterogeneities in Bioreactors. *Molecular Biotechnology 34* (2006), 355–381.

[178] Lee, J. Y., Na, Y. A., Kim, E., Lee, H. S., and Kim, P. The actinobacterium *Corynebacterium glutamicum*, an industrial workhorse. *Journal of Microbiology and Biotechnology 26*, 5 (2016), 807–822.

[179] Lee, K. S., Hong, M. E., Jung, S. C., Ha, S. J., Yu, B. J., Koo, H. M., Park, S. M., Seo, J. H., Kweon, D. H., Park, J. C., and Jin, Y. S. Improved galactose fermentation of *Saccharomyces cerevisiae* through inverse metabolic engineering. *Biotechnology and Bioengineering 108*, 3 (2011), 621–631.

[180] Lee, S. Y., Kim, H. U., Chae, T. U., Cho, J. S., Kim, J. W., Shin, J. H., Kim, D. I., Ko, Y. S., Jang, W. D., and Jang, Y. S. A comprehensive metabolic map for production of bio-based chemicals. *Nature Catalysis 2*, 1 (2019), 18–33.

[181] Legras, J. L., Merdinoglu, D., Cornuet, J. M., and Karst, F. Bread, beer and wine: *Saccharomyces cerevisiae* diversity reflects human history. *Molecular Ecology 16*, 10 (2007), 2091–2102.

[182] Lesage, G., and Bussey, H. Cell Wall Assembly in *Saccharomyces cerevisiae*. *Microbiology and Molecular Biology Reviews 70*, 2 (2006), 317–343.

[183] Levin, D. E. Cell Wall Integrity Signaling in *Saccharomyces cerevisiae*. *Microbiology and Molecular Biology Reviews 69*, 2 (2005), 262–291.

[184] Levin, D. E. Regulation of cell wall biogenesis in *Saccharomyces cerevisiae*: the cell wall integrity signaling pathway. *Genetics 189*, 4 (dec 2011), 1145–75.

[185] Li, H., and Durbin, R. Fast and accurate long-read alignment with Burrows-Wheeler transform. *Bioinformatics 26*, 5 (2010), 589–595.

[186] Li, H., Handsaker, B., Wysoker, A., Fennell, T., Ruan, J., Homer, N., Marth, G., Abecasis, G., Durbin, R., and Subgroup, . G. P. D. P. The Sequence Alignment/Map format and SAMtools. *Bioinformatics 25*, 16 (2009), 2078–2079.

[187] Li, M., and Borodina, I. Application of synthetic biology for production of chemicals in yeast *Saccharomyces cerevisiae*. *FEMS yeast research* (sep 2014), n/a–n/a.

[188] Lindahl, L., Santos, A. X., Olsson, H., Olsson, L., and Bettiga, M. Membrane engineering of *S. cerevisiae* targeting sphingolipid metabolism. *Scientific Reports 7* (2017), 1–10.

[189] Liti, G. The fascinating and secret wild life of the budding yeast *S. cerevisiae*. *eLife 4* (2015), 1–9.

[190] Liu, X., Jia, B., Sun, X., Ai, J., Wang, L., Wang, C., Zhao, F., Zhan, J., and Huang, W. Effect ofinitial pH on growth characteristics and fermentation properties of *Saccharomyces cerevisiae*. *Journal of Food Science 80*, 4 (2015), M800–M808.

[191] Liu, Y., el Bouhaddani, A., Pronk, J., and van Gulik, W. M. Quantitative physiology of non-energy-limited retentostat cultures of *Saccharomyces cerevisiae* at near-zero specific growth rates. *BioRxiv* (2019).

[192] Liu, Z., Hou, J., Martínez, J. L., Petranovic, D., and Nielsen, J. Correlation of cell growth and heterologous protein production by *Saccharomyces cerevisiae*. *Applied microbiology and biotechnology 97*, 20 (oct 2013), 8955–62.

[193] Lõoke, M., Kristjuhan, K., and Kirstjuhan, A. Extraction of genomic DNA from yeasts for PCR-based applications. *Biotechniques 50*, 5 (2011), 325–328.

[194] Lu, C., Brauer, M. J., and Botstein, D. Slow Growth Induces Heat-Shock Resistance in Normal and Respiratory-deficient Yeast. *Molecular biology of the cell 20* (2009), 891–903.

[195] Lu, S., Eiteman, M. A., and Altman, E. Effect of CO_2 on succinate production in dual-phase *Escherichia coli* fermentations. *Journal of Biotechnology 143*, 3 (2009), 213–223.

[196] Ludovico, P., Sousa, M. J., Silva, M. T., Leão, C., and Côrte-Real, M. *Saccharomyces cerevisiae* commits to a programmed cell death process in response to acetic acid. *Microbiology 147*, 9 (2001), 2409–2415.

[197] Luttik, M. A. H., Kötter, P., Salomons, F. A., Van der Klei, I. J., Van Dijken, J. P., and Pronk, J. T. The *Saccharomyces cerevisiae ICL2* gene encodes a mitochondrial 2-methylisocitrate lyase involved in propionyl-coenzyme a metabolism. *Journal of Bacteriology 182*, 24 (2000), 7007–7013.

[198] Madeira, A., Leitão, L., Soveral, G., Dias, P., Prista, C., Moura, T., and Loureiro-Dias, M. C. Effect of ethanol on fluxes of water and protons across the plasma membrane of *Saccharomyces cerevisiae*. *FEMS Yeast Research 10*, 3 (2010), 252–258.

[199] Madeo, F., Herker, E., Wissing, S., Jungwirth, H., Eisenberg, T., and Fröhlich, K. U. Apoptosis in yeast. *Current Opinion in Microbiology 7*, 6 (2004), 655–660.

[200] Magoc, Magoc, Derrick Wood, and Salzberg. EDGE-pro: Estimated Degree of Gene Expression in Prokaryotic Genomes. *Evolutionary Bioinformatics* (2013), 127.

[201] Magocha, T. A., Zabed, H., Yang, M., Yun, J., Zhang, H., and Qi, X. Improvement of industrially important microbial strains by genome shuffling: Current status and future prospects. *Bioresource Technology 257*, December 2017 (2018), 281–289.

[202] Mandal, D., Rulli, S. J., and Rao, R. Packing interactions between transmembrane helices alter ion selectivity of the yeast Golgi Ca^{2+}/Mn^{2+}-ATPase *PMR1*. *Journal of Biological Chemistry 278*, 37 (2003), 35292–35298.

[203] Mans, R., Daran, J. M. G., and Pronk, J. T. Under pressure: evolutionary engineering of yeast strains for improved performance in fuels and chemicals production. *Current Opinion in Biotechnology 50* (2018), 47–56.

[204] Mans, R., van Rossum, H. M., Wijsman, M., Backx, A., Kuijpers, N. G. A., van den Broek, M., Daran-Lapujade, P., Pronk, J. T., van Maris, A., and Daran, J.-M. G. CRISPR/Cas9: a molecular Swiss army knife for simultaneous introduction of multiple genetic modifications in *Saccharomyces cerevisiae*. *FEMS Yeast Research*, January (mar 2015), 1–15.

[205] Marcellin, E., and Nielsen, L. K. Advances in analytical tools for high throughput strain engineering. *Current Opinion in Biotechnology 54*, Figure 2 (2018), 33–40.

[206] Marques, W. L., Mans, R., Henderson, R. K., Marella, E. R., ter Horst, J., de Hulster, E., Poolman, B., Daran, J. M., Pronk, J. T., Gombert, A. K., and van Maris, A. J. Combined engineering of disaccharide transport and phosphorolysis for enhanced ATP yield from sucrose fermentation in *Saccharomyces cerevisiae*. *Metabolic Engineering 45*, June 2017 (2018), 121–133.

[207] Marques, W. L., Raghavendran, V., Stambuk, B. U., and Gombert, A. K. Sucrose and *Saccharomyces cerevisiae*: a relationship most sweet. *FEMS Yeast Research 16*, 1 (2016).

[208] Mascaraque, V., Hernáez, M. L., Jiménez-Sánchez, M., Hansen, R., Gil, C., Martín, H., Cid, V. J., and Molina, M. Phosphoproteomic Analysis of Protein Kinase C Signaling in *Saccharomyces cerevisiae* Reveals Slt2 Mitogen-activated Protein Kinase (MAPK)-dependent Phosphorylation of Eisosome Core Components. *Molecular & Cellular Proteomics 12*, 3 (2013), 557–574.

[209] Mashego, M. R., van Gulik, W. M., Vinke, J. L., and Heijnen, J. J. Critical evaluation of sampling techniques for residual glucose determination in carbon-limited chemostat culture of *Saccharomyces cerevisiae*. *Biotechnology and bioengineering 83*, 4 (aug 2003), 395–9.

[210] Matsushika, A., Negi, K., Suzuki, T., Goshima, T., and Hoshino, T. Identification and characterization of a novel *Issatchenkia orientalis* GPI-anchored protein, IoGas1, required for resistance to low pH and salt stress. *PLoS ONE 11*, 9 (2016), 1–25.

[211] Matsushika, A., Suzuki, T., Goshima, T., and Hoshino, T. Evaluation of *Saccharomyces cerevisiae GAS1* with respect to its involvement in tolerance to low pH and salt stress. *Journal of Bioscience and Bioengineering 124*, 2 (2017), 164–170.

[212] Maurer, M., Kühleitner, M., Gasser, B., and Mattanovich, D. Versatile modeling and optimization of fed batch processes for the production of secreted heterologous proteins with *Pichia pastoris*. *Microbial cell factories 5* (jan 2006), 37.

[213] Mendes, F., Sieuwerts, S., de Hulster, E., Almering, M. J. H., Luttik, M. A. H., Pronk, J. T., Smid, E. J., Bron, P. A., and Daran-Lapujadea, P. Transcriptome-based characterization of interactions between *Saccharomyces cerevisiae* and *Lactobacillus delbrueckii* subsp. bulgaricus in lactose-grown chemostat cocultures. *Applied and Environmental Microbiology 79*, 19 (2013), 5949–5961.

[214] Mengel, M., Nauels, A., Rogelj, J., and Schleussner, C. F. Committed sea-level rise under the Paris Agreement and the legacy of delayed mitigation action. *Nature Communications 9*, 1 (2018), 1–10.

[215] Mira, N. P., Teixeira, M. C., and Sá-Correia, I. Adaptive response and tolerance to weak acids in *Saccharomyces cerevisiae*: A genome-wide view. *Omics 14*, 5 (2010), 525–40.

[216] Mohanty, S. K., and Swain, M. R. *Bioethanol Production From Corn and Wheat: Food, Fuel, and Future*. Elsevier Inc., 2018.

[217] Monod, J. The growth of bacterial cultures. *annual review of microbiology 3* (1949), 371–394.

[218] Monod, J. La technique de culture continue théorie et applications. *Annales de l'Institut Pasteur 79* (1950), 390–412.

[219] Morano, K. A., Grant, C. M., and Moye-Rowley, W. S. The response to heat shock and oxidative stress in *Saccharomyces cerevisiae*. *Genetics 190*, 4 (apr 2012), 1157–95.

[220] Motizuki, M., Yokota, S., and Tsurugi, K. Effect of low pH on organization of the actin cytoskeleton in *Saccharomyces cerevisiae*. *Biochimica et biophysica acta 1780*, 2 (2008), 179–84.

[221] Muntean, M., Guizzardi, D., Schaaf, E., Crippa, M., Solazzo, E., Olivier, J., and Vignati, E. Fossil CO_2 emissions of all world countries - 2018 report. Tech. rep., Publication Office of the european Union, Luxembourg, 2018.

[222] Murphy, M. P. Slip and leak in mitochondrial oxidative phosphorylation. *BBA - Bioenergetics 977*, 2 (1989), 123–141.

[223] Nakajima-Shimada, J., Iida, H., Tsuji, F., and Anraku, Y. Monitoring of intracellular calcium in *Saccharomyces cerevisiae* with an apoaequorin cDNA expression system. *Proc Natl Acad Sci USA 88*, August (1991), 6878–6882.

[224] Nakamura, C. E., and Whited, G. M. Metabolic engineering for the microbial production of 1,3-propanediol. *Current Opinion in Biotechnology 14*, 5 (2003), 454–459.

[225] Nandy, S. K., and Srivastava, R. K. A review on sustainable yeast biotechnological processes and applications. *Microbiological Research 207*, November 2017 (2018), 83–90.

[226] Nielsen, J., and Keasling, J. D. Engineering Cellular Metabolism. *Cell 164*, 6 (2016), 1185–1197.

[227] Nielsen, J., Larsson, C., van Maris, A., and Pronk, J. Metabolic engineering of yeast for production of fuels and chemicals. *Current Opinion in Biotechnology* (apr 2013), 1–7.

[228] Nijkamp, J. F., van den Broek, M., Datema, E., de Kok, S., Bosman, L., Luttik, M. A., Daran-Lapujade, P., Vongsangnak, W., Nielsen, J., Heijne, W. H. M., Klaassen, P., Paddon, C. J., Platt, D., Kotter, P., van Ham, R. C., Reinders, M. J., Pronk, J. T., Ridder, D. D., and Daran, J.-M. *De novo* sequencing, assembly and analysis of the genome of the laboratory strain *Saccharomyces cerevisiae* CEN.PK113-7D, a model for modern industrial biotechnology. *Microbial Cell Factories 11*, 1 (2012), 36.

[229] Novick, A., and Szilard, L. Description of the Chemostat. *Science 112*, 2920 (1950).

[230] Novick, A., and Szilard, L. Experiments with the chemostat on spontaneous mutations in bacteria. *Proceedings of the National Academy of Sciences of the United States of America* (1950), 708–719.

[231] Nueda, M. J., Tarazona, S., and Conesa, A. Next maSigPro: Updating maSigPro bioconductor package for RNA-seq time series. *Bioinformatics 30*, 18 (2014), 2598–2602.

[232] Odani, T., Shimma, Y.-i., Wang, X.-H., and Jigami, Y. Mannosylphosphate transfer to cell wall mannan is regulated by the transcriptional level of the *MNN4* gene in *Saccharomyces cerevisiae*. *FEBS Letters 420*, 2-3 (1997), 186–190.

[233] Orij, R., Brul, S., and Smits, G. J. Intracellular pH is a tightly controlled signal in yeast. *Biochimica et biophysica acta 1810*, 10 (2011), 933–44.

[234] Orij, R., Postmus, J., Beek, A. T., Brul, S., and Smits, G. J. *In vivo* measurement of cytosolic and mitochondrial pH using a pH-sensitive GFP derivative in *Saccharomyces cerevisiae* reveals a relation between intracellular pH and growth. *Microbiology 155*, 1 (2009), 268–278.

[235] Orij, R., Urbanus, M. L., Vizeacoumar, F. J., Giaever, G., Boone, C., Nislow, C., Brul, S., and Smits, G. J. Genome-wide analysis of intracellular pH reveals quantitative control of cell division rate by pHc in *Saccharomyces cerevisiae*. *Genome Biology 13*, 9 (2012), R80.

[236] Otero, J. M., Cimini, D., Patil, K. R., Poulsen, S. G., Olsson, L., and Nielsen, J. Industrial systems biology of *Saccharomyces cerevisiae* enables novel succinic acid cell factory. *PloS one 8*, 1 (jan 2013), e54144.

[237] Oyetunde, T., Bao, F. S., Chen, J. W., Martin, H. G., and Tang, Y. J. Leveraging knowledge engineering and machine learning for microbial bio-manufacturing. *Biotechnology Advances 36*, 4 (2018), 1308–1315.

[238] Pais, C., Franco-Duarte, R., Sampaio, P., Wildner, J., Carolas, A., Figueira, D., and Ferreira, B. S. *Production of Dicarboxylic Acid Platform Chemicals Using Yeasts: Focus on Succinic Acid*. Elsevier Inc., 2016.

[239] Palma, M., Guerreiro, J. F., and Sá-Correia, I. Adaptive response and tolerance to acetic acid in *Saccharomyces cerevisiae* and *Zygosaccharomyces bailii*: A physiological genomics perspective. *Frontiers in Microbiology 9*, FEB (2018), 1–16.

[240] Papapetridis, I., van Dijk, M., Dobbe, A. P., Metz, B., van Maris, A. J. A., and Pronk, J. T. Improving ethanol yield in acetate-reducing Saccharomyces cerevisiae by cofactor engineering of 6-phosphogluconate dehydrogenase and deletion of *ALD6*. *Microbial Cell Factories 15*, 1 (2016), 1–16.

[241] Parrou, J. L., and François, J. A simplified procedure for a rapid and reliable assay of both glycogen and trehalose in whole yeast cells. *Analytical biochemistry 248*, 1 (may 1997), 186–8.

[242] Partow, S., Siewers, V., Bjørn, S., J., N., and Maury, J. Characterization of different promoters for designing a new expression vector in *Saccharomyces cerevisiae*. *Yeast 27* (2010), 955–964.

[243] Paulsel, A. L., Merz, A. J., and Nickerson, D. P. Vps9 family protein Muk1 is the second Rab5 guanosine nucleotide exchange factor in budding yeast. *Journal of Biological Chemistry 288*, 25 (2013), 18162–18171.

[244] Pawelzik, P., Carus, M., Hotchkiss, J., Narayan, R., Selke, S., Wellisch, M., Weiss, M., Wicke, B., and Patel, M. Critical aspects in the life cycle assessment (LCA) of bio-based materials – Reviewing methodologies and deriving recommendations. *Resources, Conservation and Recycling 73* (apr 2013), 211–228.

[245] Petitjean, M., Teste, M. A., François, J. M., and Parrou, J. L. Yeast tolerance to various stresses relies on the trehalose-6P synthase (Tps1) protein, not on trehalose. *Journal of Biological Chemistry 290*, 26 (2015), 16177–16190.

[246] Pham, H. T. B., Larsson, G., and Enfors, S. O. Growth and energy metabolism in aerobic fed-batch cultures of *Saccharomyces cerevisiae*: Simulation and model verification. *Biotechnology and Bioengineering 60*, 4 (1998), 474–482.

[247] Piper, M. D. W., Daran-Lapujade, P., Bro, C., Regenberg, B., Knudsen, S., Nielsen, J., and Pronk, J. T. Reproducibility of Oligonucleotide Microarray Transcriptome Analyses. *Journal of Biological Chemistry 277*, 40 (2002), 37001–37008.

[248] Piper, P., Calderon, C. O., Hatzixanthis, K., and Mollapour, M. Weak acid adaptation: The stress response that confers yeasts with resistance to organic acid food preservatives. *Microbiology 147*, 10 (2001), 2635–2642.

[249] Piper, P., Mahé, Y., Thompson, S., Pandjaitan, R., Holyoak, C., Egner, R., Muhlbauer, M., Coote, P., and Kuchler, K. The Pdr12 ATP-binding cassette (ABC) transporter is required for development of weak organic acid resistance in yeast. *The EMBO Journal 17*, 15 (1998), 4257–4265.

[250] Pirt, S. The Maintenance Energy of Bacteria in Growing Cultures. *Proceedings of the Royal Society of London 163*, 991 (1965), 224–231.

[251] Pirt, S. Maintenance Energy: a General Model for Energy-Limited and Energy-Sufficient Growth. *Archives of Microbiology 133* (1982), 300–302.

[252] Pirt, S., and Kurowski, W. M. An extension of the theory of the chemostat with feedback of organisms. Its experimental realization with a yeast culture. *Journal of general microbiology 63*, 3 (nov 1970), 357–66.

[253] Pirt, S. J., and Righelato, R. C. Effect of Growth Rate on the Synthesis of Penicillin by *Penicillium chrysogenum* in Batch and Chemostat Cultures. *Applied microbiology 15*, 6 (1967), 1284–90.

[254] Pohlers, S., Martin, R., Kruger, T., Hellwig, D., Hanel, F., Kniemeyer, O., Saluz, H., Van Dijck, P., Ernst, J., Brakhage, A., Muhlschlegel, F., and Kurzai, O. Lipid Signaling via Pkh1/2 Regulates Fungal CO_2 Sensing Through the Kinase Sch9. *mBio* (2017), 1–15.

[255] Popolo, L., and Vai, M. The Gas1 glycoprotein, a putative wall polymer cross-linker. *Biochimica et Biophysica Acta - General Subjects 1426*, 2 (1999), 385–400.

[256] Popolo, L., Vai, M., Gatti, E., Porello, S., Bonfante, P., Balestrini, R., and Alberghina, L. Physiological analysis of mutants indicates involvement of the *Saccharomyces cerevisiae* GPI-anchored protein gp115 in morphogenesis and cell separation. *Journal of Bacteriology 175*, 7 (1993), 1879–1885.

[257] Postma, E., Verduyn, C., Scheffers, W. A., and Van Dijken, J. P. Enzymic analysis of the crabtree effect in glucose-limited chemostat cultures of *Saccharomyces cerevisiae*. *Applied and Environmental Microbiology 55*, 2 (1989), 468–477.

[258] Ram, A. F. J., Brekelmans, S. S. C., Oehlen, L. J. W. M., and Klis, F. M. Identification of two cell cycle regulated genes affecting the β1,3-glucan content of cell walls in *Saccharomyces cerevisiae*. *FEBS Letters 358*, 2 (1995), 165–170.

[259] Rebnegger, C., Graf, A. B., Valli, M., Steiger, M. G., Gasser, B., Maurer, M., and Mattanovich, D. In *Pichia pastoris*, growth rate regulates protein synthesis and secretion, mating and stress response. *Biotechnology Journal 9*, 4 (2014), 511–525.

[260] Regenberg, B., Grotkjaer, T., Winther, O., Fausbøll, A., Akesson, M., Bro, C., Hansen, L. K., Brunak, S., and Nielsen, J. Growth-rate regulated genes have profound impact on interpretation of transcriptome profiling in *Saccharomyces cerevisiae*. *Genome biology 7*, 11 (jan 2006), R107.

[261] Reich, M., Liefeld, T., Gould, J., Lerner, J., Tamayo, P., and Mesirov, J. GenePattern 2.0. *Nature Genetics 38* (2006), 500–501.

[262] Resnick, M. A., and Martin, P. The repair of double-strand breaks in the nuclear DNA of *Saccharomyces cerevisiae* and its genetic control. *MGG Molecular & General Genetics 143*, 2 (1976), 119–129.

[263] Richard, L., Guillouet, S. E., and Uribelarrea, J.-L. Quantification of the transient and long-term response of *Saccharomyces cerevisiae* to carbon dioxide stresses of various intensities. *Process Biochemistry 49*, 11 (nov 2014), 1808–1818.

[264] Rintala, E., Jouhten, P., Toivari, M., Wiebe, M. G., and Maaheimo, H. Transcriptional Responses of *Saccharomyces cerevisiae* to Shift from Respiratory and Respirofermentative to Fully Fermentative Metabolism. *OMICS A journal of Integrative Biology 15* (2011).

[265] Ro, D. K., Paradise, E. M., Quellet, M., Fisher, K. J., Newman, K. L., Ndungu, J. M., Ho, K. A., Eachus, R. A., Ham, T. S., Kirby, J., Chang, M. C., Withers, S. T., Shiba, Y., Sarpong, R., and Keasling, J. D. Production of the antimalarial drug precursor artemisinic acid in engineered yeast. *Nature 440*, 7086 (2006), 940–943.

[266] Robinson, M. D., McCarthy, D. J., and Smyth, G. K. edgeR: A Bioconductor package for differential expression analysis of digital gene expression data. *Bioinformatics 26*, 1 (2009), 139–140.

[267] Rodriguez-Pena, J., Garcia, R., Nombela, C., and Arroyo, J. The high-osmolarity glycerol (HOG) and cell wall integrity (CWI) signalling pathways interplay: a yeast dialogue between MAPK routes. *Yeast (Chichester, England) 26*, 10 (2010), 545–551.

[268] Roelants, F., Torrance, P., Bezman, N., and Thorner, J. Pkh1 and Pkh2 Differentially Phosphorylate and Activate Ypk1 and Ykr2 and Define Protein Kinase Modules Required for Maintenance of Cell Wall Integrity. *Molecular Biology of the Cell 13* (2002), 3005–3028.

[269] Rogers, P. J., and Stewart, P. R. Energetic efficiency and maintenance. Energy characteristics of *Saccharomyces cerevisiae* (wild type and petite) and *Candida parapsilosis* grown aerobically and micro-aerobically in continuous culture. *Archives of microbiology 99*, 1 (jan 1974), 25–46.

[270] Roohvand, F., Shokri, M., Abdollahpour-Alitappeh, M., and Ehsani, P. Biomedical applications of yeast- a patent view, part one: yeasts as workhorses for the production of therapeutics and vaccines. *Expert Opinion on Therapeutic Patents 27*, 8 (2017), 929–951.

[271] Rossum, H. M. V., Kozak, B. U., Niemeijer, M. S., Dykstra, J. C., Luttik, M. A. H., Daran, J.-M. G., van Maris, A. J., and Pronk, J. Requirements for carnitine shuttle-mediated translocation of mitochondrial acetyl moieties to the yeast cytosol. *mBio 7*, 3 (2016), 1–14.

[272] Rowley, B. I., and Pirt, S. J. Melanin Production by *Aspergillus nidulans* in Batch and Chemostat Cultures. *Journal of General Microbiology 72*, 3 (2009), 553–563.

[273] Salazar, A. N., Gorter De Vries, A. R., Broek, M. V. D., De la Torre Cortés, P., Brickwedde, A., Brouwers, N., Daran, J.-m. G., and Abeel, T. Nanopore sequencing enables near-complete *de novo* assembly of *Saccharomyces cerevisiae* reference strain CEN.PK113-7D. *FEMS Yeast Research 17* (2017), 1–35.

[274] Sandoval, C. M., Ayson, M., Moss, N., Lieu, B., Jackson, P., Gaucher, S. P., Horning, T., Dahl, R. H., Denery, J. R., Abbott, D. A., and Meadows, A. L. Use of pantothenate as a metabolic switch increases the genetic stability of farnesene producing *Saccharomyces cerevisiae*. *Metabolic Engineering 25* (2014), 215–226.

[275] Santangelo, G. M. Glucose Signaling in *Saccharomyces cerevisiae*. *Microbiology and Molecular Biology Reviews 70*, 1 (2006), 253–282.

[276] Sauer, M., Porro, D., Mattanovich, D., and Branduardi, P. Microbial production of organic acids: expanding the markets. *Trends in biotechnology 26*, 2 (feb 2008), 100–8.

[277] Schmelzle, T., Helliwell, S. B., and Hall, M. N. Yeast Protein Kinases and the RHO1 Exchange Factor TUS1 Are Novel Components of the Cell Integrity Pathway in Yeast. *Molecular and Cellular Biology 22*, 5 (2002), 1329–1339.

[278] Schmidt, F. R. Optimization and scale up of industrial fermentation processes. *Applied Microbiology and Biotechnology 68*, 4 (2005), 425–435.

[279] Schmitt, M. E., Brown, T. A., and Trumpower, B. L. A rapid and simple method for preparation of RNA from *Saccharomyces cerevisiae*. *Nucleic Acids Research 18*, 10 (1990), 3091–3092.

[280] Schrickx, J., Readts, M., Stouthamer, A., and Van Verseveld, H. Organic Acid Production by *Aspergllus niger* in Recycling Culture Analyzed by Capillary Electrophoresis. *Analytical Biochemistry 231* (1995), 175–181.

[281] Schrickx, J. M., Stouthamer, A. H., and van Verseveld, H. W. Growth behaviour and glucoamylase production by *Aspergillus niger* N402 and a glucoamylase overproducing transformant in recycling culture without a nitrogen source. *Applied Microbiology and Biotechnology 43*, 1 (1995), 109–116.

[282] Schwartz, R., Ting, C. S., and King, J. Whole Proteome pI Values Correlate with Subcellular Localizations of Proteins for Organisms within the Three Domains of Life. *Genome Research 11* (2001), 703–709.

[283] Schwarz, D. S., and Blower, M. D. The endoplasmic reticulum: Structure, function and response to cellular signaling. *Cellular and Molecular Life Sciences 73*, 1 (2016), 79–94.

[284] Sevella, B., and Bertalan, G. Development of a MATLAB based bioprocess simulation tool. *Bioprocess engineering 23*, December 1999 (2000), 621–626.

[285] Sheldon, J. G., Williams, S. P., Fulton, A. M., and Brindle, K. M. ^{31}P NMR magnetization transfer study of the control of ATP turnover in *Saccharomyces cerevisiae*. *Proceedings of the National Academy of Sciences 93*, 13 (1996), 6399–6404.

[286] Shi, L., Sutter, B. M., Ye, X., and Tu, B. P. Trehalose is a Key Determinant of the Quiescent Metabolic State That Fuels Cell Cycle Progression upon Return to Growth. *Molecular biology of the cell 21* (2010).

[287] Shideler, T., Nickerson, D. P., Merz, A. J., and Odorizzi, G. Ubiquitin binding by the CUE domain promotes endosomal localization of the Rab5 GEF Vps9. *Molecular biology of the cell 26*, 7 (2015), 1345–56.

[288] Show, P. L., Oladele, K. O., Siew, Q. Y., Aziz Zakry, F. A., Lan, J. C. W., and Ling, T. C. Overview of citric acid production from *Aspergillus niger*. *Frontiers in Life Science 8*, 3 (2015), 271–283.

[289] Si, T., Chao, R., Min, Y., Wu, Y., Ren, W., and Zhao, H. Automated multiplex genome-scale engineering in yeast. *Nature Communications 8*, May (2017), 1–12.

[290] Smets, B., Ghillebert, R., De Snijder, P., Binda, M., Swinnen, E., De Virgilio, C., and Winderickx, J. Life in the midst of scarcity: adaptations to nutrient availability in *Saccharomyces cerevisiae*. *Current genetics 56* (feb 2010), 1–32.

[291] Snoep, J. L., Mrwebi, M., Schuurmans, J. M., Rohwer, J. M., and Teixeira de Mattos, M. J. Control of specific growth rate in *Saccharomyces cerevisiae*. *Microbiology (Reading, England) 155*, Pt 5 (may 2009), 1699–707.

[292] Solis-Escalante, D., Kuijpers, N. G., Barrajon-Simancas, N., van den Broek, M., Pronk, J. T., Daran, J. M., and Daran-Lapujade, P. A minimal set of glycolytic genes reveals strong redundancies in *Saccharomyces cerevisiae* central metabolism. *Eukaryotic Cell 14*, 8 (2015), 804–816.

[293] Solis-Escalante, D., Kuijpers, N. G. a., Bongaerts, N., Bolat, I., Bosman, L., Pronk, J. T., Daran, J.-M., and Daran-Lapujade, P. *amdSYM*, a new dominant recyclable marker cassette for Saccharomyces cerevisiae. *FEMS yeast research 13*, 1 (feb 2013), 126–39.

[294] Stanley, D., Fraser, S., Chambers, P. J., Rogers, P., and Stanley, G. A. Generation and characterisation of stable ethanol-tolerant mutants of *Saccharomyces cerevisiae*. *Journal of Industrial Microbiology and Biotechnology 37*, 2 (2010), 139–149.

[295] Steen, E. J., Chan, R., Prasad, N., Myers, S., Petzold, C. J., Redding, A., Ouellet, M., and Keasling, J. D. Metabolic engineering of *Saccharomyces cerevisiae* for the production of n-butanol. *Microbial Cell Factories 7* (2008), 1–8.

[296] Steensels, J., Gorkovskiy, A., and Verstrepen, K. J. SCRaMbLEing to understand and exploit structural variation in genomes. *Nature Communications 9*, 1 (2018), 9–11.

[297] Stips, A., MacIas, D., Coughlan, C., Garcia-Gorriz, E., and Liang, X. S. On the causal structure between CO_2 and global temperature. *Scientific Reports 6*, February (2016), 1–9.

[298] Stouthamer, A. H. A theoretical study on the amount of ATP required for synthesis of microbial cell material. *Antonie van Leeuwenhoek 39*, 1 (1973), 545–565.

[299] Suarez-Mendez, C., Sousa, A., Heijnen, J., and Wahl, A. Fast "Feast/Famine" Cycles for Studying Microbial Physiology Under Dynamic Conditions: A Case Study with *Saccharomyces cerevisiae*. *Metabolites 4*, 2 (2014), 347–372.

[300] Swiat, M. A., Dashko, S., Den Ridder, M., Wijsman, M., Van Der Oost, J., Daran, J. M., and Daran-Lapujade, P. FnCpf1: A novel and efficient genome editing tool for *Saccharomyces cerevisiae*. *Nucleic Acids Research 45*, 21 (2017), 12585–12598.

[301] Święciło, A. Cross-stress resistance in *Saccharomyces cerevisiae* yeast - new insight into an old phenomenon. *Cell Stress and Chaperones 21*, 2 (2016), 187–200.

[302] Tagoe, D., and Ansah, F. K. Computer Keyboard and Mice : Potential Sources of Disease Transmission and Infections. *The Internet Journal of Public Health 1*, 2 (2010), 1–6.

[303] Tai, S. L., Boer, V. M., Daran-Lapujade, P., Walsh, M. C., De Winde, J. H., Daran, J. M., and Pronk, J. T. Two-dimensional transcriptome analysis in chemostat cultures: Combinatorial effects of oxygen availability and macronutrient limitation in *Saccharomyces cerevisiae*. *Journal of Biological Chemistry 280*, 1 (2005), 437–447.

[304] Tännler, S., Decasper, S., and Sauer, U. Maintenance metabolism and carbon fluxes in *Bacillus species*. *Microbial Cell Factories 7*, 1 (2008), 19.

[305] Tappe, W., Laverman, A., Bohland, M., Braster, M., Groeneweg, J., and Verseveld, H. W. V. Maintenance Energy Demand and Starvation Recovery Dynamics of *Nitrosomonas europaea* and *Nitrobacter winogradskyi* Cultivated in a Retentostat with Complete Biomass Retention. *Applied and Environmental Microbiology 65*, 6 (1999), 2471–2477.

[306] Tempest, David, W., and Neijssel, Oense, M. The status of Y_{ATP} and maintenance energy as biologically interpretable phenomena. *Annual Review of Microbiology 38*, 34 (1984), 259–513.

[307] Teste, M.-A., Duquenne, M., François, J. M., and Parrou, J.-L. Validation of reference genes for quantitative expression analysis by real-time RT-PCR in *Saccharomyces cerevisiae*. *BMC Molecular Biology 10*, 1 (2009), 99.

[308] Thakker, C., Martínez, I., Li, W., San, K.-Y., and Bennett, G. N. Metabolic engineering of carbon and redox flow in the production of small organic acids. *Journal of industrial microbiology & biotechnology 42*, 3 (2015), 403–22.

[309] Thomas, R. C. The effect of carbon dioxide on the intracellular pH and buffering power of snail neurones. *The Journal of Physiology 255*, 3 (1976), 715–735.

[310] Ton, V.-K., and Rao, R. Functional expression of heterologous proteins in yeast: insights into Ca2+ signaling and Ca2+-transporting ATPases. *American Journal of Physiology-Cell Physiology 287*, 3 (2004), C580–C589.

[311] Tu, L., and Banfield, D. K. Localization of Golgi-resident glycosyltransferases. *Cellular and Molecular Life Sciences 67*, 1 (2010), 29–41.

[312] Turrens, J. F. Mitochondrial formation of reactive oxygen species. *The Journal of physiology 552*, Pt 2 (oct 2003), 335–44.

[313] Ullah, A., Orij, R., Brul, S., and Smits, G. J. Quantitative analysis of the modes of growth inhibition by weak organic acids in *Saccharomyces cerevisiae*. *Applied and Environmental Microbiology 78*, 23 (2012), 8377–8387.

[314] van Bodegom, P. Microbial maintenance: a critical review on its quantification. *Microbial ecology 53*, 4 (may 2007), 513–23.

[315] Van Den Berg, M. A., Albang, R., Albermann, K., Badger, J. H., Daran, J. M., M Driessen, A. J., Garcia-Estrada, C., Fedorova, N. D., Harris, D. M., Heijne, W. H., Joardar, V., W Kiel, J. A., Kovalchuk, A., Martín, J. F., Nierman, W. C., Nijland, J. G., Pronk, J. T., Roubos, J. A., Van Der Klei, I. J., Van Peij, N. N., Veenhuis, M., Von Döhren, H., Wagner, C., Wortman, J., and Bovenberg, R. A. Genome

sequencing and analysis of the filamentous fungus *Penicillium chrysogenum*. *Nature Biotechnology 26*, 10 (2008), 1161–1168.

[316] Van den Brink, J., Daran-Lapujade, P., Pronk, J. T., and de Winde, J. H. New insights into the *Saccharomyces cerevisiae* fermentation switch: Dynamic transcriptional response to anaerobicity and glucose-excess. *BMC Genomics 9* (2008), 1–14.

[317] Van der Beek, C., and Roels, J. Penicillin production: Biotechnology at its finest. *Antonie van Leeuwenhoek 50* (1984), 625–639.

[318] van Dijken, J., Bauer, J., Brambilla, L., Duboc, P., Francois, J., Gancedo, C., Giuseppin, M., Heijnen, J., Hoare, M., Lange, H., Madden, E., Niederberger, P., Nielsen, J., Parrou, J., Petit, T., Porro, D., Reuss, M., van Riel, N., Rizzi, M., Steensma, H., Verrips, C., Vindeløv, J., and Pronk, J. An interlaboratory comparison of physiological and genetic properties of four *Saccharomyces cerevisiae* strains. *Enzyme and Microbial Technology 26*, 9-10 (2000), 706–714.

[319] van Dijken, J. P., Weusthuis, R. A., and Pronk, J. T. Kinetics of growth and sugar consumption in yeasts. *Antonie van Leeuwenhoek 63* (1993), 343–352.

[320] van Hoek, P., de Hulster, E., van Dijken, J. P., and Pronk, J. T. Fermentative capacity in high-cell-density fed-batch cultures of baker's yeast. *Biotechnology and bioengineering 68*, 5 (jun 2000), 517–23.

[321] van Hoek, P., van Dijken, J., and Pronk, J. T. Effect of Specific Growth Rate on Fermentative Capacity of Baker's Yeast. *Applied and Environmental Microbiology 64*, 11 (1998), 4226–4233.

[322] Van Hoek, P., Van Dijken, J. P., and Pronk, J. T. Regulation of fermentative capacity and levels of glycolytic enzymes in chemostat cultures of *Saccharomyces cerevisiae*. *Enzyme and Microbial Technology 26*, 9-10 (2000), 724–736.

[323] van Maris, A. J., Abbott, D. A., Bellissimi, E., van den Brink, J., Kuyper, M., Luttik, M. A., Wisselink, H. W., Scheffers, W. A., van Dijken, J. P., and Pronk, J. T. Alcoholic fermentation of carbon sources in biomass hydrolysates by *Saccharomyces cerevisiae*: Current status. *Antonie van Leeuwenhoek, International Journal of General and Molecular Microbiology 90*, 4 (2006), 391–418.

[324] van Maris, A. J. A., Geertman, J.-M. A., Vermeulen, A., Groothuizen, M. K., Winkler, A. A., Piper, M. D. W., van Dijken, J. P., and Pronk, J. T. Directed evolution of pyruvate decarboxylase-negative *Saccharomyces cerevisiae*, yielding a C_2-independent, glucose-tolerant, and pyruvate-hyperproducing yeast. *Applied and Environmental Microbiology 70*, 1 (jan 2004), 159–166.

[325] van Uden, N. Transport-Limited Growth in the Chemostat and its Competitive Inhibition; A Theoretical Treatment. *Archiv für Mikrobiologie 154* (1967), 145–154.

[326] van Verseveld, H. W., Arbige, M., and R. Chesbro, W. Continuous culture of bacteria with biomass retention. *Trends in Biotechnology 2*, 1 (1984), 8–12.

[327] van Verseveld, H. W., de Hollander, J. A., Frankena, J., Braster, M., Leeuwerik, F. J., and Stouthamer, A. H. Modeling of microbial substrate conversion, growth and product formation in a recycling fermentor. *Antonie van Leeuwenhoek 52*, 4 (jan 1986), 325–42.

[328] Vanholme, B., Desmet, T., Ronsse, F., Rabaey, K., Breusegem, F. V., Mey, M. D., Soetaert, W., and Boerjan, W. Towards a carbon-negative sustainable bio-based economy. *Frontiers in Plant Science 4*, June (2013), 1–17.

[329] Vanrolleghem, P., de Jong-Gubbels, P., van Gulik, W., Pronk, J., van Dijken, J., and Heijnen, S. Validation of a Metabolic Network for *Saccharomyces cerevisiae* Using Mixed Substrate Studies. *Biotechnology Progress 12*, 4 (1996), 434–448.

[330] Väremo, L., Nielsen, J., and Nookaew, I. Enriching the gene set analysis of genome-wide data by incorporating directionality of gene expression and combining statistical hypotheses and methods. *Nucleic Acids Research 41*, 8 (2013), 4378–4391.

[331] Verduyn, C., Postma, E., Scheffers, W. A., and van Dijken, J. P. Physiology of *Saccharomyces cerevisiae* in anaerobic glucose-limited chemostat cultures. *Journal of general microbiology 136*, 3 (mar 1990), 405–412.

[332] Verduyn, C., Postma, E., Scheffers, W. A., and Van Dijken, J. P. Effect of benzoic acid on metabolic fluxes in yeasts: a continuous-culture study on the regulation of respiration and alcoholic fermentation. *Yeast (Chichester, England) 8* (1992), 501–17.

[333] Verduyn, C., Stouthamer, A. H., Scheffers, W. A., and van Dijken, J. P. A theoretical evaluation of growth yields of yeasts. *Antonie van Leeuwenhoek 59*, 1 (jan 1991), 49–63.

[334] Verghese, J., Abrams, J., Wang, Y., and Morano, K. A. Biology of the Heat Shock Response and Protein Chaperones: Budding Yeast (*Saccharomyces cerevisiae*) as a Model System. *Microbiology and Molecular Biology Reviews 76*, 2 (2012), 115–158.

[335] Verhoeven, M. D., Lee, M., Kamoen, L., van den Broek, M., Janssen, D. B., Daran, J.-M. G., van Maris, A. J. A., and Pronk, J. T. Mutations in *PMR1* stimulate xylose isomerase activity and anaerobic growth on xylose of engineered *Saccharomyces cerevisiae* by influencing manganese homeostasis. *Scientific Reports 7*, October 2016 (2017), 46155.

[336] Viaggi, D. Towards an economics of the bioeconomy: Four years later. *Bio-based and Applied Economics 5*, 2 (2016), 101–112.

[337] Virgilio, C., Hottinger, T., Dominguez, J., Boller, T., and Wiemken, A. The role of trehalose synthesis for the acquisition of thermotolerance in yeast. I. Genetic evidence that trehalose is a thermoprotectant. *European Journal of Biochemistry 219* (1994), 179–186.

[338] Voordeckers, K., Kominek, J., Das, A., and Espinosa-cantú, A. Adaptation to high ethanol reveals complex evolutionary pathways. *PLoS Genetics 11*, 11 (2015).

[339] Vos, T., de la Torre Cortés, P., van Gulik, W. M., Pronk, J. T., and Daran-Lapujade, P. Growth-rate dependency of *de novo* resveratrol production in chemostat cultures of an engineered *Saccharomyces cerevisiae* strain. *Microbial Cell Factories 14*, 1 (2015), 1–15.

[340] Vos, T., Hakkaart, X. D. V., de Hulster, E. A. F., van Maris, A. J. A., Pronk, J. T., and Daran-Lapujade, P. Maintenance-energy requirements and robustness of *Saccharomyces cerevisiae* at aerobic near-zero specific growth rates. *Microbial Cell Factories 15*, 1 (2016), 111.

[341] Wahl, S. A., Bernal Martinez, C., Zhao, Z., van Gulik, W. M., and Jansen, M. L. A. Intracellular product recycling in high succinic acid producing yeast at low pH. *Microbial Cell Factories 16*, 1 (2017), 90.

[342] Walker, B. J., Abeel, T., Shea, T., Priest, M., Abouelliel, A., Sakthikumar, S., Cuomo, C. A., Zeng, Q., Wortman, J., Young, S. K., and Earl, A. M. Pilon: An integrated tool for comprehensive microbial variant detection and genome assembly improvement. *PLoS ONE 9*, 11 (2014).

[343] Walsh, G. Therapeutic insulins and their large-scale manufacture. *Applied Microbiology and Biotechnology 67*, 2 (2005), 151–159.

[344] Werner-Washburne, M., Braun, E., Johnston, G. C., and Singer, R. a. Stationary phase in the yeast *Saccharomyces cerevisiae*. *Microbiological reviews 57*, 2 (jun 1993), 383–401.

[345] Wiebe, M. G., Rintala, E., Tamminen, A., Simolin, H., Salusjärvi, L., Toivari, M., Kokkonen, J. T., Kiuru, J., Ketola, R. A., Jouhten, P., Huuskonen, A., Maaheimo, H., Ruohonen, L., and Penttilä, M. Central carbon metabolism of *Saccharomyces cerevisiae* in anaerobic, oxygen-limited and fully aerobic steady-state conditions and following a shift to anaerobic conditions. *FEMS Yeast Research 8*, 1 (2008), 140–154.

[346] Wilson, K., and McLeod, B. J. The influence of conditions of growth on the endogenous metabolism of *Saccharomyces cerevisiae*: effect on protein, carbohydrate, sterol and fatty acid content and on viability. *Antonie van Leeuwenhoek 42*, 4 (1976), 397–410.

[347] Wisselink, H. W., Toirkens, M. J., del Rosario Franco Berriel, M., Winkler, A. a., van Dijken, J. P., Pronk, J. T., and van Maris, A. J. a. Engineering of *Saccharomyces cerevisiae* for efficient anaerobic alcoholic fermentation of L-arabinose. *Applied and environmental microbiology 73*, 15 (aug 2007), 4881–91.

[348] Wisselink, H. W., Toirkens, M. J., Wu, Q., Pronk, J. T., and van Maris, A. J. a. Novel evolutionary engineering approach for accelerated utilization of glucose, xylose, and arabinose mixtures by engineered *Saccharomyces cerevisiae* strains. *Applied and environmental microbiology 75*, 4 (feb 2009), 907–14.

[349] Wloch-Salamon, D. M., and Bem, A. E. Types of cell death and methods of their detection in yeast *Saccharomyces cerevisiae*. *Journal of Applied Microbiology 114*, 2 (2013), 287–298.

[350] Woodley, J. M., Breuer, M., and Mink, D. A future perspective on the role of industrial biotechnology for chemicals production. *Chemical Engineering Research and Design 91*, 10 (2013), 2029–2036.

[351] Xia, Z., Webster, A., Du, F., Piatkov, K., Ghislain, M., and Varshavsky, A. Substrate-binding sites of *UBR1*, the ubiquitin ligase of the N-end Rule pathway. *Journal of Biological Chemistry 283*, 35 (2008), 24011–24028.

[352] Xiberras, J., Klein, M., and Nevoigt, E. Glycerol as a substrate for *Saccharomyces cerevisiae* based bioprocesses – Knowledge gaps regarding the central carbon catabolism of this 'non-fermentable' carbon source. *Biotechnology Advances* (2019).

[353] Xie, Y., and Vershavsky, A. The E2-E3 interaction in the N-end rule pathway: the RING-H2 finger of E3 is required for the synthesis of multiubiquitin chain. *The EMBO Journal 18*, 23 (1999), 6832–6844.

[354] Yin, X., Li, J., Shin, H.-d., Du, G., Liu, L., and Chen, J. Metabolic engineering in the biotechnological production of organic acids in the tricarboxylic acid cycle of microorganisms: Advances and prospects. *Biotechnology Advances 33*, 6 (2015), 830–841.

[355] Zakrzewska, A., van Eikenhorst, G., Burggraaff, J. E. C., Vis, D. J., Hoefsloot, H., Delneri, D., Oliver, S. G., Brul, S., and Smits, G. J. Genome-wide analysis of yeast stress survival and tolerance acquisition to analyze the central trade-off between growth rate and cellular robustness. *Molecular biology of the cell 22*, 22 (nov 2011), 4435–46.

[356] Zelle, R. M., de Hulster, E., Kloezen, W., Pronk, J. T., and van Maris, A. J. a. Key process conditions for production of C(4) dicarboxylic acids in bioreactor batch cultures of an engineered *Saccharomyces cerevisiae* strain. *Applied and environmental microbiology 76*, 3 (feb 2010), 744–50.

[357] Zhang, Y., Wang, J., Wang, Z., Zhang, Y., Shi, S., Nielsen, J., and Liu, Z. A gRNA-tRNA array for CRISPR-Cas9 based rapid multiplexed genome editing in *Saccharomyces cerevisiae*. *Nature Communications 10*, 1 (2019), 1–10.

[358] Zhao, C., Liu, B., Piao, S., Wang, X., Lobell, D. B., Huang, Y., Huang, M., Yao, Y., Bassu, S., Ciais, P., Durand, J.-L., Elliott, J., Ewert, F., Janssens, I. A., Li, T., Lin, E., Liu, Q., Martre, P., Müller, C., Peng, S., Peñuelas, J., Ruane, A. C., Wallach, D., Wang, T., Wu, D., Liu, Z., Zhu, Y., Zhu, Z., and Asseng, S. Temperature increase reduces global yields of major crops in four independent estimates. *Proceedings of the National Academy of Sciences 114*, 35 (2017), 9326–9331.

[359] Zingaro, K. A., and Terry Papoutsakis, E. GroESL overexpression imparts *Escherichia coli* tolerance to i-, n-, and 2-butanol, 1,2,4-butanetriol and ethanol with complex and unpredictable patterns. *Metabolic Engineering 15*, 1 (2013), 196–205.

Curriculum vitæ

On Friday the 13th of July 1990 Xavier Dominique Vincent Hakkaart first saw the light in Hilversum, The Netherlands. In the eighteen following years, Xavier moved from Primary education (Hilversumse Schoolvereniging, Hilversum), to secondary education (Alberdingk Thijm College, Hilversum). There he completed pre-university education (Gymnasium) with the specialization in Science and Technology subjects and chose French, Latin and Ancient Greek as electives.

In 2008, driven by a fascination for biology and chemistry, Xavier embarked on the Bachelor programme in Life Science & Technology offered by Delft University of Technology (TU Delft) and Leiden University. During his BSc study, Xavier took electives in biochemistry and biotechnology at Imperial College London (United Kingdom) in the Erasmus Exchange Program provided by the European Union.

The final research project to become BSc in Life Science & Technology was performed in the Industrial Microbiology group at TU Delft. The daily supervision of this study of putative lactic acid transporters in *Saccharomyces cerevisiae* was done by ir. Stefan de Kok. This project sparked Xavier's interest in industrially inspired research. Upon completion of this project, in 2011, Xavier was awarded the BSc degree in Life Science & Technology, with the distinction *cum laude*.

Right after obtaining his BSc degree, Xavier became a one-year full-time board member of Study Association LIFE in the position of treasurer. The highlights of this year included a symposium on Synthetic Biology and a study-tour to Lyon and Zürich. In 2012 Xavier enrolled for the MSc programme Life Science & Technology at TU Delft. At the end of the first year, the Design project on a second generation bio-refinery in the Port of Rotterdam was won by the team in which Xavier took part.

Determined to return to industrially inspired research, Xavier started his academic research project of the MSc programme in the Industrial Microbiology group under the supervision of Dr. Pascale Daran-Lapujade and daily supervision by ir. Tim Vos. This project focussed on the physiological responses of *S. cerevisiae* under near-zero growth rates. Upon finishing this project in May 2014, Xavier moved to New Hampshire in the United States to work at Mascoma Corp. for his industrial internship. Finishing this project marked the end of the student life of Xavier with the completion of the MSc degree in Life Science & Technology with the distinction *cum laude*.

After moving back to the Netherlands at the end of 2014, Xavier joined the Industrial Microbiology group at the TU Delft yet again to continue his studies of yeast under industrially relevant conditions as a PhD candidate. This project was performed under the supervision of Prof. dr. Pascale Daran-Lapujade and Prof. dr. Jack Pronk. After four years, the PhD project resulted in this thesis. As from June 2019 Xavier works as Bioprocess engineer with Evonik Industries AG in Germany.

List of Publications

5. Juergens, H.*, **Hakkaart X.D.V.***, Bras J.E., Vente, A., Pronk J.T., Mans, R., Investigation of the contribution of respiratory Complex I towards NADH reoxidation in glucose-grown cultures of the Crabtree-negative yeast *Ogataea parapolymorpha*, In preparation for publication in Applied and Environmental Microbiology. ** Joint first authorship*
4. **Hakkaart, X.D.V.**, Geelhoed J., de Groot P.A., Luttik M.A.H., Kranendonk E.M.M., Dijksman D., Daran J.M.G., Pronk J.T., Daran-Lapujade P., Adaptive laboratory evolution and reverse engineering of low pH tolerance in *Saccharomyces cerevisiae*, Submitted for publication in Applied and Environmental Microbiology.
3. **Hakkaart X.D.V.***, Liu Y*, Hulst M.B., el Masoudi A., Peuscher E.J., Pronk J.T., van Gulik W.M., Daran-Lapujade P.A.S.., Physiological responses of *Saccharomyces cerevisiae* grown under industrially- relevant conditions: slow growth, low pH and high CO_2 levels, Submitted for publication in Biotechnology & Bioengineering. ** Joint first authorship*
2. **Hakkaart X.D.V.**, Pronk J.T., van Maris A.J.A. , A Simulator-Assisted Workshop for Teaching Chemostat Cultivation in Academic Classes on Microbial Physiology, J Microbiol Biol Educ **18** (2017).
1. Vos T, **Hakkaart X.D.V.**, de Hulster E.A.F., van Maris A.J.A., Pronk J.T., Daran-Lapujade P., Maintenance-energy requirements and robustness of *Saccharomyces cerevisiae* at aerobic near-zero specific growth rates, Microb Cell Fact **15**, 111 (2016).